THE MINERALOGY AND CHEMISTRY OF GRANITE WEATHERING

BY

JILLIAN F. BANFIELD

A THESIS SUBMITTED FOR THE DEGREE OF

MASTER OF SCIENCE

AT

THE AUSTRALIAN NATIONAL UNIVERSITY

APRIL, 1985.

STATEMENT

This thesis is based on work carried out in the Department of Geology, the Scanning Electron Microscope Facility, The Research School of Chemistry, and the Research School of Earth Sciences, of the Australian National University; The Division of Soils and the Division of Plant Industry, C.S.I.R.O; Canberra, A.C.T.

All results and conclusions are those of the author unless otherwise acknowledged.

Jill Banfield.

J Banfield

ABSTRACT

The weathering of granite has been studied by examining the mineralogical and chemical changes which occur. In the early stages weathering proceeds by crystallographically controlled dissolution of parent minerals focussed initially at energetically favoured sites such as dislocations, twin and cleavage planes. Secondary phases may form in a variety of ways: from solution, from an amorphous or gel-like component, or by recrystallization. The pathway observed in any specific case is dependent primarily upon the structures of the parent mineral and the secondary phase.

In the granites studied, the framework silicates plagioclase, K-feldspar, and the chain silicate amphibole weather by the breakdown of their structures to form an amorphous or semi- amorphous component. This recrystallizes by nucleation and growth of small units which form increasingly large aggregates of clay, generally smectite. The chemistry of this clay clearly reflects the composition of the parent phase. Consequently, the first formed phase replacing amphibole is an Al poor, Fe rich smectite (nontronite), whereas the feldspars are replaced by Al rich smectite. Smectite is a transitional phase, and is converted to an allophane-like material which recrystallizes to form spherical halloysite. Kaolinite is also a weathering product, developing epitactically onto available sheet silicate structures. Fe which is present in the smectite appears to recrystallize to form oxides.

Tubular halloysite is another abundant alteration product, particularly of plagioclase. This phase grows outward, apparently via solution, into cavities produced by dissolution. Recrystallization to kaolinite can be observed in some areas.

Phases such as biotite and muscovite have sheet silicate structures which facilitate their direct conversion to 2:1 clay minerals. Biotite alters to vermiculite via two direct mechanisms. The most common transformation involves the introduction of cations and water, converting the 10 Å biotite sheet to 14 Å vermiculite. The second, relatively uncommon mechanism involves the replacement of two biotite sheets by a single vermiculite layer. Both reactions contribute to the development of interstratified biotite-vermiculite. As weathering

proceeds biotite-vermiculite is increasingly converted to kaolinite which crystallizes by templating onto existing sheet silicate structures. Fe released recrystallizes via an apparently semi-amorphous material to form increasingly regular, oriented laths of goethite.

Muscovite derived by hydrothermal alteration of feldspar alters via illite and interstratified illite-smectite to a smectite. The chemistry of muscovite derived illite clearly distinguishes it from plagioclase derived smectite. This chemical distinction is preserved although phases develop in close proximity, and regardless of whether transformations proceed via an amorphous component or by direct structural modification. This suggests that the chemistry of the parent mineral is a major factor in determining the nature of early formed replacement phases.

Apatite undergoes dissolution and replacement during the earliest stages of weathering. In two profiles studied this phase is replaced by a range of REE-Al-phosphate and REE-phosphate phases. Minerals with an enormous range in morphology and chemistry develop, the average size of which is <5μm. This process involves the introduction of large quantities of REE (except Ce) from elsewhere in the weathering granite which are then fixed in phases which appear to be resistant to further alteration. The net effect of the mobilization and fixation of REE is enrichment, not fractionation, despite the fact that the phases which accommodate these elements fractionate them dramatically.

In the granites studied many minerals are replaced sequentially by transitional phases which provide temporary sites for elements which are subsequently released. Kaolin and oxides appear to be the final alteration products stable under the conditions which are encountered in the profile.

The chemical composition of weathered material is determined by the relative rates at which primary phases weather, and the extent to which elements released are retained in secondary phases. These relative weathering rates appear to remain constant, at least in the early stages of weathering. A comparison of calculated weathering rates for minerals in the three profiles indicates that calcic feldspar is rapidly destroyed, whereas K-feldspar is relatively resistant to weathering. However, significant differences in the relative weathering rates between the weathering profiles are indicated, possibly arising from differences in original mineralogy.

The extent to which individual components, particularly the trace elements, are hosted in the clay fraction varies dramatically. These elements appear to be strongly retained when vermiculite is a major component, and very weakly when kaolin is a major component of the assemblage.

If an element is immobile during weathering it must either be hosted in a phase which does not weather, or be completely retained by the alteration products. Results of this study indicate that no phase is clearly completely resistant to weathering, and that no element can be assumed to be retained in the clay fraction. Furthermore, it has been demonstrated that elements (such as the lanthanides) may migrate from one region of the profile to concentrate in another. Hence the abundance of components in the weathering profile must be seen as the result of a complex interaction of processes.

ACKNOWLEDGEMENTS

During the past two years there have been many people who have made available their expertise and time, and I am indebted to them all. Firstly I would like to thank my supervisor, Dr Tony Eggleton, whose guidance, assistance, and interest has been invaluable.

Secondly, there are many people who have provided technical assistance; I take this opportunity to thank them. From the Geology Department: Ross Cliff, Chris Foudoulis, Raudi Popovic, Henry Zapasnik, Ross Freeman, Liz Webber, Jack Wasik, Mary MacDougall; from the Research School of Chemistry: Peter Barlow; from the Scanning Electron Microscope Facility: John Preston and Roger Heady; from CSIRO Soils Division: John Hutka and CSIRO Division of Plant Industry: Celia Miller. Professor Brown translated some Russian text. The staff at IRU were involved with the production of plates in this thesis.

A third group of people who provided access to equipment, assistance, and results, includes Dr Bruce Chappell (chemical analyses), Nick Ware (microprobe data), Dr John Fitzgerald (TEM), Dr Alan Chivas (isotope results), Dr Pat Walker (particle size analysis), Mr Jim Beatty (CEC results). The facilities of the Research School of Chemistry were made available by Prof. Hyde, and of the Geology Department by Prof. Campbell. The help of all these people is gratefully acknowledged. I express particular thanks to Dr David Goodchild who encouraged me to use the analytical TEM and STEM belonging to CSIRO, and showed me how to operate this equipment.

Numerous people at conferences, from the university, and CSIRO provided advice, information and discussion on many topics. Although it is not possible to name all of these people, thanks are extended to them. In particular, the contributions of Dr. Keith Norrish, Dr Colin Chartres, Prof. Steve Guggenheim, and Dane Varkevisser are noted. Similarly, fellow students, particularly: Richard Holmes, Wayne Sawka, Imants Kavalieris, Wang Qiming, Donal Windrim, Scott Haley, Clinton Holtzhauer, Brian Harrold participated in discussions and provided assistance.

Finally, I thank Peter for help with sampling, and Sally, Jim, and Perry for assistance with proof reading.

The research for this thesis was funded in part by ARGS grant E 8115611 R. I am grateful for the receipt of an ANU postgraduate scholarship.

TABLE OF CONTENTS:

PLATES

FIGURES

TABLES

Chapter 1

INTRODUCTION

Crystalline rocks formed within the crust are composed of an assemblage of minerals which, when exposed to conditions at the surface of the earth frequently become unstable, and begin to alter. Primary minerals within these rocks are replaced largely by an assemblage of clays, oxides, and hydroxides whose mineralogy and chemistry differs significantly from that of the unweathered material.

Through the interaction of chemical and mechanical weathering and the processes of erosion and transportation, the composition and nature of materials available for the development of sediments is determined. In turn, the composition of sediments is an important factor in determining the nature of the granite produced by partial melting of these rocks (Chappell and White, 1974). Weathering can therefore be seen as part of an important fractionation in the chemical evolution of the crust, and as such represents one of the only steps in this process which can be directly studied as it occurs. An application of some of the observations of the weathering process to an understanding of granite source regions has already been demonstrated (Sawka, Banfield, and Chappell; manuscript: Appendix 1). Furthermore, in its role in the development of surficial materials, the nature of the weathering process exerts an influence upon the quality and fertility of soil.

A considerable volume of literature has been devoted to the study of weathering. Many workers have examined the relative degree of weathering of individual minerals, the way in which the breakdown of these minerals occurs, and the phases which are produced. Considerable attention has also been focused upon determining the variation in chemistry and morphology of phases produced, and the dependence of the nature of these assemblages upon aspects of the environment. Many other studies have been directed toward elucidating the geochemical characteristics of the bulk changes within weathering profiles. Almost

all of these studies have been largely dependent upon bulk chemical data, optical microscopy, mineral chemistry, XRD, and in some cases, Scanning Electron Microscopy (SEM). Other studies based upon experimental alteration of minerals have contributed both explanations for aspects of naturally observed processes, and provided mechanisms by which certain steps of weathering reactions may occur.

Aims

This thesis aims to contribute to an understanding of the details of a number of individual weathering reactions, and to examine the ways in which they control the distribution, and pathways of elements through the weathering process. To carry out this study emphasis has been placed upon the contribution which Transmission Electron Microscopy (TEM) (used in conjunction with Scanning Transmission Electron Microscopy (STEM) - Microanalysis) can make to determining the details of weathering reactions at the unit cell level. These techniques provide the means by which relatively small volumes of material can be chemically analysed, and allows the recognition of phases by their cell dimensions in images, and by their diffraction patterns. An important aspect of this work has been the use of ion-beam thinned samples as well as grain-crushed samples.

In this study of granite weathering, three profiles have been examined. Every aspect of these profiles will not be discussed in detail. Rather, these profiles have been used to provide a range of minerals, (and mineral assemblages) for the study of weathering reactions, as well as to allow comparisons to be made. It is hoped that observations from one profile can be considered to be more generally applicable if similar processes can be observed in other profiles.

Thesis structure

The nature of the three granites, and the details of the weathering profiles developed upon them are discussed in Chapter 3. The central portion of this thesis is then devoted to the investigation of the way in which primary minerals weather, and the sequential development of secondary phases which occurs as the rock becomes increasingly exposed to the surficial environment. Metamorphically derived phases are also identified in the granite which have been produced by a greenschist facies episode of alteration. The form and distribution of these phases

is considered briefly to allow a distinction between these minerals and those produced by weathering. The weathering reactions of some of these alteration products are also described.

The bulk geochemical trends for the three profiles are discussed in Chapter 8. The behavior of individual elements is interpreted in light of the mineralogical pathways which have been recognised. The general conclusions to this study are then presented in the final section of this thesis.

Chapter 2

INSTRUMENTATION AND EXPERIMENTAL TECHNIQUES

The initial investigation of weathering was directed toward a general understanding of the nature of phases replacing the primary minerals. This was undertaken by disaggregating the granite or saprolite in a mortar and pestle and sieving so that the material passed through a 2mm sieve. This ensured that the majority of the minerals were present as isolated crystals. Crystals of individual minerals were handpicked under a binocular microscope, washed in water, crushed, and deposited on glass slides as oriented mounts for XRD. Samples were X-rayed using a Philips 1010 generator and Philips goniometer, using Co radiation and a graphite monochromator. The equipment was operated at 40kV and 20mA.

Samples of the bulk clay fraction from weathered material were also obtained, and X-rayed using the above equipment. These samples were prepared at the CSIRO Division of Soils with the assistance of Dr P. Walker and Mr J. Hutka. The percent clay in individual samples, and the size distribution of this clay were also determined, and samples of clay were extracted for major and trace element analysis, and for CEC measurements (CEC determinations by J. Beatty, CSIRO Soils Divisions). The method used for the clay extractions and the particle size analysis is given in Appendix 3.

Handpicked minerals were washed, split, and mounted on aluminium or carbon stubs, coated with either gold or carbon, and examined in a Cambridge Stereoscan 180 scanning electron microscope operated at 30kV. This microscope, which is located in the Forestry Department, ANU, is fitted with an energy dispersive* detector and provided qualitative chemical analyses for parent phases and clays. For the study of etching, samples were prepared by mounting grains which had been ultrasonically cleaned for 40 minutes, washed, and dried at 105°C (by-products of the particle size analysis).

* x-ray

The transmission electron microscope (TEM) study of alteration involved the use of both grain mount and ion-beam thinned samples. Grain mount samples were prepared by crushing handpicked phases in a mortar and pestle, dispersing the powder in alcohol, and placing drops of the suspension onto three millimetre, 400 mesh holey carbon grids. Ion-beam thinned samples were prepared from thin sections which had been mounted on crystal bond. Two and three millimetre Cu grids were stuck over selected minerals using an epoxy resin. By cutting around grids and heating the sections to about 90°C, thin slices of rock could be removed. These samples were then placed in one of three ion beam thinners available. Ar gas atoms were fired at 22° to the sample from two opposing guns after the ions had been accelerated across a high voltage (4-5kV) in a vacuum of about 10^{-4} torr.

The majority of the images and diffraction patterns presented in this thesis were obtained using the JEOL 100CX transmission electron microscope with a side entry double tilt goniometer operating at 100kV which belongs to the Research School of Chemistry, ANU. Some micrographs were obtained from the 200kV JEOL 200B TEM (operated largely by Dr J. Fitzgerald), which belongs to the Research School of Earth Sciences, ANU. Some electron micrographs presented in Chapter 5 were obtained using the RSC 200CX JEOL TEM which is fitted with an ultra high resolution top entry goniometer stage.

Qualitative chemical analyses for very small regions, generally of ion beam thinned samples were obtained using a JEOL 100CX TEM fitted with an energy dispersive detector (with a hard X-ray suppressor in the column), and a scanning - transmission imaging system. Analytical data were obtained from the margins of ion-beam thinned samples placed in the column at, or near the eucentric position. As it was critical that the exact nature of the phases analysed was known at all times, only material which could be clearly imaged in the STEM could be examined. This implies that the requirement for constant thickness of sample probed was approximately met. Spectra produced by this system were characterised by very low background to peak ratio, and only small Cu peaks from the grid and instrumentation. Contamination marks produced during analysis were 500-1000 Å in diameter. This appeared to represent the size of the area from which analyses were obtained, as complete separations in the compositions of phases were obtained over comparable distances.

Spectral data produced by this system were recorded as total counts in each peak, and in appropriate sections of the background. After subtraction of background counts, peak data for each element was ratiod to the Si peak. By comparison with peak ratios for phases with known chemistry (such as K-feldspar, biotite, and amphibole) an estimate of the molecular proportions of the components in an unknown phase could be obtained.

Quantitative determinations of mineral chemistry, the range in composition exhibited by plagioclase feldspar, and the nature of accessory and replacement phases were made on an energy dispersive Technisch Physich Dienst (TPD) electron microprobe at the RSES. Semi-quantitative determinations of the compositions of very small volumes of phases replacing apatite were made with the assistance of Mr N. Ware (RSES) who calibrated the wavelength dispersive CAMECA microprobe (belonging to the RSES) specifically for measurement of lanthanide and trace element abundances in these phases.

The chemical composition of samples of fresh and weathered rock, and of the clay fractions associated with these samples were determined by Dr B. Chappell (Geology, ANU) using XRF analysis. Wet chemical analysis was also performed to determine the abundance of some components. Neutron activation analysis was employed to determine the abundance of certain elements, primarily the lanthanides, in a range of samples of weathered rock, clay and mineral separates. Neutron activation results* were also obtained by Dr B. Chappell.

* | see amendments: p 230

Chapter 3

PROFILE DATA AND ENVIRONMENT

THE PROFILES

The mineralogical and chemical changes which occur in three weathering profiles are examined in this thesis. Profiles have been studied from fresh rock through until original texture is just retained, and before soil forming processes commence.

Two of the profiles are developed in I-type granite, the third is in S-type granite.* All of the profiles are exposed in road cuttings in southeastern New South Wales. The first two profiles formed by the weathering of the I-type Bemboka granodiorite, and the Island Bend adamellite; the S-type Bullenbalong granodiorite is the host for the third profile.

The Bemboka profile is located on the Snowy Mountains highway between Nimitabel and Bemboka. The site selected was at the base of a south-facing cutting at the top of Brown Mountain (GR 148 445), (Plate 3.1a).

Samples from the Bullenbalong profile (Plate 3.1b) were obtained from the middle of a cutting on the approach road to Lake Jindabyne, and the Jindabyne township (GR 472 691). This is referred to as the Jindabyne profile in this thesis.

The Island Bend profile is located in the Snowy Mountains on the approach to the Island Bend Pondage (GR 790 328). The samples were collected from fairly high in the cutting on the northern side of the divided road (Plate 3.1c). All of the three profiles studied are located between 36.3 - 36.6°S of the equator, and between the longitudes of 148.5 and 149.5°E (Figure 3.1).

The granitic rocks from which the weathering profiles have

* see amendments: p 230

PLATE 3.1A: The Bemboka Profile

PLATE 3.1Bi: The Jindabyne Profile

PLATE 3.1Bii: The Jindabyne Profile, distant view.

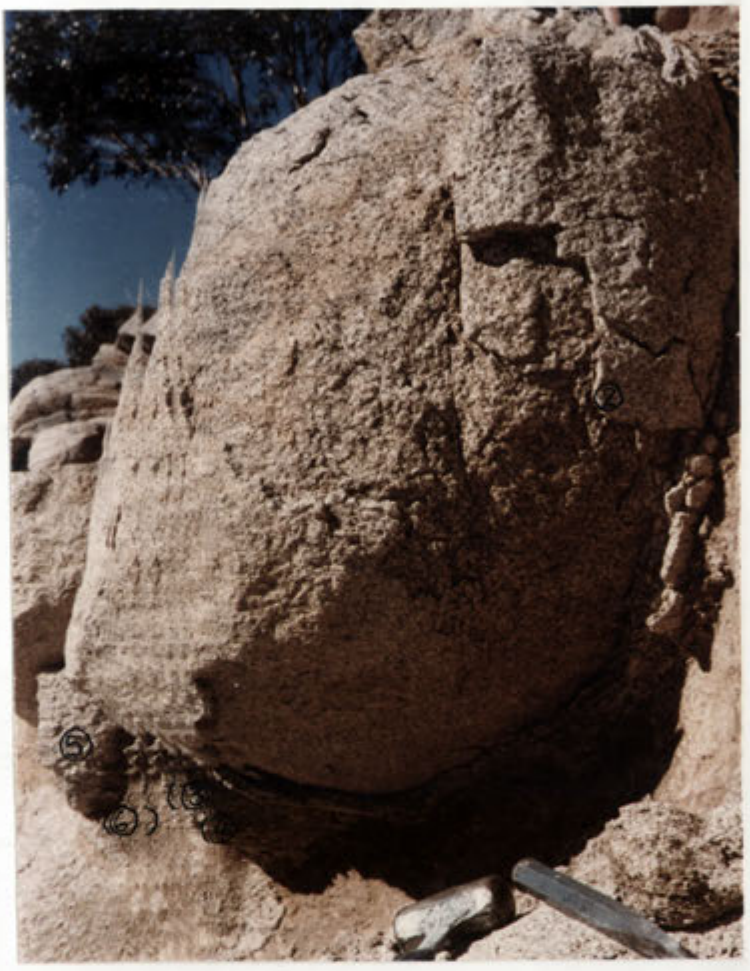

PLATE 3.11c: The Island Bend Profile.

FIGURE 3.1: LOCATION MAP

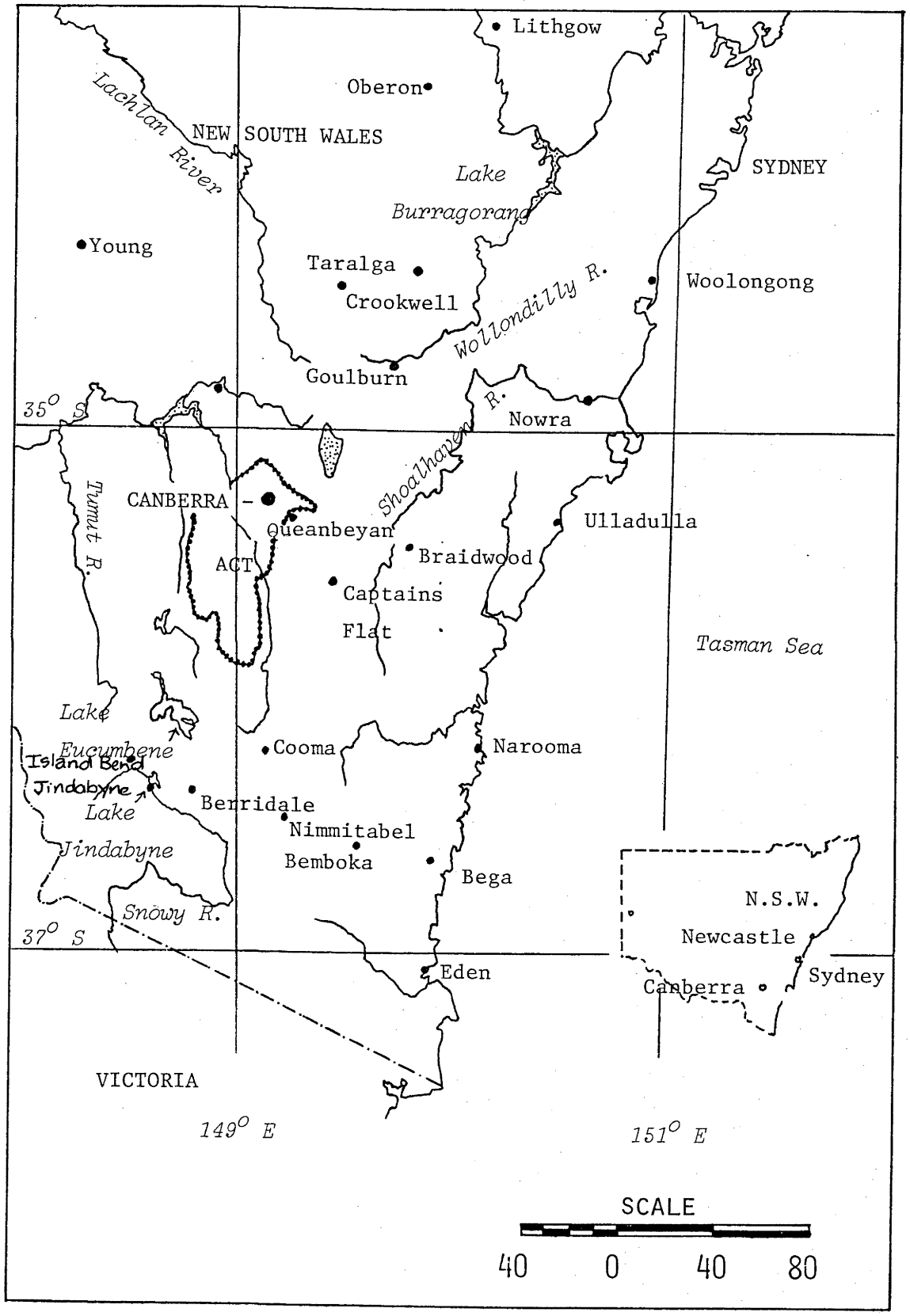

developed have been studied by a number of authors who discuss their mineralogy, chemistry, and origin. The Bemboka granodiorite has been described by Beams (1980), the Bullenbalong granodiorite by White et. al. (1977), and the Island Bend adamellite by Hine et. al. (1978).

SAMPLING

Several kilograms of material were obtained for each of the samples collected for chemical analysis, and separation of clays and primary minerals. Two series of chemical analyses have been combined for two of the three profiles. Analyses prefixed 'R' in Chapter 8 for the Island Bend and Bemboka profiles were collected by R.A.E. before this study commenced. All TEM, SEM, clay extraction etc. was carried out on the second series of samples collected by the author. The second series of samples for the Island Bend and Bemboka profiles were obtained from the same locations as the first. This second series contains three sets of six samples for the profiles which are labelled from 1 representing fresh material, to 6, representing strongly weathered material. Samples were generally collected outward from a less altered granite core, and hence their numbers reflect the relative distance from fresh rock. The correlation between these sample numbers and the analytical numbers is given in Table 3.1. This table also lists the clay and mineral separates which have been analysed, and the samples from which they were extracted.

PROFILE DATA: WEATHERING INDEXES

The samples were arranged into a sequence based on the appearance, particularly the colour and texture of the weathered granite (Plate 3.2). Other properties and characteristics of the profile which also reflect the extent of alteration include density, clay content, water content of samples etc. These data are listed in Table 3.2 The method used to determine the abundance of material in each size fraction is described in Appendix 3. The 'powderability' of material in Table 3.2 reflects the abundance of material measured to be in the 31.2 - 2μm size range after samples were crushed so all material passed through a 2mm sieve.

WEATHERING ENVIRONMENT

The climatic conditions under which current weathering is occurring

PLATE 3.2

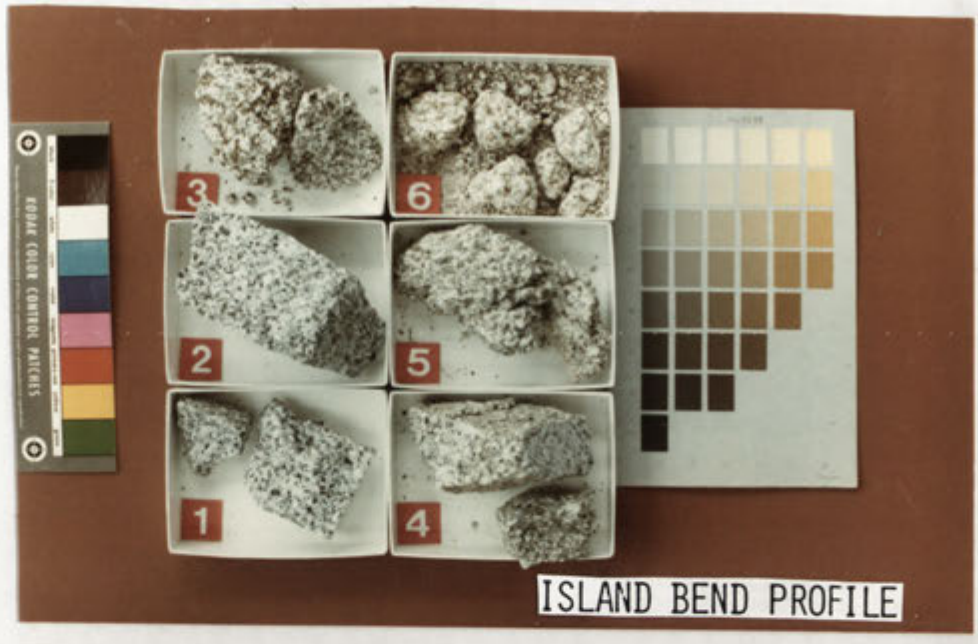
KODAK COLOR CONTROL PATCHES
3
6
2
5
1
4
ISLAND BEND PROFILE

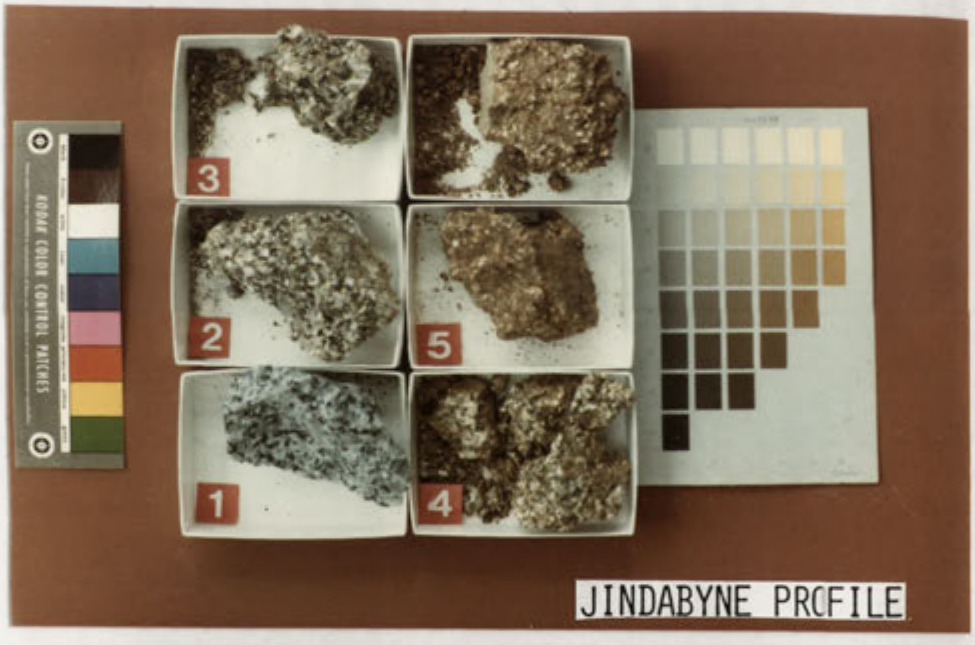
KODAK COLOR CONTROL PATCHES
3
2
5
1
4
JINDABYNE PROFILE


KODAK COLOR CONTROL PATCHES
3
6
2
5
1
4
BEMBOKA PROFILE

TABLE 3.1

	ANALYTICAL SAMPLE NMBER	PROFILE SAMPLE NUMBER	
ANU ROCK NUMBER	47451 JFB 1	IB 1	ISLAND BEND PROFILE
"	47452 JFB 2	IB 2	
"	47453 JFB 3	IB 3	
"	47454 JFB 4	IB 4	
"	47455 JFB 5	IB 5	
"	47456 JFB 6	IB 6	
"	47457 JFB 7	JIN 1	JINDABYNE PROFILE
"	47458 JFB 8	JIN 2	
"	47459 JFB 9	JIN 3	
"	47460 JFB 10	JIN 4	
"	47461 JFB 11	JIN 5	
"	47462 JFB 12	JIN 6	
"	47463 JFB 13	BEM 1	BEMBOKA PROFILE
"	47464 JFB 14	BEM 2	
"	47465 JFB 15	BEM 3	
"	47466 JFB 16	BEM 4	
"	47467 JFB 17	BEM 5	
"	47468 JFB 18	BEM 6	

JFB 19 - CLAY FROM IB 6

JFB 20 - CLAY FROM JIN 6

JFB 21 - CLAY FROM JIN 5

JFB 22 - CLAY FROM BEM 6

JFB 23 - CLAY FROM BEM 5

JFB 24 - CLAY FROM BEM 4

JFB 25 ..... BIOTITE EXTRACTED FROM BEM 1

JFB 26 ..... BIOTITE EXTRACTED FROM BEM 4

R.A.E. SAMPLES

RAE 22 - RAE 28 ..... ISLAND BEND PROFILE

RAE 1 - RAE 9 ..... BEMBOKA PROFILE

TABLE 3.2:

SAMPLE NUMBER	% 2um CLAY	% .24um CLAY	DENSITY	POWDERABILITY	FeO/ tot. FeO*	H_2O^+ %
IB 1	--	--	2.56	↓	.57	1.14
IB 2	--	--	2.62		.53	1.14
IB 3	2.01	0.94	2.51		.44	1.32
IB 4	1.73	0.19	2.40		.39	1.49
IB 5	3.45	0.39	2.39		.28	2.00
IB 6	14.87	4.83	1.60		.13	4.97
JIN 1	--	--	2.73	↓	.92	1.31
JIN 3	3.76	1.62	2.61		.76	1.46
JIN 2	--	--	2.55		.66	1.52
JIN 4	11.56	4.44	2.35		.17	2.14
JIN 6	12.21	5.01	2.30		.11	2.49
JIN 5	18.75	7.31	2.18		.07	2.93
BEM 1	--	--	2.71	↓	.75	.93
BEM 2	--	--	2.61		.66	1.27
BEM 3	5.62	1.92	2.36		.45	3.19
BEM 4	9.31	3.12	2.46		.42	3.38
BEM 5	14.43	4.69	1.93		.34	4.27
BEM 6	17.23	5.05	1.83		.11	4.41

RESULTS FOR CATION EXCHANGE CAPACITY MEASUREMENTS OBTAINED BY Mr J. BEATTY (CSIRO DIVISION OF SOILS)

SAMPLE	Ca ml%	Mg ml%	Na ml%	K ml%	CEC meq/100gm
BEM 5	0.00	0.03	25.2	0.35	27.2
BEM 6	0.00	0.08	23.2	0.23	26.0
JIN 5 + 6	0.80	0.29	27.0	0.86	31.2
IB 6	0.00	0.06	18.8	0.61	20.0

Results obtained for clays extracted using a Na dispersing agent.

* total FeO expressed as FeO

vary to some extent, but could be broadly described as temperate to sub-alpine. All profiles have developed under fairly sparse eucalypt forest. Although the age of weathering profiles is not known, it is probable that a considerable proportion of their evolution occurred under climatic conditions which differed from those observable today.* Available information about Quaternary and Holocene climate change in southeastern Australia has been summarised by McConnell (1979). The data is presented in Table 3.3 (From Hough, 1982). Hough (1982) notes that Walker and Coventry (1976) have suggested that although the change in climate in the non-alpine areas during the last 30,000 years may have modified the rate of soil weathering and leaching, it has not been sufficient to alter the general direction of pedogenesis.

*

OXYGEN ISOTOPE DATA

Oxygen isotope data was obtained for separates of minerals from the Bemboka profile. Eight quite pure samples of minerals extracted from the fresh rock: quartz, biotite, plagioclase feldspar, K-feldspar, amphibole, magnetite, epidote, and chlorite, and a sample of clay (fairly pure halloysite extracted from Bemboka 4 using heavy liquid) were submitted to Dr Allan Chivas (RSES) for oxygen isotope analysis. Results are listed in Table 3.4.

Oxygen isotope data have been employed to determine the temperatures of formation of various phases in the Bemboka granite. As noted by Faure (1977), the use of isotope geothermometers is based on three assumptions, 1. that exchange reactions reached isotopic equilibrium, 2. that isotopic compositions were not subsequently altered, and 3. that the temperature dependence of fractionation factors is known from experimental determinations. If these assumptions can be made, the difference in the $\delta\ ^{18}O$ values of two minerals depends upon the final temperature of equilibration of that rock. Concordance of temperatures for isotopically equilibrated assemblages of minerals must be demonstrated. Results for equilibration temperatures of the primary granitic minerals from Bemboka 1 are listed in Table 3.5. Temperatures were determined using equations of O'Neil and Taylor (1969, (1)); Bottinga and Javoy (1973, (2); 1975, (3)); Anderson et. al. (1971, (4)); and Shieh & Schwarcz (1974, (5)).

Results in Table 3.5 indicate that plagioclase, quartz, magnetite,

* see amendments: p 230

Table 3.3 Summary of Holocene and Quaternary climatic changes, from McConnell (1979).

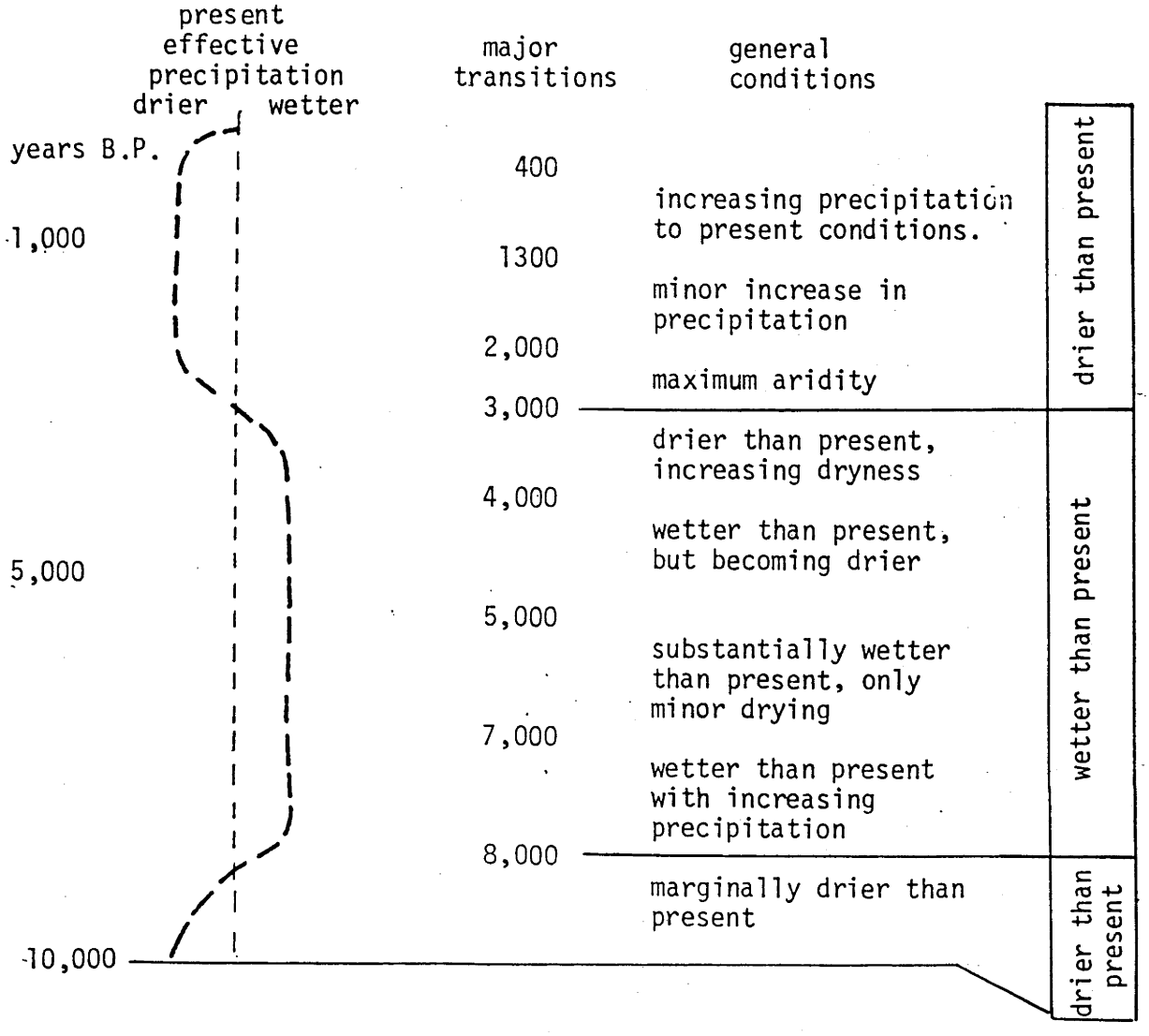

stage (year B.P.)	climatic conditions
10,000-22,000 24,000	lowest effective precipitation recorded - associated phase of major aridity
22,000-26,000 24,000	higher effective precipitation than at present
26,000-30,000	slightly lower effective precipitation than at present.
30,000-40,000	higher effective precipitation than at present, associated lake full period.
40,000-50,000	lower effective precipitation than at present.

TAKEN FROM HOUGH, 1982; p 14.

TABLE 3.4

MINERAL	$\delta^{18}O_{SMOW}$	D_{SMOW}
QUARTZ	9.0	
K-FELDSPAR	7.1	
PLAGIOCLASE	7.1	
AMPHIBOLE	5.2	
BIOTITE	2.6	
MAGNETITE	1.4	
CHLORITE	4.0	
EPIDOTE	3.8	
CLAY (HALLOYSITE)	16.0	-73

PRIMARY MINERALS AND SECONDARY PHASES (CHLORITE AND EPIDOTE) EXTRACTED FROM BEMBOKA 1. CLAY EXTRACTED FROM BEMBOKA 4 USING HEAVY LIQUIDS, AND IDENTIFIED AS HALLOYSITE USING XRD. (see below).

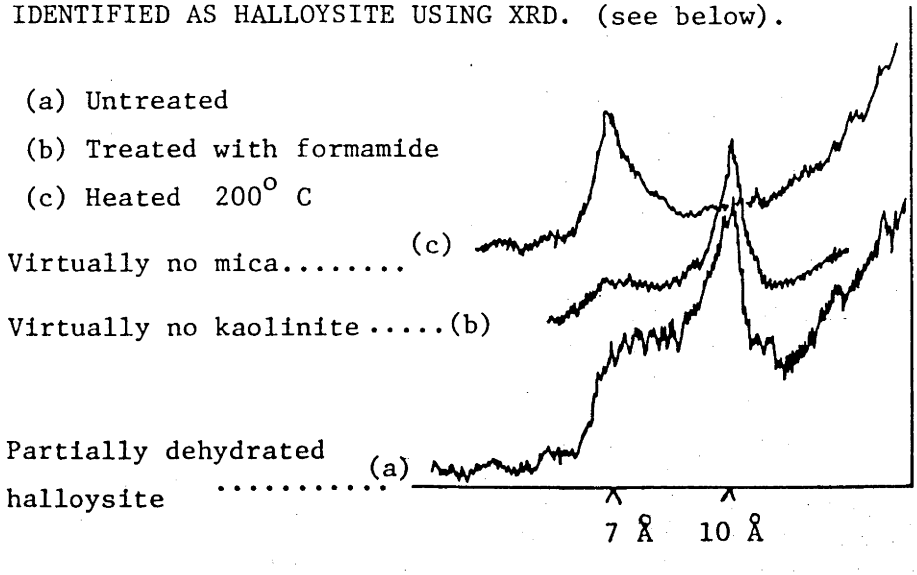

TABLE 3.5

CALCULATION OF RESULTS FOR TEMPERATURES OF EQUILIBRATION OF THE PRIMARY MINERALS

QUARTZ - MAGNETITE	583° C	(2,3)
PLAGIOCLASE - AMPHIBOLE	635° C	(3)
QUARTZ - PLAGIOCLASE	564° C	(2,3)
PLAGIOCLASE - BIOTITE	407° C	(3)
QUARTZ - BIOTITE	404° C	(5)
PLAGIOCLASE - MAGNETITE	590° C	(2,3)
	596° C	(4)
K-FELDSPAR - MAGNETITE	627° C	(1,2)
K-FELDSPAR - QUARTZ	464° C	(2)

(1) O'Neil and Taylor (1969)

(2) Bottinga and Javoy (1973)

(3) Bottinga and Javoy (1975)

(4) Anderson et. al. (1971)

(5) Shieh and Schwarcz (1974)

and K-feldspar equilibrated at approximately 590°C, or 863°K. This observation can be used to calculate the composition of the water which was present when they equilibrated (using mineral-water equations of the above authors). Results for the δ values of water were calculated for K-feldspar to be 6.6; for plagioclase 7.09; for quartz 7.19; and for magnetite 7.07. As illustrated in Figure 3.2a (from O'Neil & Silberman, 1974) these results are consistent with the composition of magmatic water.

In contrast, equilibrium temperatures derived for biotite are considerably lower (404°C , 407°C). This indicates that biotite recrystallized, possibly during the metamorphic episode when chlorite and epidote formed.

Isotope data was also obtained by Dr Chivas (RSES), for a clay sample. The isotopic composition of clay minerals is dependent upon 1. the water present when the clay formed, 2. the isotopic fractionation factors for O and H for clay-water, the approach to equilibrium, and the temperature of the environment (Faure, 1977). Taylor (1974) notes that clay rich soils lie close to the kaolinite line, whereas hydrothermal clay minerals plot closer to the meteoric water line. Hence it is possible to distinguish hypogene for supergene clays equilibrated at surface temperatures. Results for the determinations of δ O and δ H are listed in Table 3.4, and are plotted in Figure 3.2b (from Faure, 1977). The results plot close to the kaolinite line, confirming a low temperature origin for the clay products.

The composition of the water in equilibrium with the clay (at 25°C or 298°K can be determined from the equation for kaolinite-water fractionation of Kulla & Anderson (1978). The result of -3.23 for water is plotted in Figure 3.3 (from Lawrence and Taylor, 1971). On the meteoric water line this corresponds to a point which would seem to indicate that weathering to produce this clay proceeded under conditions which were slightly warmer than those currently experienced in the area.

An isotopic composition can also be derived for water in equilibrium with biotite. The value of -2.31 lies much closer to the meteoric water line than the value for magmatic water. This is consistent with the prediction of Taylor (1974) that phases which formed under metamorphic conditions will be associated with δ values which

FIGURE 3.2A

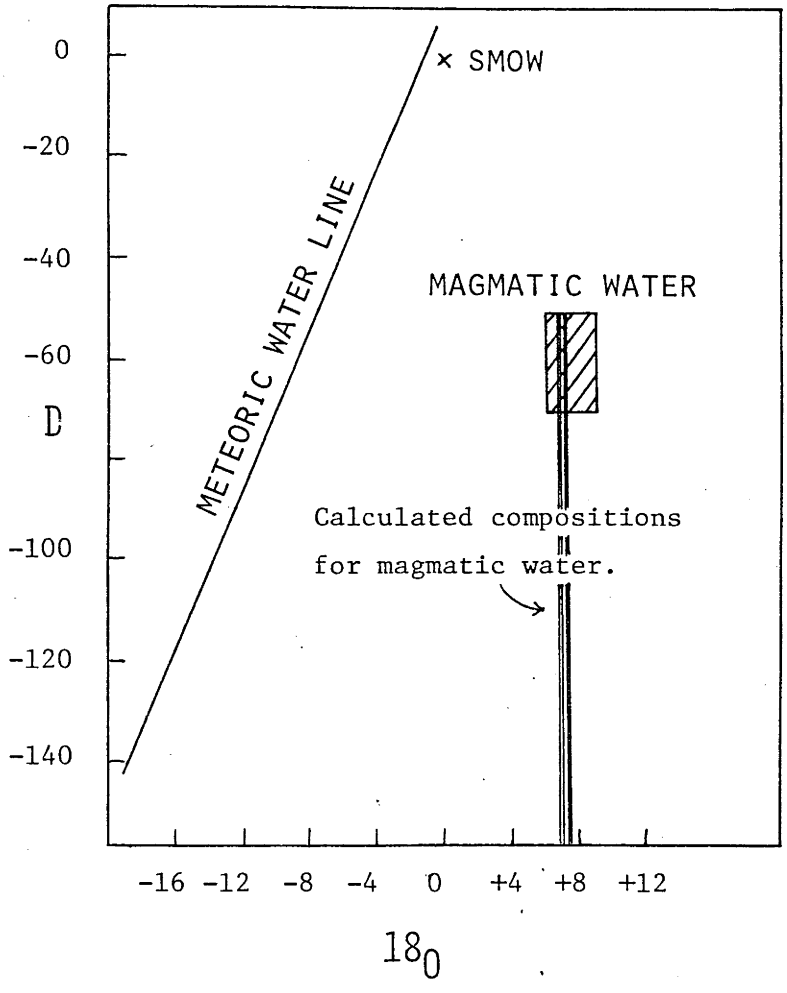

From O'Neil and Silberman, 1974.

FIGURE 3.2B

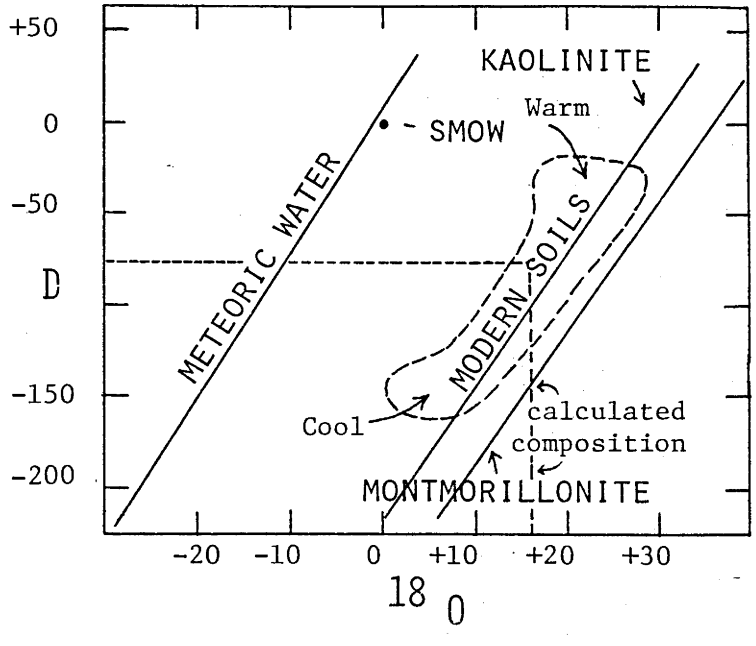

The relationships between D and ^{18}O of clay minerals at Earth-surface temperatures.

From Faure, 1977; Fig. 19.7

FIGURE 3.3

-Taken from Lawrence and Taylor, 1971 for Quaternary soils, USA.

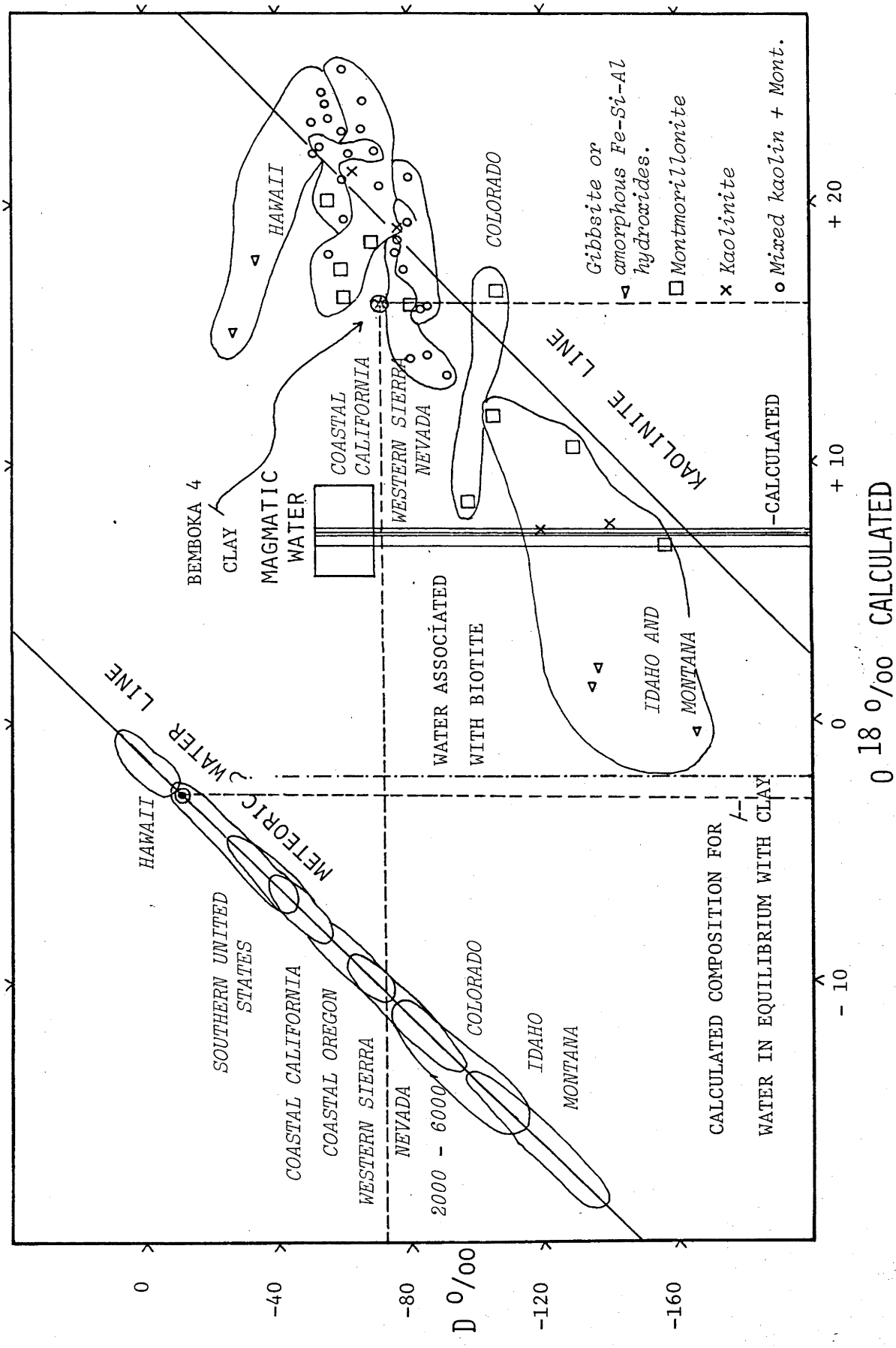

approach the meteoric water line as temperatures of equilibration increase. This result, and those for the magmatic water are plotted with data for the clay in Figure 3.3, summarising these data.

Although isotopic results were also obtained for chlorite and epidote, there is insufficient data in the literature to provide clear indications of the temperature of formation of these phases. For chlorite, comparative results of δ values of 5.3 (Hoefs and Binns, 1978), and 4.7, 4.9 (Hiroji & Honma, 1978) are available. The measured value of 4.0 for Bemboka chlorite can be plotted onto the empirical curve of Taylor (1979) to generate a temperature of ~150°C (Figure 3.4). This result is probably meaningless, due to the poorly understood variation of isotopic composition with temperature, and the variation in the isotopic fractionation associated with changes in the composition of chlorite.

Conclusions from isotopic results.

Isotopic data would appear to be consistent with an interpretation of the mineral assemblage based upon the formation of magnetite, quartz, and the feldspars at magmatic temperatures, and equilibration finally at about 600°C with magmatic water. Subsequently, magmatic biotite recrystallized at intermediate temperatures. Chlorite and epidote were probably formed during this episode, although empirical curves indicate a significantly lower final temperature of equilibration. The clay sample is associated with δ values for O and H which are consistent with formation of alteration products at surface temperatures.

FIGURE 3.4

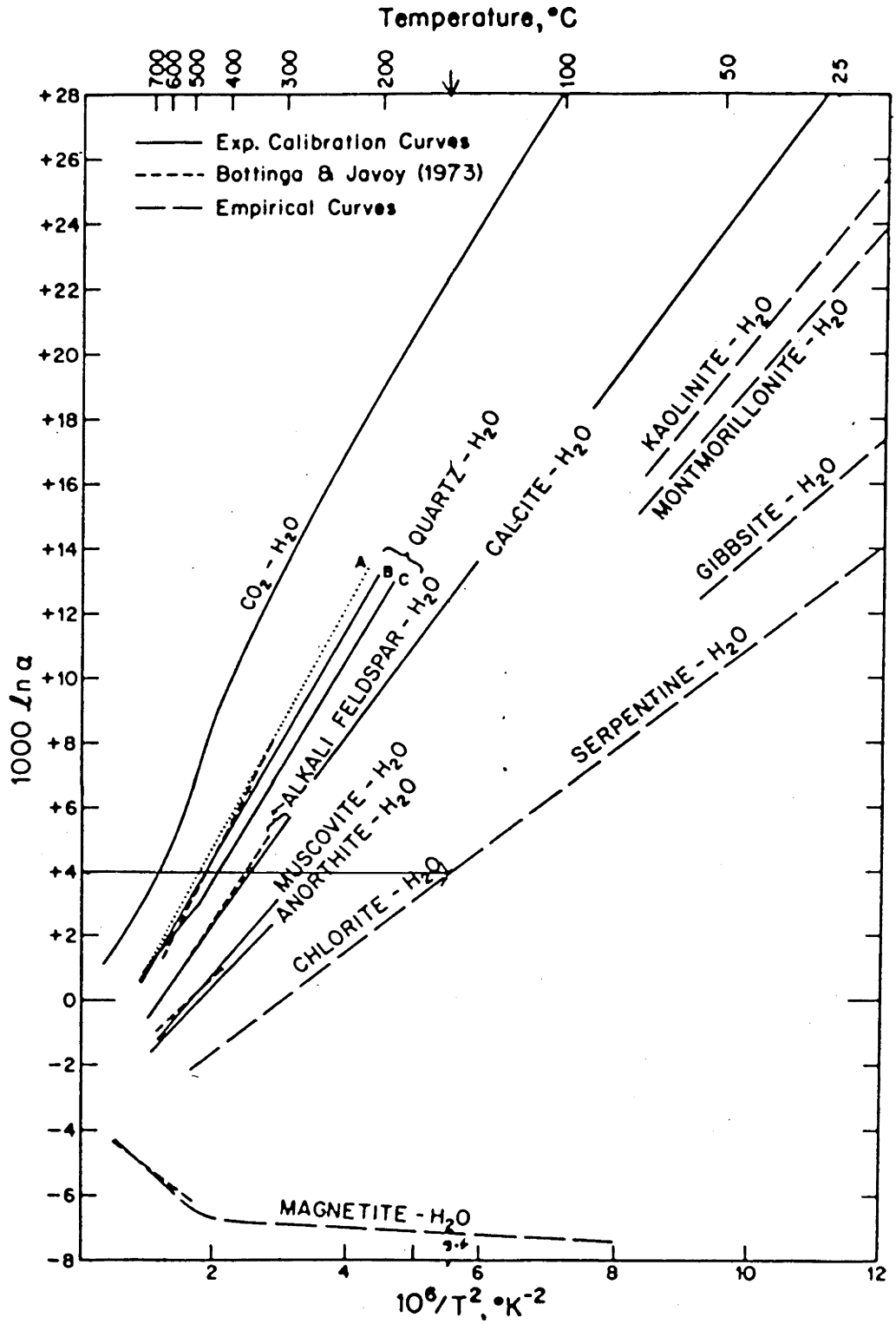

Experimentally determined equilibrium oxygen isotope fractionation curves for various mineral water systems.

From Taylor, 1979; Figure 6.1.

Chapter 4

THE WEATHERING OF GRANITIC FELDSPAR

ABSTRACT

Alteration of plagioclase and included K-mica laths occurs via a number of stages. Plagioclase weathers firstly to an apparently amorphous material and then to smectite with a Ca, Fe, K-montmorillonite composition. This phase is transitional, and is converted to an amorphous component which recrystallizes to form spherical halloysite. Tubular halloysite is also an abundant alteration product. Tubes generally grow outward (possibly via solution) from the corroded feldspar surface into cavities formed by dissolution, and then recrystallize to form kaolin. Well formed muscovite laths within plagioclase are converted to illite by loss of K. Illite is altered then to randomly interstratified illite-smectite, and subsequently smectite. This muscovite derived smectite differs from that produced by direct alteration of plagioclase in that it is more aluminous, contains Mg, is less Fe rich, contains little K, and virtually no Ca. This difference in smectite chemistry reflects both the parent composition, and selective addition of externally derived elements. Smectite is converted to spherical halloysite via an amorphous stage, or is replaced epitactically by kaolin.

K-feldspar is markedly more resistant to weathering than plagioclase. After a protracted initial stage of etching, larger scale alteration commences with the conversion of feldspar to an amorphous component along an irregular front. This material contains abundant, but variable quantities of introduced Fe. The smectite produced by recrystallization of this material is quite aluminous, and contains considerably less Fe than its amorphous precursor. Excess Fe may concentrate in the amorphous phase until goethite crystallizes. The presence of Fe in the alteration products is not understood. Fe may simply be scavenged by the amorphous phase or may actively participate in the breakdown of K-feldspar or recrystallization of clays. Spherical

halloysite is also observed to crystallize from an amorphous precursor, possibly derived from smectite. Kaolinite also forms crinkly films in cracks and channels where access to solution is greater, and as irregular laths, possibly by replacement of smectite.

In the weathering of both plagioclase and K-feldspar the sequential development of amorphous material, smectite and kaolin is associated with the stepwise increase in the Al:Si ratio, and removal of excess octahedral, and interlayer cations. Recrystallization of halloysite is occasionally observed suggesting that kaolinite is the stable weathering product of feldspars in this environment.

SECTION 4.1

PREVIOUS WORK

Members of the feldspar group are the most abundant constituents of igneous rocks, and their weathering products form major components of sediments and soils. Consequently the alteration of these phases has received considerable attention. Numerous studies have been published which discuss the mechanisms by which the feldspar structure is broken down, and document the assemblages of secondary phases which develop in response to a range of environmental conditions. Topics such as the nature of the feldspar surface during alteration and the morphology of alteration products (especially halloysite) have also received considerable attention. Some of this literature is based on experimental studies; reactions are discussed for temperatures ranging up to about 200°C.

Low temperature hydrothermal alteration:

Studies of natural rocks indicate that assemblages of secondary minerals produced by hydrothermal alteration resemble those produced by weathering. For example, Exley (1976) examined granitic feldspars and found that K-feldspar was replaced by a micaceous mineral and montmorillonite which were intermediate between plagioclase and kaolinite. Meunier and Velde (1982) examined a low temperature metasomatised granite and found that the feldspars were replaced by potassic beidellite, (and later Ca-montmorillonite), kaolinite, and Al-illite. Muscovite was replaced by ferrous-magnesian phengite. These authors note that the alteration assemblage is temperature dependent, micas appearing at intermediate temperatures, and smectite at low temperatures.

Products of feldspar weathering:

A number of minerals are reported to be produced by weathering of feldspar, including amorphous material, smectite, mica, kaolin minerals (including halloysite), and gibbsite. Various combinations of these phases have been recognised; feldspar has been observed to alter to an amorphous phase (Eswaran and Bin, 1978; Rimsaite, 1978; Eggleton and Buseck,1980); K-feldspar to illite-muscovite (Eggleton and Buseck, 1980); to kaolin and illite (for K-feldspar: Field, manuscript;

Loughnan, 1969); to smectite (Wilson et. al., 1971; Proust and Velde, 1978- with an aluminous intergrade precursor); to an amorphous phase and smectite (Guilbert and Sloane, 1968); to kaolin and smectite (Field, manuscript; Loughnan, 1969); smectite, kaolin and gibbsite (Tardy et. al., 1973; Carroll, 1970); kaolin and gibbsite (Anand et. al., manuscript); kaolin including a number of forms of halloysite (Keller, 1978; Hughes and Brown, 1977; Wilke et. al., 1978); and to gibbsite (Lodding, 1972; Praham, 1969).

It has been noted by several of these authors that alteration products develop sequentially, with smectites developing early under conditions of mild leaching or under semi-arid conditions. This phase is replaced primarily by kaolin under conditions of greater leaching (Carroll, 1970; Loughnan, 1969; Tardy et. al., 1973). Gibbsite apparently develops as a result of more extreme degrees of weathering. This sequence can be predicted on thermodynamic grounds by examination of phase diagrams such as those produced by Feth et. al.(1964), Helgeson (1971), and Garrels (1984).

The mechanisms of feldspar breakdown:

The concept that feldspars dissolve incongruently (Correns and Von Engelhardt, 1938; Correns, 1940 and 1963; Keller et. al., 1963; Marshall and Mc Dowell, 1965; Reesman and Keller, 1965; Huang and Keller, 1970) led to the hypothesis that a protective residual surface layer developed on the altered feldspar, and that reactions were controlled by diffusion through this zone. This formed the basis for many models of feldspar alteration advanced over the last half century.

As noted by Aagaard and Helgeson (1982), the work of many authors supports the view that precipitation of a surface layer of reaction products is consistent with the incongruent nature of silicate hydrolysis. The presence of such a diffusion limiting layer has never been demonstrated. Petrovic (1976) concluded that the precipitates formed by aqueous dissolution of feldspar could not control the rate of feldspar dissolution. Petrovic et. al. (1976) demonstrated using XPS that a continuous precipitate layer does not develop on alkali feldspar. Similarly, Holdren and Berner (1979) used SEM and XPS to show that the clay which is present on feldspar surfaces is Al-rich, hydrous, patchy, and probably has a high permeability. These authors attributed non

linear kinetics observed at the beginning of most experiments to rapid dissolution of hyperfine particles. They support the view first advanced by Lagache, Wyart, and Sabatier (1961) that weathering of feldspar is a surface controlled reaction. Some authors (eg. Velbel, 1983; Anand et. al., manuscript) argue on this basis that dissolution occurs congruently.

The rate at which silicates hydrolyse is controlled by the kinetics of reactions at activated sites where Al-O and Si-O bonds are disrupted, (Aagaard and Helgeson (1982). Many authors have argued that hydrogen is involved in the disruption of these bonds, and that this ion replaces K, Na, or Ca in the feldspar structure (Frederickson, 1951; Garrels and Howard, 1957; Marshall, 1962; Wollast, 1967).

Aagaard and Helgeson (1982) summarized the results of a number of studies which indicated that it is H_3O^+ and not H^+ which enters the exchange position. These authors noted the parallel between such models and models which propose that H_2O dissolution in silicate melts occurs by breaking bridging oxygens and formation of (OH) groups (eg. Burnham, 1975). Aagaard and Helgeson (1982), proposed that the hydronium ion plays the dominant role in forming a rate limiting complex with a stoichiometry of (H_3O) Al Si (H_3O^+). This complex corresponds to a localized surface configuration of atoms formed from the disrupted silicate network. A schematic representation of the formation of this complex as the result of the interaction of a hydronium ion with the surface of a feldspar crystal was presented by Aagaard and Helgeson (1982), and is reproduced in Figure 4.1. Their model involves the exchange of H_3O^+ for K^+, addition of an interstitial hydronium ion from solution which acts with the hydronium in the exchange position to break down the feldspar structure.

Gardner (1983) attributed the nonstoichiometric release of alkalis relative to Si to a two step mechanism for Si release, whereby exchange of H^+ for alkalis is followed by release of Al and Si. Aagaard and Helgeson (1982) suggested that this process is focused at the local surpluses of negative charge associated with the presence of tetrahedral Al. Finally, an activated complex is released from the feldspar surface; this is suggested by these authors to be the rate limiting step in the hydrolytic process (see Figure 4.1e)

FIGURE 4.1: BREAKDOWN OF K-FELDSPAR BY SOLUTION.

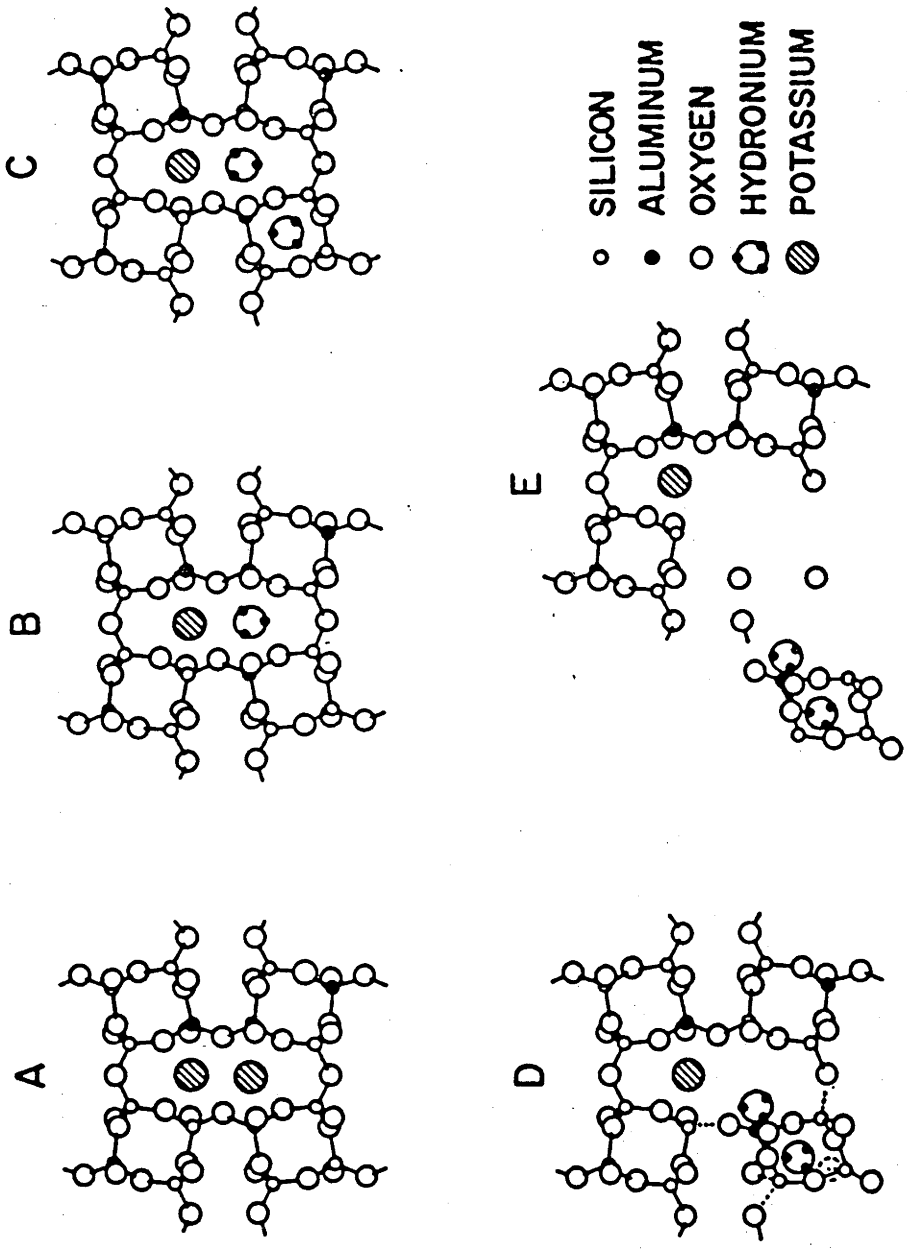

Fig. 1 Schematic representation of the formation of an activated complex corresponding in stoichiometry to $((H_2O)AlSi_2O_8(H_2O))^+$ on the surface of a K-feldspar grain reacting with an acid aqueous solution .

FROM AAGAARD AND HELGESON, 1982, PAGE 255.

Access of solution to the feldspar structure is probably controlled by the presence of defects, cleavages, twin planes, cracks, etc. Many workers have reported that dissolution proceeds by preferential attack at energetically favoured sites, commonly dislocations (eg. Berner and Holdren, 1977; Nixon, 1979). Studies of the surface textures of weathered minerals indicate that this results in the development of solution pits (Seifert, 1967; Greer, 1970; Lundstrom, 1970; Parham, 1969; Berner and Holdren, 1977).

The nature of the intermediate phase:

Anand et. al. (manuscript) notes that considerable uncertainty still exists as to whether secondary minerals crystallize from solution or develop from transient amorphous aluminosilicate intermediaries. These authors propose that crystallization of kaolinite, halloysite, and gibbsite occurs from solution within pits. Tzuki and Kawabe (1983) suggested that the dissolution reprecipitation mechanism may be responsible for the entire sequence from feldspar to kaolin, including polymorphic transformations of kaolin minerals. Keller (1978) stated that the most logical mechanism for production of kaolin minerals was via solution. Eswaran and Bin (1978) proposed that feldspar alters via solution to kaolin and gibbsite, but via an amorphous stage to halloysite. In contrast to the views noted above, Fieldes and Swindale (1954) stated that with the exception of micas, all primary silicates must pass through an amorphous stage in transition to secondary phases. Guilbert and Sloane (1968) proposed formation of montmorillonite from feldspar by the merging of allophane discoids, while Eggleton and Buseck (1980) described the crystallization of illite or montmorillonite from amorphous ring shaped structures 250 Å in diameter.

Synthesis of clay minerals

A number of workers have synthesized clay minerals (see Petrovic, 1976) by combining solutions and precipitating amorphous materials which on aging polymerize, dehydrate, and reorder. Petrovic (1976) suggested that the mechanism for this transformation is dissolution-reprecipitation.

Conclusions

The weathering of feldspar has been examined using both naturally

and experimentally weathered materials, and the process has been considered from a theoretical standpoint. An examination of the literature suggests that current thinking supports the views that:

1. A range of secondary products can occur in the alteration assemblage produced by feldspar weathering. Compositional variations in this assemblage have been attributed to differences in both the climate under which weathering occurs, and the extent of weathering.

2. Weathering is initiated at energetically favoured sites on the feldspar surface, such as dislocations.

3. The view that weathering results in the development of a protective, diffusion limiting surface layer which controls the breakdown of feldspar, has lost favour. Much of the literature supports the concept that weathering is surface controlled, focused at sites on the feldspar surface where reactivity is enhanced. Although some authors believe that dissolution occurs congruently, many argue that incongruent dissolution is associated with the formation of a narrow zone (<20 Å) of H-feldspar which is followed by release of Al and Si.

4. Any stable or metastable products formed during the incongruent dissolution of feldspar do not form a continuous and coherent surface layer on altered grains. Any coating which forms is patchy, and apparently hydrous, and therefore not diffusion limiting.

5. Most workers support the view that alteration of feldspar and conversion of secondary phases and polymorphs occurs via solution. The view that amorphous or semi-amorphous intermediate phases are involved in feldspar weathering was advanced largely by earlier workers and has generally not been supported in more recently published literature.

SECTION 4.2

WEATHERING OF PLAGIOCLASE, K-MICA, AND K-FELDSPAR

INTRODUCTION

The relative extent of K-feldspar and plagioclase feldspar alteration, and the distribution of secondary products within feldspar crystals can be determined using an optical microscope. Descriptions of thin sections from fresh through to strongly weathered granite are given in Appendix 2. Optical micrographs illustrating the nature of the hydrothermal alteration, and of strongly weathered material are presented in Plate 4.1.

This chapter commences with a discussion of plagioclase feldspar weathering based largely on electron microscope data. Hydrothermal alteration has resulted in the development within plagioclase of an assemblage of alteration products. The nature of these alteration products is examined briefly in Section 4.2.2, and the weathering of muscovite, is then considered in Section 4.2.3. This is followed by a description of the weathering of K-feldspar in Section 4.2.4. Section 4.3, discusses the general comments and conclusions which can be made from this study.

SECTION 4.2.1

PLAGIOCLASE FELDSPAR WEATHERING

.1: Initiation of Weathering

The weathering of plagioclase is commonly initiated at sites on dislocations (Plate 4.2a), and less commonly, on twin planes (Plate 4.2b) and cleavages. During the early stages of weathering dissolution is controlled strongly by crystallographic planes so that the resulting etches tend to resemble negative crystals, often with a prismatic form. TEM images illustrate that amorphous material can be observed in some of these etches. This phase appears to be transitory, and is replaced by clays with 11-15 $\mathring{A}$ basal spacings (Plate 4.3), or by spherical halloysite.

Alteration appears to accelerate once dissolution has improved

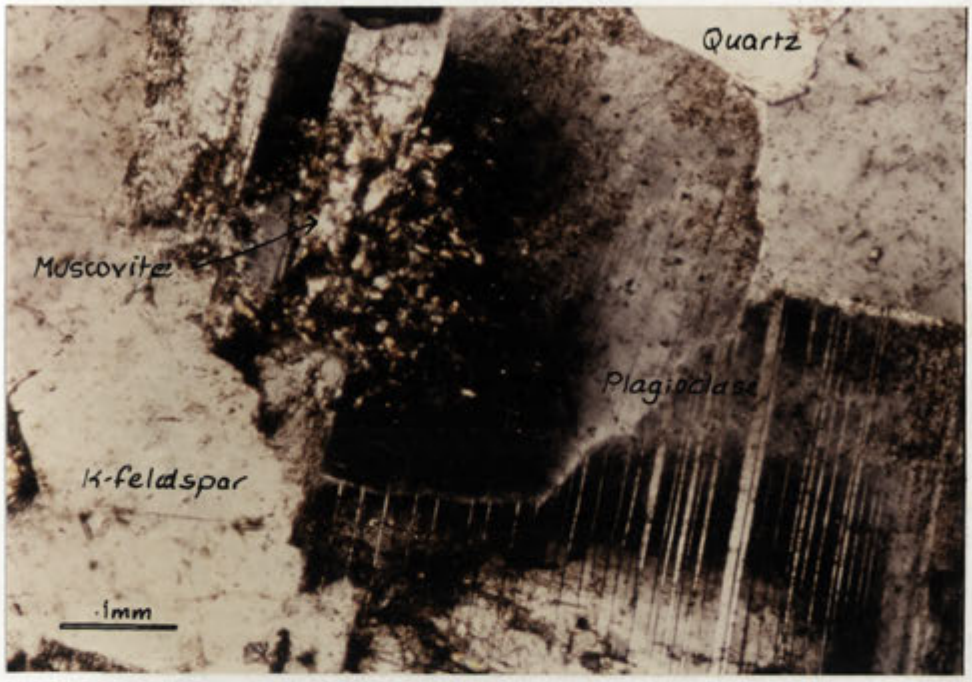

PLATE 4.1A: Fresh Bemboka Granodiorite. Plagioclase contains hydrothermally derived muscovite. K-feldspar has not been altered.

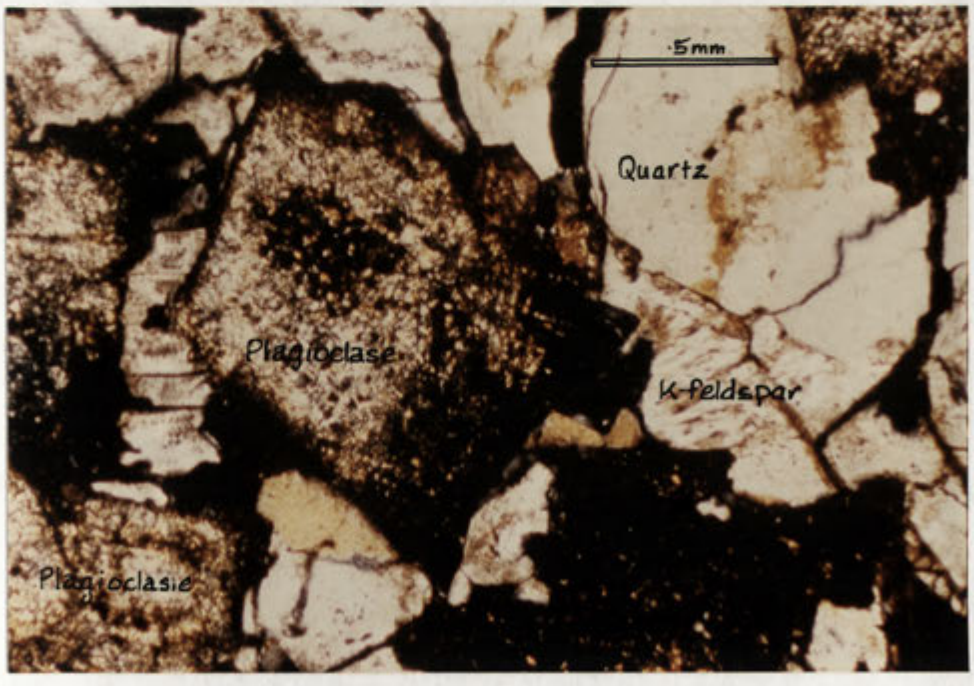

PLATE 4.1B: Strongly weathered Bemboka Granodiorite. Plagioclase has been almost completely replaced by clay. K-feldspar is only moderately weathered at this stage.

PLATE42A: ETCHING ALONG DISLOCATIONS IN FELDSPAR.

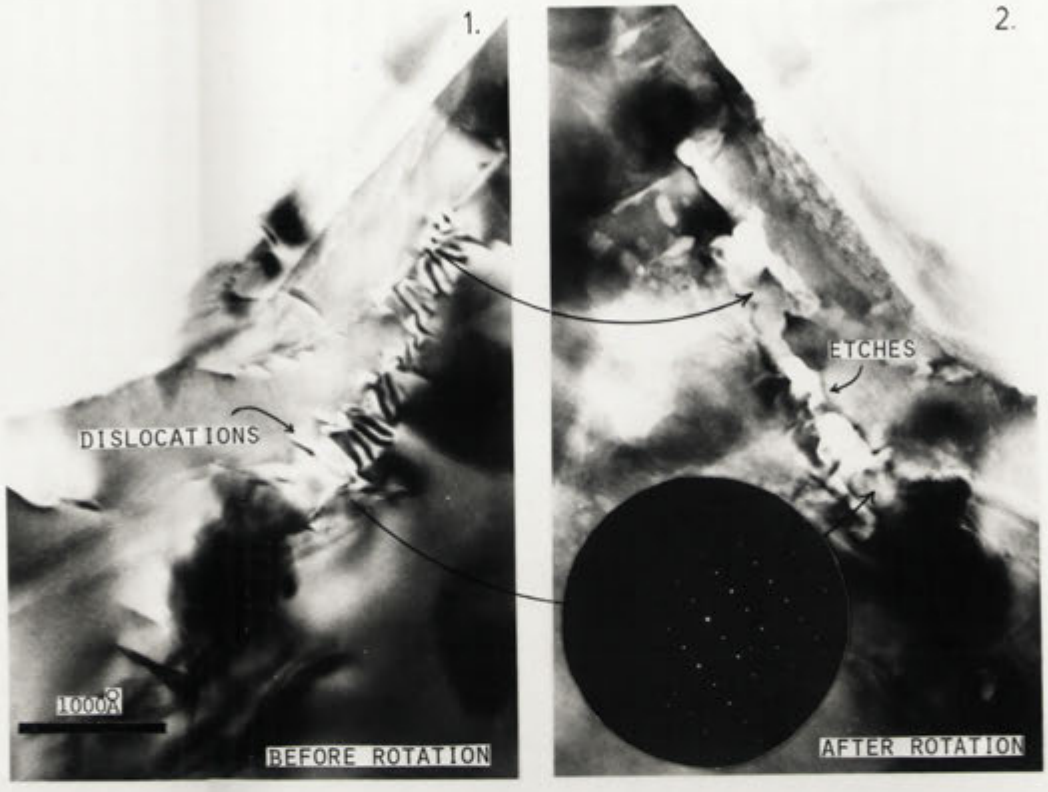

PLATE42B: ETCHING ALONG TWIN PLANES IN PLAGIOCLASE.

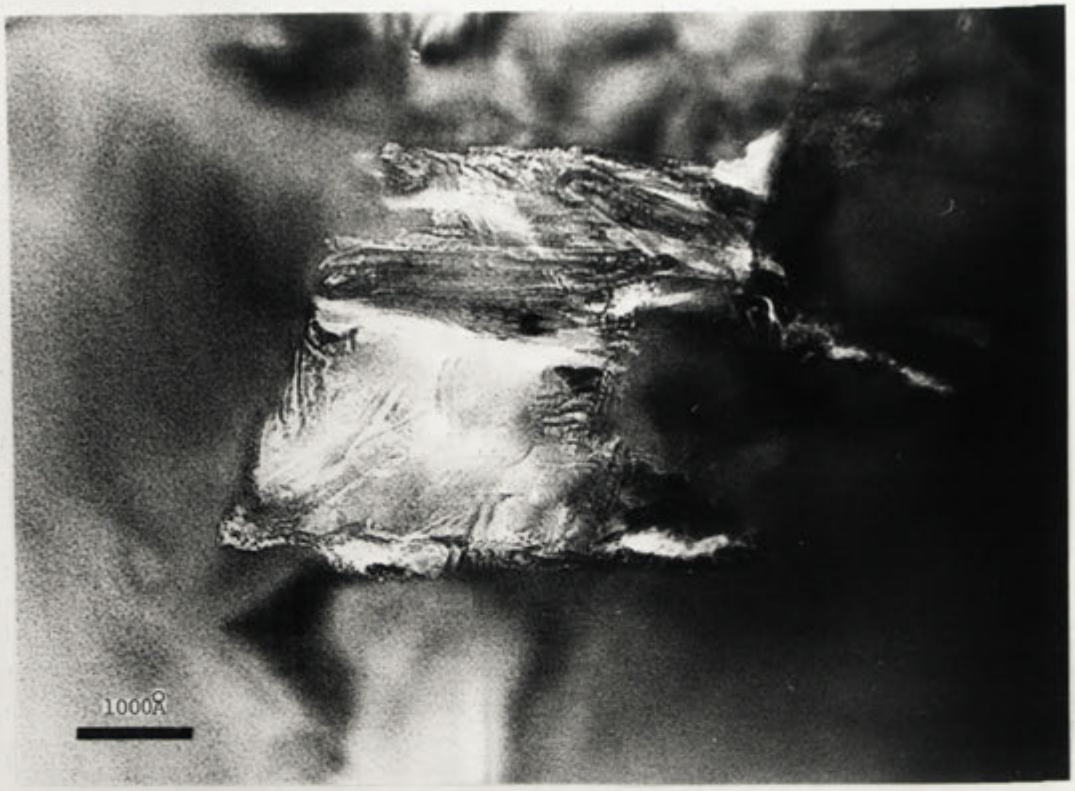

PLATE 43A: ETCH CONTAINING PARRTTLY CRYSTALLINE MATERIAL AND CLAY.

PLATE 43B: THIN STRIPS OF CLAYY IN FELDSPAR.

access of water to the feldspar. The role of lattice planes in controlling removal of feldspar is reduced, and the dissolution frontier becomes more irregular (see Plate 4.6). In general however, crystallography controls etching, resulting in the development of a very sculpted surface, honeycombed by prismatic pits and cracks (Plate 4.4). This process has been well documented by many authors, particularly Berner and Holdren (1977).

.2: Development of clays

The early stages of weathering are characterised by the removal of large quantities of material in solution. A TEM examination of the surface of the reacting feldspar indicates that a small quantity of patchily distributed, apparently unstructured material has been developed adjacent to these etched surfaces. This early product of feldspar alteration initially has an even cellular texture with individual units (possibly compressed spheres) between 30 Å and 60 Å in diameter. With subsequent reorganisation an alignment of this material can be observed. Individual units become more elongate, and strips about 30 Å wide form within a zone or domain. These poorly defined domains are generally up to 1000 Å wide and 2000 Å long, and are randomly oriented with respect to each other. The 30 Å wide strips developed within these zones are essentially parallel, and in more advanced stages of crystallization can be recognised as narrow strips of clay, generally only 2 or 3 unit cells wide (Plate 4.5a). The formation of curving bunches of clay with basal spacings of 11-15 Å can be observed with increasing degrees of recrystallization (Plate 4.5c). The abundance of unstructured material decreases with increasing abundance of clay, and outwards from the reacting feldspar surface, until it is entirely replaced by this phase (Plates 4.6 and 4.7).

Diffraction patterns obtained from this apparently unstructured material typically show quite diffuse rings at d spacings of 3.4 Å, 2.3 Å, 1.6 Å, 1.4 Å, and 1.3 Å (Plate 4.5b). Material retains a cellular appearance regardless of the orientation in which the material is viewed. This phase is described in later sections of this chapter, and in following chapters. On the basis of texture, the observed evolutionary sequence toward more crystalline material, and comparisons with diffraction characteristics and morphology of allophane as described in the literature (eg. Hemni and Wada, 1976) it is suggested

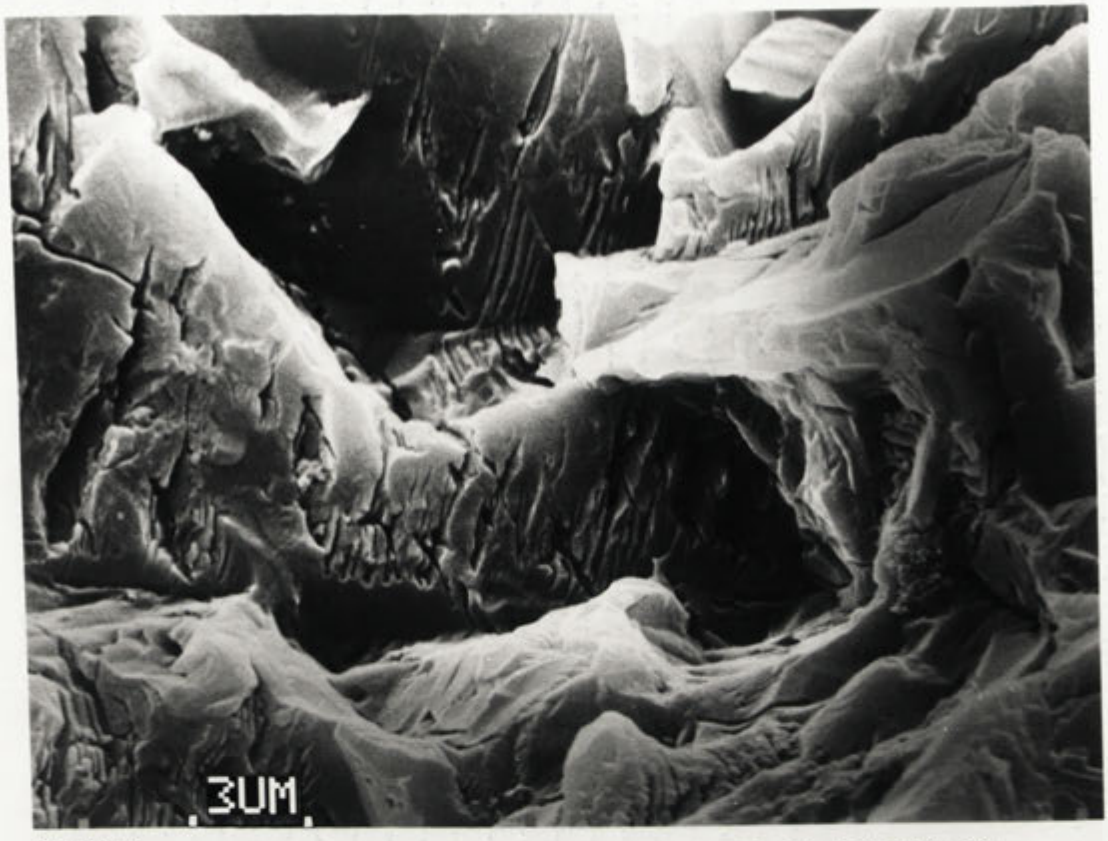

PLATE44A: CRYSTALLOGRAPHICALLY CONTROLLED ETCHES IN PLAGIOCLASE.

PLATE44B: NUMEROUS ETCHES DEVELOPED IN PLAGIOCLASE FELDSPAR.

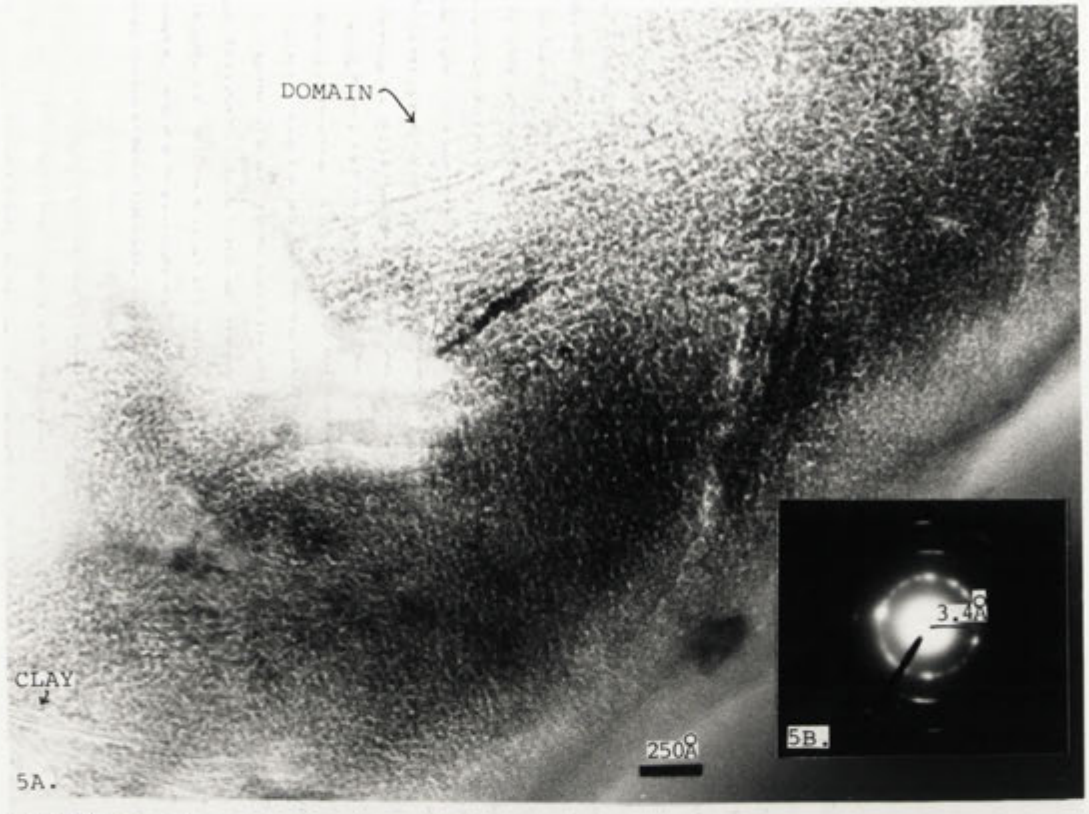

PLATE 45A: ALLIGNMENT OF POORLY CRYSTALLINE MATERIAL TO PRODUCE NARROW STRIPS 30--50Å WIDE. PLATE 45B: DIFFRACTION PATTERN.

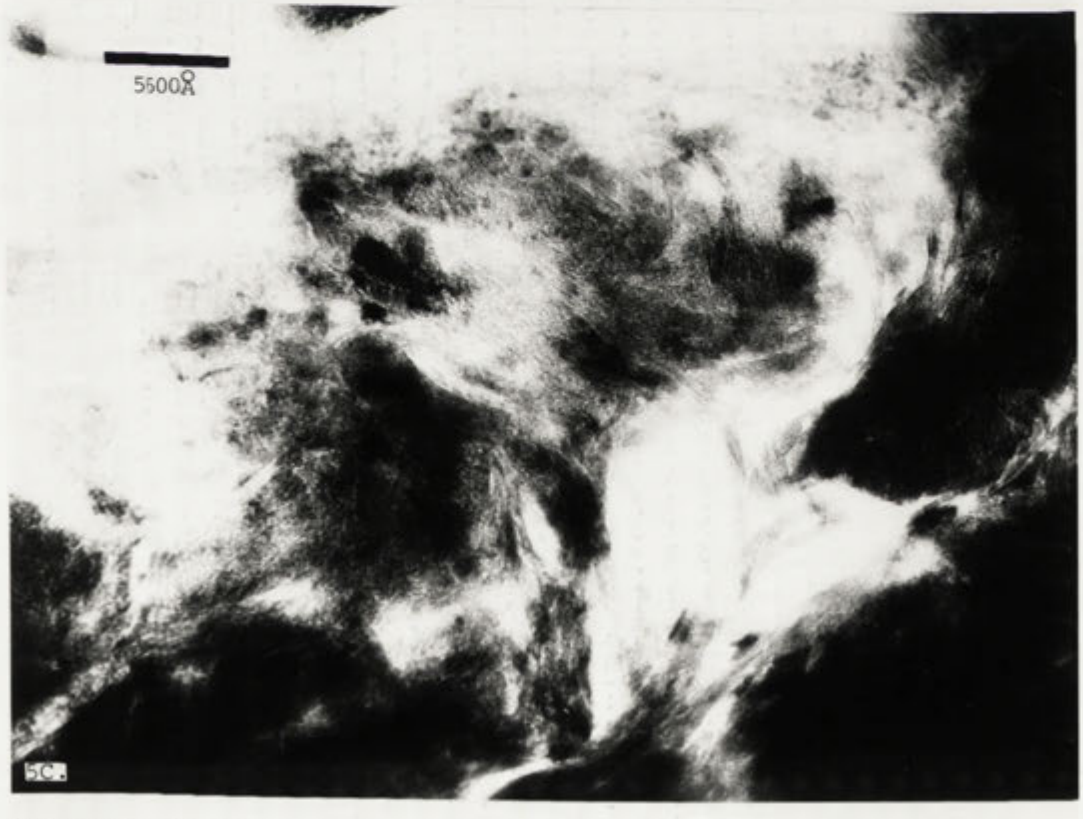

PLATE 45C: NARROW, CURVED BUNCHES OF CLAY DEVELOPING FROM POORLY CRYSTALLINIE MATERIAL.

PLATE 46: AMORPHOUS MATERIAL DEVELOPED ADJACENT TO FELDSPAR IS CONVERTED TO SMECTITE.

PLATE 47A: SMECTITE FORMED BY RECRYSTALLIZATION OF APPARENTLY UNSTRUCTURED MATERIAL.

PLATE 47B: SMECTITE PRODUCED BY FELDSPAR WEATHERING.

that this material is semi-amorphous. Diffraction data indicate that this phase can not be considered completely amorphous as d spacings suggest the presence of units possibly resembling octahedral sheets.

The chemistry of the 11-15 Å product of the recrystallization of the semi-amorphous phase was investigated using the STEM. Data were processed using the method outlined in the experimental techniques section at the beginning of this thesis. Results have been plotted on Al:Si:K+Na+Ca, and Al:Si:Fe triangular diagrams in Figures 4.2 and 4.3, with analyses for the host plagioclase and co-existing spherical halloysite.

Figure 4.2 illustrates that smectites produced by alteration of plagioclase are more aluminous than the parent phase, and may also be quite enriched in alkali and alkali earth metals. Although the actual extent to which the smectite is enriched in these metals (particularly Ca) is not known, it would appear that the quantities are sufficiently large that they could not be readily accommodated in the smectite structure, or by adsorption onto it. Although no evidence has been observed for the presence of a second phase (such as calcite) these data may indicate such a mineral exists in the alteration assemblage at this stage.

Smectites display an approximately linear range in chemistry in Figure 4.2, the trend of which can be extrapolated to the halloysite composition. This is interpreted as reflecting kaolinite crystallization, possibly epitactically, onto smectite sheets in a similar manner to that described in Section 4.2.3. The Al:Si:Fe plot reveals that smectite contains appreciably more Fe than its parent feldspar. Fe may have been introduced in solution, and has been either scavenged by the smectite or its amorphous precursor, or adsorbed at an early stage onto the corroded feldspar surface. The possibility that Fe actually plays a specific role in the breakdown of feldspar, or in the crystallization of clay products is examined later in this chapter.

The recrystallization of amorphous material results in a smectite with a composition which is estimated to be: $(K_{.3}Ca_x)^1(Fe_{.25}Al_{3.78})$

---

[1]Ca omitted as this element is difficult to calibrate due to interference from the K K-alpha peak. The amount is apparently larger than could be accommodated into the smectite structure

FIGURE 3.2

TRIANGULAR DIAGRAM FOR Al - ALKALI - Si OF WEATHERING PRODUCTS OF PLAGIOCLASE.

Linear trend toward kaolinite for the smectite analyses suggests that they are interlayered with kaolin.

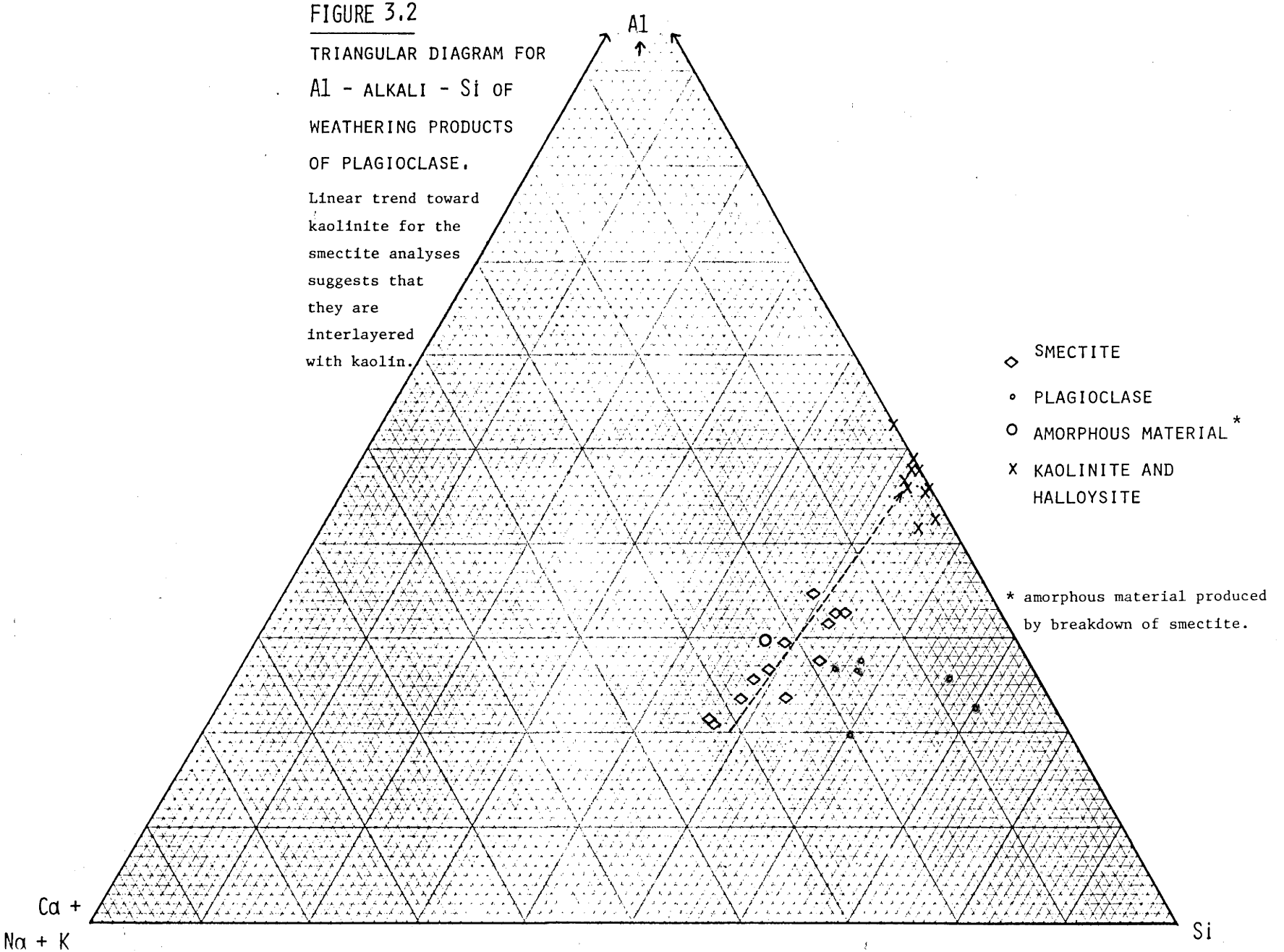

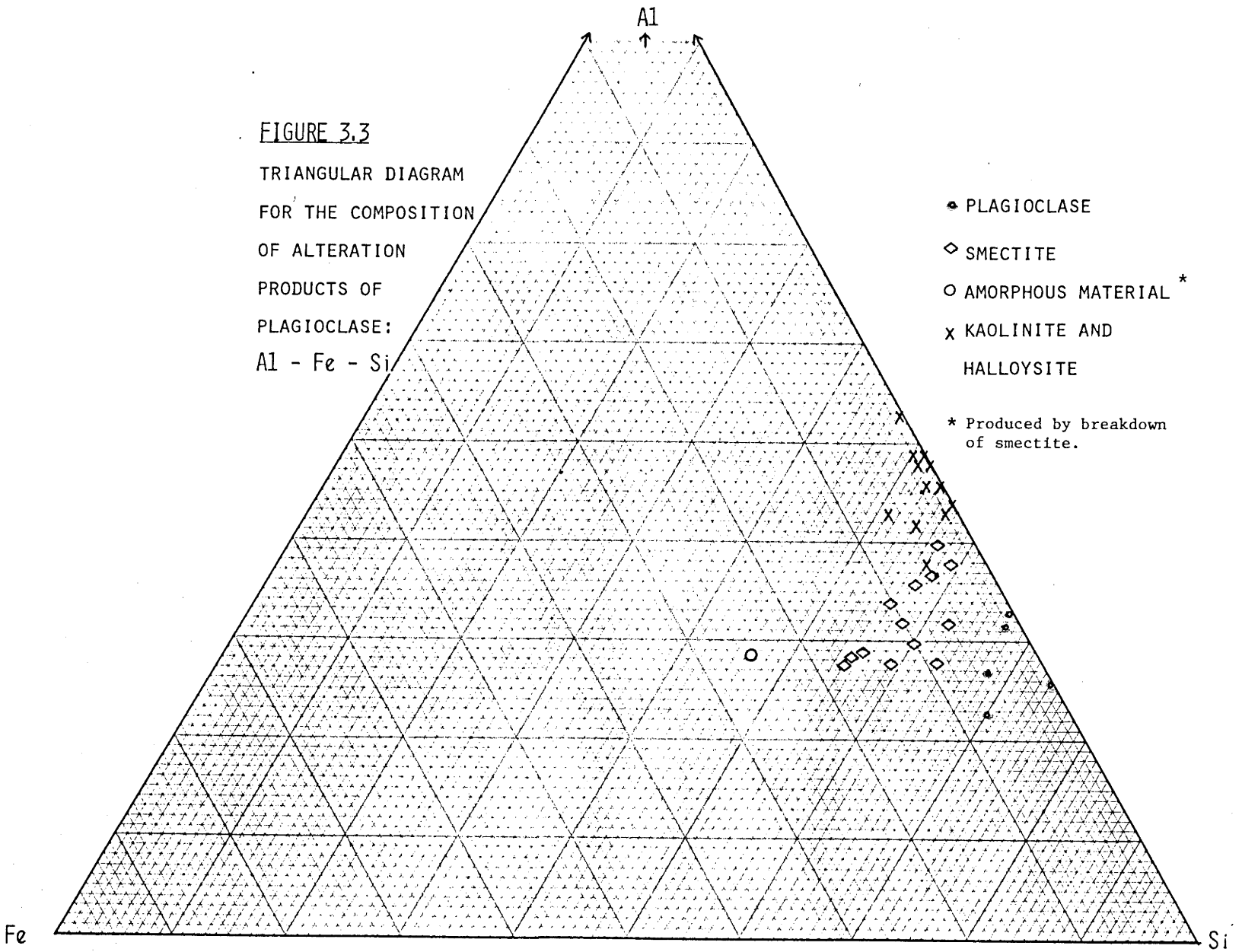

FIGURE 3.3

TRIANGULAR DIAGRAM FOR THE COMPOSITION OF ALTERATION PRODUCTS OF PLAGIOCLASE: Al - Fe - Si

$(Si_{7.6}Al_{.4})O_{20}(OH)_4nH_2O$. This analysis, selected as representative, is from smectite shown in Plate 4.9a.

Smectite is a transitional or metastable phase in the feldspar weathering sequence, and is converted along a reaction front to amorphous material. The breakdown of this phase may correspond to an increased throughflow of solution and probably indicates a decrease in the pH of the local environment. Amorphous material is subsequently replaced by halloysite, generally with a spherical form (Plates 4.8 and 4.9). In most cases the relationship between smectite and spherical halloysite is not readily apparent, and it is common simply to find an association of these two phases (Plate 4.10). The sequential development of amorphous material and then smectite during weathering allows a stepwise increase in the Al:Si ratio. Consequently, when smectite is replaced by amorphous material and the efficiency of Si removal is improved, the remaining material has a composition appropriate for the crystallization of halloysite.

An STEM analysis for the semi-amorphous material which replaces smectite is also plotted in Figure 4.3. This component contains significant quantities of Fe. This is probably due to the concentration of Fe released from smectite and not accommodated in halloysite. Goethite will probably crystallize when a sufficient concentration of Fe is attained.

The mineralogical pathway described above is only one of two sequences observed for the transformation of feldspar to clay. In the second case the alteration product is tubular halloysite. This phase develops abundantly in cavities, growing outward from the surface of the corroded plagioclase (Plate 4.11). The interface between the feldspar and halloysite tubes consists of a narrow zone (<250 Å wide) of partially disrupted material (Plate 4.12). Simultaneously Fe in the system precipitated as goethite. This phase can be observed to coexist with halloysite in Plate 4.12b. It would appear that after dissolution forms networks of cavities, precipitation of Al and Si from solution results in the growth of halloysite.

The space filling nature of halloysite tubes can also be illustrated in SEM photomicrographs (Plate 4.13). In most cases tubes grow outward from a substrate into cavities. Photographs do not show

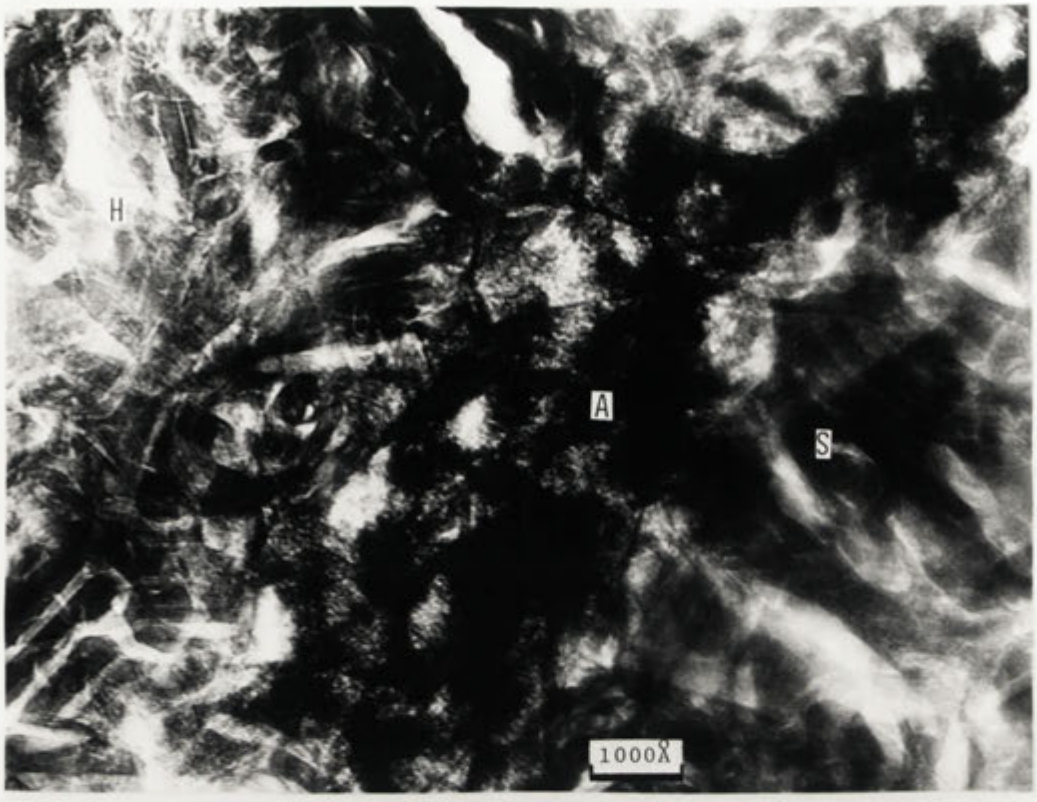

PLATE48A: SMECTITE (S) IS CONVERTED VIA APPARENTLY AMORPHOUS MATERIAL (A) TO SPHERICAL HALLOYSITE (H).

PLATE48B: SPHERICAL HALLOYSITE (H) ASSOCIATED WITH APPARENTLY AMORPHOUS MATERIAL (A), AND SMECTITE (S).

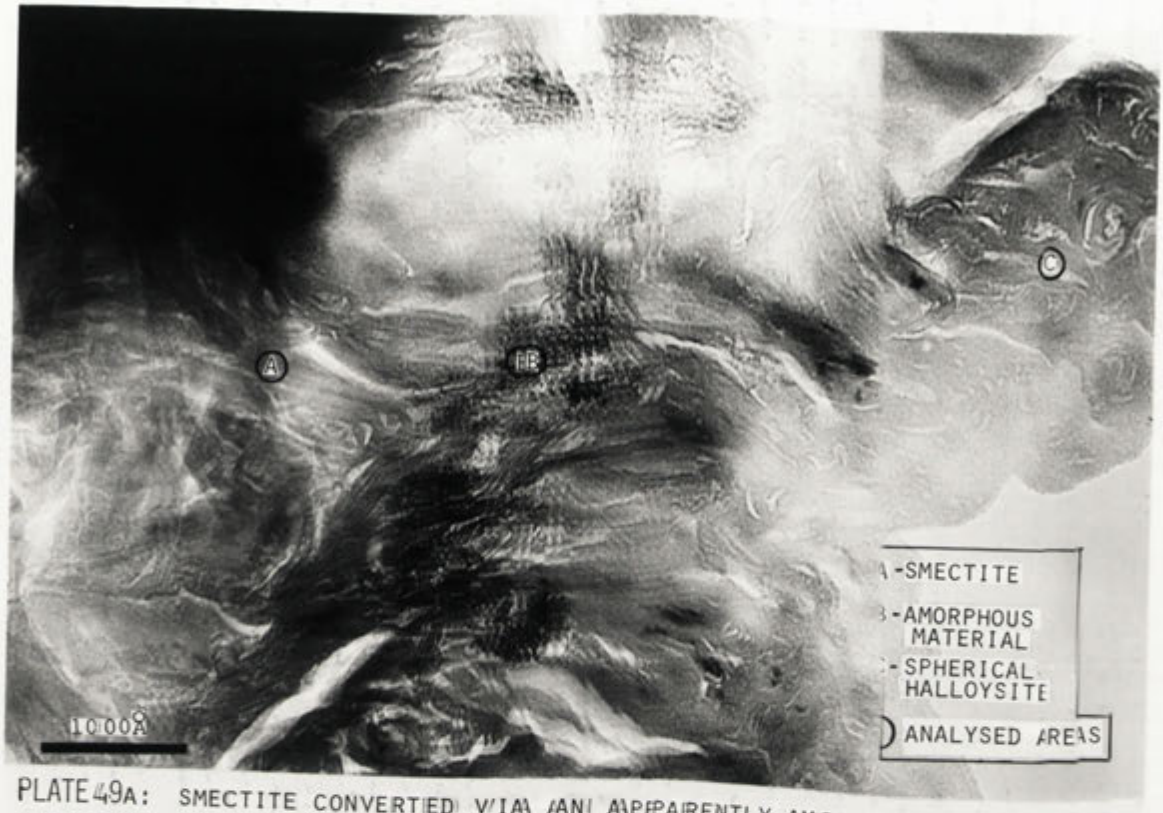

PLATE 49A: SMECTITE CONVERTIED VIA AN APPARENTLY AMORPOUS STAGE TO SPHERICAL HALLOYSITEE.

PLATE 49B: SMECTITE CONVERTING TO SPHERICAL HALLOYSITE.

PLATE 410A: SPHERICAL HALLOYSITE ASSOCIATED WITH SMECTITE.

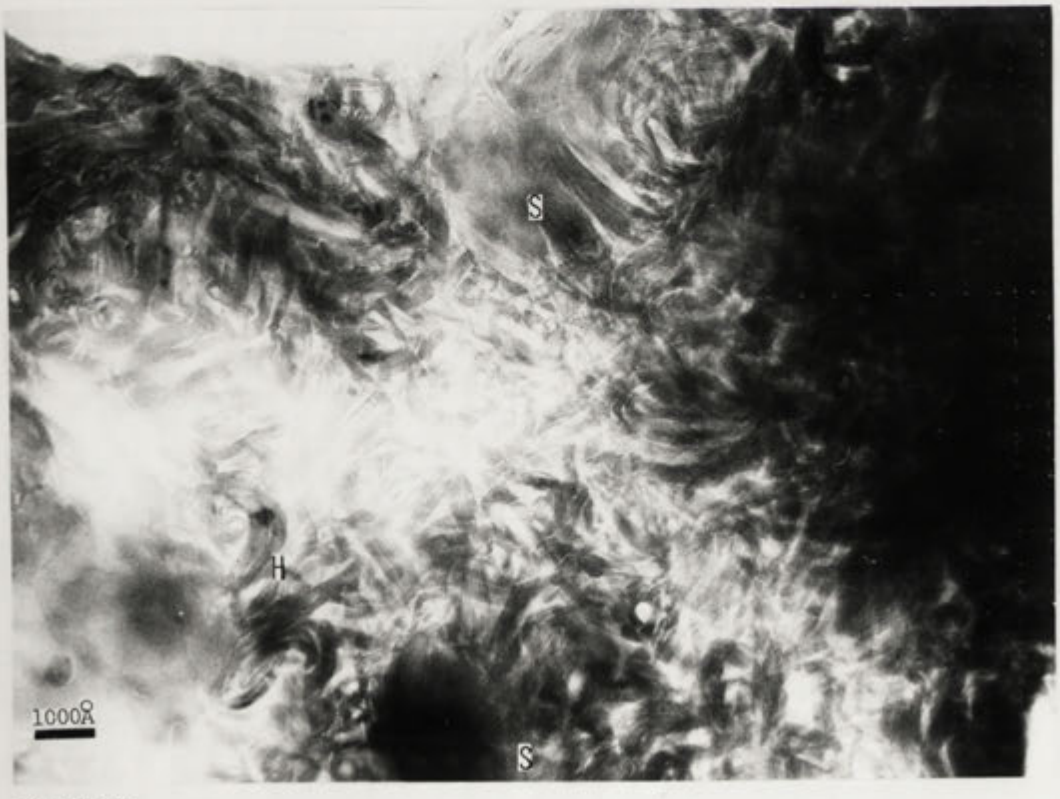

PLATE 410B: ABUNDANT SPHERICAL HALLOYSITE ASSOCIATED WITH SMECTITE.

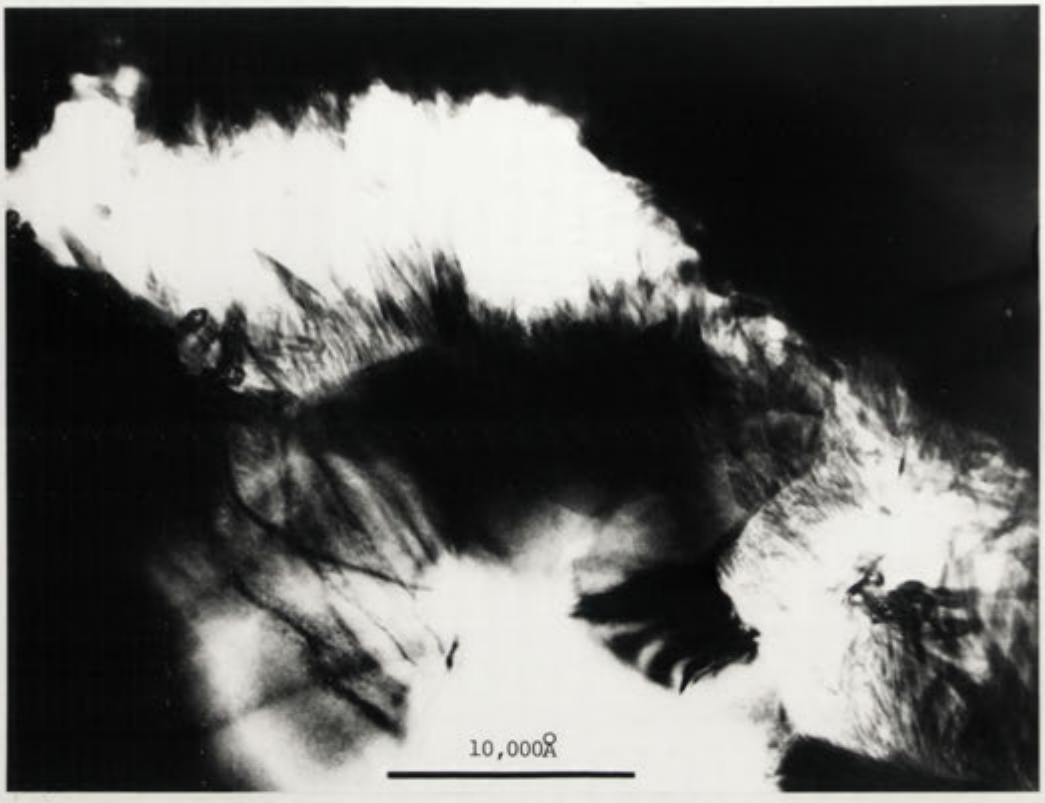

PLATE 11A: TUBULAR HALLOYSITE GROWING OUTWARD FROM THE SURFACE OF ETCHES.

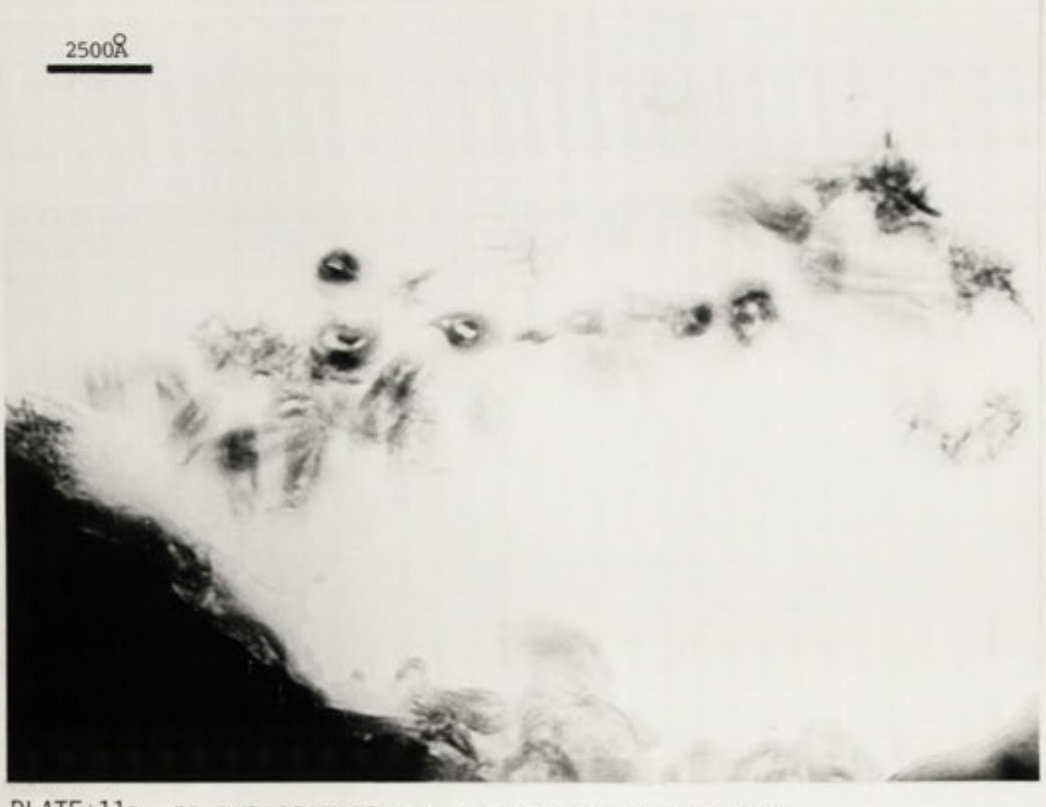

PLATE 11B: Fe PRECIPITATES IN SOME AREAS AS GOETHITE.

PLATE 12: TUBES OF HALLOYSITE GROWING OUTWARD FROM THE CORRODED SURFACE OF PLAGIOCLASE.

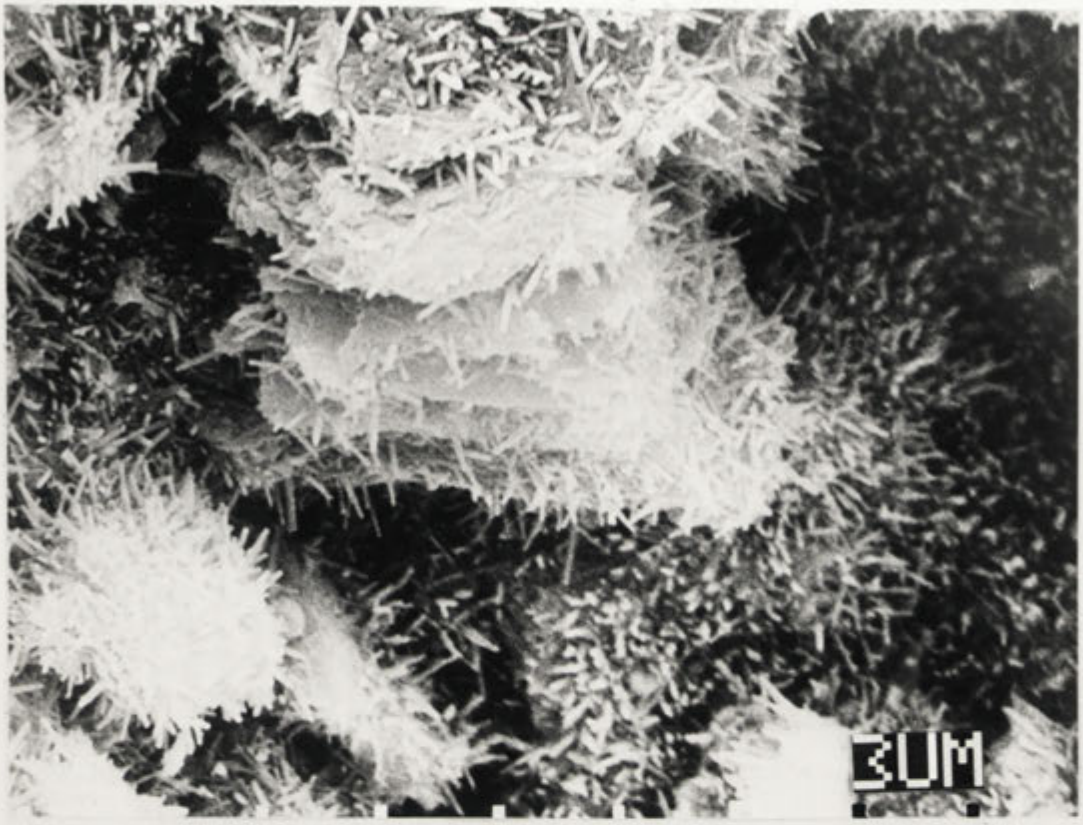

PLATE 413A: HALLOYSITE TUBES GROWING OUTWARD INTO DISSOLUTION CAVITIES IN FELDSPAR.

PLATE 413B: HALLOYSITE TUBES AND SPHERICAL HALLOYSITE ON A CORRODED FELDSPAR SURFACE.

tube openings although these are known to be present. Kirkman (1981) offers explanations for this by suggesting that either the tube ends are obscured by the carbon coating, or that secondary electron emissions may swamp out contrast. Kirkman (1981) proposes a spiral mechanism of growth for halloysite tubes, and claims that this is supported by the tapered ends of tubes. Similar terminations of tubes can be observed in Plate 4.14a.

It has been commonly suggested that halloysite on aging converts to kaolinite. This process can be clearly illustrated for material from the Bemboka profile in Plates 4.14b, 4.15, and 4.16. The first stage in this process appears to be the development of halloysite 'tee-pees' by coalescing the tops of adjacent tubes. These areas merge, and gradually form sheets of platy kaolinite.

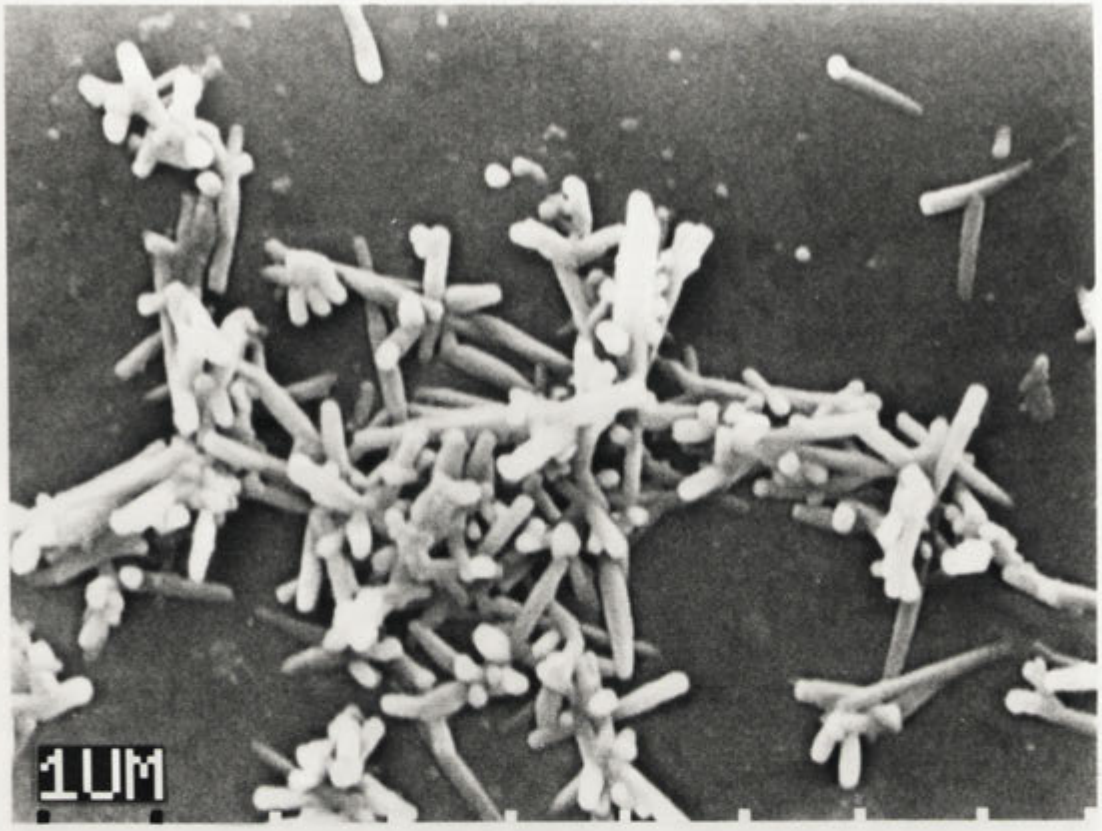

PLATE414A: HALLOYSITE TUBES EXHIBITING TAPERED ENDS.

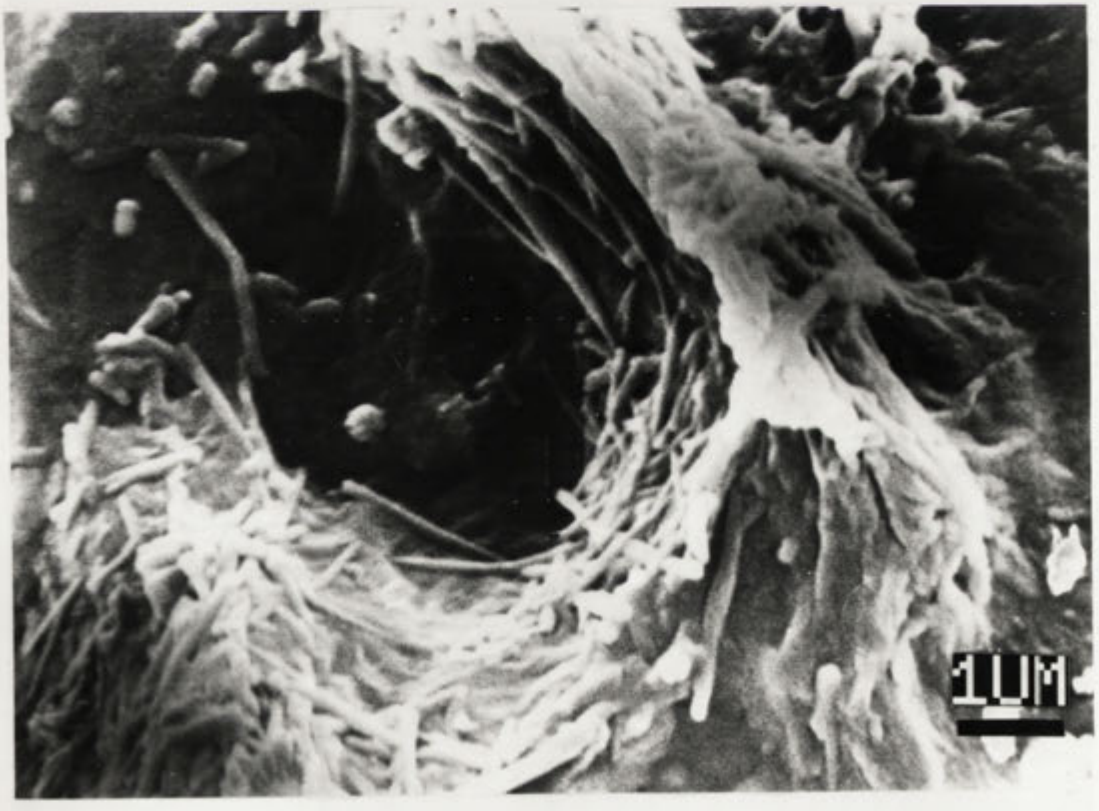

PLATE414B: AGGREGATES OF HALLOYSITE TUBES SHOWING SOME TENDENCY TO COALESCE.

PLATE 415A: 'T-PEES' DEVELOP AS THE TOPS OF HALLOYSITE TUBES COALESCE.

PLATE 415B: FILMS OF KAOLINITE FORM BY RECRYSTALLIZATION OF HALLOYSITE.

PLATE 416. Halloysite tubes coalescing to form kaolinite. 3UM

SECTION 4.2.2: HYDROTHERMAL ALTERATION OF PLAGIOCLASE

Late stage subsolidus, or metamorphic alteration has resulted in the development of muscovite and clinozoisite within plagioclase feldspar. Muscovite ($2M_1$ polymorph) is distinguished from illite by its greater crystallinity and high interlayer occupancy. These phases form part of a greenschist facies assemblage developed in the granite which also includes actinolite, talc, chlorite, epidote, and sphene. An optical microscope study of alteration phases replacing plagioclase indicates that these phases are concentrated in the calcic cores of the feldspar. The chemistry of these phases is shown in Figure 4.4.

Hydrothermal alteration products can be generally distinguished from weathering products by their well developed lath form, and their straight sharp contacts with their host (Plate 4.17). Generally laths are randomly oriented with respect to their parent structure. This lack of structural continuity is illustrated in Plate 4.18. Alteration also occasionally results in the development of some phases within etches. This material is generally present as clay which spans the etch pit (Plate 4.19).

Products of hydrothermal alteration are not stable in the weathering environment. The following section discusses the degradation of muscovite, which is the most abundant hydrothermally produced phase in plagioclase feldspar.

SECTION 4.2.3

WEATHERING OF MUSCOVITE

.1: Previous Work

The natural weathering of muscovite has received relatively little attention in the literature. Several studies of the diagenetic transformation of smectite to illite have been published, and the hydrothermal alteration of magmatic muscovite has received some attention. The literature also contains several studies based on the artificial weathering of micas.

On the basis of X-ray and chemical evidence Churchman (1980) showed that muscovite weathered by loss of K from alternate interlayers. This

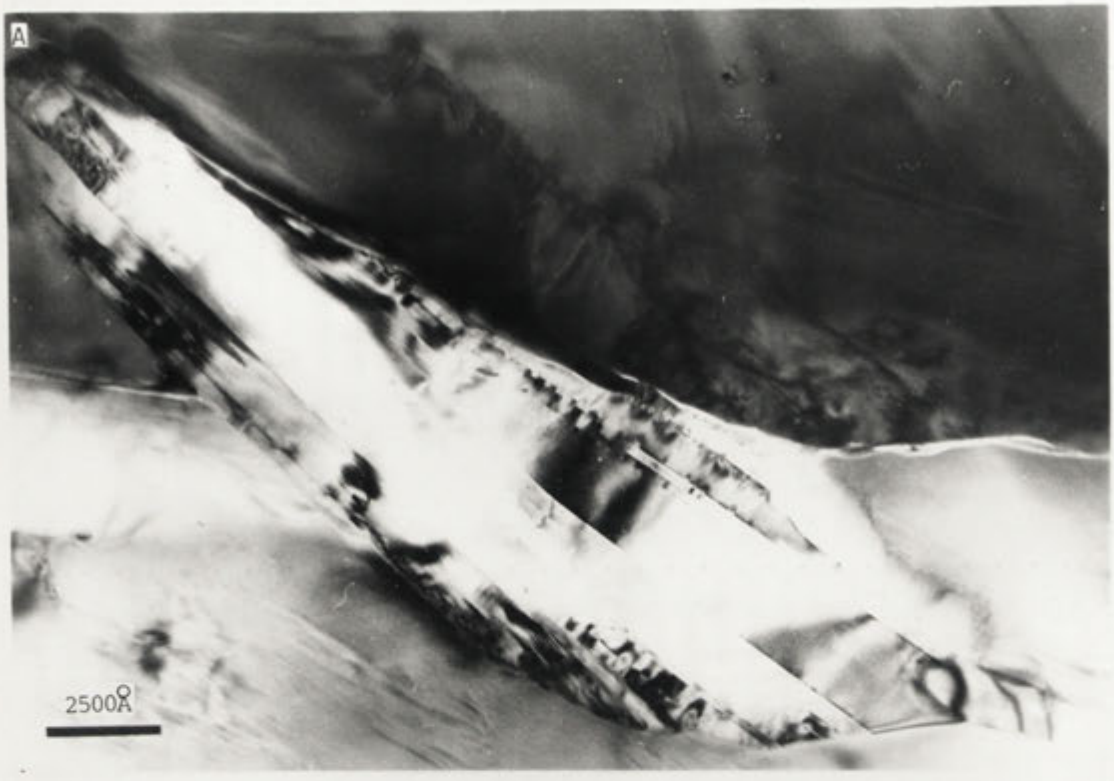

PLATE 417A: HYDROTHERMALLY DERIVED LATH IN PLAGIOCLASE FELDSPAR.

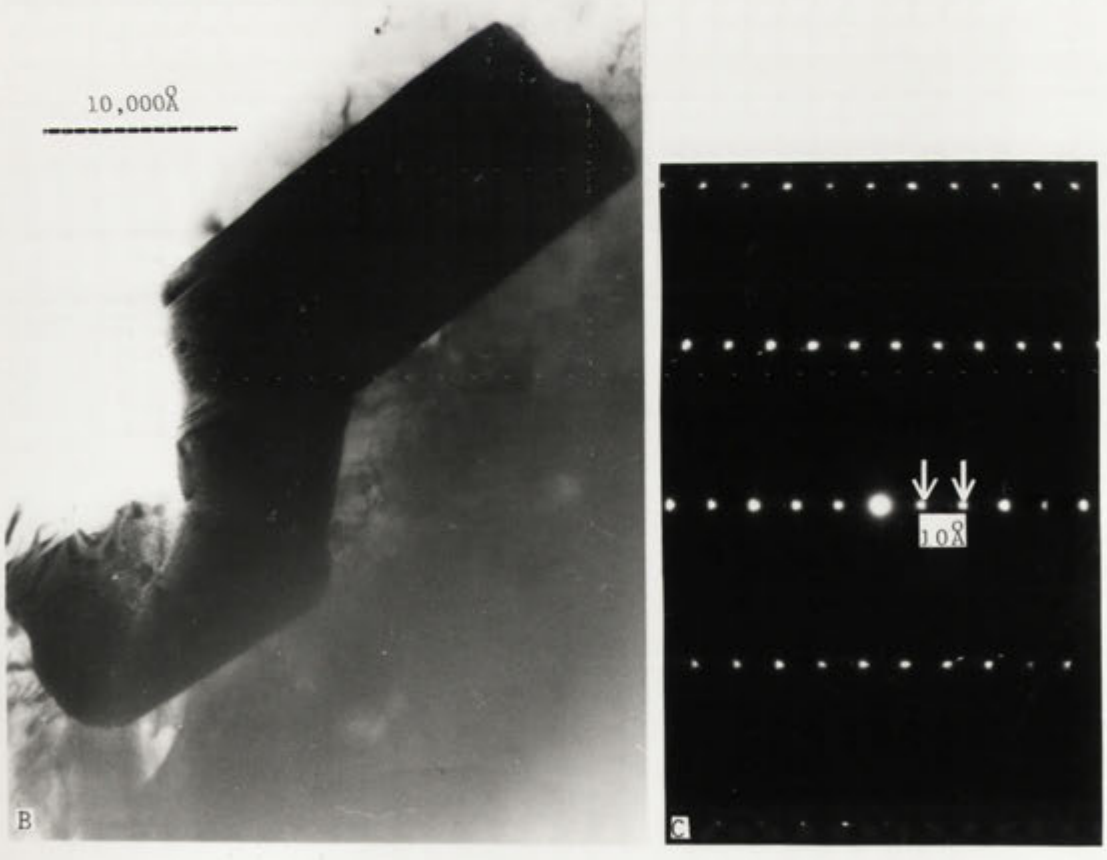

PLATE 417B: MUSCOVITE LATH IN PLAGIOCLASE. PLATE 417C: DIFFRACTION PATTERN.

PLATE 18A: MICA LATH IN PLAGIOCLASE FELDSPAR.

10Å

PLATE 18B: DIFFRACTION PATTERN FOR LATH IN 18A. FELDSPAR REFLECTIONS SUGGEST THAT THE MICA IS RANDOMLY ORIENTED WITHIN THE HOST.

PLATE 18C: DIFFRACTION PATTERN FOR THE CLOSEST FELDSPAR ZONE TO 18B.

PLATE 419A: HYDROTHERMALLY DERIVED STRIPS OF CLAY SPANNING AN ETCH IN PLAGIOCLASE FELDSPAR.

PLATE 419B: DIFFRACTION PATTERN FOR THE HOST FELDSPAR.

Figure 4:4 Hydrothermal alteration products of plagioclase
PROBE ANALYSES

Clinozosoite			Altered Core Plagioclase		
SiO_2	39.52	6.163	SiO_2	41.30	7.984
TiO_2	0.00	0.000	Al_2O_3	30.67	6.987
Al_2O_3	28.53	5.244	FeO	3.21	.52
V_2O_3	0.00	0.000	CaO	23.96	4.96
Cr_2O_3	0.00	0.000	Na_2O	.37	.14
FeO	6.24	.813			
MnO	0.00	0.000	Total	99.50	20.591
MgO	0.00	0.000			-32.0
CaO	23.90	3.993		Na:K:Ca	
				2.7:0:97.3	
Total	98.19	16.214			
		25.0			

Muscovite			Muscovite		
SiO_2	45.11	6.106		46.43	6.110
TiO_2	0.000	0.000		0.00	0.000
Al_2O_3	36.56	5.833		37.55	5.824
FeO	.15	.017		0.00	0.000
MnO	0.00	0.000		0.00	0.000
MgO	.28	.057		.16	.032
CaO	.24	.035		.35	.049
K_2O	10.25	1.769		10.25	1.721
Na_2O	.34	.089		.80	.204
Cl	0.00	0.000		0.00	0.000
Total	92.93	13.906		95.54	13.940
		22.0			22.0
	Na:K:Ca			Na:K:Ca	
	4.7:93.5:1.8			10.3:87.2:2.5	

resulted in the development of a sequence of mica-dioctahedral vermiculite, interstratified mica-beidellite, beidellite minerals or mica, vermiculite, beidellite depending on the nature of the overlying vegetation. On the basis of the similarity in the composition of part of the structures he suggested that smectite inherited the octahedral sheet of muscovite.

Studies of the diagenetic transformation of smectite to illite have been published by a number of authors, including Eberl and Hower (1976); Eberl et. al. (1978); Robertson and Lahann (1981). Eberl and Hower (1976) and Eberl et. al. (1978) noted that the smectite-illite transformation occurred when the negative charge on the 2:1 layer was increased by substitution of Al for Si; substitution of Mg or another divalent cation for octahedral Al; or by reduction of iron. As a result, K is fixed in the interlayer position. For the reverse process, (transformation of illite to smectite by weathering) Eberl et. al. (1978) proposed replacement of K by cations with greater hydration energies, (H_3O^+, Ca). Charge on the 2:1 layer is decreased in this reaction by substitution of Si for Al or oxidation of Fe^{++}.

The product of low temperature hydrothermal alteration of muscovite was reported by Meunier and Velde (1982) to be ferrous-magnesian phengite. Their microprobe analyses of this phase indicated that it contained more Si, Mg, and Fe than the magmatic mica. These authors also observed recrystallization of muscovite to a 1M polymorph which contained more Mg than the parent phase.

Alteration of muscovite has been studied experimentally by Rausell-Colom et. al. (1965) who reported that although K is readily removed from biotite and phlogopite, its removal from muscovite was extremely difficult. These authors considered that this was due to the inclined orientation of the hydroxyl bonding which led to stronger bonding of K; and extreme sensitivity to K in solution. T'Serstevens et. al. (1978) also studied this reaction and suggested that formation of mica-vermiculite intergrades from muscovite occurred by concomitant hydrolysis of K and dissolution of Si. Artificial muscovite dissolution was also studied by Lin and Clemency (1981) who reported that dissolution was incongruent, and that the reaction rate was probably controlled by the rate of destruction of tetrahedral sheets.

SECTION 4.2.3: MUSCOVITE WEATHERING

Relatively well formed laths of muscovite such as those shown in Plate 4.17 alter initially to illite by loss of K. This reaction appears to proceed simultaneously with, or following alteration of the surrounding feldspar (Plate 4.20a), and is associated with the formation of more disorganised, radiating lath structures (Plate 4.20b). In view of the observation of Rausell- Colom et. al. (1965) the relatively late stage at which muscovite degradation occurs may reflect a requirement for increased access of water to the altering phases to allow efficient removal of K.

The process of muscovite alteration has been studied by observation of changes in chemistry, degree of crystallinity, and lath form, and is reflected in the increased degree of beam sensitivity of phases in the TEM. Changes in chemistry have been recorded using data from the STEM. These data reveal that loss of K is accompanied by introduction of a small quantity of Mg and in some cases, traces of Fe. The Al:Si ratio remains constant during this process. Data for the degradation of muscovite to illite are presented in an alkali:Al:Si plot in Figure 4.5.

During, or following the removal of K from muscovite, smectite layers begin to develop. This phase is recognised in TEM images of laths by the presence of 12-15 Å lattice spacings distributed fairly randomly amongst the 10 Å mica sheets (Plates 4.21 and 4.22). Subsequent alteration results in the replacement of illite by smectite, primarily through modification of interlayer chemistry. This is concomitant with a further change in lath form, resulting in the development of fanning areas of smectite.

The chemistry of smectite produced by direct alteration of illite can be clearly distinguished from the smectite formed by recrystallization of amorphous, plagioclase derived material. On the alkali:Al:Si plot (Figure 4.5) mica derived smectite analyses fall on the extrapolation of the muscovite-illite-illite/smectite trend, close to the Al-Si join. This material is distinguished from plagioclase derived smectite by higher Al:Si ratios (reflecting the more aluminous parent); considerably lower abundances of Ca and K; lower Fe contents; and the presence of Mg in the structure.

PLATE420A: PARTIALLY REPLACED MUSCOVITE LATH SURROUNDED BY THE WEATHERING PRODUCTS OF THE HOST FELDSPAR.

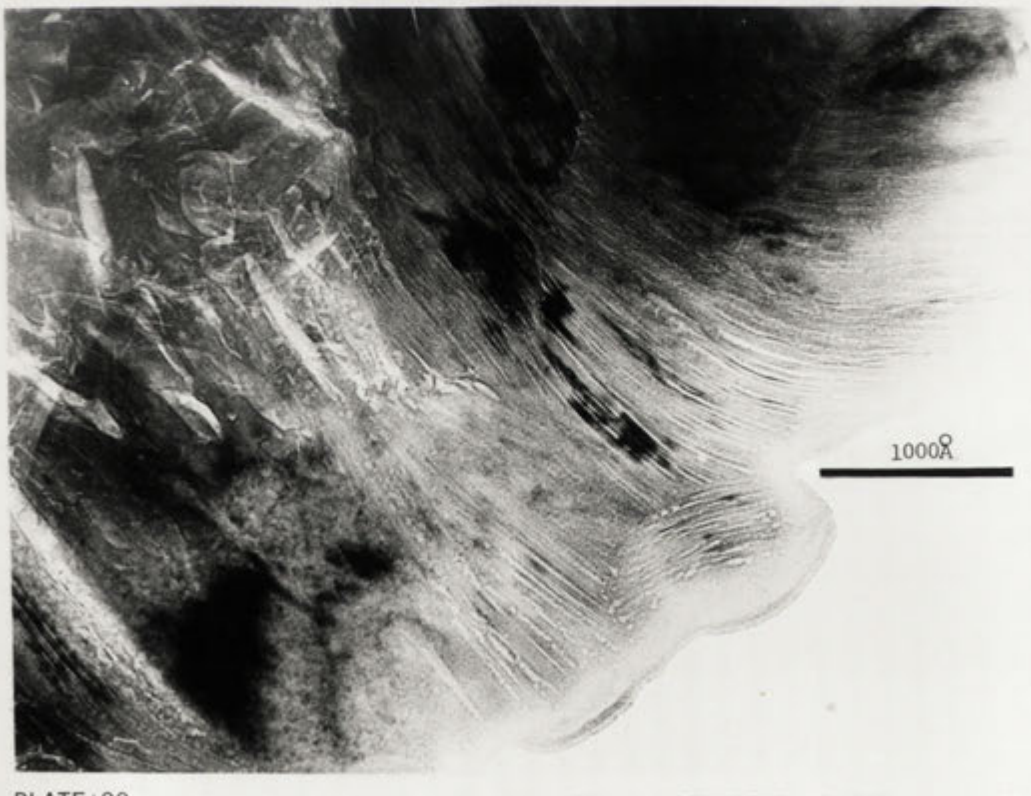

PLATE420B: WEATHERING OF MICA IS ASSOCIATED WITH DEVELOPMENT OF A LESS REGULAR LATH FORM.

PLATE421A: ILLITE LATH (I) CONTAINING SMECTITE (S) INTERLAYERS.

PLATE421B: PARTIALLY REPLACED ILLITE LATH IN FELDSPAR.

PLATE 422: 12Å SMECTITE LAYERS DEVELOP WITHIN LATHS BY REPLACEMENT OF ILLITE.

PLAGIOCLASE, MUSCOVITE, ILLITE, ILLITE-SMECTITE, SMECTITE, HALLOYSITE AND KAOLINITE COMPOSITIONS.

FIGURE 4.5

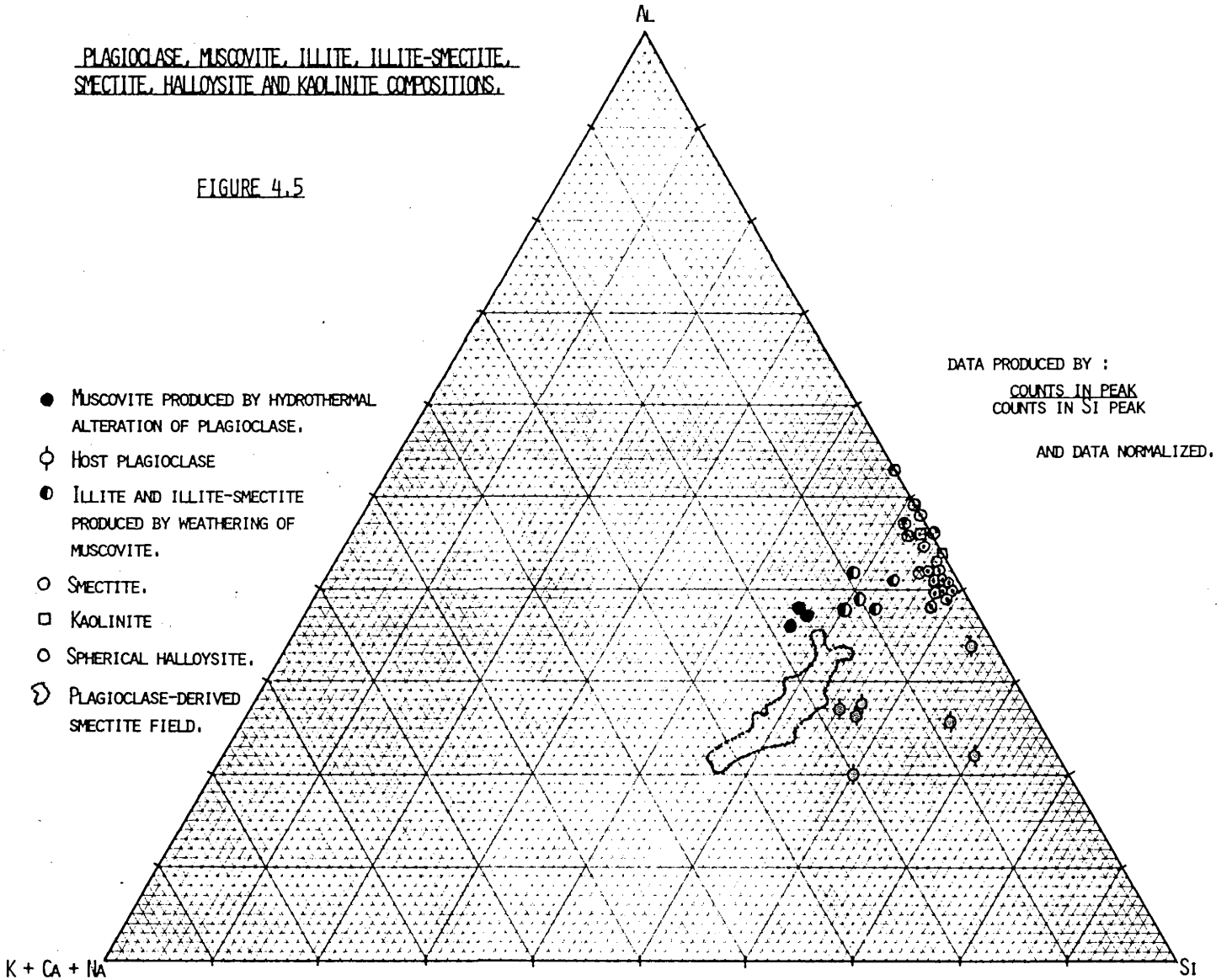

Smectite produced by mica replacement is, like the plagioclase derived smectite, a transitionary phase, and is subsequently replaced by either kaolinite or spherical halloysite.

Replacement by spherical halloysite occurs by the same process as that observed for plagioclase derived smectite. Material at the margins of radiating smectite laths is converted to an amorphous phase which recrystallizes, to form spherical halloysite presumably by spherical growth of nuclei in this relatively unstructured material (Plate 4.23).

Platy kaolinite is also a late stage weathering product of K-mica, apparently developing by templating onto existing sheet silicate structures, and eventually pseudomorphing them (Plate 4.24). It appears that transfer of material is by solution as no evidence can be observed for an amorphous stage. Direct conversion of the structures can not be completely ruled out as the abundance and distribution of Al and Si in muscovite and smectite requires comparatively little modification for the formation of kaolinite. The distribution of this phase adjacent to pre-existing smectite (and illite) rather than randomly throughout these phases suggests that crystallization occurs by epitactic growth. This mechanism of kaolinite crystallization is also inferred for replacement of 2:1 sheet silicates in other mineral weathering reactions (for example, see Chapter 5), and may represent the process by which much of the plagioclase derived kaolinite forms. At a later stage, recrystallization of halloysite may also contribute to the abundance of this phase in the weathering profile.

SECTION 4.2.4

K-FELDSPAR WEATHERING

Primary K-feldspar

Fresh K-feldspar contains no phases developed in response to the period of low grade metamorphism.* The effect of this episode can, however, be observed within K-feldspar crystals where solutions have promoted the dissolution of material and resulted in etches. These etches have been initiated at dislocations and twin planes, and have developed with lattice planes controlling subsequent removal of material (Plate 4.25). Weathering also proceeds in this manner in the early

* see amendments: p230

PLATE 423. ILLITE - SMECTITE LATH CONVERTED TO SPHERICAL HALLOYSITE.

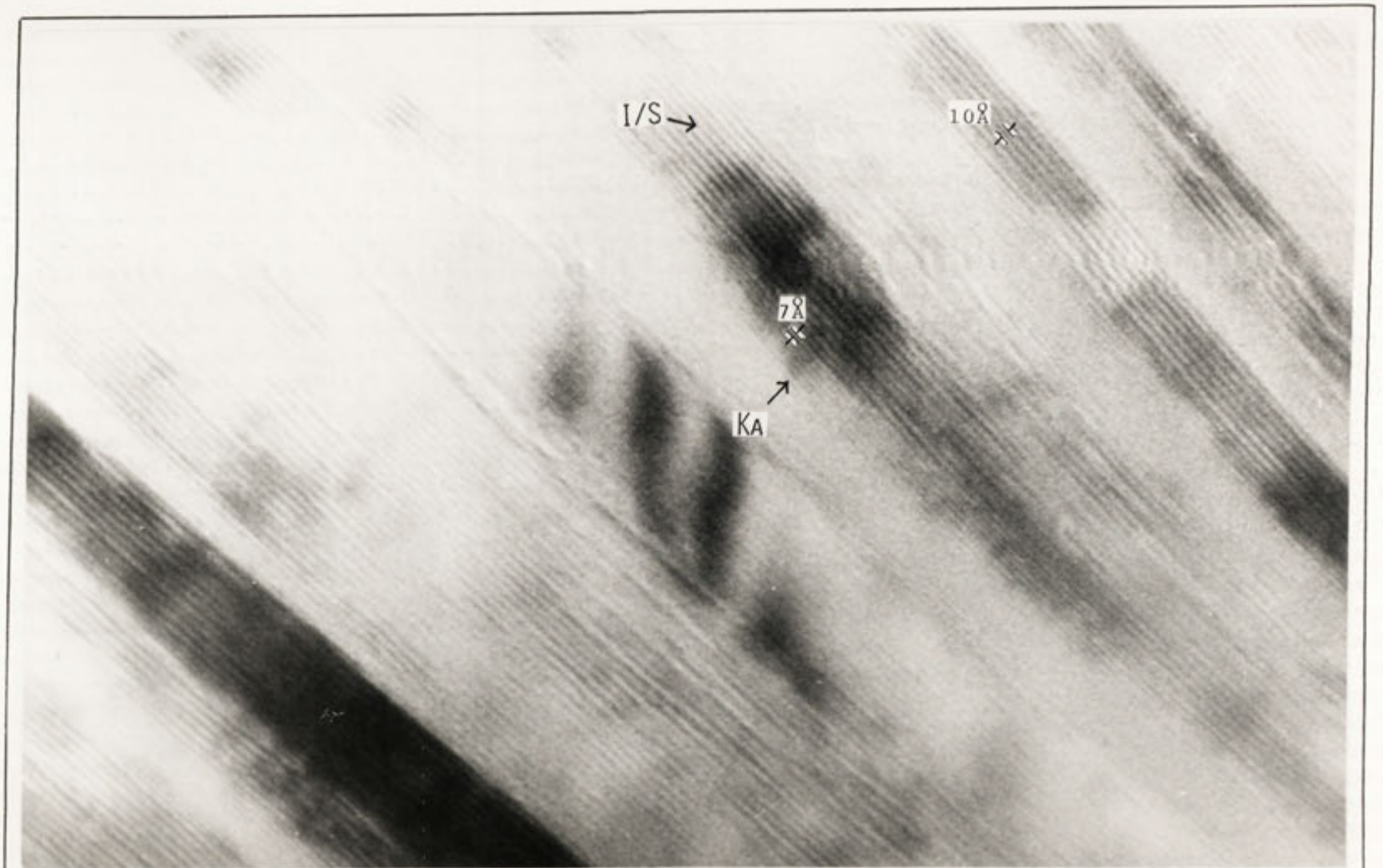

PLATE 424. ILLITE-SMECTITE LATH (I/S) REPLACED BY EPITAXIALLY CRYSTALLIZED KAOLIN (KA).

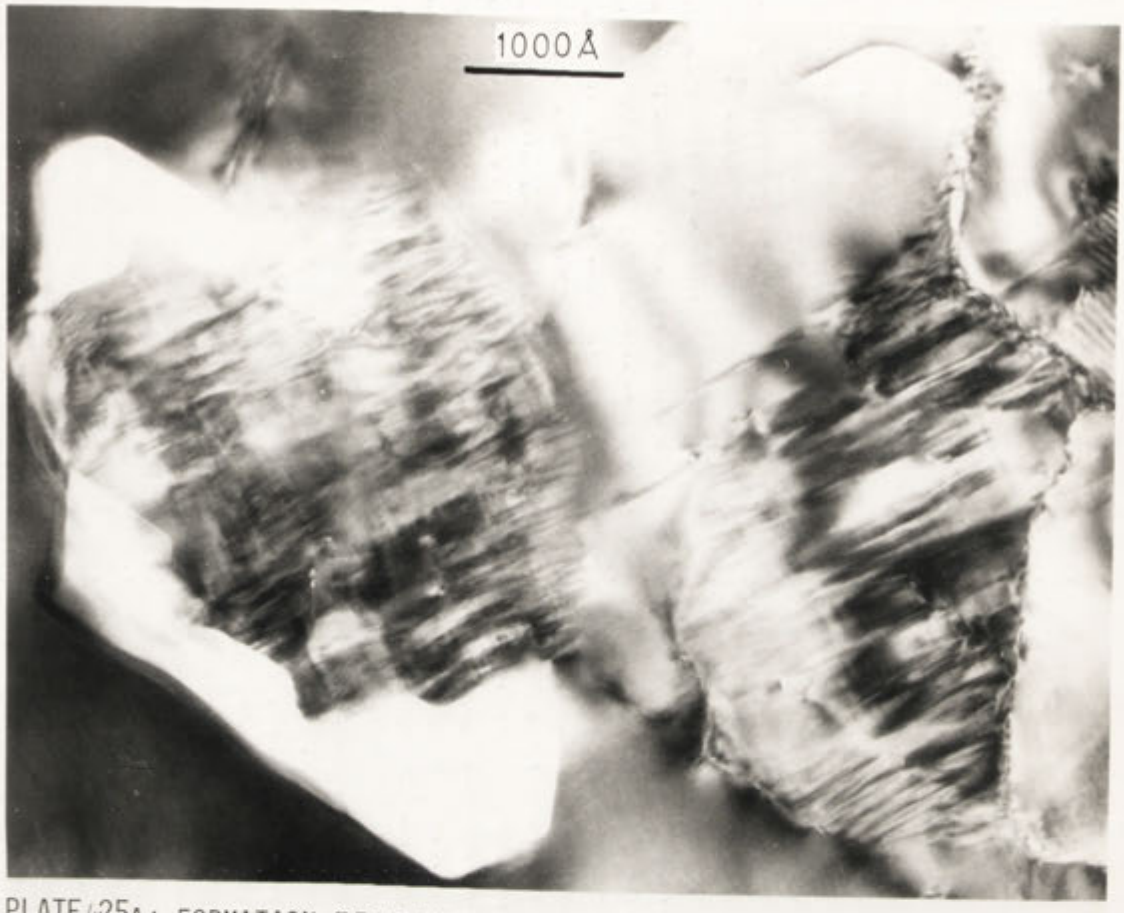

PLATE 425A: FORMATION OF ETCHES IN K-FELDSPAR WHICH RESEMBLE NEGATIVE CRYSTALS.

PLATE 425B: ETCHING INITIATED AT DISLOCATIONS.

stages, and it is not until most of the other minerals in the granite have been largely replaced that the K-feldspar is converted into secondary phases.

The early stages of weathering

Early stage dissolution of the K-feldspar, like that of the plagioclase, results in the development of etches which contain amorphous material and strips of clay. These clay laths frequently span etches, suggesting that in this microenvironment secondary phases may adopt an orientation which resembles that of the parent phase. For example, Plate 4.26 illustrates the development of replacement phases in etches controlled by twin planes. Plate 4.27 depicts the development of clay with lattice spacings of 10-12.5-15 Å which rapidly collapse to 10 Å as a result of beam damage. This material is probably smectite.

Main stage of weathering

The first formed replacement phases produced by large scale alteration of K-feldspar from the Bemboka profile differ from those produced in the Jindabyne profile in morphology and chemistry.

.1 Bemboka Profile

The main stage of alteration of K-feldspar commences with the development of a strip of semi-amorphous cell-textured material up to .5μm thick which forms adjacent to the corroded edge of the parent phase (Plate 4.28a). Crystallization of this component occurs in a similar manner to that described for the semi-amorphous product of the initial stage of plagioclase weathering. Zones within the semi-amorphous material develop internal foliations which, as reorganisation becomes more pronounced, show characteristics of simple strands of clay (Plate 4.28a). With further crystallization, curving bands develop. These clays have the characteristic 10-15 Å lattice spacings of smectite (Plates 4.28b, 4.29).

The transformation of K-feldspar to smectite is clearly demonstrated in Plates 4.30 and 4.31. Plate 4.30 also illustrates the way in which advancing alteration develops along an uneven front, with early breakdown of feldspar occurring by opening cracks along cleavages, and isolating blocks of unaltered K-feldspar. These areas are subsequently converted to apparently amorphous material.

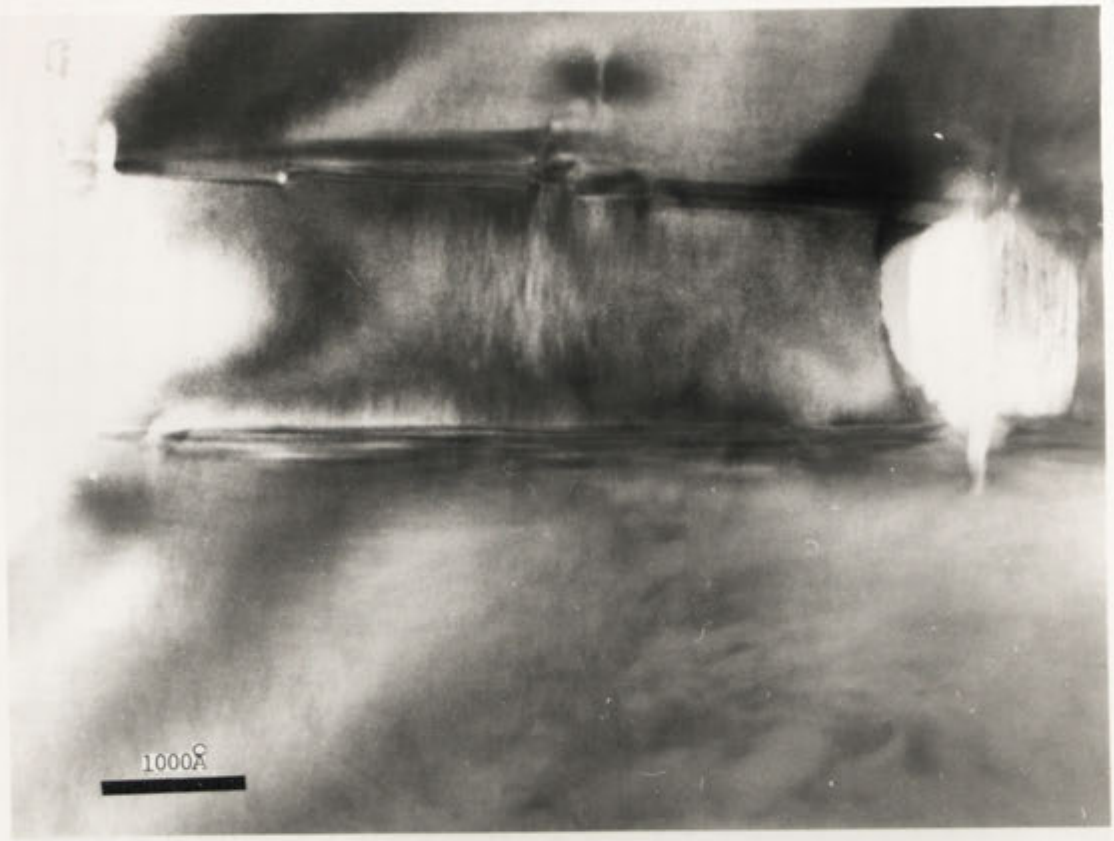

PLATE 426A: DEVELOPMENT OF CLAY IN AN ETCH DEVELOPED BETWEEN TWIN PLANES.

PLATE 426B: DEVELOPMENT OF STRIPS OF CLAY IN AN ETCH BOUND BY THE PRESENCE OF TWIN PLANES.

PLATE 427A: NARROW STRIPS OF SMECTITE DEVELOPED IN AN ETCH PIT.

PLATE 427B: LATHS OF SMECTITE FORMED IN AN ETCH PIT IN K-FELDSPAR.

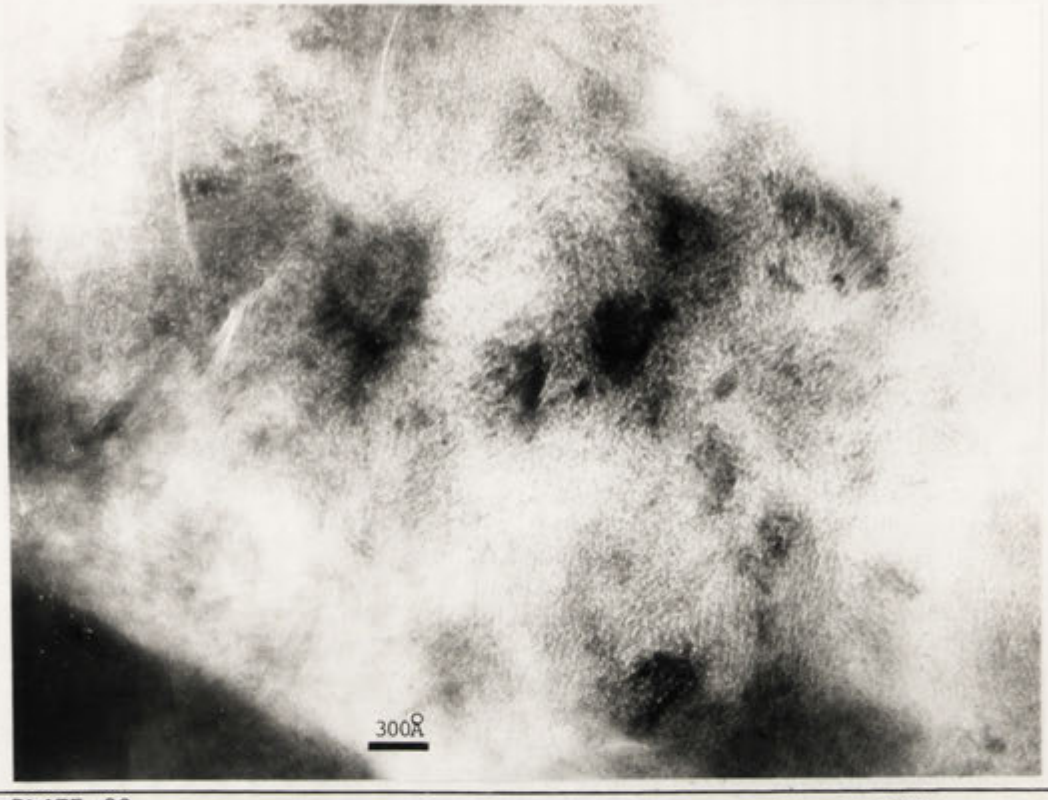

PLATE 28A: DEVELOPMENT OF VERY NARROW STRIPS OF CLAY FROM EVEN, CELL-TEXTURED, APPARENTLY AMORPHOUS MATERIAL.

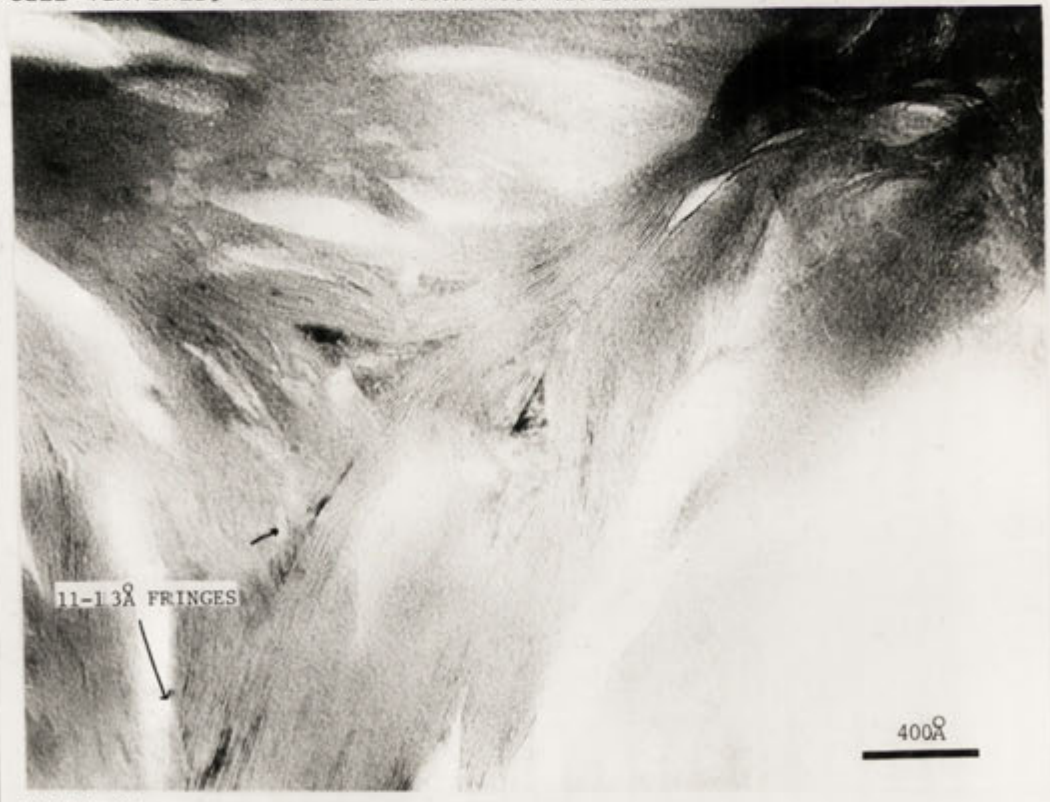

PLATE 28B: WAVY STRIPS OF CLAY, PROBABLY SMECTITE.

PLATE 429A: DEVELOPMENT OF VERY NARROW STRIPS OF CLAY FROM APPARENTLY SEMI-AMORPHOUS MATERIAL.

PLATE 429B: CRYSTALLIZATION OF SMECTITE FROM A POORLY CRYSTALLINE MATERIAL ADJACENT TO CORRODED K-FELDSPAR.

PLATE430. K-FELDSPAR (K) CONVERTED VIA AN AMORPHOUS STAGE (A) TO SMECTITE (S).

PLATE431

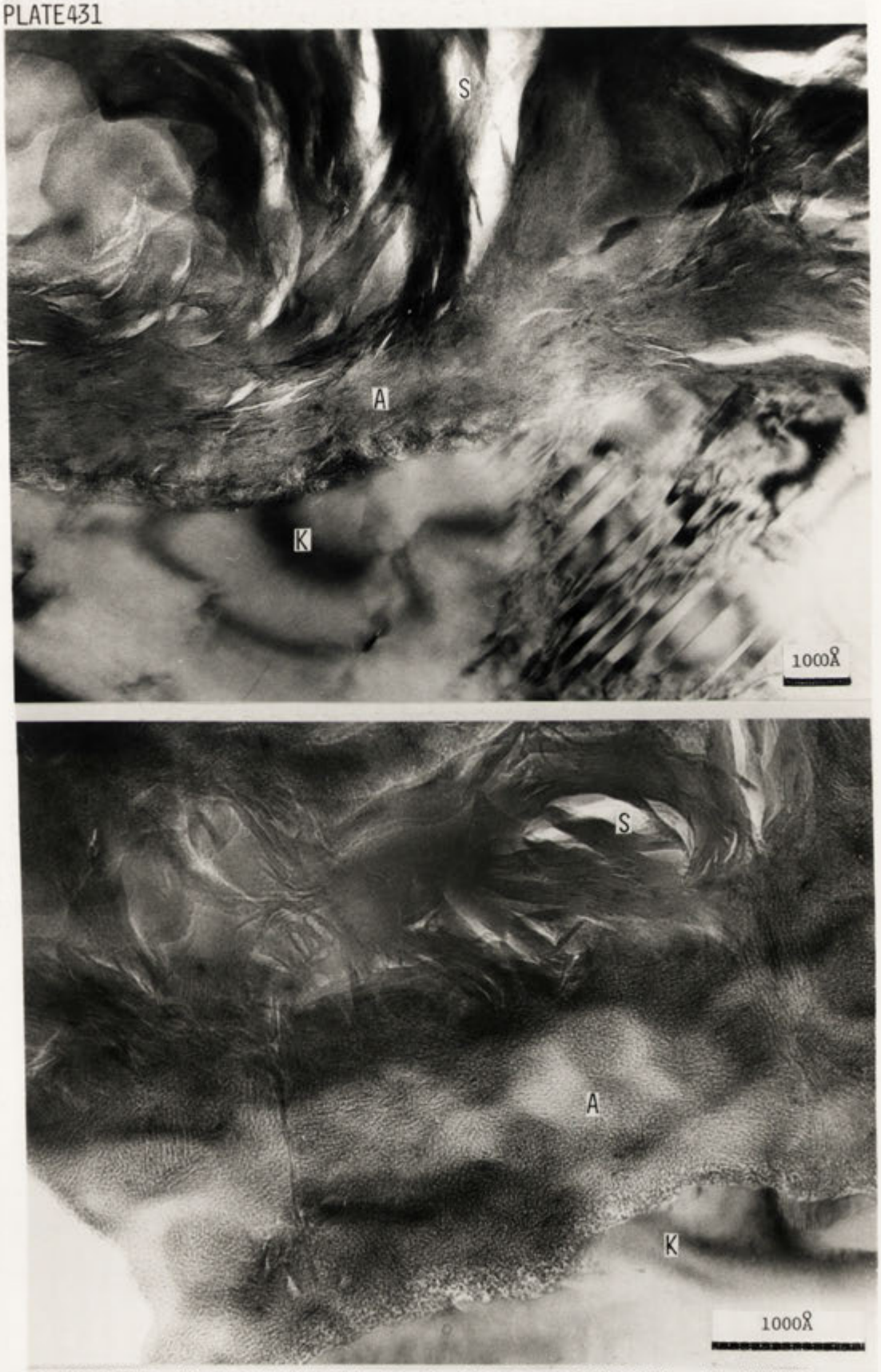

K-FELDSPAR (K) IS CONVERTED TO AN AMORPHOUS MATERIAL (A) WHICH GRADUALLY RECRYSTALLIZES TO FORM SMECTITE (S).

.2 Jindabyne profile

K-feldspar in the Jindabyne profile also undergoes a very similar sequence of alteration characterised initially by the conversion of feldspar to amorphous material. However, the morphology of the smectite formed differs in that this phase crystallizes to form more regular, elongate laths. This sequence is illustrated in Plates 4.32 and 4.33.

The chemistry of weathering products

The compositions of the K-feldspar, amorphous phase, and smectites produced in the Bemboka and Jindabyne profiles are plotted on K:Al:Si and Fe:Al:Si triangular diagrams in Figures 4.6 and 4.7, which have been constructed using peak count data. From these plots, average data for smectites and amorphous material have been estimated.[2]

.1 Jindabyne smectite chemistry

Estimated average Al:Si:K:Fe = .66:1:.07:.27 which is interpreted as representing a smectite with a formula of: $K_{.5}(Fe_{.3}Mg_{small}Al_{3.6})(Si_7Al_1)O_{20}(OH)_4nH_2O$.

Bemboka amorphous material

Estimated average Al:Si:K:Fe = .50:1:.05:x where x varies independently of Al:Si. The composition represented in Figure 4.7 corresponds to proportions of .50:1:.05:1.63 and can be expressed as: $K_{.4}(Fe_{1.3}(OH)_{3.7})(Fe_{.9}Al_{3.1})(Si_{7.4}Al_{.6})O_{20}\ (OH)_4nH_2O$.

Bemboka smectite

Estimated average Al:Si:K:Fe = .5:1:.05:.5 which is interpreted to represent a composition: $K_{.4}(Mg_{small}Fe_{.7}Al_{3.1})(Si_{7.4}Al_{.6})O_{20}\ (OH)_4nH_2O$.

Discussion of chemical data

The amorphous material contains Fe which can not be accommodated in the smectite structure. This surplus apparently remains and concentrates in the amorphous component, explaining the very variable

---

[2]Qualitative data has been semi-quantified using the procedure outlined in the Instrumentation and Experimental techniques section.

PLATE 432A: EARLY STAGE IN CRYSTALLIZATION OF SMECTITE. ABUNDANT POORLY CRYSTALLINE MATERIAL IS PRESENT. PLATE 4.32B: DIFFRACTION PATTERN.

PLATE 432C: MIDDLE STAGE IN THE CRYSTALLIZATION OF SMECTITE. LATH-LIKE AGGREGATES ARE PRESENT. 4.32D: DIFFRACTION PATTERN.

PLATE433A: MORE ADVANCED STAGE IN FORMATION OF SMECTITE LATHS. NARROW STRIPS OF CLAY CAN BE IDENTIFIED.

PLATE433B: QUITE WELL CRYSTALLIZED STRIPS OF SMECTITE.

FIGURE 4.6

TRIANGULAR DIAGRAM FOR K-Al-Si FOR BEMBOKA AMORPHOUS MATERIAL, BEMBOKA SMECTITE, AND JINDABYNE SMECTITE

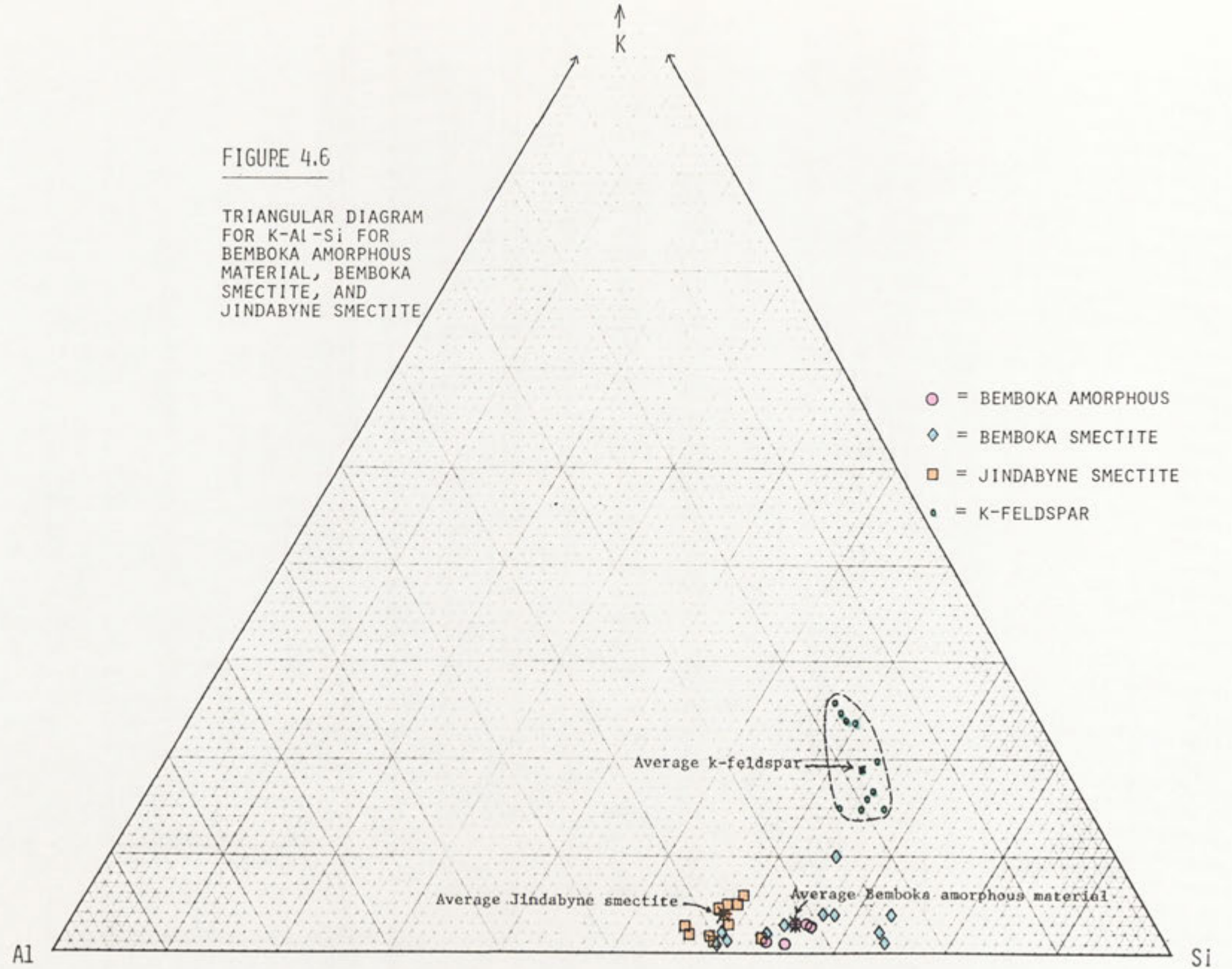

FIGURE 4.7

TRIANGULAR DIAGRAM FOR Al-Si-Fe FOR JINDABYNE, BEMBOKA SMECTITE AND BEMBOKA AMORPHOUS MATERIAL.

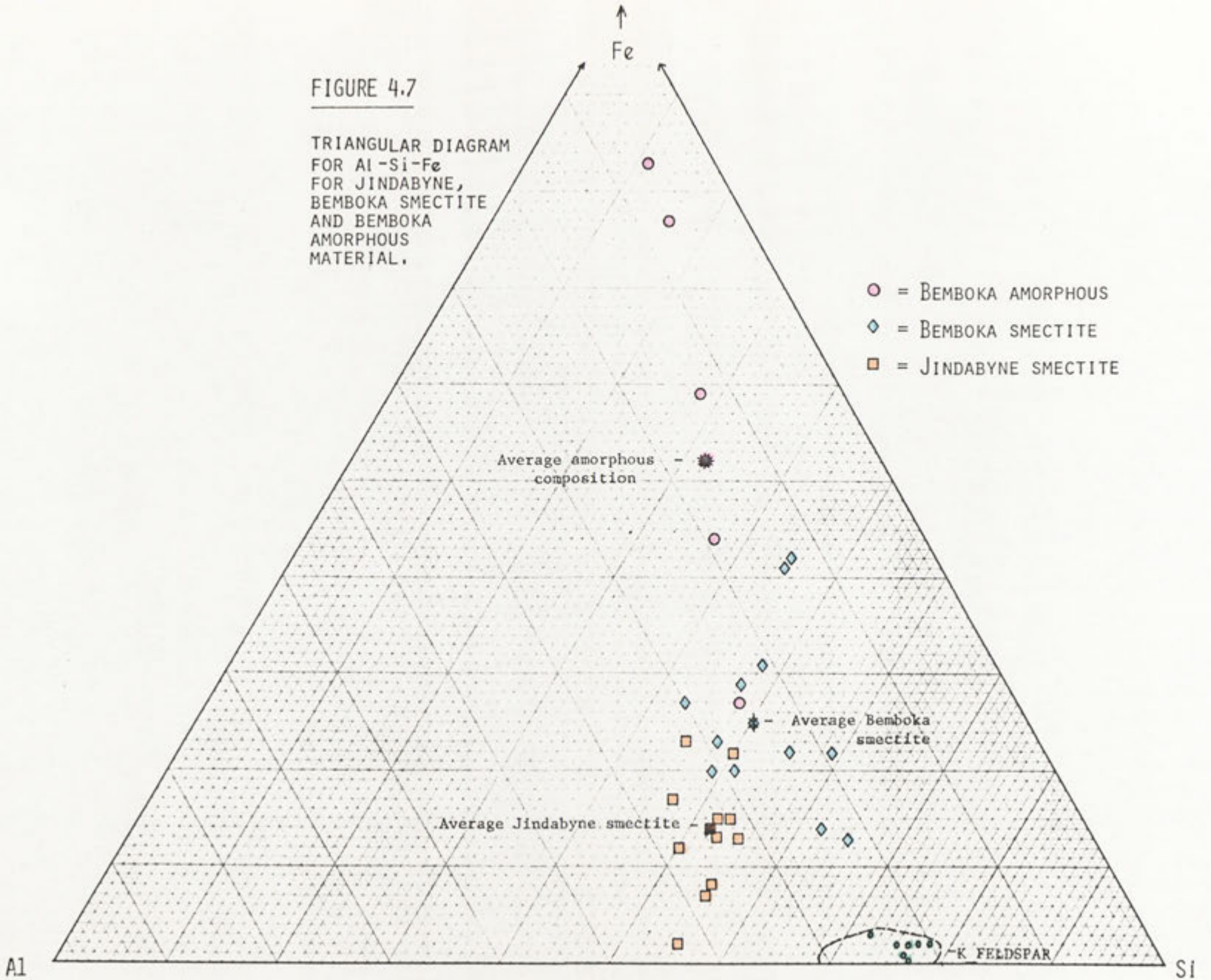

and often high Fe content of this material. Presumably with time and increasing Fe content, goethite will crystallize.

K-feldspar contains virtually no Fe. Consequently for the Fe present in the amorphous phase to be derived from feldspar by concentration, very large quantities of material would have to be consumed. As illustrated in Plate 4.34, this has not occurred, as smectite and amorphous material appear to have replaced about half the volume originally occupied by the feldspar. Analyses which were obtained from the marked areas in this photograph are amongst those included in Figures 4.6 and 4.7. It would appear, therefore, that Fe has been introduced to the altering feldspar from an external source, presumably by migrating solutions. This feature of K-feldspar weathering appears to be consistently noted in both the Bemboka and the Jindabyne profiles. It is not clear whether Fe is simply scavenged by the amorphous material, or if this element assumes a more active role in the weathering reaction.

Fe in K-feldspar weathering

Most models of feldspar alteration propose hydrolysis of water provides H^+ or H_3O^+, which disrupts the structure by bonding to oxygen atoms associated with tetrahedral Al. K then becomes redundant in the structure, and is released. This probably will not occur readily, as the K ion is large, an it is unlikely that it can be released without breaking several bonds in the feldspar structure.

It is possible to visualise a number of ways in which Fe may participate in the breakdown of K-feldspar. During the earlier stages of weathering a significant proportion of Fe is in the reduced state. Fe must be mobile at this stage as its abundance in the amorphous component and smectite indicates that it has been introduced. If solutions in this environment are not strongly oxidizing, Fe may be transported from sites of release in adjacent phases and be adsorbed, or bound to the K-feldspar surface as a hydrated Fe^{2+} compound. This will probably occur preferentially in regions where the presence of unsaturated Al tetrahedra at the surface present a locus of negative charge.

As weathering proceeds and permeability increases, oxygen will be

PLATE 434: K-FELDSPAR REPLACED BY SEMI-AMORPHOUS MATERIAL WHICH RECRYSTALLIZES TO FORM SMECTITE. ALTERATION PRODUCTS OCCUPY A SIGNIFICANT PROPORTION OF THE ORIGINAL VOLUME.

introduced in increasing abundance, and result in the transformation of Fe^{2+} to Fe^{3+}. This may be associated with the liberation of H^+. Such a reaction can be represented in simplified form by an equation between the feldspar surface, Fe, oxygen and water (Figure 4.8). H^+ or H_3O^+ may then participate in the breakdown of feldspar in the manner described by previous workers. The generation of H^+ is coupled with an increase in the charge on Fe, hence stronger bonds may develop between the surface oxygens and this ion. This could disrupt the surface bonding configuration and result in the incorporation of Fe into Si-Al-O polymers generated when feldspar bonds are broken and K released.

On the basis of an unexpected concentration of Fe at the interface between altering feldspar and clays a suggestion has been made as to a way in which this element may participate in the early stages of weathering. Such a concept can not be easily proven, particularly as scavenging of Fe may be a simpler alternative explanation. The proposition can, however, be tested to some extent as the mechanism places some constraints on the redox state of the profile during the early stages of weathering.

K-feldspar does not develop any appreciable quantity of secondary phases until relatively late in weathering. Consequently if Fe is to participate in this reaction in the manner described above, solutions must not become strongly oxidising until this stage. A late episode of oxidation is observed, probably corresponding with the development of abundant kaolin and goethite in biotite (see Chapter 5). In the Bemboka profile the FeO/total FeO ratios decrease gradually from .76 in fresh rock to .41, and then rapidly to .07 in very strongly weathered material. As discussed in Chapter 8, this does not reflect a preferential loss of Fe^{2+}, but does reflect oxidation of Fe; and is associated with an increased abundance of Fe^{3+}. Consequently, there are some data to support a changeover from mildly oxidizing conditions earlier in weathering to strongly oxidizing conditions at about the stage when significant breakdown and replacement of K-feldspar begins to occur.

An alternate role for Fe in the weathering of K-feldspar may involve oxidation of this element by introduced solutions, and generation of H^+. Hydrated Fe^{2+} may be scavenged by the amorphous material in which it is first detected. Subsequent oxidation of Fe may

FIGURE 4.8 A REPRESENTATION OF THE WAY IN WHICH Fe MAY PARTICIPATE IN THE BREAKDOWN OF K-FELDSPAR

$$2Fe(H_2O)_6^{++} + 1/2\ O_2 + (KAlSi_{2.75}O_8)^{-1} \Rightarrow (H_3O^+)\ AlSi_{2.75}O_8\ Fe_2O(OH)_3 + K^+ + 2H_3O^+ + 6H_2O$$

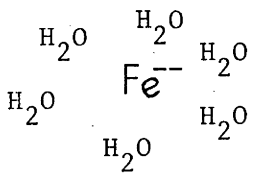

Fe introduced as a hydrated species in solution.

Unsaturated tetrahedra at the surface of K-feldspar.

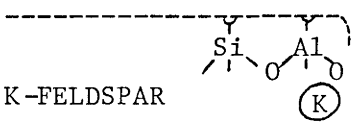

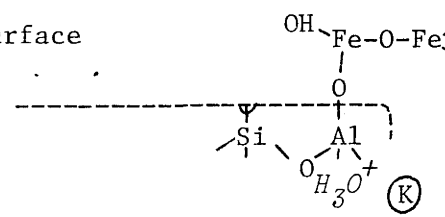

Al presents a locus of excess surface negative charge = 1, and distributed between the 4 oxygens.

Fe bonds weakly to the surface of the K-feldspar. Oxidation of Fe may result in the generation of H^+ according to the above equation.

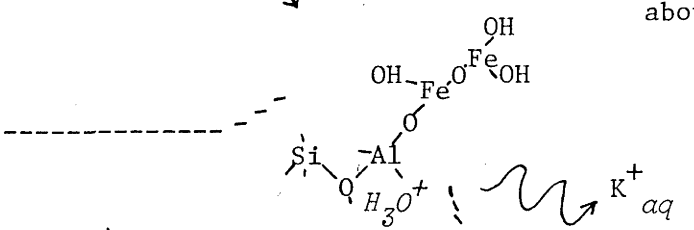

H^+ or H_3O^+ migrates through the structure and bonds to one or several of the O associated with Al tetrahedra. K becomes redundant in the structure, and is released into solution. Fe may become incorporated into products generated as the feldspar breaks down.

then provide a mechanism which initiates, or facilitates the crystallization of clay. This is consistent with the presence of Fe within the smectite structure.

Kaolin alteration products

Halloysite and kaolinite are also products of K-feldspar weathering. Spherical halloysite is fairly commonly developed in association with smectite, and appears to be derived from an amorphous precursor in a similar fashion to that described for plagioclase feldspar alteration (Plate 4.35). Some tubular halloysite also develops occasionally in more altered areas. In some cases this material can be observed growing outward from feldspar and spherical halloysite aggregates (Plate 4.36a).

Of the K-feldspar derived kaolin minerals, kaolinite is the most abundant. This phase develops in two forms, the first of which appears to be the end result of a series of transformations similar to those noted in plagioclase weathering. The second kaolin-like mineral has a different morphology, and is generally developed in zones of greater leaching.

The first form of kaolinite develops as irregular, often radiating laths late in K-feldspar weathering. Although this mineral is often associated with smectite and amorphous material the relationship between these phases is not clear. Kaolinite does not appear to crystallize from the amorphous material, but develops in areas adjacent to these reactions (Plate 4.36b). In other cases, kaolinite parallels the K-feldspar surface without displaying any clear association with any other alteration products (Plate 4.37a). The possibility that kaolinite crystallizes epitactically onto smectite is suggested to some extent by the morphology of the kaolinite (Plates 4.37b, 4.38a).

The second kaolin-like phase develops as crinkled films in cracks and channels within Bemboka K-feldspar (Plate 4.38b) quite early in weathering. Films which develop in these areas are composed primarily of Al, Si, Fe, and Mn, and minor K, Ti and Cl in some samples. The Al:Si ratio ranges from 1:1 up to 1.3:1, while Mn and Fe display dramatic variations in abundance. The chemistry, morphology, and distribution of this material closely resembles the black coating developed on crystals in strongly weathered Bemboka granite.

K-FELDSPAR DERIVED SMECTITE (S) CONVERTED TO SPHERICAL HALLOYSITE (H)

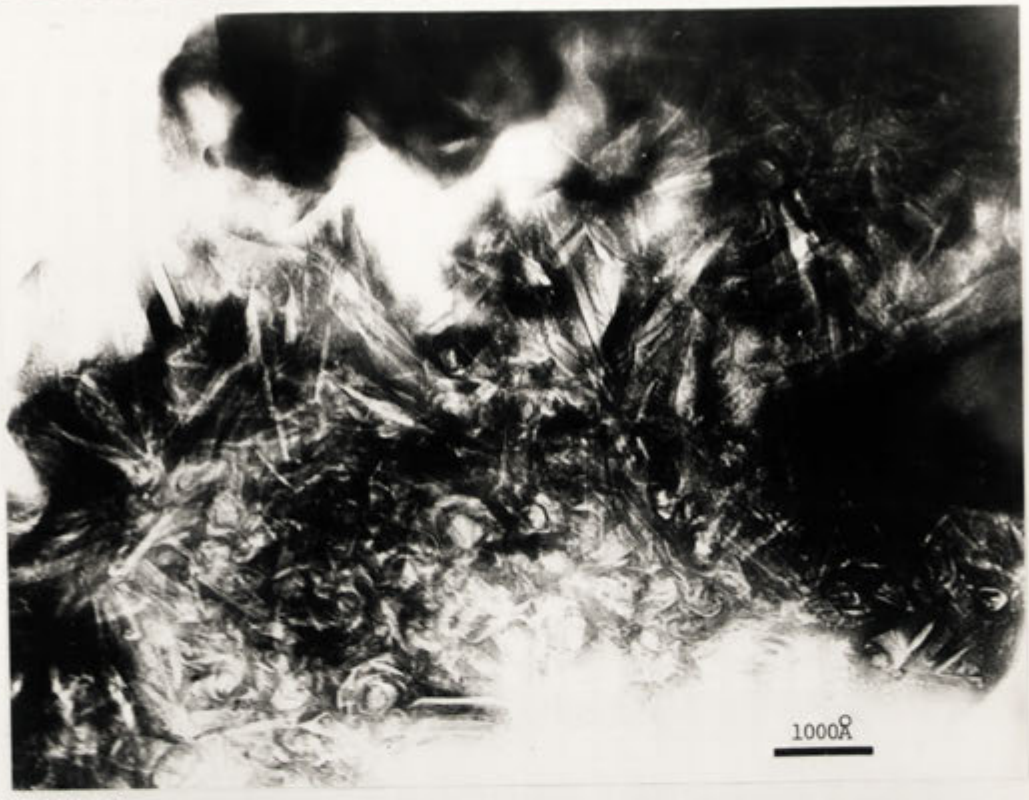

PLATE436A: HALLOYSITE TUBES AND SPHERICAL HALLOYSITE AGGREGATES.

PLATE436B: DEVELOPMENT OF KAOLINITE (BEAM SENSITIVE) IN AREAS ADJACENT TO SEMI-AMORPHOUS MATERIAL AND SMECTITE.

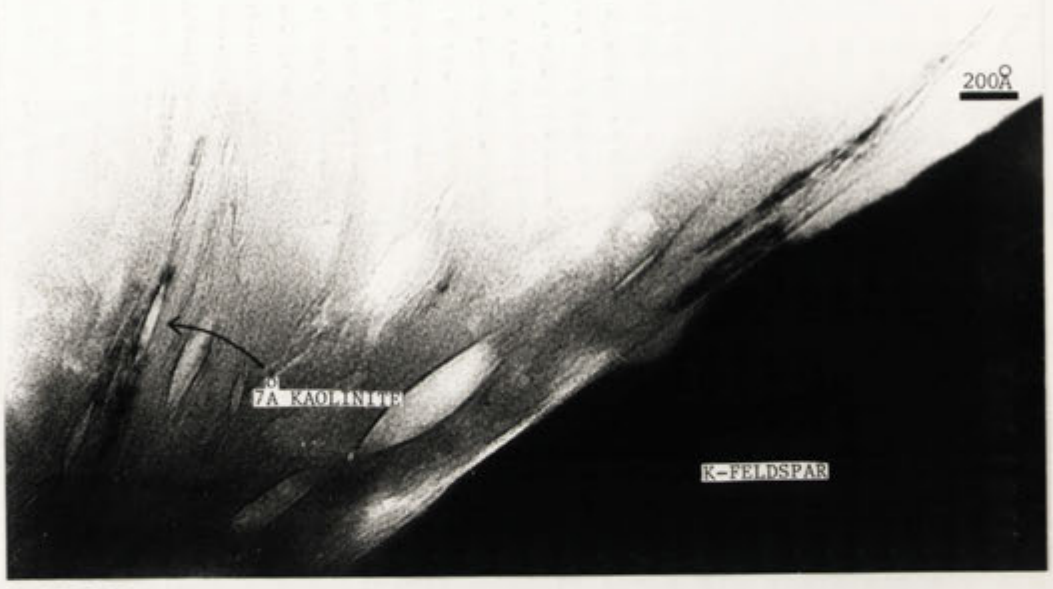

PLATE437A: KAOLINITE DEVELOPED PARALLEL TO THE FELDSPAR SURFACE.

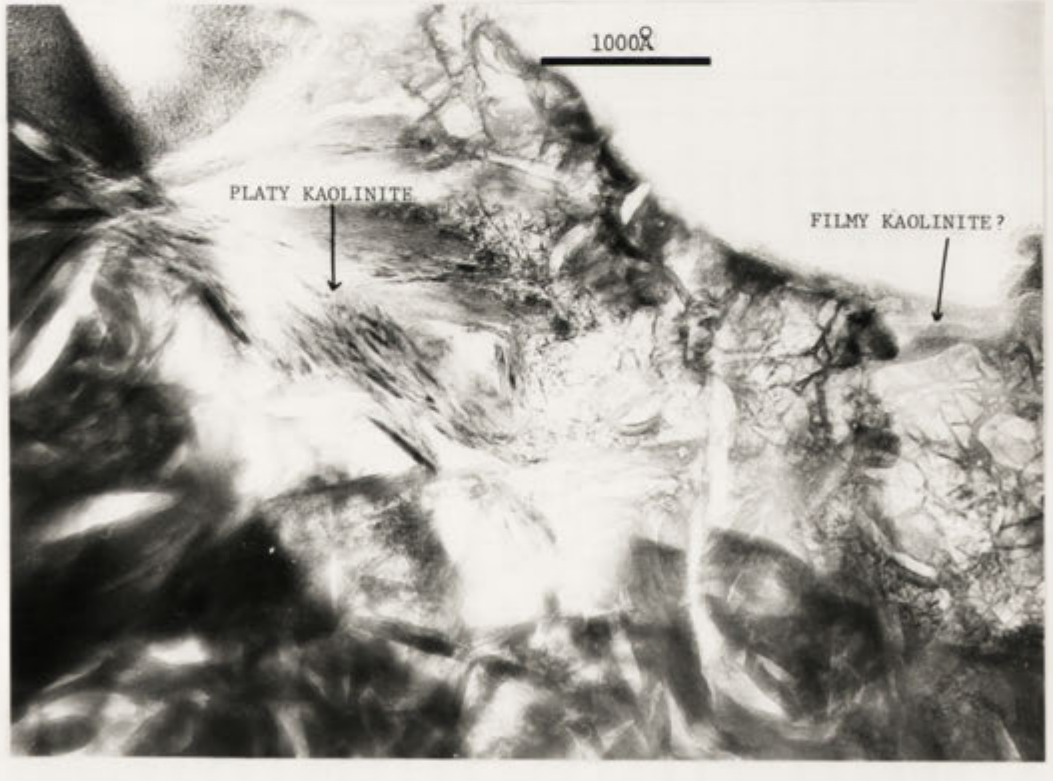

PLATE437B: PLATY KAOLINITE AND FILMY KAOLINITE-LIKE PHASE.

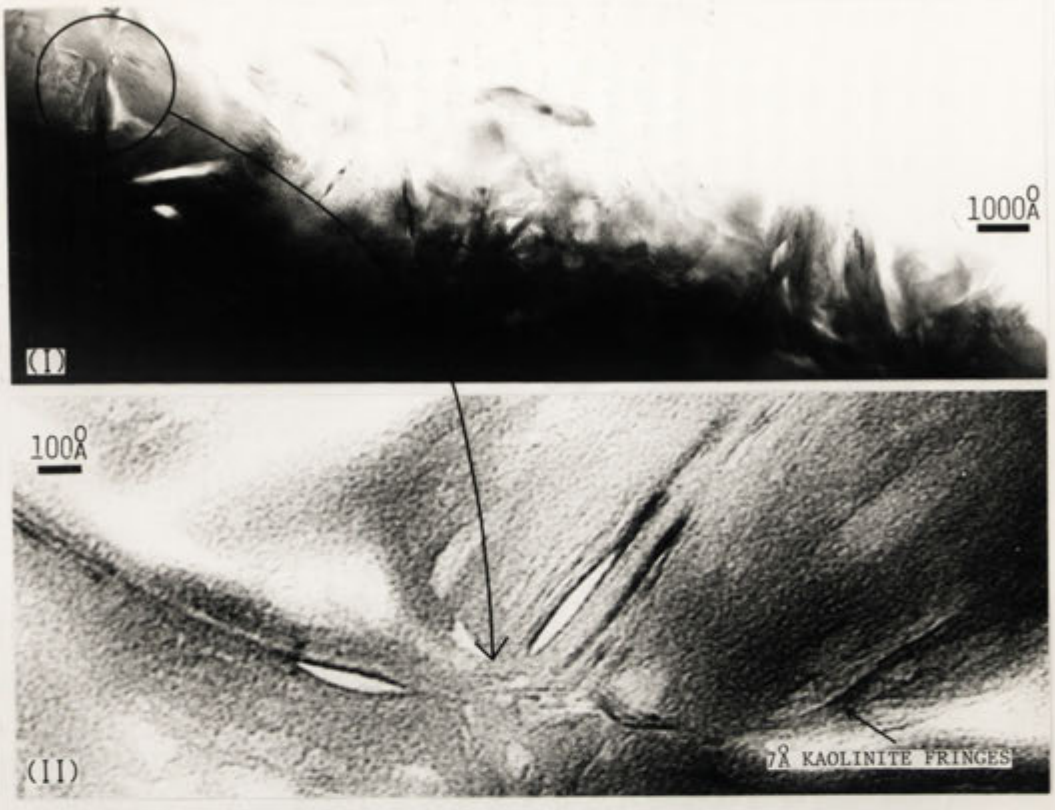

PLATE438A: GENERAL REGION OF FELDSPAR ALTERATION - (I). ENLARGEMENT OF KAOLINITE IN (I); - (II).

PLATE438B: FILMY KAOLINITE DEVELOPED TYPICALLY IN CRACKS AND CHANNELS.

SECTION 4.3

GENERAL COMMENTS AND CONCLUSIONS

A diagram describing the way in which feldspars and K-mica weather is given in Figure 4.9.

Both plagioclase and K-feldspar have been observed to alter initially to a relatively unstructured, or semi-amorphous material whose composition differs from that of the parent feldspar, and which recrystallizes to form smectite.

Several sequences of transitional phases have been observed to develop during the weathering of K-feldspar, plagioclase feldspar, and included K-mica. Some of these intermediate steps involve the direct transformation of structures, some require the development of amorphous or partly crystalline material, and others appear to proceed by dissolution and reprecipitation. These processes seem to allow sufficient change in chemistry for crystallization of new minerals to proceed. Transitional phases develop in a local environments where they are temporarily stable. These environments alter with further weathering, particularly with increased access of dilute oxygenated water. Consequently these phases provide only temporary sites for elements such as Ca, K, (Na), Mg, Fe, and Si, which are subsequently removed in solution, or precipitate as other alteration products.

The pathways of cations during weathering appear to be more complex than the stepwise progression described above. Mg and Fe are introduced in solution and incorporated to varying degrees in different phases. Fe is more abundant in the amorphous phase than in minerals which replace it. This element is included in plagioclase derived smectite to a lesser extent than K-feldspar derived smectite, yet more strongly than in mica derived smectite. Mg is incorporated into illite and illite derived smectite, yet not into plagioclase derived smectite to any significant extent. K is an important cation in all three smectites, and is a major component of two of the parent minerals. K is present in plagioclase in only minor quantities, and appears to be introduced to form the smectite which develops from this phase.

Not only are introduced components added differently to these

FELDSPAR WEATHERING - SUMMARY

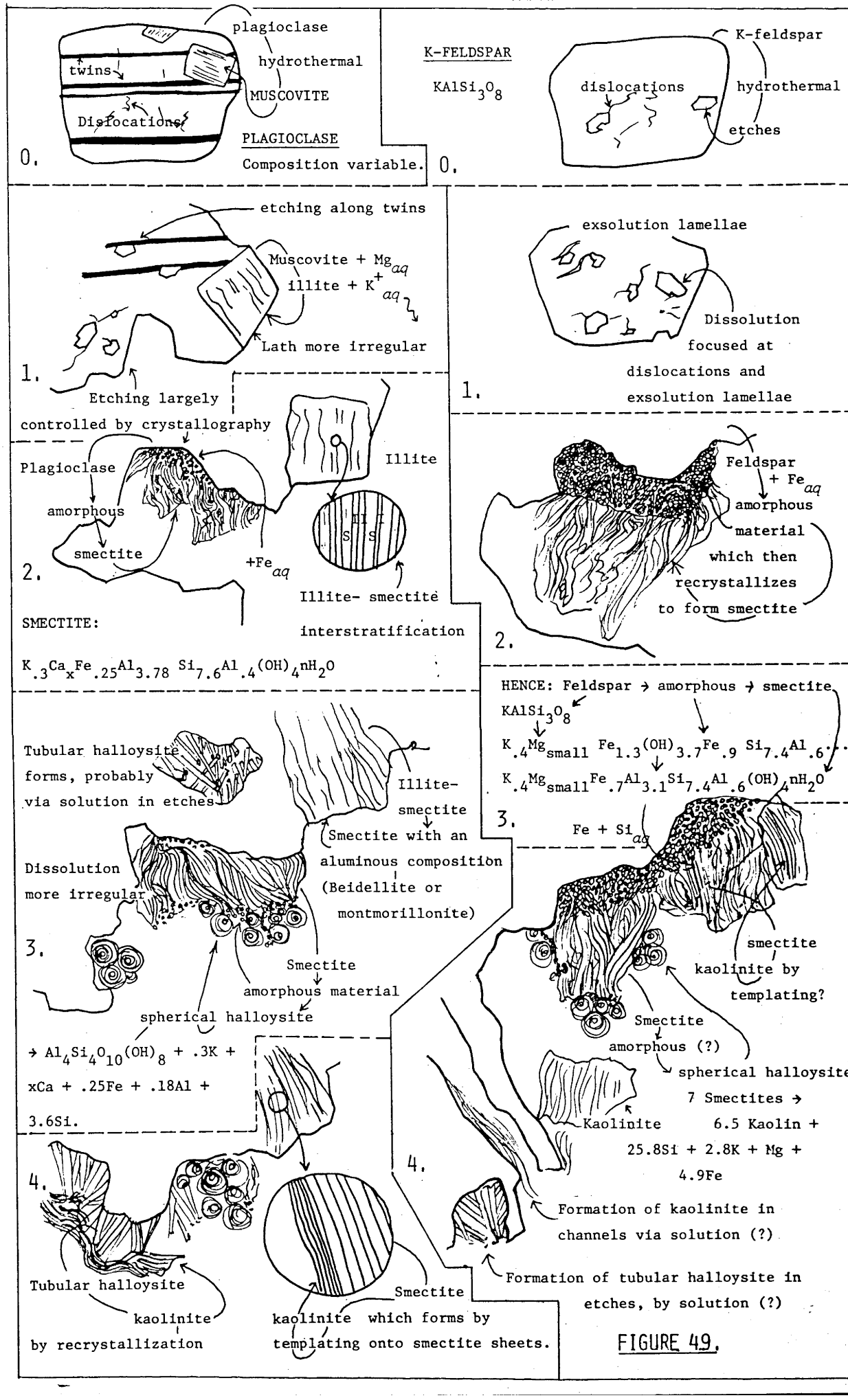

FIGURE 49.

alteration products, but each smectite phase retains the signature of its parent mineral. Consequently the plagioclase derived smectite is less aluminous, and more Ca rich than the muscovite derived phase, and more Ca rich than the K-feldspar derived smectite (which contains virtually no Ca). However, it is not clear whether Ca is completely accommodated by, or adsorbed onto plagioclase derived smectite, or whether it forms a separate phase.

The chemical distinction between the compositions of smectites produced by alteration of different minerals is retained although phases may exist in close proximity. This suggests that the distinctive chemistry of alteration products may not necessarily reflect development in different microenvironments, but may be a direct consequence of the nature of the parent phases. This control appears to be exerted regardless of whether transformations proceed by direct structural modification, via an amorphous stage, or possibly via solution.

A prediction that plagioclase feldspar will be replaced sequentially by smectite and kaolinite can be made by examination of phase diagrams such as those of Feth et. al. (1964), Loughnan (1969), Keller (1970), and those for higher temperature alteration (200°C) by Helgeson (1971). Similarly, the pathway for the replacement of muscovite by illite, smectite, and kaolin minerals can be traced on a $\log(aK^+/aH^+)$ vs $\log {}^{a}SiO_2$ diagrams such as those of Garrels (1984). Diagrams from the work of Keller (1970) and that of Garrels (1984) are presented in Figures 4.10a,b. The pathways on these diagrams appear to reflect the progressive change in composition of solutions within the rock during alteration, possibly reflecting increased porosity and throughflow of water as weathering proceeds. The overall trend is towards an assemblage of minerals which is in equilibrium with fluid with the composition of meteoric water (Figure 4.10c, from Loughnan, 1969).

Most phase diagrams constructed for the alteration of K-feldspar predict the development of K-mica or illite as the intermediate phase between feldspar and kaolinite (Figure 4.10d, from Keller, 1970). In the profiles examined in this study K-feldspar does not develop secondary phases until late in weathering. More efficient removal of K at this stage may promote the replacement of K-feldspar by smectite rather than illite.

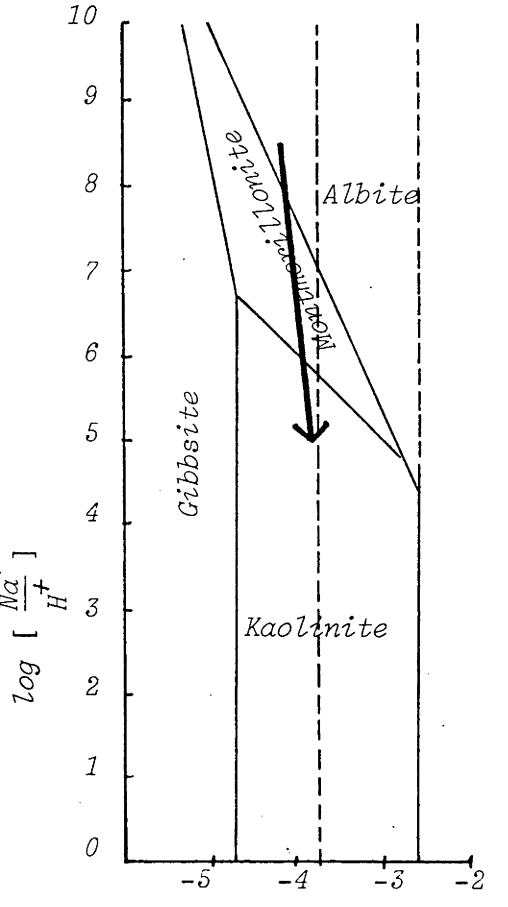

FIGURE 8A

Taken from Keller, 1970.

FIGURE 4.10

Theoretical pathways for mineral reactions. Arrows indicate sequence of phases observed. 8a: Plagioclase, 8b: Muscovite 8c: K-feldspar.

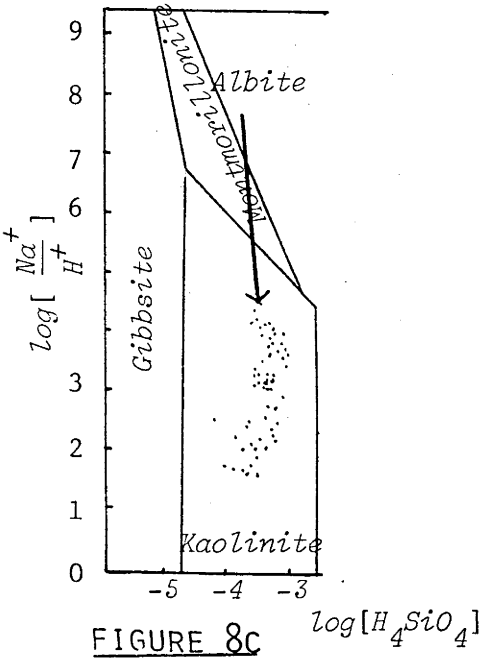

FIGURE 8C

Taken from Loughnan, 1969.

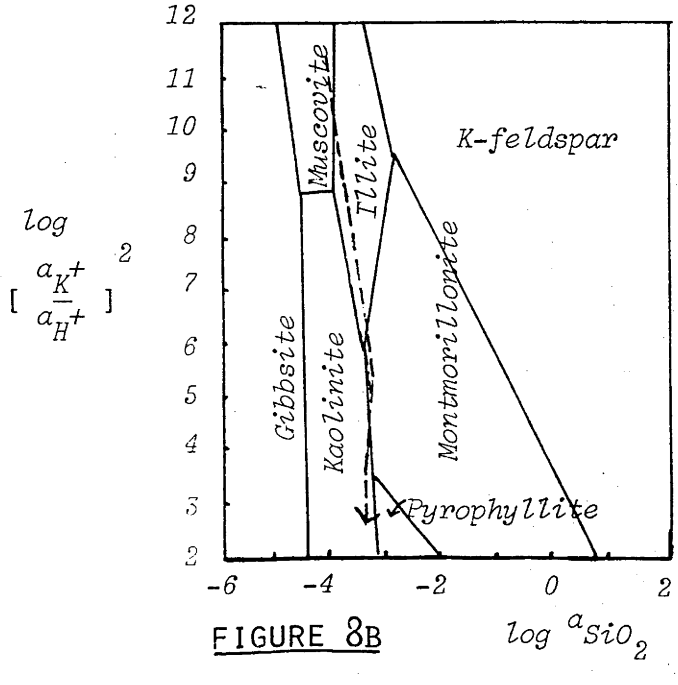

FIGURE 8B

Taken from Garrells, 1984.

A number of models have been advanced to explain the relationship between the various forms of halloysite, kaolin and amorphous material. Tazaki (1978) noted that amorphous or allophane material merged to form crinkled sheets containing over 10% FeO. Tazaki proposed that sheets transform to spherical particles by reduction of Fe. As tubular halloysite did not contain appreciable Fe, Tazaki proposed that these tubes formed from an Fe poor parent, or by removal of Fe from the crinkly film. Wilke et. al. (1978) claim that different degrees of enrolment result in the formation of platy, tubular, and spheroidal halloysite. Nagasawa and Miyazaki (1976) suggested that the morphology of halloysite is closely related to its genesis. Balls and scrolls were developed by alteration of pyroclastics, whereas long tubes formed by weathering of granitic feldspar. Kurabayashi and others (in Sudo and Shimoda, 1978) described a sequence where (rhyolitic) glass transformed into allophane then to 'chestnut-shell' like particles which subsequently formed 10 Å tubular halloysite. Minato (1981) proposed that kaolinite formed from more acidic solutions than halloysite.

It can be seen that many suggestions have been advanced to explain the development, coexistence, and distribution of various forms of kaolin. These include varying Fe content, degree of enrolment, origin of parent material, degree of evolution of form, and acidity of altering solutions. Within the sequences examined in this study there is some evidence to suggest that three separate mechanisms are responsible for the development of three distinctive kaolin types. Spherical halloysite is observed to crystallize from an amorphous or semi-amorphous precursor; tubular halloysite develops as a space filling phase, growing outward, probably via solution from corroded feldspar surfaces; and kaolinite appears to crystallize by templating onto existing sheet silicate phases. No chemical distinction between these forms of kaolin could be detected using the STEM whose spot size for analysis is apparently comparable with that of a single spherical halloysite particle. These crystallization mechanisms appear to provide a means by which the development and distribution of the different forms of halloysite can be explained within altering feldspars. The extent to which this provides a general explanation for the coexistence of these phases is not known.

Chapter 5

BIOTITE WEATHERING

ABSTRACT

Many studies have been made of the way in which biotite weathers, and the phases which are produced by this reaction. These studies have generally relied upon XRD, optical microscopy, mineral chemistry, and rarely, electron microscopy. A variety of experimental approaches have been used to explain aspects of this reaction. In the following chapter transmission electron microscopy is combined with more conventional methods of investigation to illustrate the way in which biotite weathers. The study of this process has concentrated upon examination of biotite from the Jindabyne profile as this phase contains only very minor quantities of metamorphic chlorite.

Biotite is the only abundant sheet silicate phase in the granitic rocks studied, and as such is the only major mineral which has a structure which facilitates direct transformation to secondary clay minerals. Examination of this process indicates that dissolution is the initial stage, resulting in the removal of quite appreciable quantities of material. In rare cases prismatic etch pits filled with amorphous material and crystallizing clays are recognised. Generally however, biotite is transformed to vermiculite by direct modification of the layer structure.

In most cases where the conversion of biotite to vermiculite is observed at the unit cell level it would appear that K is removed and replaced by hydrated interlayer cations which are introduced, apparently from adjacent areas where dissolution has occurred. A second mechanism is suggested by the presence in some areas of a second biotite sheet which terminates where vermiculite is initiated. This gives rise to a model where two biotites are replaced by one vermiculite layer.

Regardless of whether one or two biotites are replaced by a

vermiculite sheet, a volume change must occur in the immediate vicinity of the reaction. To minimise disruption of the structure it would appear that adjacent transformations commence, and proceed initially in opposite directions, the second layer possibly altering in response to the disruption caused by the first. Further propagation of these vermiculite layers to complete the conversion of the sheets allows weathering of the biotite to proceed with minimal disruption of the structure. Distortion induced alteration may also possibly contribute to the development of an early, reasonably regular interstratification of vermiculite and biotite. Wedge shaped gaps also develop, and serve to remove distortion caused by transformations.

Biotite is also replaced by kaolin and goethite. These phases appear only in minor quantities early in weathering; goethite at this stage tends to be poorly crystalline. Kaolinite initially crystallizes epitactically onto existing sheet silicate layers, while goethite develops from an amorphous, or semi-amorphous precursor to form laths which are generally oriented perpendicular to enclosing sheets.

Weathering of biotite proceeds by the development of a series of fairly regularly interstratified vermiculite-biotite phases which display an increasing vermiculite content as weathering proceeds. In the later stages kaolinite and goethite dominate the weathering assemblage. An equation representing the maximum stoichiometry of one biotite replaced by one kaolinite and two goethite unit cells can be written, conserving both iron and aluminium. Some evidence can be observed in TEM images to support the development of kaolin and goethite in approximately these proportions.

Chlorite is unstable in the weathering environment, and can be observed in the optical microscope to be replaced by an orange phase. Although vermiculite is the commonly reported alteration product of chlorite, and replaces this phase where it is hosted in amphibole, no evidence is observed for the conversion of biotite derived chlorite to vermiculite. Some evidence is observed for the replacement of this phase late in weathering by goethite, and kaolinite which grows, apparently epitactically onto chlorite sheets.

SECTION 5.1

BIOTITE WEATHERING

PREVIOUS WORK

The alteration of biotite has been studied by many workers, particularly over the last twenty five years. This topic has attracted interest as biotite is an important source of K in soils, hence factors affecting the breakdown of this phase exert some influence upon soil fertility. Attempts to understand this process have been made by observation of naturally weathered materials, and by studying the artificial alteration of mica in the laboratory.

.1 Products of natural weathering:

Published accounts of the development of weathering products under a range of environmental conditions include those of Walker (1949); Coleman et. al. (1963); Wilson (1966, 1970); Ojanuga (1973); Rimsaite, (1975); Stoch and Sikora (1976); Meunier and Velde (1978); Gilkes and Suddhiprakarn (1979). These authors identified a range of phases developed as a result of weathering of biotite, including variously interstratified biotite and vermiculite; chlorite-vermiculite (a soil chlorite described as Al-hydroxy- interlayered vermiculite by Farmer pers. comm; 1984) vermiculite; kaolin minerals; Fe- and Ti- oxides (generally goethite, hematite, and anatase); and gibbsite. Montmorillonite has also been identified as an alteration product of biotite in poorly drained soils (MacEwan, 1953). The variety in the assemblage of phases observed led to the suggestion that biotite weathering resulted in different end products under differing weathering conditions, (eg. Wilson, 1966). Conversely, Meunier and Velde (1978) found that although final products of biotite weathering were the same, the nature of the intermediate phase varied as a result of changes in the chemical environment such as variation in the composition of the altering fluid.

The development of biotite alteration products whose orientations were controlled by the parent phase has been noted in a number of studies. For example, Wilson (1966) describes the epitactic crystallization of gibbsite and kaolinite onto biotite. Gilkes and Suddhiprakarn (1979) noted the orientational relationship between the

parent phase and secondary products applies not only to clays, but also to goethite. This phase crystallizes with goethite z / biotite y, presumably by nucleation of octahedral chains parallel to octahedra in biotite.

.2 Hydrothermal weathering products; Weathering of chlorite:

Products of the hydrothermal alteration of biotite include chlorite, sphene, rutile, carbonate, epidote, and magnetite, (Sales and Meyer, 1948; Schwarz, 1958; Ferry, 1979; Pary and Downey, 1982; Eggleton and Banfield, in press). Alteration facies of biotite distributed in a granite were described by Parneix and Meunier (1982) who reported that propylitic alteration (220-280°C) resulted in the replacement of biotite by magnesian chlorite and Fe-Mn chlorite associated with Fe rich epidotes. Lower temperature (<100°C) argillic alteration resulted in the development of chlorite-smectite-calcite, and kaolinite-K-beidellite-carbonate assemblages. Under weathering conditions chlorite was replaced by a vermiculite like mineral and Fe-oxides. Several other studies of the reactions of chlorite to weathering products (primarily vermiculite-chlorite intergrade phases and vermiculite) have been made. This literature will be discussed in Chapter 6, where weathering of amphibole derived chlorite is considered.

.3 Experimental studies:

The mechanisms by which micas weather to vermiculite have been studied by examining the artificial weathering of micas using a number of reagents and techniques. Norrish (1972) discussed much of this work and noted that the form of artificially weathered mica differs from that of naturally weathered micas. On this basis he suggests that a difference may exist between laboratory and natural weathering, possibly as a result of the dramatic way in which the laboratory transformation occurs. These studies, however, provide valuable insights into several important aspects of the biotite-vermiculite reaction. In particular, they contribute explanations for the ease of removal of K, describe the effect of the K concentration of the solution, and offer mechanisms for charge reduction and interlayering.

In a summary of the conclusions of this experimental work, Norrish (1972) notes that micas will exchange their interlayer K with hydrated cations from solution to produce an expanded lattice. The exchange

appeared to be diffusion controlled and was observed to proceed inwards in an orderly manner from the margins of the crystal. He suggested that the fast exchange of K in biotite was due to the orientation of the (OH) bond, which is normal to the silicate sheet. As the proton is then close to the interlayer K this element is held less firmly than, for example, in muscovite, where the inclined orientation of the (OH) allows a greater bond strength due to the separation of the cation and proton.

The sensitivity of the reaction to large monovalent cations in solution (particularly K) is stressed by Rausell-Colom et. al.(1965). These authors proposed that this was the most important property of micas during weathering, explaning the slow rate of natural weathering, the development of interstratification, and the tendency of alteration to concentrate in areas where interlayer regions have already been opened up.

Formation of vermiculite is associated with a decrease in layer charge, generally attributed to oxidation of ferrous to ferric iron. Norrish (1972) examined the chemistry of a large number of vermiculites and concluded that data supported the view that in the natural weathering of biotite to vermiculite charge reduction is primarily due to, and does not exceed the oxidation of ferrous iron. Farmer et. al. (1971) noted that biotite can be converted experimentally to vermiculite with little oxidation of Fe. Furthermore, Farmer (pers. comm., 1984) suggested that opening up of the interlayer must occur before Fe can be oxidised. Oxidation of Fe may be accommodated by one of three mechanisms: loss of interlayer cations, loss of hydroxyl protons, or loss of octahedral Fe, (Farmer et. al., 1971). These authors presented evidence to suggest that oxidation of Fe is compensated first by loss of protons, and subsequently by loss of octahedral Fe.

Regularly interstratified micas (hydrobiotites) are commonly listed among the weathering products of biotites. A mechanism to explain the development of interlayering was advanced by Norrish (1972). He proposed that as the (OH) bond direction changes in the absence of K (Serratosa and Bradley, 1958), there may be an associated decrease in the angle of the (OH) bond of the other hydroxyl attached to the same octahedral cation (facing the adjacent interlayer). As bonding of interlayer K is dependent on the (OH) orientation, reduction in the other (OH) bond angle will result in stronger bonding of the K in the

adjacent sheet. This may result in the development of regular interlayering.

.4 Concluding remarks:

It would appear that the way in which biotite weathers is controlled firstly by the structure of the sheet silicate, where the orientation of the (OH) bonds facilitate the early removal of K. In the absence of K the (OH) bond may readjust, possibly resulting in firmer bonding of K in the adjacent layer, and explaining the tendency of biotite to weather to a regularly interstratified phase. These processes may be associated with oxidation of Fe in the octahedral layer, apparently accounting for the decrease in layer charge associated with the formation of vermiculite.

Differences in the exact nature of the alteration products are reported to reflect changes in the weathering environment. Factors include efficiency of removal of K, composition of the altering solutions, and pH. Norrish (1972) noted that the effect of pH is complex, H may cause destruction of the structure, and possibly increase the exchange rate. The extent of weathering also appears to dictate the weathering products observed. Although kaolinite and oxides begin to form early in weathering, these phases are reported to dominate the final assemblage, (eg. Meunier and Velde, 1978).

One other factor, metamorphic preconditioning, is reported to exert a control on biotite weathering. Meunier and Velde (1978) for example, noted that biotites which have undergone a slight metamorphism alter more completely, and at an earlier stage than their unmetamorphosed counterparts.

BIOTITE WEATHERING

SECTION 5.2

INTRODUCTION:

Although compared with other granitic minerals, biotite begins to weather relatively early, alteration initially proceeds slowly. It is not until quite late in weathering that replacement by secondary phases becomes pronounced.

Examination of biotite in an optical microscope indicates that the extent to which biotite is weathered and the stage at which alteration occurs is affected both by previous metamorphic alteration and proximity to other phases in the granite. The presence of chloritic layers in the biotite structure apparently promotes the development of secondary phases, (Plate 5.1A), probably due to increased access of solutions. Where biotite is in the vicinity of minerals which alter early in weathering, particularly amphibole, replacement is noticeably more pronounced (Plate 5.1B). However, no evidence has been found to suggest that chloritic layers in the biotite, or amphibole close to it change either the process by which weathering occurs, or the phases which are produced.

X-RAY DIFFRACTION

The alteration products of biotite were identified by XRD. Samples were prepared by handpicking crystals of biotite from granite which had undergone various degrees of weathering. Standard procedures, such as those documented in Brindley and Brown (Eds., 1980), were used to establish the identity of phases. Figure 5.1 presents some of this data. These results indicate that early in weathering vermiculite is the only phase developed in sufficient abundance to be identified. Kaolin becomes increasingly abundant with subsequent weathering, as does vermiculite (and goethite). In more strongly weathered material there is an asymmetric widening of the 10 Å peak towards the 14 Å peak, and eventually a discrete 12 Å peak can be recognised. This is interpreted to reflect the formation of interstratified biotite and vermiculite. Halloysite appears to be a minor component of the alteration assemblage, and was diagnosed using the formamide treatment advocated by Churchman et. al.(1984). Goethite peaks were detected in some cases. These peaks

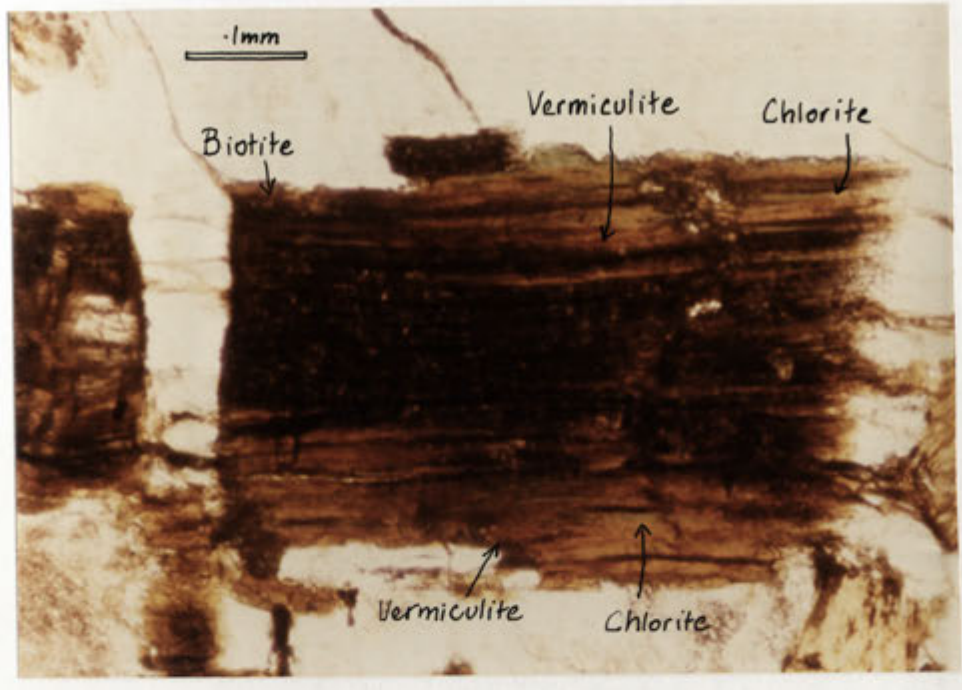

PLATE 5.1A: Biotite is more extensively weathered where it contains metamorphic chlorite.

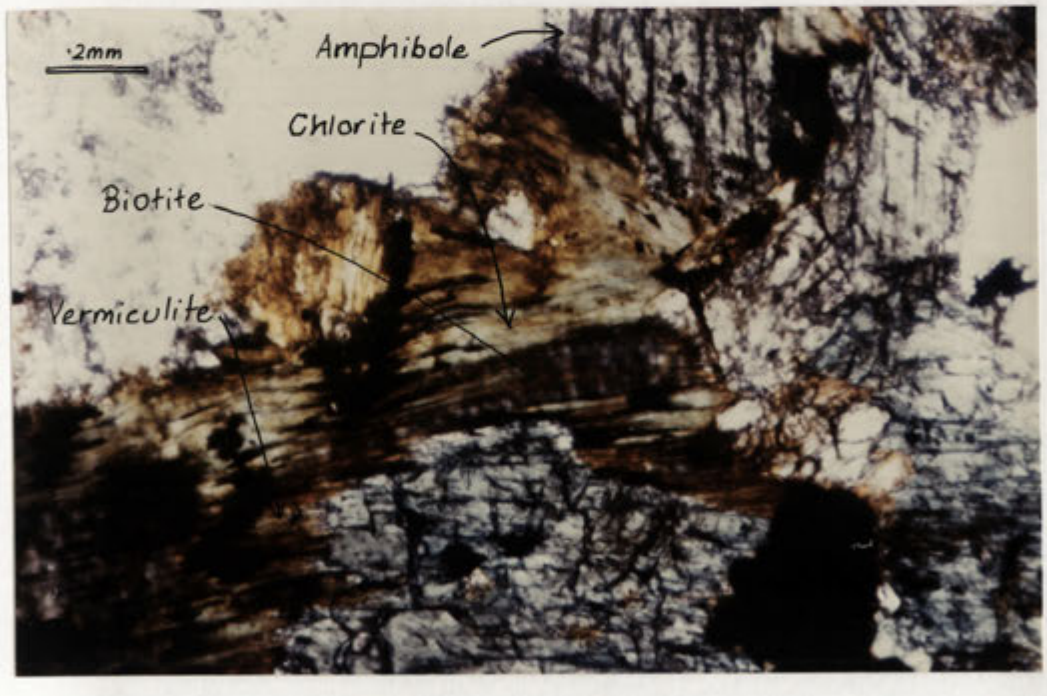

PLATE 5.1B: Biotite is more weathered where it is close to amphibole crystals.

BIOTITE WEATHERING-SUMMARY X.R.D. SCANS.

FIGURE 5.1

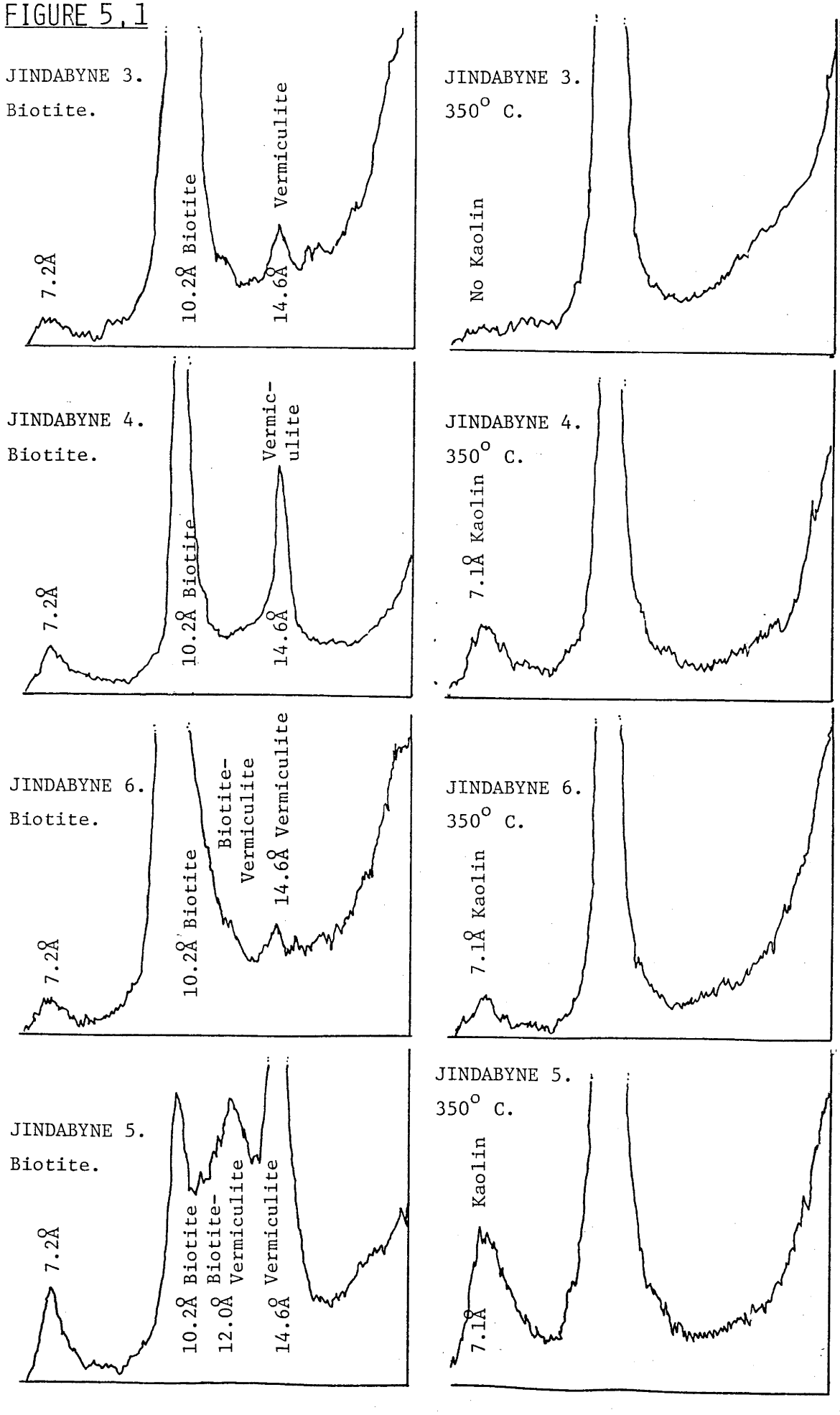

were broad and not well defined, indicating the poorly crystalline nature of this phase.

SECTION 5.2.1

EARLY STAGES OF WEATHERING

The initial stage of biotite weathering is characterised by the development of occasional elongate, prismatic etches. These etches form by destruction of biotite layers, and their long dimensions parallel enclosing sheets. Apparently amorphous material may develop in these etches and recrystallize to form clays (Plate 5.2A). As shown in this plate, clays are characterised by 12-14 Å lattice spacings, suggesting that they may be either vermiculite or smectite.

More commonly, long, extremely narrow zones develop within the biotite where alteration has either resulted in the removal of material in solution, or in the development of an amorphous phase which also recrystallizes to form clays, (Plate 5.2B).

Destruction of biotite and removal of material in solution is an important stage early in biotite weathering. This provides components for the formation of vermiculite, space to accommodate volume changes, and increased access of solution to the lattice. TEM evidence suggests that dissolution is concentrated in clearly defined zones where disaggregation is accompanied by the development of wider, and brighter interlayer regions. Termination of sheets is commonly observed, indicating that dissolution of individual layers may be an important early step. This results in distortion of surrounding sheets and the development of channels, probably further accelerating the process (Plate 5.3).

SECTION 5.2.2

MAIN STAGE OF BIOTITE WEATHERING

.1 THE BIOTITE - VERMICULITE STAGE:

It would appear that where weathering can proceed rapidly, removal of material in solution and the development of an amorphous phase are the predominant processes. Where weathering proceeds slowly biotite is

5.2.1: PRISMATIC ETCH IN BIOTITE CONTAINING AMORPHOUS MATERIAL (↓) AND NEWLY CRYSTALLIZING CLAYS.

5.2.2: ZONE WITHIN BIOTITE WHERE BIOTITE HAS APPARENTLY BEEN CONVERTED TO SEMI-AMORPHOUS MATERIAL (↑) WHICH SHOWS SOME DEVELOPMENT OF NEWLY CRYSTALLIZING CLAYS.

5.3.1: ZONE OF DISAGGREGATION AND DISSOLUTION OF BIOTITE.

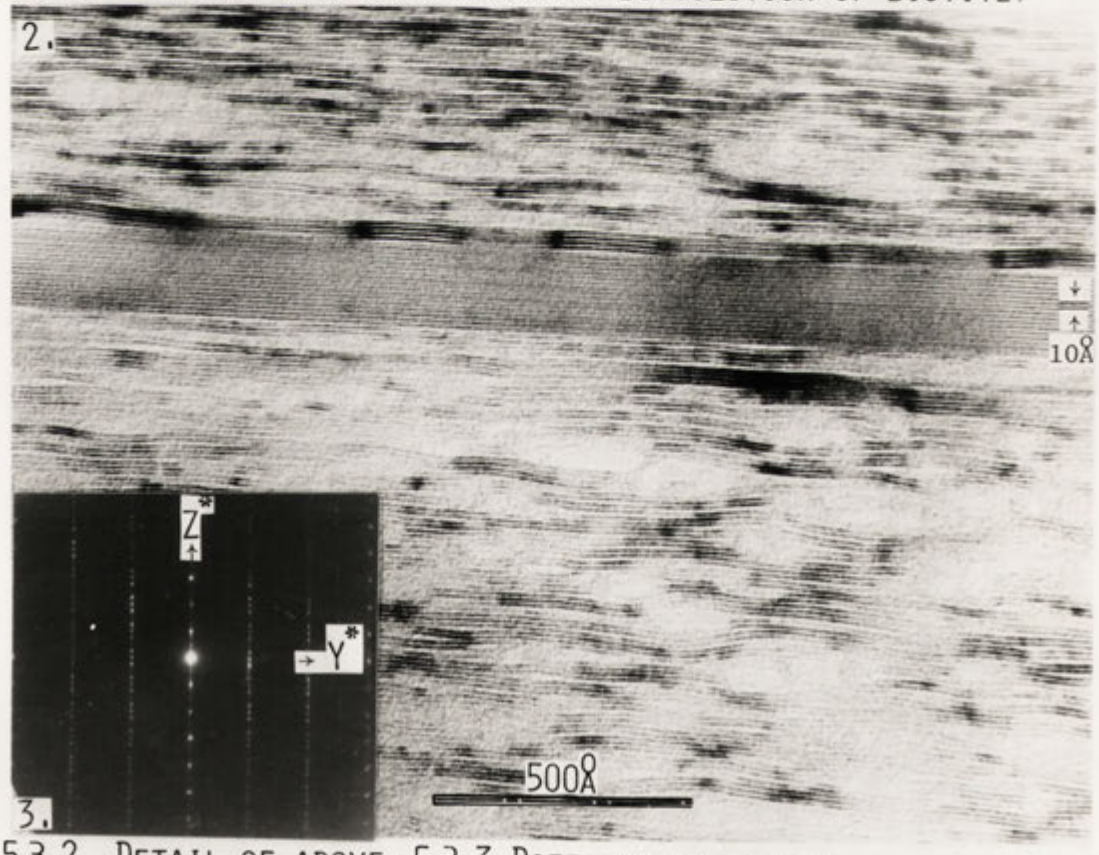

5.3.2 DETAIL OF ABOVE. 5.3.3 DIFFRACTION PATTERN.

converted to vermiculite by direct modification of the structure. In electron micrographs this conversion appears to proceed by replacement of K by hydrated cations which swell the layer from 10 to 14 Å (Plates 5.4 and 5.5). A second mechanism also appears to operate occasionally, and involves the conversion of two biotite layers to one vermiculite layer, (Plates 5.6 and 5.7). The presence of the second biotite sheet before the appearance of the vermiculite can not be firmly established as vermiculite may simply have developed by the first mechanism at an edge dislocation. The dislocation could have provided a pathway for the introduction of cations and water, and thus acted to focus alteration. It would appear, however, that the very gradual reduction of the second biotite sheet, and the apparent continuity of the reduced layer with the vermiculite (also see Plate 5.10B) supports the view that one vermiculite is actually replacing two biotites.

The development of a brighter interlayer region in electron micrographs of biotite just prior to replacement by vermiculite is observed in some cases, and may be associated with an increase in layer width from 10 Å to 12 Å (Plates 5.8 and 5.9A). Brighter interlayer regions are interpreted to reflect lower electron density, hence the appearance of these immediately before the appearance of a recognisable vermiculite layer may indicate that K has been removed. The increase in layer width which accompanies this may result from the partial hydration of the region, or be a consequence of decreased cohesion between the layers. In the later case the increased width of the interlayer zone may serve to accommodate some deformation resulting from the development of vermiculite.

A link between the distortion of the lattice surrounding the initiation of one vermiculite layer, and the initiation of a second layer is suggested by observations such as those illustrated in Plate 5.9. The layers immediately adjacent to the expanding layer remain attached, and bend around the distortion. This flexure is commonly transfered through the structure for a few unit cells, (often less than 10) until another biotite is converted to vermiculite. This second vermiculite initially propagates in the opposite direction, hence effectively reduces the distortion. The replacement of the remainder of these layers can subsequently proceed with minimal disruption of the surrounding region.

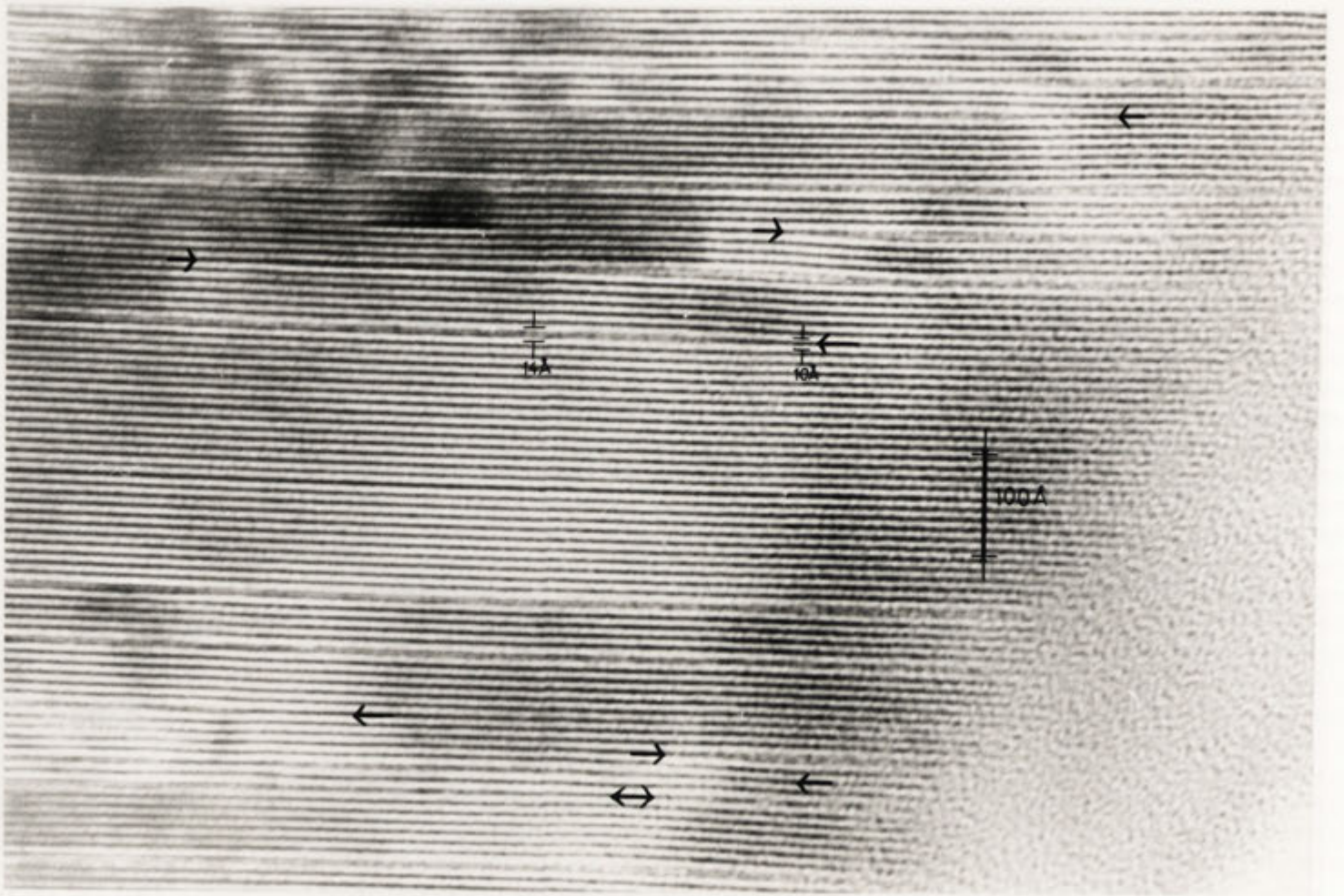

Plate 5.4:
Biotite converts directly to vermiculite by introduction of cations and water which swell the layer.

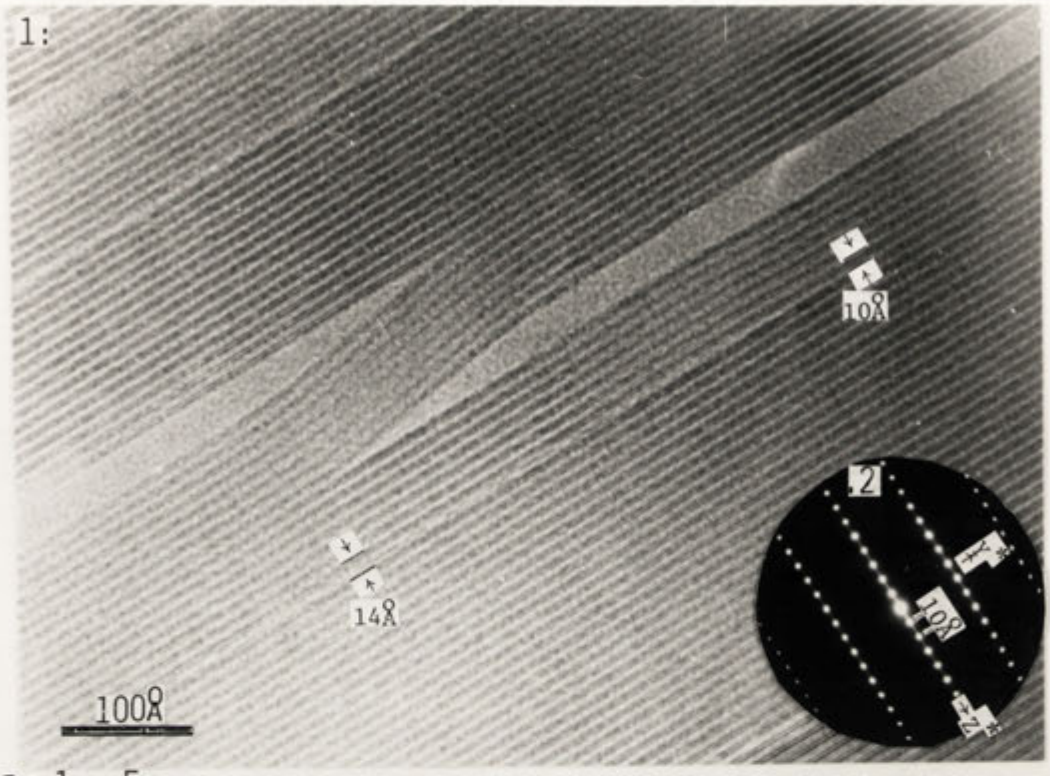

5.5.1: FORMATION OF ONE VERMICULITE LAYER BY DIRECT MODIFICATION OF AN EXISTING BIOTITE SHEET. 5.5.2: DIFFRACTION PATTERN.

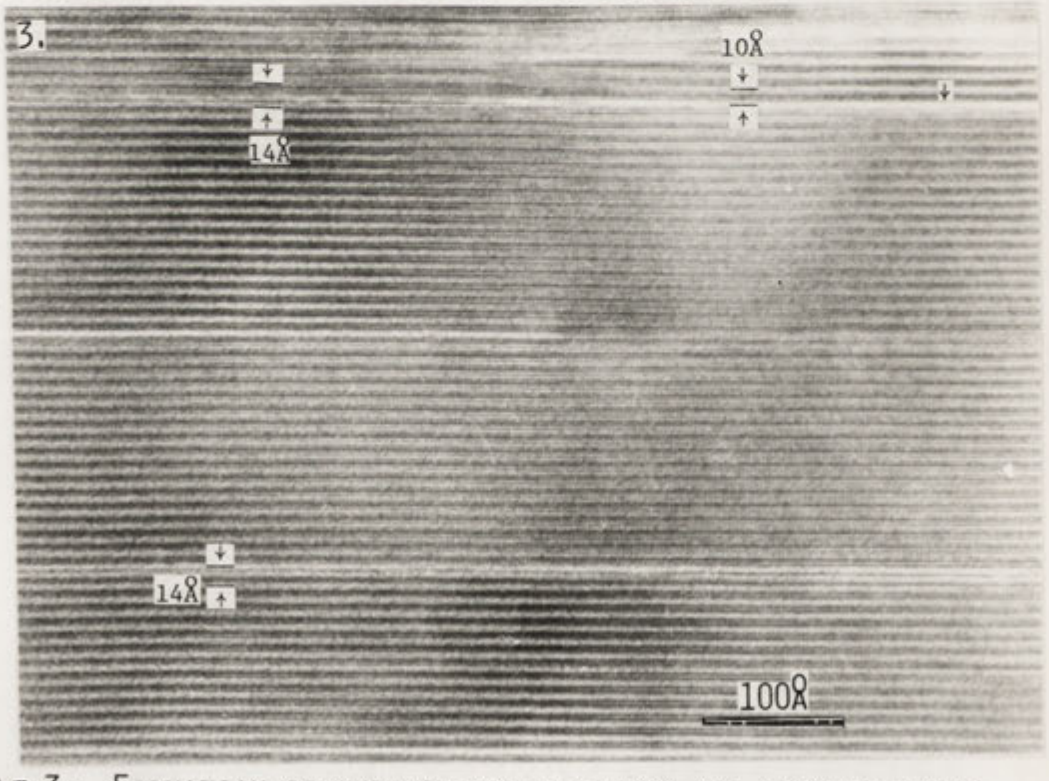

5.5.3: FORMATION OF ONE VERMICULITE FROM ONE BIOTITE LAYER. A BRIGHTER INTERLAYER ZONE IS PRESENT PRIOR TO THE FORMATION OF VERMICULITE, (↓).

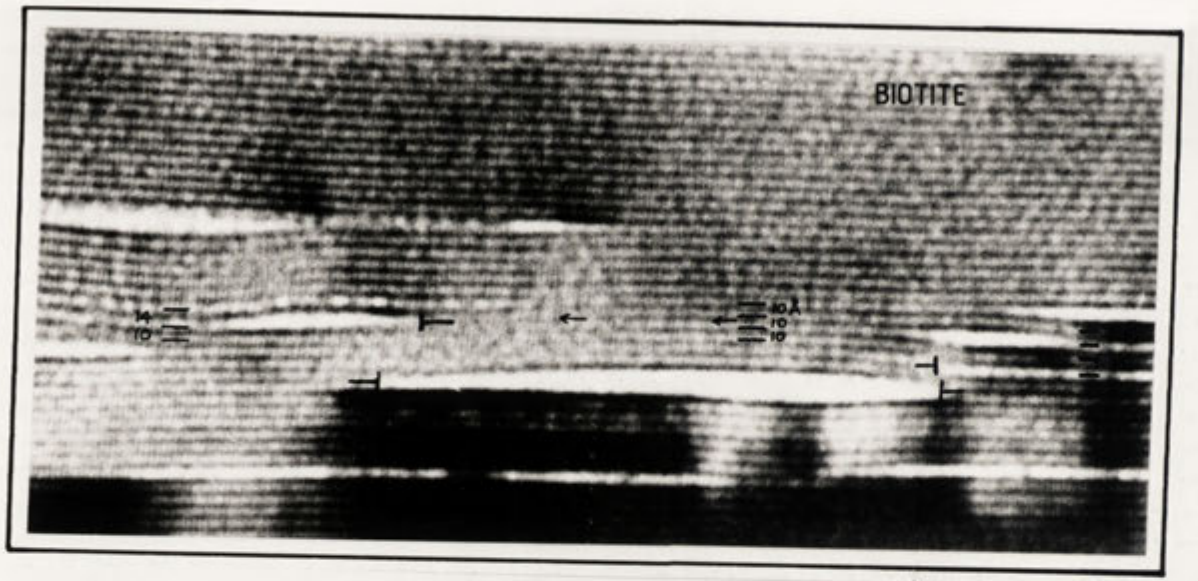

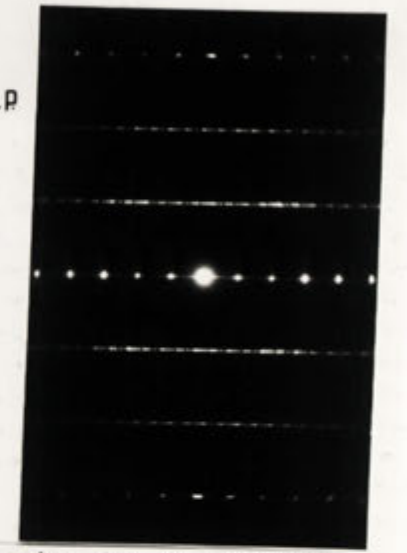

Plate 5.6: Biotite altering to vermiculite.

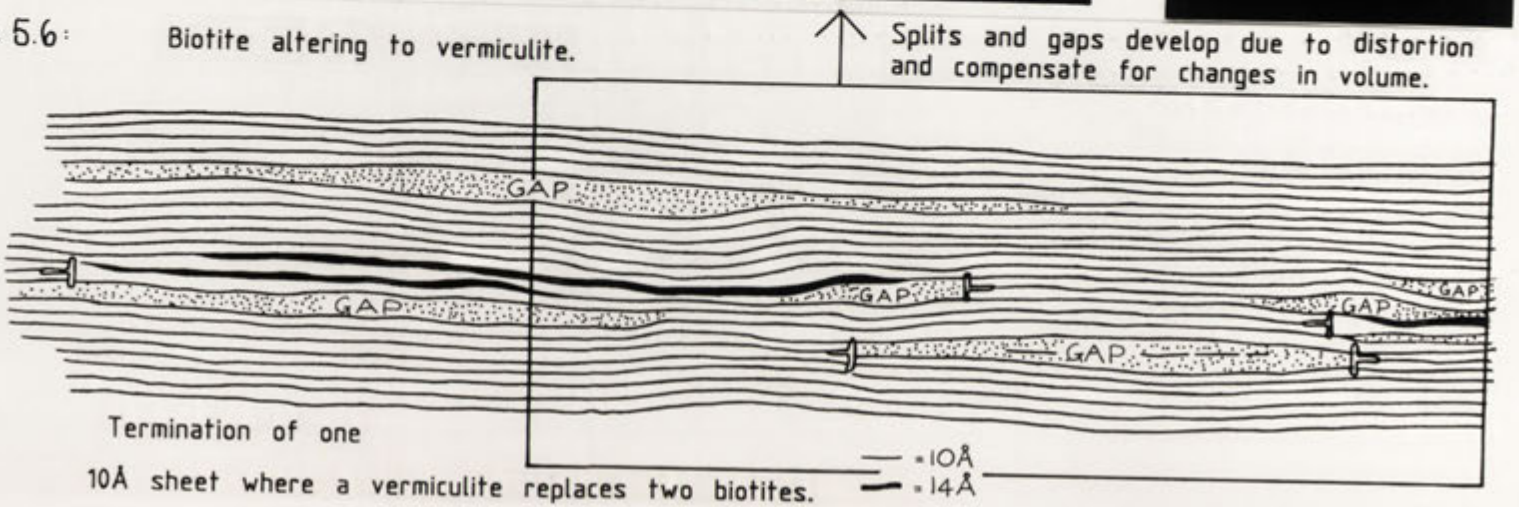

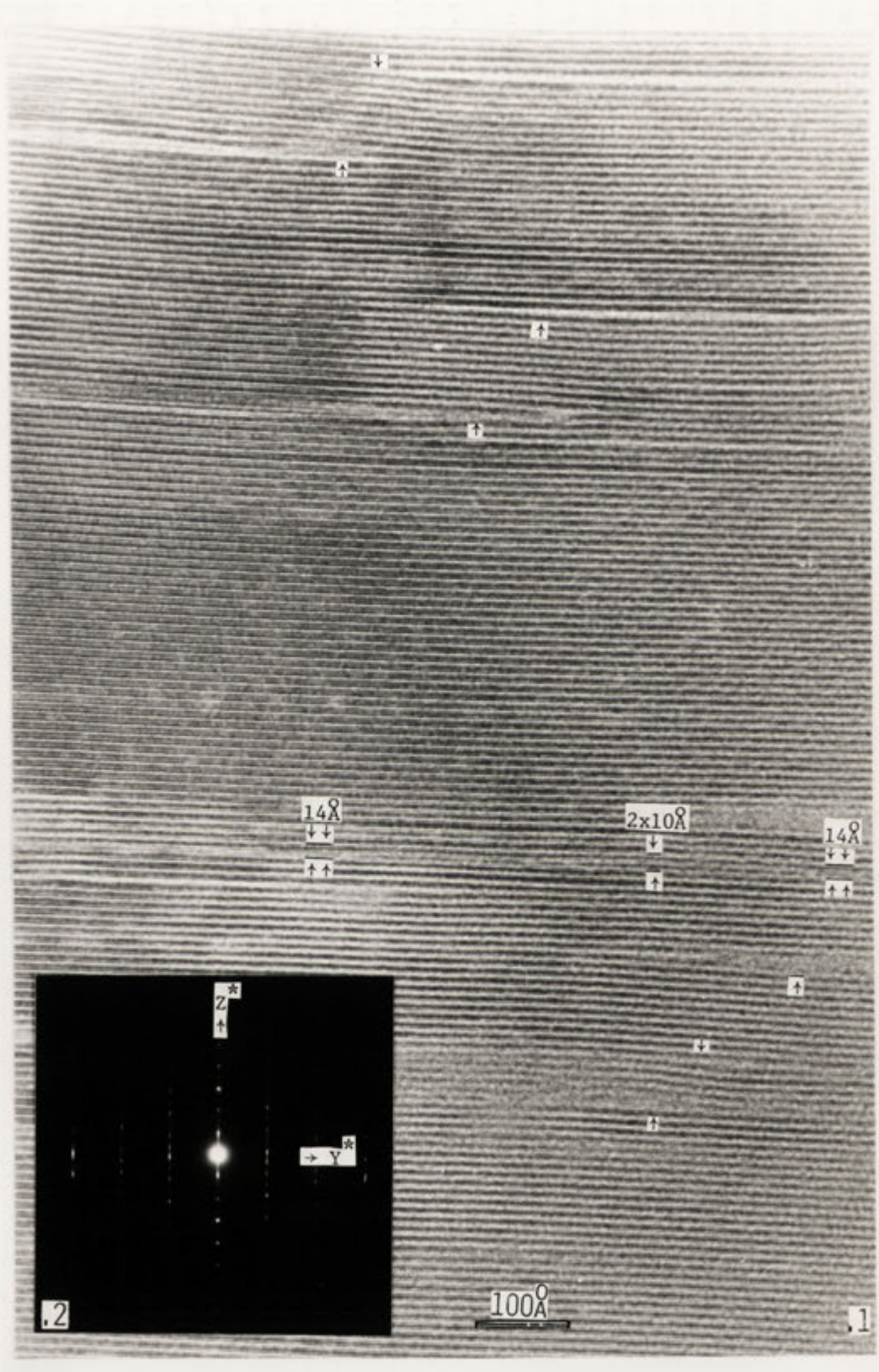

5.7.1: TRANSFORMATION OF BIOTITE TO VERMICULITE BOTH BY CONVERSION OF TWO LAYERS OF BIOTITE TO ONE LAYER OF VERMICULITE, AND BY DIRECT MODIFICATION OF THE EXISTING SHEET (↑).

5.7.2 DIFFRACTION PATTERN.

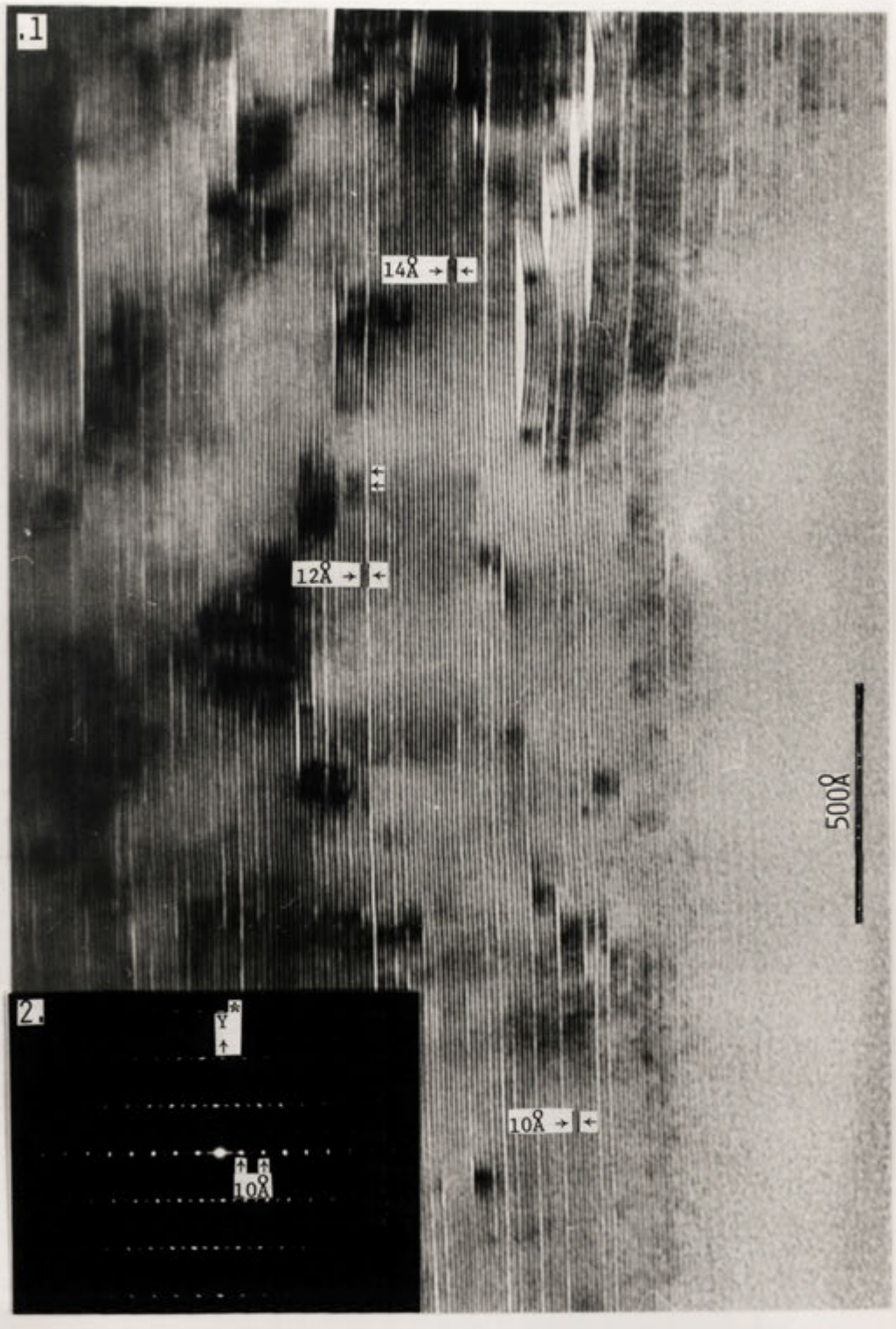

5.8.1: BIOTITE SOMETIMES DEVELOPS BRIGHTER INTERLAYER REGIONS—↓↓ WITH 10-12Å SPACINGS PRIOR TO THE FORMATION OF 14Å VERMICULITE. THIS MAY REFLECT PARTIAL HYDRATION OF THE INTERLAYER WITH THE REMOVAL OF K^+. 5.8.2: DIFFRACTION PATTERN.

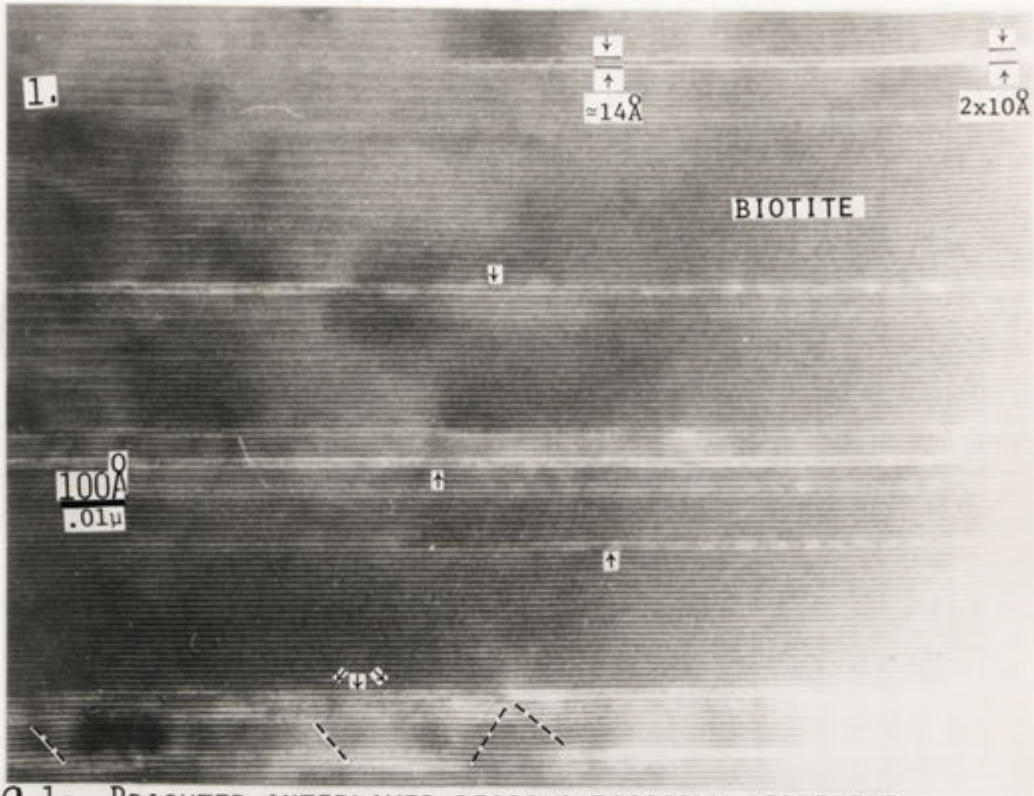

5.9.1: BRIGHTER INTERLAYER REGIONS POSSIBLY REPRESENT INCIPIENT WEATHERING (→). DISTORTION CAUSED BY ALTERATION MAY PROMOTE ALTERATION OF ADJACENT SHEETS, (---).

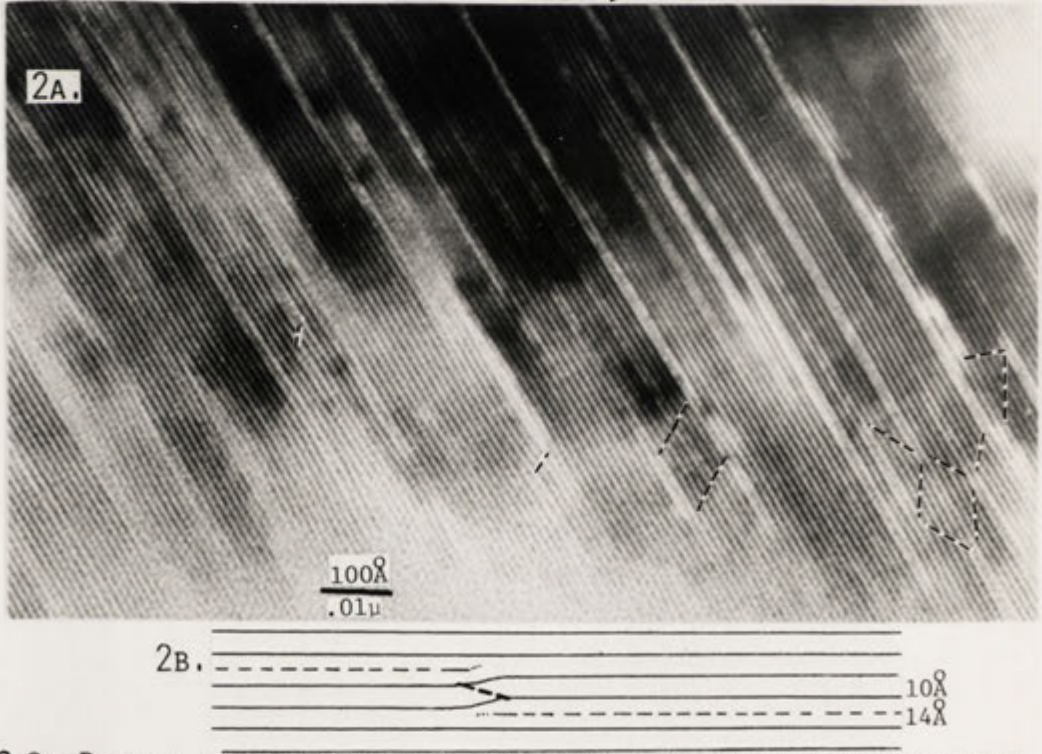

5.9.2A: DASHED LINES SUGGEST A POSSIBLE LINK BETWEEN DISTORTION CAUSED BY ALTERATION AND INITIATION OF NEW VERMICULITE LAYERS.
5.9.2B: DIAGRAM OF ABOVE.

Each conversion of one biotite to one vermiculite is associated with a volume increase of about 30%. Initially conversions occur infrequently, and the volume change is relatively small, presumably accommodated in zones where dissolution has produced space.

Extensive zones of vermiculite are generally not observed in the weathering sequences examined. Rather, biotite weathers to intergrade biotite- vermiculite phases which display some regularity in the way the phases alternate (Plates 5.10A, 5.10B). Increased weathering correlates with an increase in the proportion of vermiculite layers, and generally with an increase in the regularity of interlayering.

The development of regular interstratification is suggested by Norrish (1972) to be related to the change in (OH) orientation in the sheet adjacent to the one from where K is removed, causing firmer bonding of K in this sheet. As shown in Plate 5.10A sequences of BVB can be recognised, separated from adjacent BVB sets by a brighter interlayer region. The subsequent stage, BVVB(BVBB) is also noted in this sequence, with BVVBBVVB developing from it in the lower LHS of Plate 5.10A (Figure 5.2). Regular 1:1 interstratifications are also observed, with pairs of layers separated from adjacent pairs by brighter, lower electron density zones. This can be observed in the top RHS of Plate 5.10A. These observations provide some evidence to support the stability of BVB sets; firmer bonding of K due to re-orientation of (OH) groups may provide an explanation for this.

An examination of electron micrographs of biotite weathering (for example Plate 5.9B) indicates that biotite-vermiculite sequences do not develop sequentially outward from an initial vermiculite layer. Rather, vermiculite develops infrequently throughout the biotite, the average separation between altered layers decreasing as weathering proceeds. Some approximate early regularity can be observed in the spacing between vermiculite sheets which it would not seem possible to explain in terms of changes in (OH) orientation. This may be attributed to the development of a second vermiculite in response to warping of layers around an initial transformation, such as illustrated in Plate 5.9B. This would be particularly effective in generating an early regularity if the number of layers which deflected around a volume change before alteration was induced was fairly constant.

5.10.1: INTERSTRATIFIED BIOTITE AND VERMICULITE. A FEW REMAINING BIOTITE LAYERS CAN BE OBSERVED CONVERTING TO VERMICULITE.

5.10.2: FORMATION OF ONE VERMICULITE FROM TWO BIOTITE LAYERS. INTERSTRATIFIED BIOTITE AND VERMICULITE IS DEVELOPED IN THE LEFT OF THE PHOTOGRAPH. 5.10.3: D.P. FROM ADJACENT AREA.

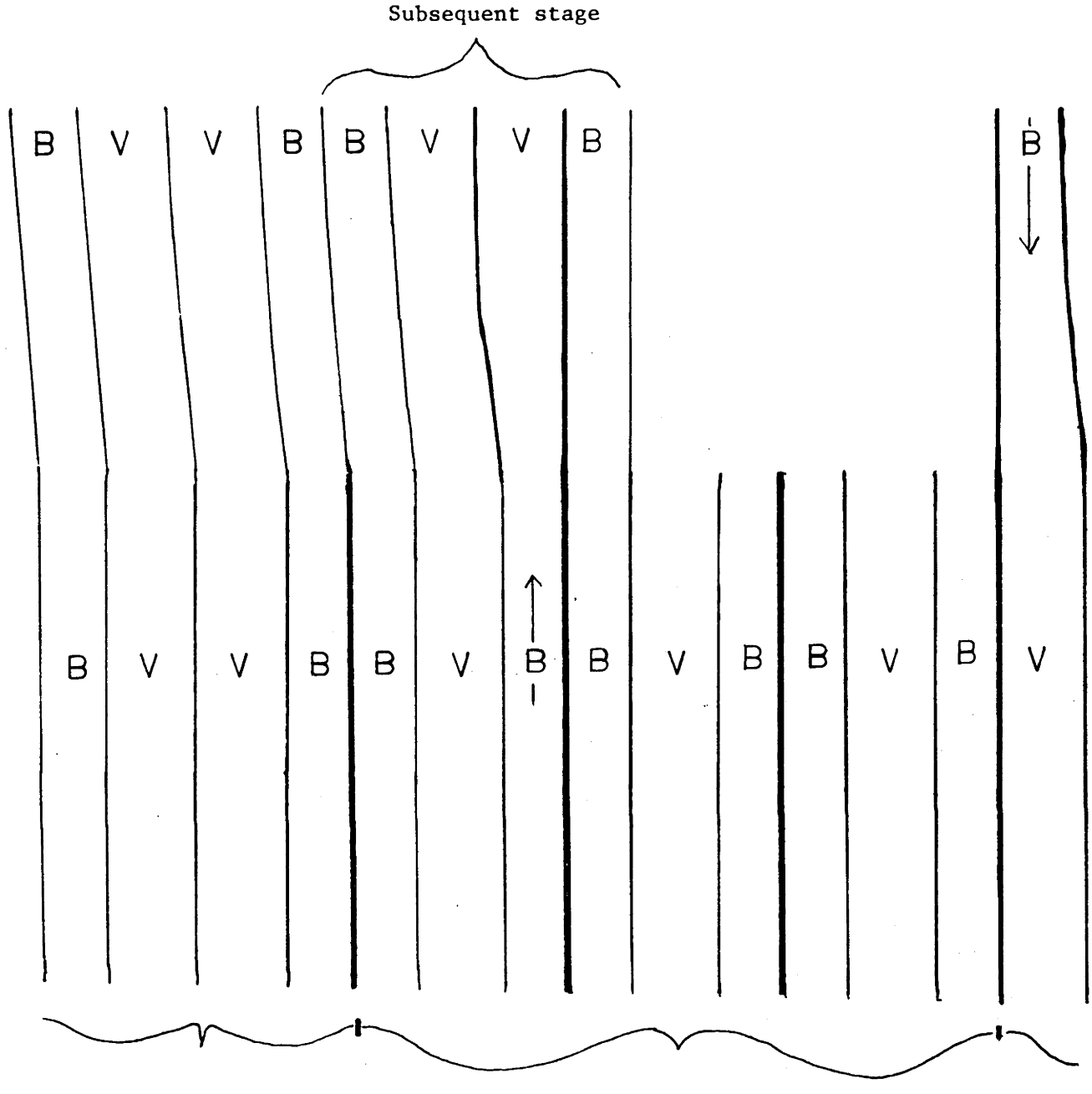

FIGURE 5.2:

Illustrating the presence of B V B sets which are replaced by B V V sequences as shown in Plate 5.10.1.

.2 THE KAOLIN - GOETHITE STAGE:

It has been noted that kaolin and goethite form minor constituents of the assemblage of weathering products in the earlier stages of weathering. In the later stages, however, these phases are the dominant products, probably replacing vermiculite as well as biotite. This stage of weathering appears to occur rapidly, and results in the destruction of most remaining biotite.

Kaolinite develops by crystallizing epitactically onto biotite, as illustrated in Plate 5.11, at a stage when a substantial amount of space has been created by dissolution of biotite. There is no evidence to suggest that this transformation occurs via an amorphous stage. Formation of kaolinite by direct modification of the biotite structure is considered unlikely. Firstly, for this reaction to occur, all Al from both tetrahedral sheets must replace most octahedral cations, Si must replace Al in the tetrahedral sheets, and many components must be removed (Figure 5.3). This would appear to constitute such a dramatic reorganisation that it would be unlikely to occur without complete destruction of the sheet. Secondly, kaolinite does not develop within zones of biotite, but is confined to formation on the surface of remaining sheets, possibly templating onto existing tetrahedral layers. On the basis of these observations, it is proposed that under more extreme weathering conditions biotite is disaggregated, and components temporarily enter a solution from which kaolinite crystallizes. In later stages of weathering kaolinite is recognised as quite well formed laths which parallel the remaining biotite parent (Plate 5.12).

Iron is an extremely abundant component in this system, composing about half the octahedral cation population of both biotite and vermiculite. With the destruction of these phases, Fe migrates to form segregations of semi-crystalline Fe-oxide-hydroxide (Plate 5.13). This material subsequently recrystallizes to form goethite.
Stages in the formation of goethite from a "proto-goethite" component are illustrated in Plate 5.14. Initially a foliation develops within evenly textured material, generally perpendicular to nearby sheets. These segregations may be 30-40 Å wide (Plate 5.14A) and have no apparent internal structure. With subsequent crystallization 10 Å b-axis fringes can be observed, generally perpendicular to (Plate 5.14B), and occasionally parallel to (Plate 5.14C) enclosing sheet

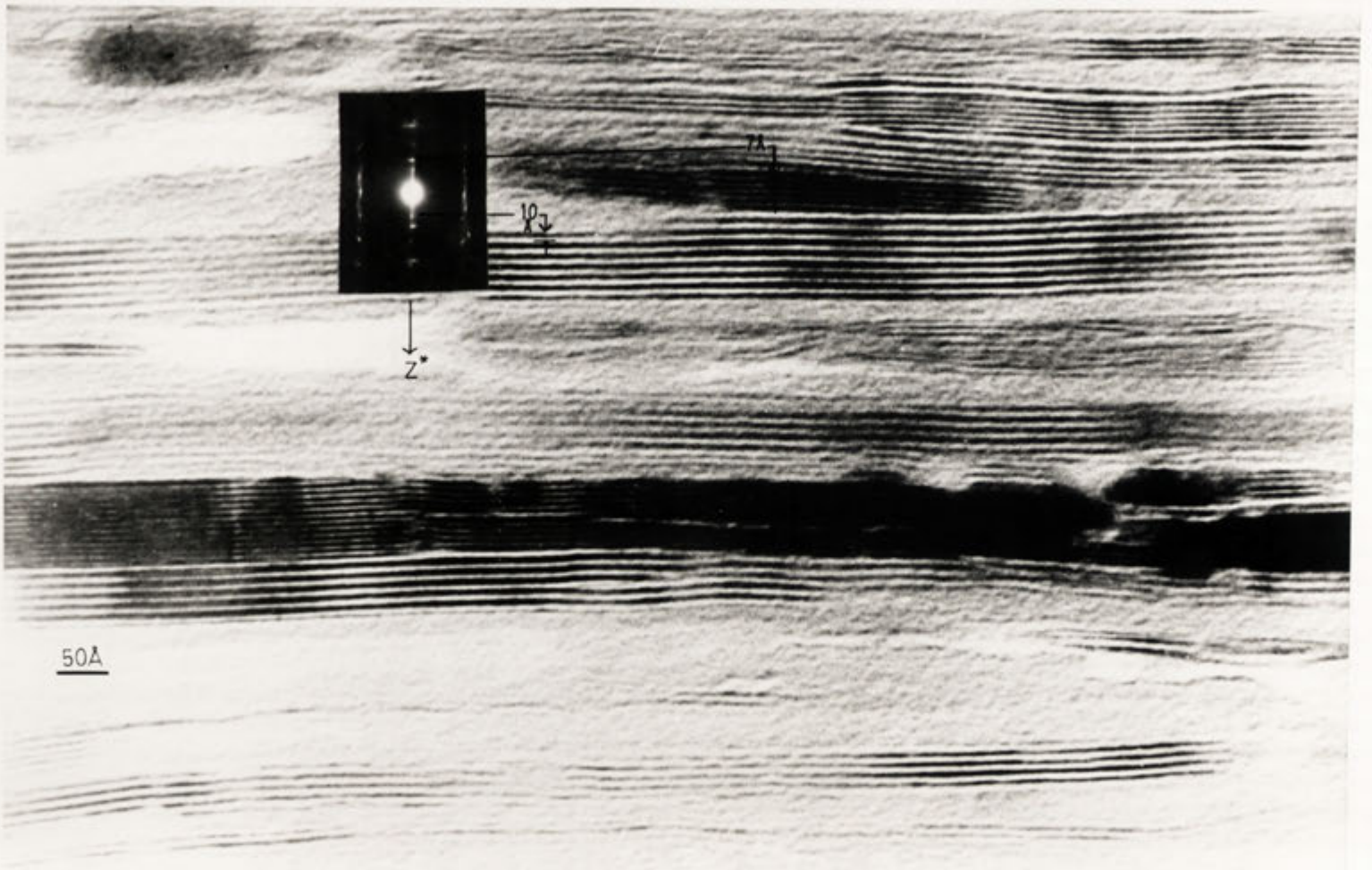

PLATE 5.11: Kaolin developing adjacent to biotite.

5.12.1: KAOLINITE EXHIBITING 7Å FRINGES. THIS MATERIAL IS CHARACTERISTICALLY EXTREMELY BEAM SENSITIVE.

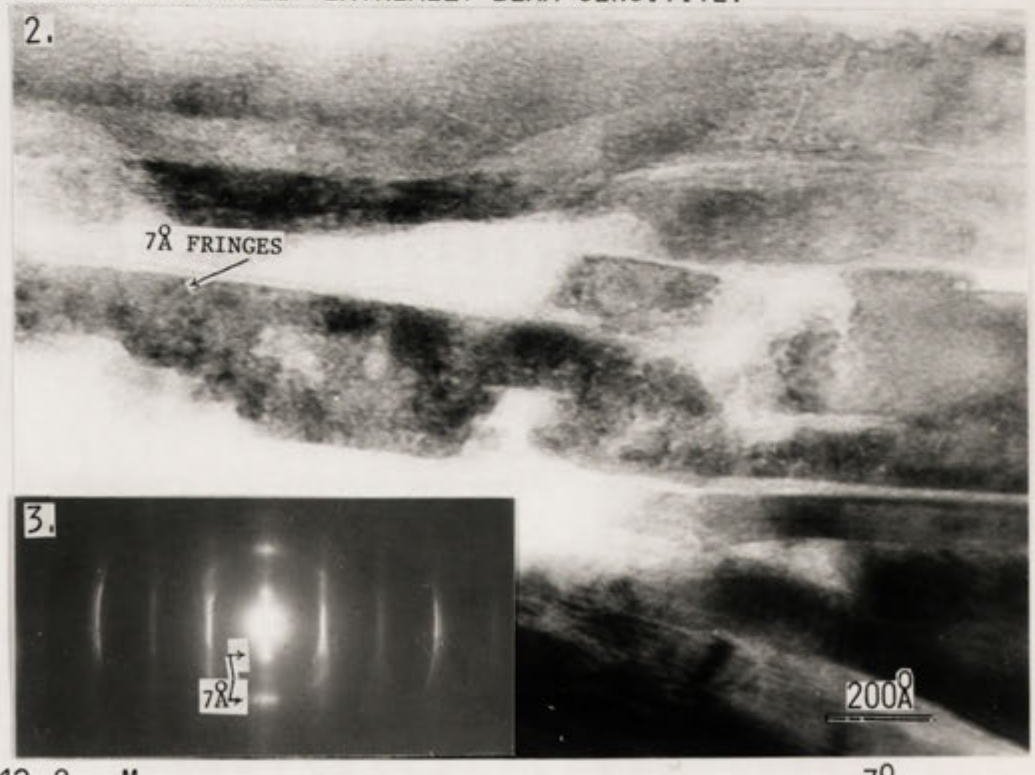

5.12.2: MODERATELY WELL FORMED KAOLINITE LATHS WITH 7Å FRINGES.
5.12.3: KAOLINITE DIFFRACTION PATTERN.

5.13.1: KAOLINITE AND PROTOGOETHITE FORMED BY ALTERATION OF BIOTITE. 5.13.2: DIFFRACTION PATTERN OF KAOLINITE SHOWING 7Å SPOTS AND RINGS PRODUCED BY GOETHITE.

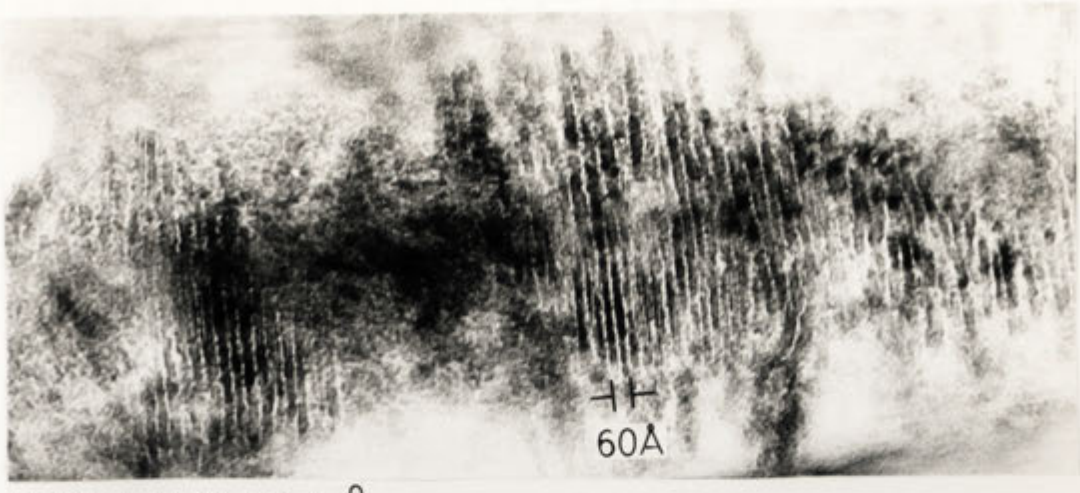

PLATE 5.14.1: 30-40Å WIDE SEGREGATIONS DEVELOPING IN PROTO-GOETHITE.

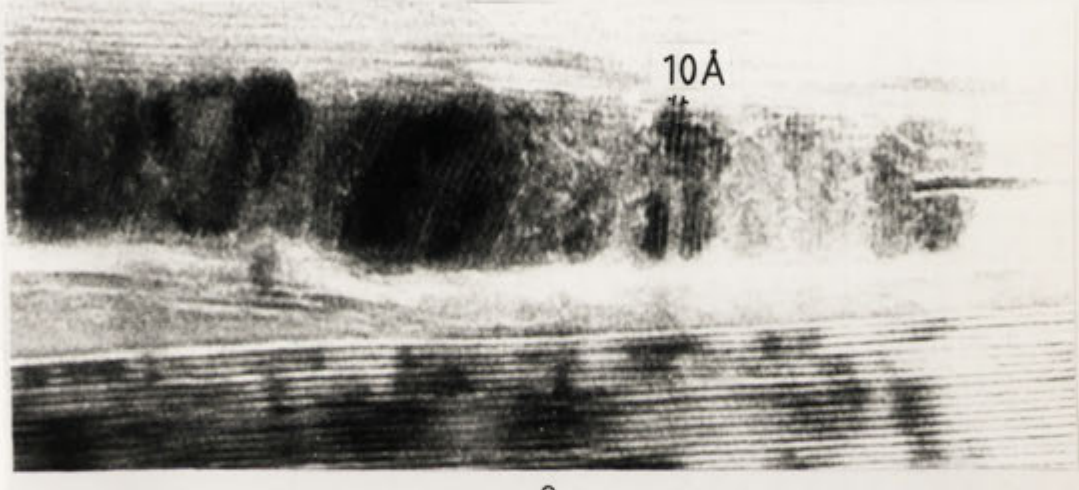

PLATE 5.14.2: GOETHITE WITH 10Å FRINGES DEVELOPED PERPENDICULAR TO ENCLOSING BIOTITE SHEETS.

PLATE 5.14.3: GOETHITE WITH 10Å FRINGES DEVELOPED PARALLEL TO ENCLOSING SHEETS.

FIGURE 5.3

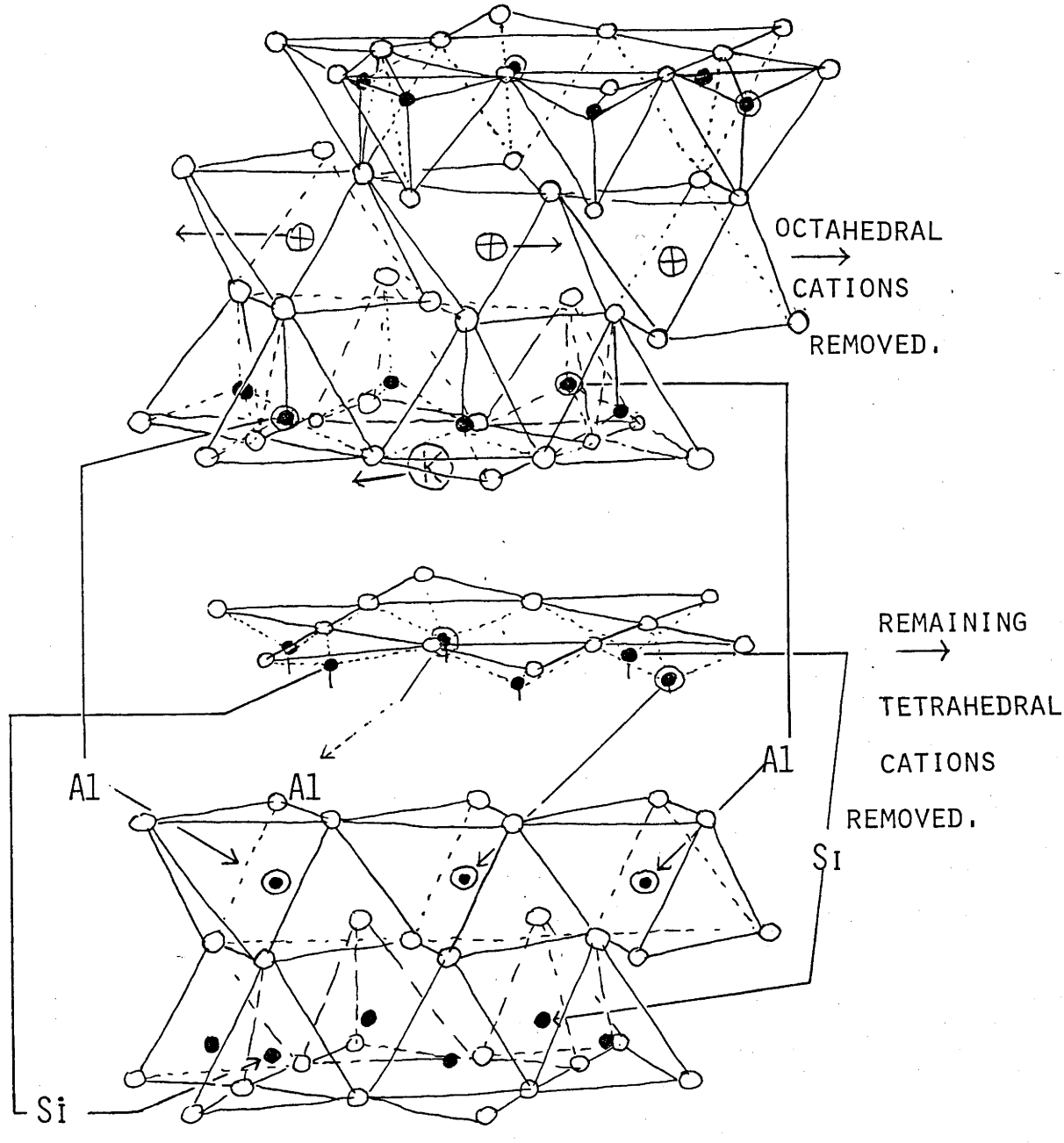

THE MODIFICATION REQUIRED FOR THE CONVERSION OF BIOTITE TO KAOLINITE.

silicate layers. Advanced stages of recrystallization result in the development of very euhedral, diamond shaped goethite crystals (not illustrated).

Of the components present within the biotite and vermiculite, K and Si are removed in large quantities in solution as a result of weathering. Mg is hosted temporarily in vermiculite, but is released into solution with the destruction of this phase. Ti apparently has at least a limited mobility, and migrates to pits or cracks where it precipitates to form anatase. This phase frequently coexists with Fe and Mn oxides, (Plate 5.15) and in some cases, halloysite. Some Fe is probably released into solution, and may then participate in other mineral alteration reactions, such as those discussed in Chapter 4, part 2.4.

SECTION 5.2.3

REACTION CHEMISTRY:

The weathering of biotite has been divided very generally into two stages, an initial stage dominated by biotite - vermiculite reactions, and a later stage dominated by the production of kaolin and goethite. These styles of alteration are depicted in low magnification TEM photographs in Plate 5.16.

Figures 5.4 and 5.5 present equations which represent the observed mechanisms for the conversion of biotite to vermiculite, and for the reaction of biotite to form kaolin and goethite. For biotite it has been estimated that 14% of the total FeO content measured is actually present in the structure as Fe_2O_3, (actual Fe determinations have not yet been received). All iron in the vermiculite is assumed to be ferric, and analyses recalculated accordingly. Formulae for biotite, vermiculite, and kaolinite used in these reactions were obtained from averages of selected microprobe data. Most microprobe data were rejected because when data were plotted on triangular diagrams, scatter clearly indicated that analyses were from mixtures of phases. This is not surprising when it is considered that the beam diameter of the probe is larger than 1μm, (10,000 Å); (for example see Plate 5.16).

The reaction for the conversion of two biotites to one vermiculite

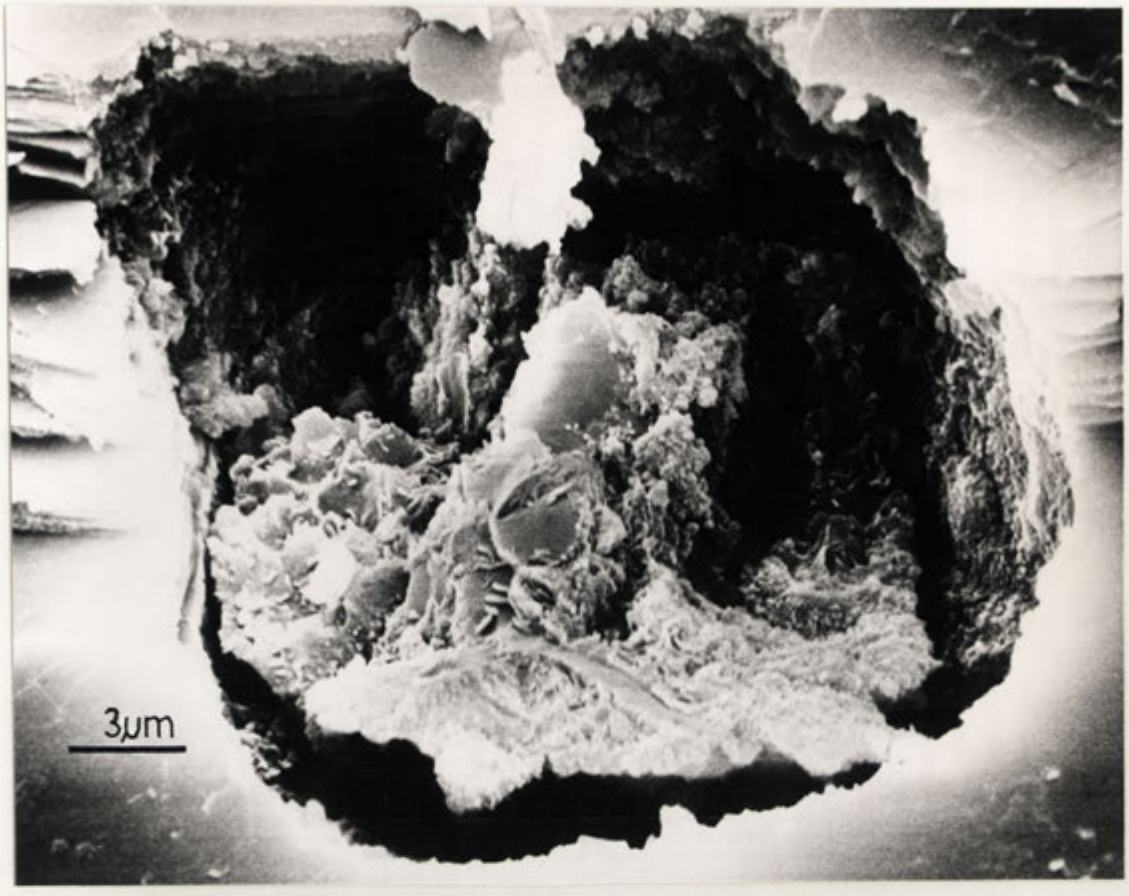

PLATE 5.15A: Fe - Ti - Mn - oxides developed in a pit in biotite.

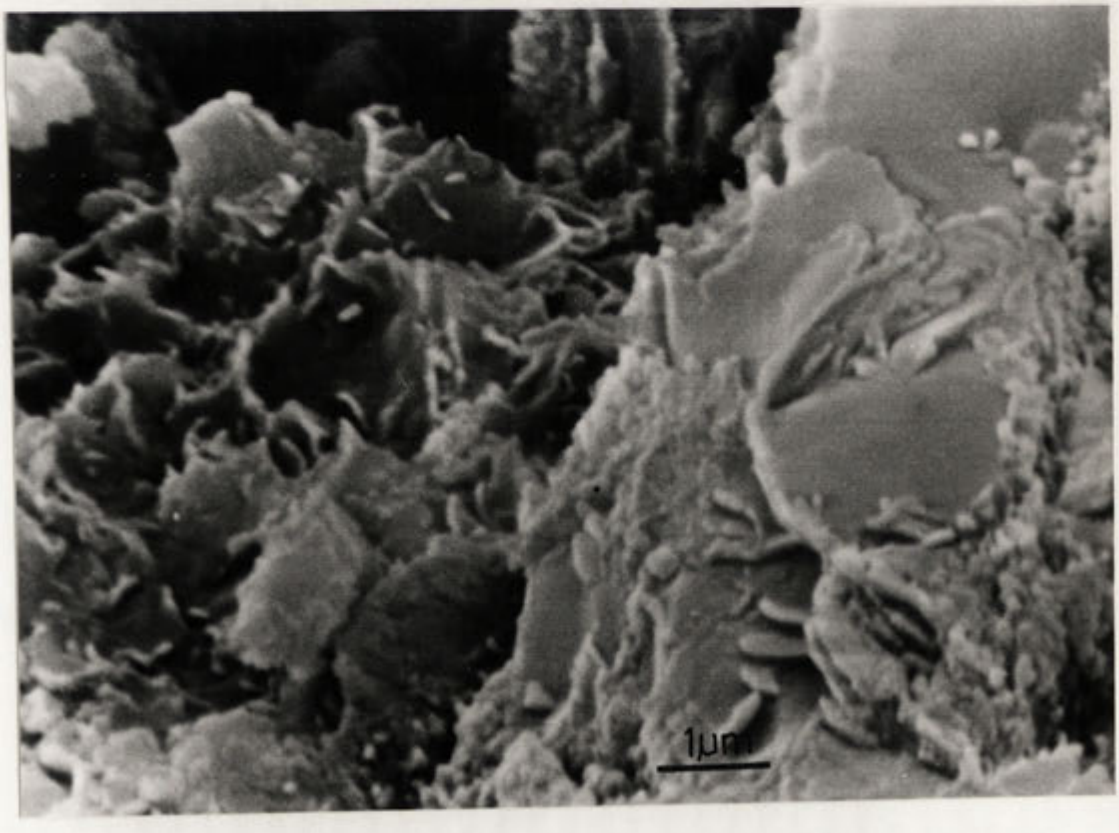

PLATE 5.15B: Higher magnification of above.

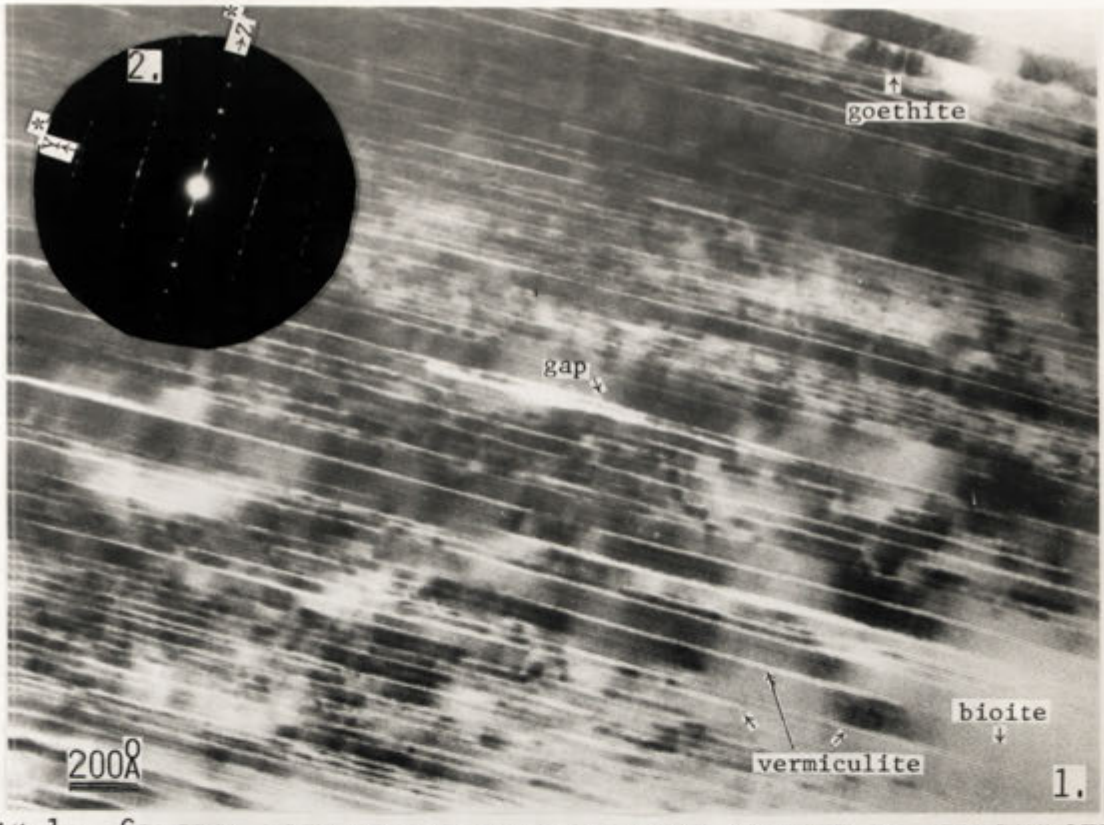

55.16.1: GENERAL VIEW OF THE ALTERATION OF BIOTITE TO VERMICULITE AND MINOR GOETHITE. 5.16.2: DIFFRACTION PATTERN.

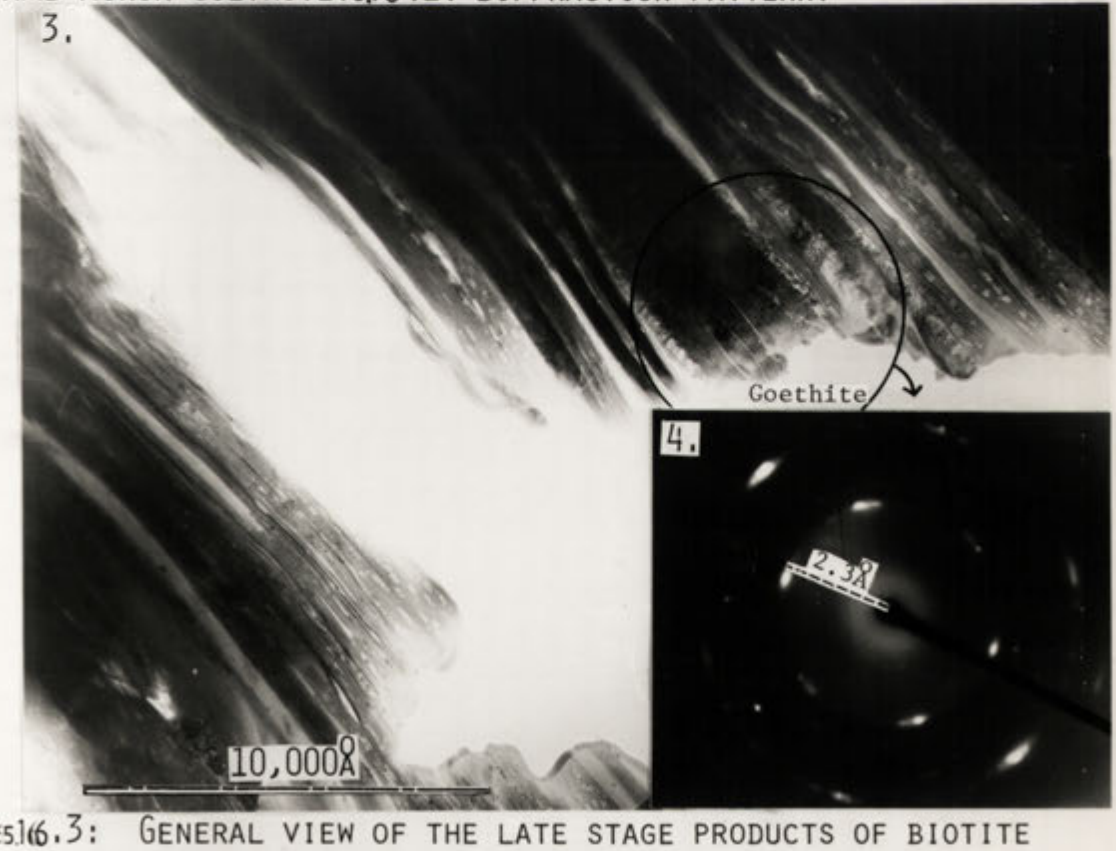

55.16.3: GENERAL VIEW OF THE LATE STAGE PRODUCTS OF BIOTITE WEATHERING. SEMI-CRYSTALLINE GOETHITE AND KAOLINITE ARE PRESENT IN APPROXIMATELY EQUAL PROPORTIONS. 5.16.4: D.P.

FIGURE 5.4

REACTION CHEMISTRY:

2 BIOTITES → 1 VERMICULITE:

$$K_{3.86}(Mg_{3.82}Fe^{+++}_{.74}\ Fe^{++}_{4.55}Al_{1.46}Ti_{.56})(Si_{10.56}Al_{5.44})O_{40}(OH)_8 + Ca_{.09} + 4.54\ H_3O^+ + 1.135\ O_2 + 1.19\ H_2O$$

$$\longrightarrow\ K_{.08}Ca_{.09}(Mg_{2.23}Fe^{+++}_{2.89}\ Al_{.48}Ti_{.03})(Si_{5.05}\ Al_{2.95})O_{20}(OH)_4\ 8H_2O + 3.78K^+ + 1.59Mg^{++} + .6Fe^{+++}$$

$$+.9Fe_2O_3 + 1.74Al_2O_3 + .53TiO_2 + 5.51SiO_2 + 4OH^-$$

---

1 BIOTITE → 1 VERMICULITE:

$$K_{1.93}(Mg_{1.91}Fe^{+++}_{.37}\ Fe^{++}_{2.27}Al_{.73}Ti_{.28})(Si_{5.23}Al_{2.72})O_{20}(OH)_4 + .32Mg^{++} + .25Fe^{2+} + .57O_2 + 2.27H_3O^+ + 4.59H_2O$$

$$+.09Ca^{++} \longrightarrow\ K_{.08}Ca_{.09}(Mg_{2.23}Fe^{+++}_{2.89}\ Al_{.43}Ti_{.03})(Si_{5.05}Al_{2.95})O_{20}(OH)_4 8H_2O + 1.85K^+ + .02Al^{+++}$$

$$+ .25Ti^{4+} + .23SiO_2.$$

FIGURE 5.5

REACTION CHEMISTRY:

BIOTITE REPLACED BY KAOLIN AND GOETHITE

$$K_{2.0}(Mg_{1.96}Fe^{++}_{2.08}\ Fe^{+++}_{.38}\ Ti_{.25}Al_{.83})(Al_{2.70}Si_{5.30})O_{20}(OH)_4 + 6.19H_2O \rightarrow$$

$$Mg_{.07}Fe^{+++}_{.38}\ Al_{3.53})(Si_{4.03})O_{10}(OH)_8 + K_2O_{aq} + 1.89MgO_{aq} + 2.08FeO(OH) + 2.08e^- + .25TiO_2 + 1.27SiO_{2\,aq} + 2.10H_3O^+$$

KAOLIN GOETHITE ANATASE

THE VOLUME OF ONE UNIT CELL OF KAOLIN IS 329.9 $\mathring{A}^3$, (V= 5.13x8.95x7.39 SIN 103.5°).

THE VOLUME OF ONE UNIT CELL OF GOETHITE IS 138.7 $\mathring{A}^3$

HENCE: IF BIOTITE IS REPLACED BY ONE MOLE OF KAOLIN AND TWO MOLES OF GOETHITE, THE GOETHITE WILL OCCUPY APPROXIMATELY 47% OF THE VOLUME OF ALTERATION PRODUCTS, EG:

$$288.4 \;/\; 329.9 + 288.4 = .47.$$

(THIS DESCRIBES THE MAXIMUM CASE). (COMPARED WITH THE ORIGINAL VOLUME OF BIOTITE OF 500.8 $\mathring{A}^3$).

can proceed with addition of only hydrogen and oxygen compounds, and liberates large quantities of cations. The alternate, and most commonly observed reaction where one biotite is replaced by one vermiculite, requires addition of Mg and Fe as well as hydrogen and oxygen. The reaction essentially conserves Al, and releases only Ti, K, and Si. In both of these reactions the exact quantity and form of H and O added are not known. The written reactions should not be interpreted as precise indications of this as their form is dependent upon the way in which equations have been balanced, primarily due to assumptions as to the nature of components released. A reaction representing the net reaction stoichiometry has not been written as the balance between the two direct pathways for the formation of vermiculite, and the contribution of components derived from the dissolution of biotite is not known.

The maximum stoichiometry for the production of kaolin and goethite from biotite is presented in Figure 5.4. This reaction, which results in the replacement of one mole of biotite by one mole of kaolinite and two moles of goethite, conserves Fe and Al, releases Si and K, (probably into solution), Ti to form anatase, and Mg either to solution, or to form vermiculite. The volumes of the main phases produced in this reaction are also listed in Figure 5.4. These data indicate that goethite should occupy 47% of the volume of weathering products developed. Examination of a number of electron micrographs indicates that at least in some cases, approximately equal proportions of goethite and kaolinite are generated, (see Plate 5.16C, and Plate 5.13).

SECTION 5.3

CHLORITE WEATHERING:

Chlorite is the major product of the hydrothermal alteration of biotite in the Island Bend and Bemboka profiles. This phase apparently develops by modification of existing biotite sheets. Observations made of this reaction in unweathered material confirm the findings of Eggleton and Banfield (in press). An example of this style of alteration is given in Plate 5.17.

Although chlorite is not stable in the weathering environment this phase does not begin to weather until comparatively late. In thin section this is characterised by a change in chlorite colour from green

Plate 5.17 : Chlorite produced by hydrothermal alteration of biotite

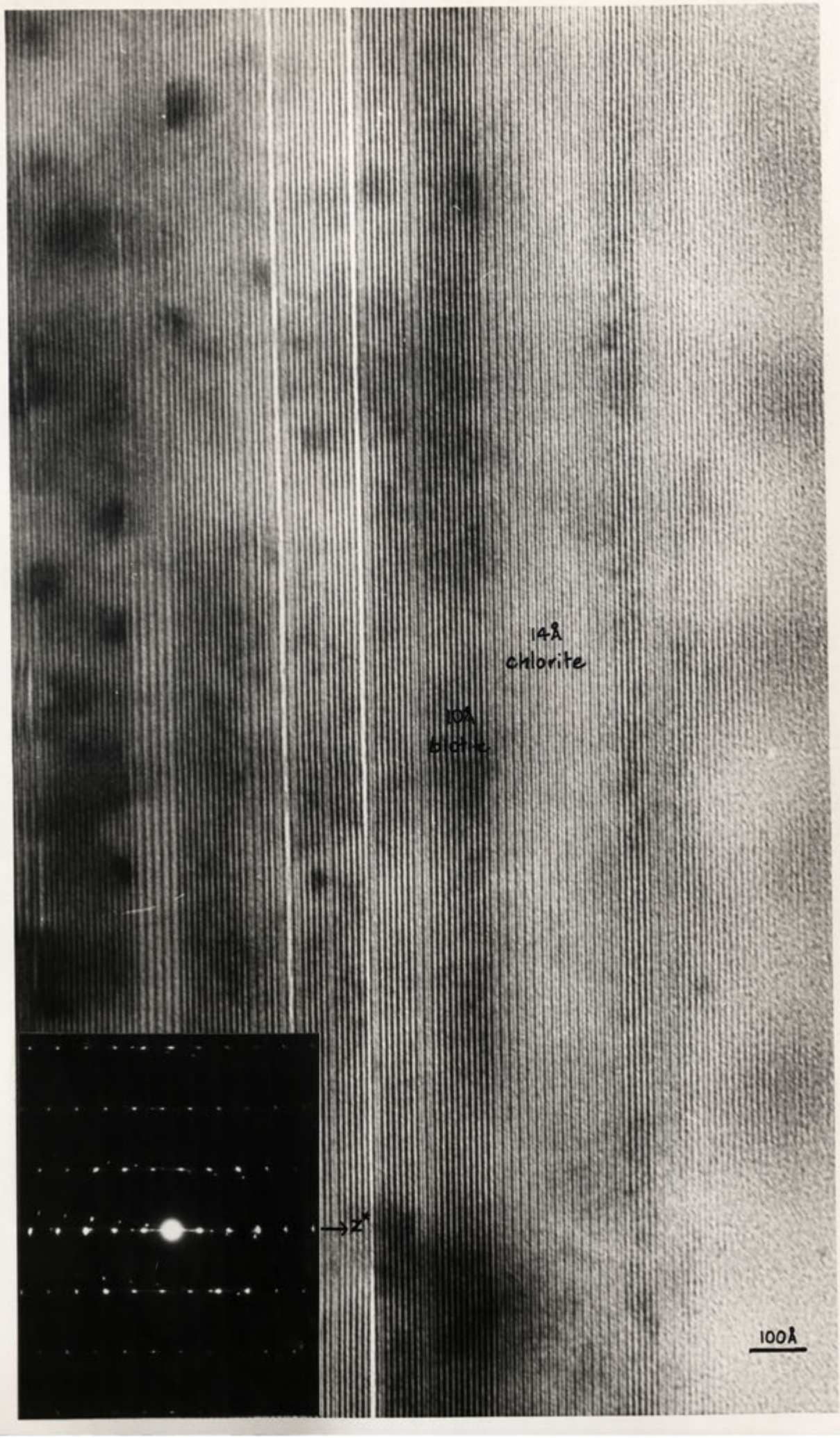

to the orange-brown generally associated with either vermiculite or kaolin and goethite.

Microprobe data for altered chlorite from Bemboka samples is variable, and difficult to interpret. Analyses do not seem to indicate that the replacement phase is vermiculite. Altered chlorite from the Island Bend profile was also examined, and data are presented below:

CHLORITE:

$$(Mg_{5.45}Mn_{0.18}Fe^{3+}{}_{.47}Fe^{2+}{}_{2.64}Al_{2.73})\ (Si_{5.70}Al_{2.30})O_{20}(OH)_8$$

ALTERED CHLORITE:

$$(Mg_{5.61}Mn_{0.16}Fe^{3+}{}_{2.91}\ Al_{2.06})\ (Si_{5.64}Al_{2.36})O_{20}(OH)_8$$

A value of 15% Fe as Fe^{3+} has been estimated for chlorite. The Fe content of the altered chlorite is not known; the above analysis has been calculated with all iron as Fe^{3+}. The result is that the abundance of most components closely resembles their abundance in the unweathered phase. This may indicate that the change in chlorite colour corresponds with the oxidation of Fe, compensated apparently by loss of Al.

Electron micrographs also fail to provide evidence for the conversion of chlorite to phases such as vermiculite; no evidence is seen for the development of any weathering products directly from the chlorite structure. At a late stage kaolinite and goethite can be observed to develop in close proximity to chlorite, apparently replacing this phase, (Plate 5.18A). Kaolinite sheets parallel existing chlorite sheets, probably indicating that they crystallized epitactically onto them, (Plates 5.18B, 5.18C). Goethite crystallizes as small laths generally developed perpendicular to enclosing sheets. If kaolinite is replacing chlorite, large quantities of Fe and Mg must be removed from the region illustrated in Plate 5.18A, Fe probably forming goethite in adjacent areas. Kaolinite probably develops from chlorite quite readily. The Al/Si ratio of chlorite is approximately .88, hence conversion to kaolinite requires far less redistribution of Al and Si than conversion of biotite to kaolinite, where the Al/Si ratio is approximately .5.

5.18.1: BIOTITE, CHLORITE, AND VERMICULITE ALTERING TO KAOLINITE (K), AND GOETHITE (G). GOETHITE FORMS LATHS ORIENTED PERPENDICULAR TO ENCLOSING SHEETS.

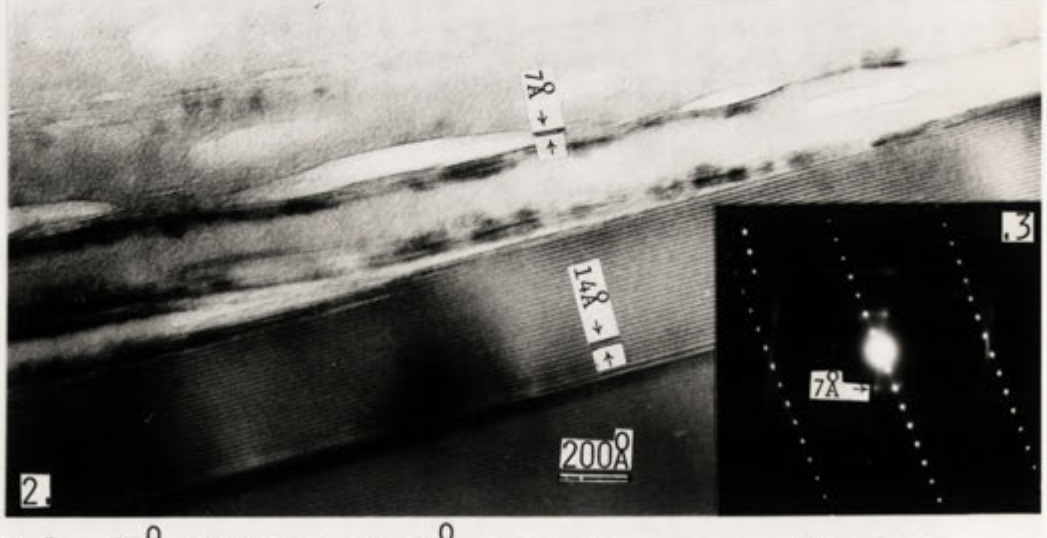

5.18.2: 14Å CHLORITE, AND 7Å KAOLINITE SHEETS. KAOLINITE IS PROBABLY CRYSTALLIZING EPITACTICALLY ONTO CHLORITE.

5.18.3: DIFFRACTION PATTERN: CHLORITE AND KAOLINITE.

SECTION 5.4

CONCLUSIONS:

Biotite weathering, as observed in the Jindabyne profile, can be generally subdivided into two stages. Initially biotite weathers gradually to intergrade biotite - vermiculite; this is associated with the crystallization of only minor quantities of goethite and kaolinite. Even in the earliest stages of biotite weathering dissolution appears to play a significant role, primarily in opening up the structure, and providing components for the development of vermiculite. Dissolution is concentrated in zones, apparently where more rapid alteration results in the disaggregation of the structure.

Vermiculite develops primarily by direct modification of the biotite structure. This may involve the introduction of cations as well as water, presumably from adjacent areas where dissolution has occurred, and results in an increase in layer width from 10 to 14 Å. The second, and far less commonly observed alteration mechanism involves the replacement of two biotites by one vermiculite layer, the second biotite layer gradually thinning until it can be recognised to form part of the vermiculite structure. This second mechanism conserves Al, and requires only the addition of water. Vermiculite layers which are developed in close proximity are frequently initiated and propagate in opposite directions from a common region. This appears to reduce the distortion of the structure associated with volume changes, and may serve to promote the early development of some regularity of interlayering.

Weathering of biotite to vermiculite only appears to proceed in the examples studied, until a locally fairly regularly interstratified 1:1 biotite-vermiculite phase develops. Subsequently only kaolinite and goethite are produced in large quantities, the development of these phases apparently corresponding with substantially more rapid alteration, and possibly with significantly more oxidising conditions.

The second stage, dominated by kaolin and goethite, is characterised by crystallization of minerals whose orientation is strongly controlled by that of the biotite. Goethite develops with its b axis either parallel or perpendicular to enclosing sheets, whereas kaolinite forms laths which parallel biotite layers. Unlike

vermiculite, which inherits much of its structure and hence orientation from biotite, kaolin and goethite appear to acquire their orientation by using existing silicate structure as a template onto which crystallization can proceed, either from solution or from an amorphous precursor.

The weathering of biotite derived chlorite is not completely understood. It would appear that this phase is not extensively altered until late in weathering, when it is replaced firstly by an orange-brown phase, possibly chlorite modified as a result of oxidation of iron. Late in weathering some evidence is observed to suggest that chlorite is replaced by kaolinite, which crystallizes, apparently epitactically onto remaining sheet silicate layers.

Chapter 6

THE WEATHERING OF AMPHIBOLE

ABSTRACT

During weathering amphibole exhibits little evidence to suggest that the development of secondary phases occurs directly from the parent structure. The first stage in alteration is dissolution, initiated at dislocations which were present in the structure before weathering commenced. Dissolution is strongly controlled by the crystallography of the parent mineral, resulting in the development of quite evenly spaced channels which coalesce to produce a sawtooth texture.

The weathered amphibole contains a complex alteration assemblage, including phases such as chlorite, vermiculite, talc, smectite, kaolin, and Fe- and Ti- oxides. Chlorite and talc are detectable in the unweathered material as euhedral laths. It is believed that these phases developed during an episode of low temperature metamorphism.

TEM evidence suggests that vermiculite associated with the altered amphibole has been derived by conversion of the chlorite to vermiculite, whereas amorphous material, smectite, Fe- and Ti-oxides, and kaolinite are produced by weathering of amphibole.

TEM and STEM data indicate degradation of amphibole results in the formation of areas of apparently amorphous material which recrystallize to simple strands of clay via material with the diffraction characteristics of allophane. The abundance and complexity of this material increases until relatively large curved laths of clay can be recognised. This clay has been chemically characterised as an Fe-smectite, or nontronite. Smectite coexists with Fe-oxide which also recrystallizes from regions of degraded amphibole, and kaolin which appears to replace it. The possibility that a phase such as stilpnomelane forms from nontronite, and in some areas is intermediate between this phase and kaolinite is tentatively suggested on the basis of diffraction data.

SECTION 6.1

PREVIOUS WORK

Weathering and Hydrothermal alteration products

Earlier workers have reported a range of secondary phases developed as a result of weathering. Proust (1982) noted that these included iron hydroxides (e.g. goethite)(Leneuf, 1959), talc (Jayaraman, 1940; Delvigne, 1965; Nicolas and Sugon, 1966), nontronite (Stringham and Taylor, 1950), chlorite - saponite (Wilson and Farmer, 1970), and chlorite - vermiculite which gave way to vermiculite (Stephen, 1952). Ildefonse et. al. (1978) reported nontronite, talc, trioctahedral vermiculite, and ferric beidellite in altered gabbro, and Ildefonse et. al. (1978) noted that early crystallizing intergrade minerals closer in composition to host hornblendes were destabilized to form beidellite.

Proust (1982) found talc - chlorite replaced hornblende as a result of metamorphic processes. He associated early supergene alteration with the development of saponite which was replaced by vermiculite. This author used microprobe data to demonstrate that phases which crystallize at hornblende surfaces could be chemically distinguished from those occurring in microcracks. He described a general trend toward the development of more aluminous phases as weathering proceeds which he attributed to increasing access of leaching solutions. Proust nominated this to be the major control on the chemistry of secondary phases in the weathering profile.

Wilson and Farmer's (1970) study of amphibole weathering revealed that the Fe-rich amphibole component was replaced by interstratified chlorite - saponite, the orientation of which was not structurally controlled. These authors proposed that amphibole could weather to either a chlorite-vermiculite or a chlorite-swelling mineral.

Chlorite is commonly present in the assemblage of hydrothermal alteration products of amphibole. This phase is generally recognised to be unstable in the weathering environment, and is replaced by vermiculite and iron oxides, (Parneix and Meunier, 1982). Vermiculite is also described as the weathering product of chlorite by Gilkes and Little, (1972). These authors, like Murray and Leininger (1956),

proposed that this reaction was related to the oxidation of iron. A more or less regularly interlayered chlorite - vermiculite mineral is reported as the intermediate stage between chlorite and vermiculite in many studies, including those of Stephen (1952), Brown and Jackson (1958), Droste et. al. (1962), Jackson (1964), and Proust (1982). Churchman (1980) described a sequence: chlorite-interlayered hydrous mica - chlorite and swelling chlorite - chlorite and vermiculite, which developed with increased weathering. Artificial alteration of chlorite to a mixed layer phase and to vermiculite has also been performed, (Ross and Kodama, 1974; Ross, 1975).

Experimental studies:

The alteration of amphibole has been studied experimentally by Schott et. al., (1981). These authors examined the dissolution of a number of ferromagnesian phases in aqueous solution and found that they released Si at a constant rate, and underwent incongruent dissolution with preferential release of Ca and Mg relative to Si from the outermost surfaces. This was interpreted to reflect greater mobility of cations from certain sites. Initial incongruent dissolution was followed by essentially congruent cation/Si dissolution indicating the formation of a constant thickness cation depleted layer. This layer, estimated to be only a few atoms thick, was suggested to result from substitution of hydrogen for calcium and/or magnesium in a modified silicate structure, and not from precipitation of a radically new surface phase. After an examination of surfaces of minerals extracted from soils, Berner & Schott (1982) estimate the thickness of this layer to be 5-20Å. Schott et. al. conclude that surface chemical reaction and not bulk diffusion is the rate controlling step in the dissolution of amphibole.

Electron Microscopy:

Berner & Schott (1982) used the SEM and XPS to study the surfaces of naturally weathered amphibole, and reported that this material dissolved by formation, enlargement, and coalescence of distinctive lens shaped etch pits. These appeared to develop mainly on dislocation outcrops, and were aligned with their long axes parallel to the Z-axis of amphibole. This resulted in the formation of distinctive saw tooth cracks and striated surfaces. These authors supported the view of Schott et. al. (1981) that dissolution is a surface controlled reaction, and does not proceed by diffusion through a surface layer such as that

nominated by Luce et. al. (1972), or Eggleton and Boland, (1981). Berner et. al. argue that any clay products formed can not be tightly adhering, as they are readily removed by sonification.

Conclusions

The literature suggests that amphibole alteration may be associated with the development of a wide range of secondary phases, some of which are also recognised by a number of workers to be part of an assemblage formed by hydrothermal alteration (such as chlorite and talc). Chlorite is described as converted to interstratified vermiculite-chlorite and to vermiculite in the weathering environment. The most commonly described weathering products of amphibole are chlorite-vermiculites, smectites, and iron oxides and hydroxides. Some evidence has been advanced to suggest that the chemistry of these phases may vary significantly in response to changing micro-environments. Where amphibole contains hydrothermally derived alteration products the assemblage produced by weathering will contain an intimate mixture of these phases and their secondary products.

Experimental studies suggest that weathering is a surface controlled reaction, secondary products not being capable of limiting diffusion. Although some evidence is observed for a very narrow (<20 Å) cation depleted surface zone this is not believed to be sufficiently well developed to control the breakdown of the amphibole.

SECTION 6.2

AMPHIBOLE WEATHERING

INTRODUCTION

Of the three granites studied, only the Bemboka profile contained sufficient amphibole to allow an examination of the way in which this phase weathered. As previous workers have researched amphibole weathering using XRD, optical microscopy, microprobe data, and the SEM, this study was directed specifically toward using the TEM to examine amphibole weathering at the unit cell level. As amphibole had been modified by an episode of hydrothermal alteration, metamorphically derived phases were also examined in order to distinguish these minerals from those produced by weathering.

SECTION 6.2.1

AMPHIBOLE CHEMISTRY AND HYDROTHERMAL ALTERATION

Microprobe analyses for the apparently unaltered amphibole are provided in Table 6.1. Unaltered amphibole is associated with a considerably paler green, or blue-green amphibole whose chemistry and optical properties suggest that it is actinolite. Actinolite appears to have developed from areas of darker green hornblende as a result of low temperature metamorphism. Analyses for actinolite are also given in Table 6.1. The observed variation in the chemistry of the amphibole probably reflects the differing degrees to which individual crystals have been modified.

Chlorite is recognised as a metamorphic alteration product of amphibole, occurring as well defined prismatic laths within the host mineral. This can be observed in Plate 6.1; a probe analysis of this material appears in Table 6.1. As seen in the following section, this form contrasts strongly with that of the weathering products, and is used to distinguish the origin of secondary phases. Laths such as those illustrated in Plate 6.1 are generally not oriented with respect to the structure of the parent phase, suggesting that they do not develop by direct modification of the amphibole.

Occasionally talc is also recognised in the alteration assemblage.

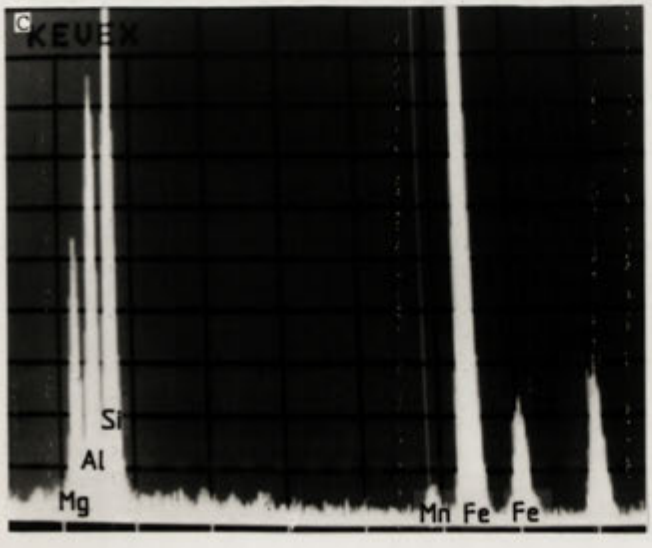

PLATE 6·1A: CHLORITE LATHS FORMED BY THE HYDROTHERMAL ALTERATION OF AMPHIBOLE.
PLATE 6·1B: DIFFRACTION PATTERN.

PLATE 6·1C: STEM SCAN OF CHLORITE.

This phase, like chlorite, appears to have formed by replacement of amphibole before weathering commenced. Microprobe analyses of talc also appear in Table 6.1.

Table 6.1: Chemistry of hydrothermal alteration products of amphibole

UNALTERED AMPHIBOLE

Ca	K	Na	/	Mg	Mn	Fe	Al	Ti	/	Al	Si
1.73	.13	.37		2.24	.10	2.60	.26	.10		1.00	7.00
1.76	.14	.40		2.09	.08	2.73	.29	.08		1.08	6.92
1.71	.14	.41		2.09	.12	2.76	.25	.10		1.06	6.94
1.74	.15	.48		2.02	.12	2.83	.20	.08		1.01	6.99

ACTINOLITE

Ca	K	Na	/	Mg	Mn	Fe	Al	Ti	/	Al	Si
1.90	-	-		2.66	.05	2.35	.06	-		.07	7.93
1.91	.02	-		1.99	.13	2.90	.08	-		.13	7.87

CHLORITE

Mg	Mn	Fe	Al	Al	Si
4.15	-	5.47	2.31	2.37	5.63
4.21	.11	5.33	2.33	2.39	5.61

TALC

Mg	Mn	Fe	Al	Al	Si
3.19	.24	2.80	-	.39	7.45
3.09	.20	2.93	-	.25	7.47

Structural formulae: amphiboles = $(-O_{22})(OH)_2$

chlorite = $(-O_{20})(OH)_{16}$

talc = $(-O_{20})(OH)_4$

Hydrothermal alteration appears to have resulted in the conversion of amphibole to two sheet silicate phases, a relatively Al rich chlorite, and Al poor talc. The hornblende itself is commonly partially replaced by another amphibole poorer in Al. The details of the relationship between these phases have not been considered.

SECTION 6.3

ELECTRON MICROSCOPY OF AMPHIBOLE WEATHERING.

.1 The initial stages of weathering.

In addition to a number of secondary phases, the unweathered amphibole contains a large number of dislocations which occur quite regularly throughout the structure, (Plate 6.2). Where dislocations have been slightly etched, possibly as a result of the metamorphic episode, removal of material has occurred along lattice planes. This crystallographic control on the way in which amphibole dissolves is also a major feature of the early stages of weathering.

Amphibole begins to weather quite early compared with other granitic phases. In thin section this is indicated by the widening of cleavages, and appearance of a small quantity of orange-brown material in the space which develops. In strongly weathered material no amphibole remains, and in many cases very little indication of the previous existence of this phase can be detected.

The initial stage in weathering of amphibole is dissolution. This process can be observed in detail using the TEM. Plate 6.3a illustrates the development of regularly spaced etches initiated along a dislocation. Dissolution commenced at energetically favoured sites along this feature, and has proceeded along a major lattice direction, (parallel to {110}). Plate 6.3b illustrates the development of dissolution channels parallel to {100}, and to a lesser extent along the lattice direction parallel to {110}. The diffraction patterns for areas where the development of these channels has occurred contain broad spots which reflect the formation of these isolated blocks of material (Plate 6.4a,b).

Dissolution most commonly occurs along {110}. This results in the development of crystallographically bound etches along two directions which intersect at ~53°, and represent the major cleavage directions. When the hk0 section of amphibole is examined (see Plate 6.4c) the tendency for dissolution to occur along these planes is clearly illustrated by the formation of regular diamond shaped etches. The removal of material along these lattice directions on a microscopic

PLATE 62A: DISLOCATIONS IN FRESH AMPHIBOLE. ETCHING OCCURS AT THE DISLOCATIONS, AND PROCEEDS ALONG CRYSTALLOGRAPHIC PLANES. 2B: DP.

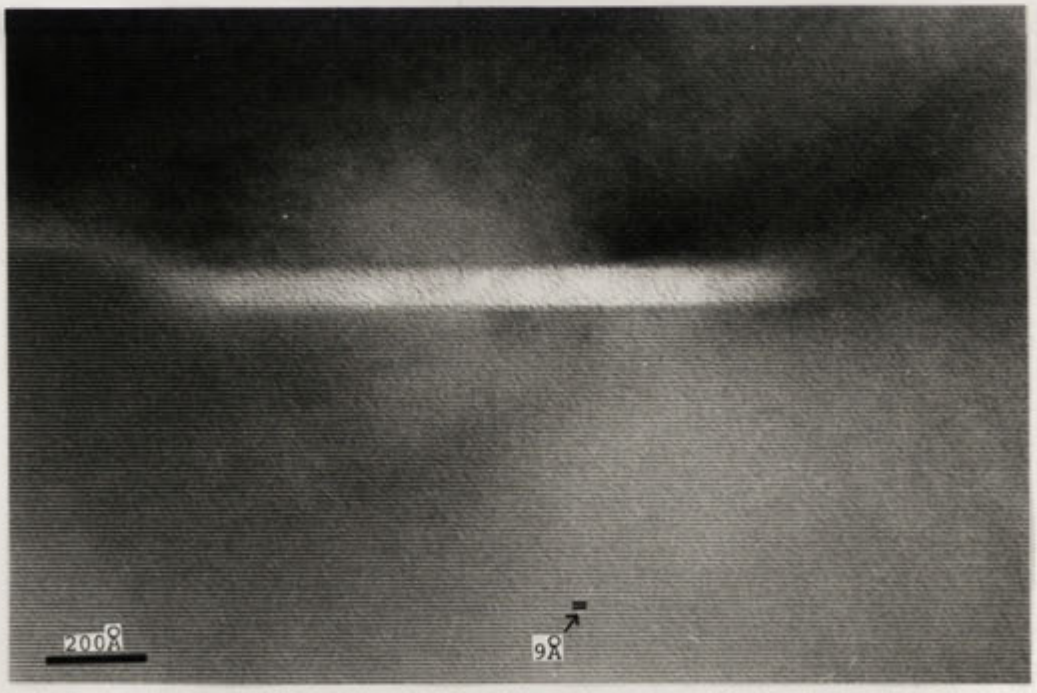

PLATE 62C: HIGH MAGNIFICATION PHOTOGRAPH OF CRYSTALLOGRAPHICALLY CONTROLLED ETCHING.

PLATE 6-3A: QUITE EVEN SPACED ETCHES INITITATED ALONG A DISLOCATION AND CONTROLLED BY LATTICE PLANES,

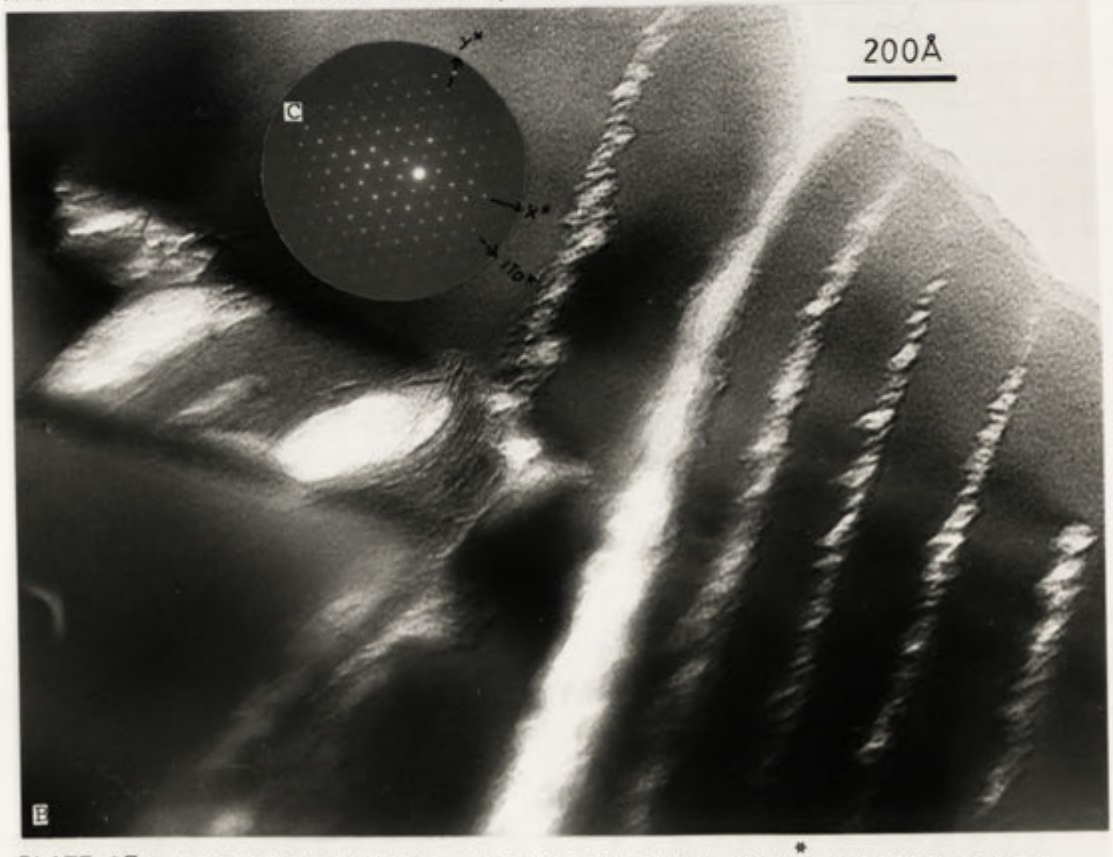

PLATE 63B: DISSOLUTION ALONG CHANNELS PARALLEL TO X* AND TO A LESSER EXTENT PARALLEL TO (110) AND ($1\bar{1}0$). PLATE 63C: DIFFRACTION PATTERN.

PLATE64A: ETCHING OF AMPHIBOLE ALONG CLEAVAGES RESULTING IN THE FORMATION OF DIAMOND SHAPED ETCHES.

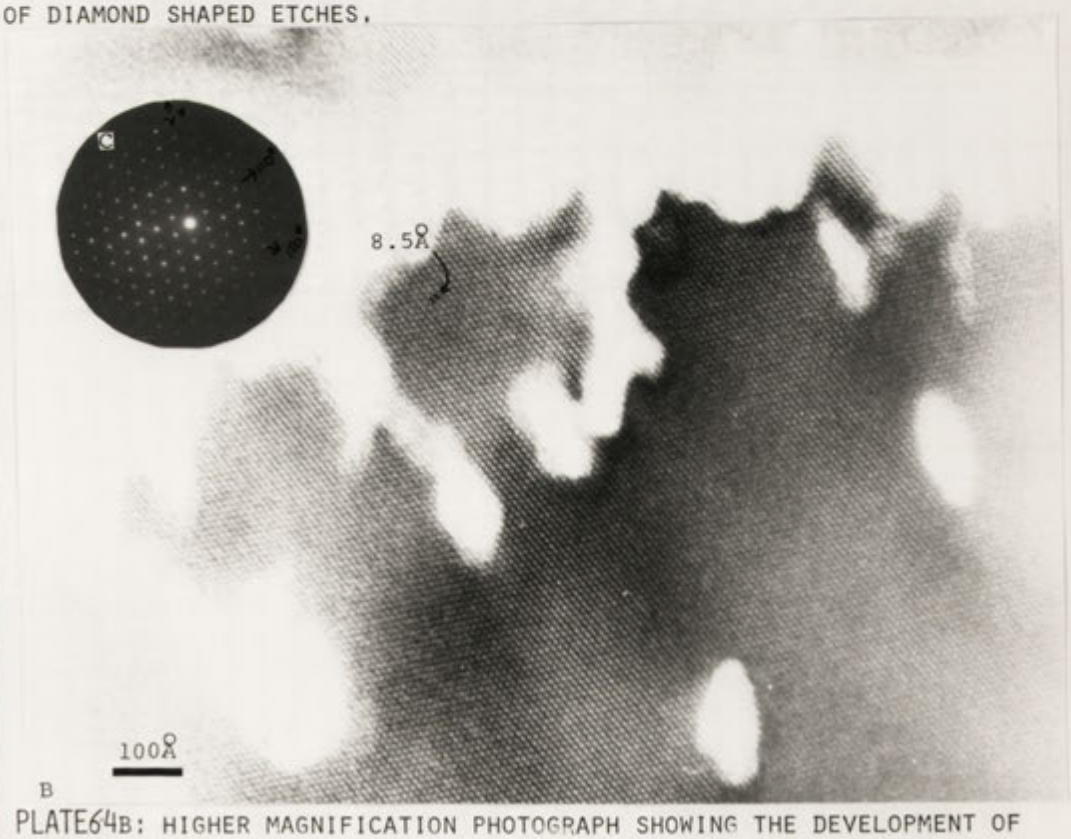

PLATE64B: HIGHER MAGNIFICATION PHOTOGRAPH SHOWING THE DEVELOPMENT OF CLEAVAGE BOUND ETCHES. PLATE64C: DIFFRACTION PATTERN.

scale parallels the process of widening of cleavages observable in the optical microscope. Plate 6.4 also illustrates the development of larger etches which contain a small quantity of clay. The process by which this material has crystallized, and the identity of the minerals which form as a result of weathering are discussed in the following section.

Main stage of amphibole weathering

The major process by which amphibole weathering occurs appears initially to involve disaggregation of the structure to form areas of semi-amorphous material. This component, which generally develops in etches produced by dissolution, subsequently recrystallizes to form simple strips of material which develop into curving laths of clay, (Plate 6.5).

The process by which recrystallization occurs is illustrated in Plate 6.6. The least crystalline material, such as that illustrated in Plate 6.6a, is characterised by an even, cell-like texture containing units about 40-60 Å in diameter. These appear to resemble a more densely packed form of the spherical particles of allophane described by Henmi and Wada, (1976). This morphology can be recognized in material in a range of orientations, suggesting that its appearance is not simply a factor of the particular view presented. On the basis of this structure, and because the diffraction patterns for material contain only a few broad rings at d spacings resembling those listed by Brindley and Brown, (1980) for allophane, it is proposed that this is a semi-amorphous, or allophane-like component. An evolutionary sequence toward more crystalline material can be observed within this component, characterised by an increase in the abundance and complexity of the clay (Plates 6.6b and 6.6c). Changes in morphology are paralleled by an increase in the definition of rings present in diffraction patterns, and in the appearance of single crystal spots from larger units of clay.

Plate 6.6b contains what appear to be tubes which are about 20 Å thick (reminiscent of imogolite), whereas Plate 6.6a illustrates the formation of 11-15 Å sheets of clay, possibly smectite or vermiculite. It is noted, however, that a measurement of the lattice dimensions of material a few unit cells thick may be very unreliable (eg. see Eggleton and Buseck, 1980). The way in which the semi-amorphous component

Saw-tooth corrosion of amphibole: (A). Abundant amorphous material containing crystallizing clay: (Am). With advanced crystallization clay forms curving bands.(C).

AMPHIBOLE

Pl. 6.6.1. Largely amorphous material.

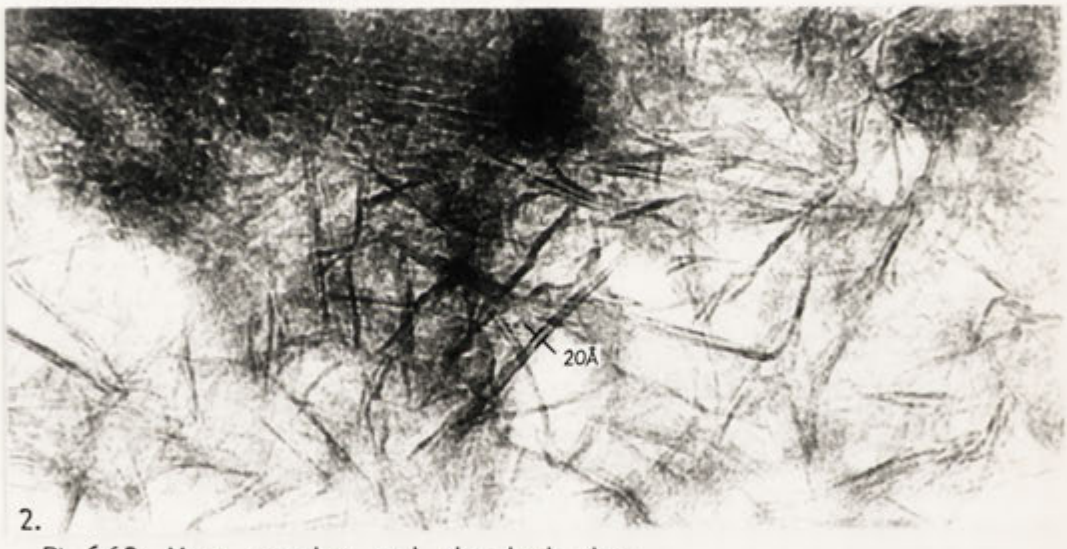

Pl. 6.6.2. More complex and abundant clays.

Pl. 6.6.3. Clays gradually re-organized to form laths.

recrystallizes is illustrated in the top part of Plate 6.6b, where a foliation develops as a result of the elongation and linkage of the sub-units in this material. Formation of subparallel groups of these strands which gradually increase in length and width eventually leads to the development of small, curved laths of clay, such as those observable in the left hand side of Plate 6.6c. Finally, larger and more regular laths appear, such as that seen in the right hand side of Plate 6.6c. Only a relatively small quantity of semi-amorphous material remains at this stage, this appears in the micrographs to be darker; STEM scans (such as shown in Plate 6.11d) indicate that it contains abundant Fe.

Examples of this crystallization sequence are given in Plate 6.7. Plate 6.7a illustrates the development of more crystalline material from a semi-amorphous component. The diffraction pattern for this material (Plate 6.7b) contains single crystal spots and relatively well defined rings which have d spacings of 4.5 Å, 2.63 Å, 1.72 Å, 1.66 Å, (etc.). These closely resemble the non-basal spacings for nontronite of 4.49 Å, 2.64, 2.57 Å, 1.72 Å, 1.67 Å, (etc.). Broad halos at about 3.4 Å, and 2.46 Å, are just recognisable in this diffraction pattern, representing the amorphous component which is also present in the area examined. Plate 6.7c illustrates material with a range of crystallinity, from an apparently near amorphous component to relatively well crystallized clay with basal spacings measured to be 11-14 Å.

In most of the examples discussed above the alteration products display no tendency to develop in orientations which are controlled by the parent phase. This is consistent with the development of these minerals from a semi-amorphous or gel-like component, rather than directly from the parent structure. In some cases, however, parallelism of clays with crystallographically controlled margins of etches is noted. This can be observed in the right hand side of Plate 6.8 where clays with 12 Å basal spacings have crystallized parallel to {110} planes of amphibole. It is not considered likely that this indicates any large scale inheritance of the parent structure by the clay (eg. topotaxy), as an examination of this plate indicates that further along the same group of sheets crystallization has proceeded perpendicular to these lattice planes. It is therefore suggested that in the few cases where parallelism of lattice directions in the clay and parent amphibole is observed that it represents the effect of a boundary which has constrained crystallization of clay, rather than suggesting the

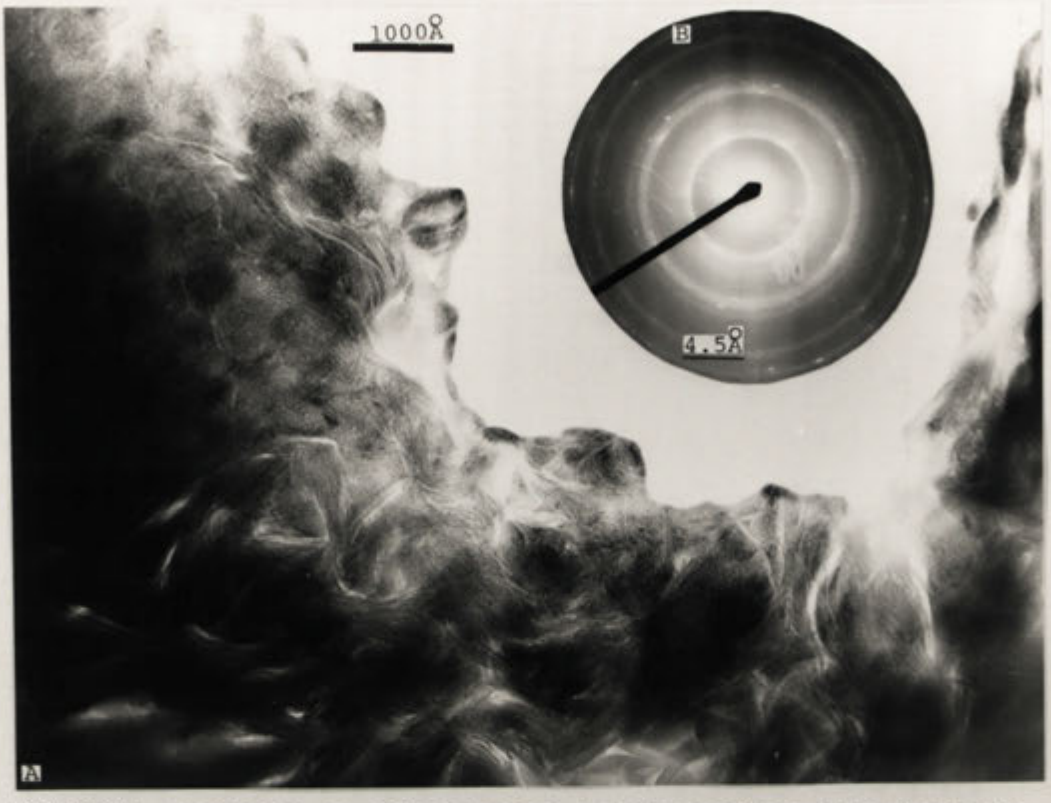

PLATE 6·7A: FORMATION OF SIMPLE STRIPS OF CLAY FROM POORLY CRYSTALLINE MATERIAL. PLATE 6·7B: DIFFRACTION PATTERN.

PLATE 6·7C: SEMI-AMORPHOUS OR POORLY CRYSTALLINE MATERIAL AND SIMPLE BUNCHES OF CLAY.

PLATE 6-8: CLAY CRYSTALLIZED PARALLEL TO (110) LATTICE PLANES, AND PERPENDICULAR TO THEM.

operation of a control exerted by the parent phase on the way in which its alteration products crystallize. A similar conclusion is suggested by Wilson and Farmer (1970), whose single crystal X-ray data indicated that during the early stages of weathering there is generally no orientational relationship between the clay and parent amphibole. They do, however, note a tendency for alteration products to parallel cleavage planes.

Regular laths of relatively well crystallized material are commonly observed in electron micrographs of weathered amphibole. Plate 6.9a illustrates a region of amphibole which has been etched, and replaced primarily by small curved bunches of clay which apparently crystallized in the manner described above. A large, far more regular lath of clay is also present in the lower right hand side of this photograph which appears to represent a more crystalline form of this material. The higher magnification image in Plate 6.9b reveals that the clay lath (which has been damaged by the electron beam) consists of a mixture of a 7 Å kaolinite component as well as what appears to be a sheet silicate with a larger basal spacing. The diffraction pattern for this material in Plate 6.9c reveals a sequence of 00$\underline{l}$ spacings at 12.4 Å, 8.36 Å, 7.4 Å, 6.29 Å(weak), 5.05 Å, 4.37 Å(weak), 3.7 Å, 3.58 Å, 3.14 Å. On the basis of these spacings, the absence of a superspacing, and the observation of 12 and 7 Å spacings in the TEM image, it could be suggested that this material represents represents a random interstratification of smectite and kaolinite. The presence of a strong ~8 Å spacing is noted by Schultz et. al., (1971) to be the most diagnostic feature of mixed layer smectite-kaolinite character after heating to 300°C, (similar to collapse of smectite in the TEM). However, it is difficult to attribute the diffraction pattern in Plate 6.9c to a randomly interstratified smectite and kaolin as reflections observed are far too clear and sharp to have been produced by such a material.

Diffraction patterns for similar laths in weathered amphibole also contain 00$\underline{l}$ reflections at many of the spacings listed above. In one example the 7 Å reflection was not detected, and in another (Plate 6.9d), a sequence of sharp reflections at 12.7 Å, 6.4 Å, 4.2 Å, 3.23 Å, 2.55 Å are present. This pattern is sufficiently clear to indicate the absence of a 25 Å reflection, and of 14 and 10 Å reflections. The image for this material was of poor quality, and has not been reproduced. It

PLATE 69A: MORE REGULAR LATHS ARE PRESENT IN THE ALTERATION ASSEMBLAGE, ASSOCIATED WITH CURVED BUNCHES OF CLAY.

PLATE 6·9B: HIGHER MAGNIFICATION PHOTOGRAPH OF LATH IN 9A, A MIXTURE OF 7Å KAOLINITE FRINGES ARE ASSOCIATED WITH LARGER LATTICE SPACINGS.
PLATE 6·9C: DIFFRACTION PATTERN.

does, however, indicate that the reflections were from a regular sequence of ~12 Å fringes. It would appear that this material is far too well crystallized to be smectite. Although the identity of this material can not be clearly established, Eggleton (pers. comm., 1985) has suggested that this phase could be stilpnomelane. Ferristilpnomelane has been detected forming in the weathering environment from nontronite after hedenbergite by Eggleton and Chappell (1978), and is reported by Macdonald and Grubb (1970) to be formed from nontronite during diagenesis. Regardless of its identity, these laths appear to coexist with the wavy textured nontronite. As illustrated in Plate 6.9b, this phase appears to be replaced by kaolinite which crystallizes onto the margins of existing sheets in a similar fashion to that observed where kaolinite replaced biotite, (Chapter 5), and illite-smectite, (Chapter 4), possibly suggesting that it forms epitactically on existing layers, and gradually replaces them.

Laths primarily composed of kaolinite (Plate 6.10a) are commonly identified by diffraction patterns such as that given in Plate 6.10b, and by their chemistry. An enlargement of the region from where this diffraction pattern was obtained is presented in Plate 6.10c. The oval shaped mark in the left hand side of this plate has been produced by contamination caused by exposure to the beam during analysis. Small dark marks in Plate 6.10a also indicate areas from where analytical data were obtained using the STEM. Qualitative chemical data obtained from these, and other areas are discussed in the following section.

Chemical characterisation of alteration products:

Energy dispersive scans obtained using the STEM are reproduced in Plate 6.11. The spectra produced by amphibole is presented in Plate 6.11a, early formed, partially crystalline material in 11b, reasonably well crystallized, curving laths of clay in 11c, remaining darker semi-amorphous material in 11d, the lath composed primarily of kaolinite illustrated in Plate 6.10c in 6.11e, and material which replaced a large regular chlorite lath in 11f. These data indicate that the early formed semi-amorphous material is richer in Al than the amphibole host. This phase appears to crystallize to curving bands of smectite rich in Fe and Mg, and poor in Al, probably nontronite. Remaining semi-amorphous material contains Ca, K, Ti and Fe which are not accommodated into the smectite structure. Analyses for the subsequent stage where

PLATE 6·10A: LATH APPARENTLY COMPOSED OF KAOLINITE.
PLATE 6·10B: DIFFRACTION PATTERN CONTAINING 10Å KAOLINITE REFLECTIONS.

PLATE 6·10C: HIGHER MAGNIFICATION PHOTOGRAPH OF LATH IN 10A, THE MARK INDICATES WHERE THIS MATERIAL WAS ANALYSED IN THE STEM.

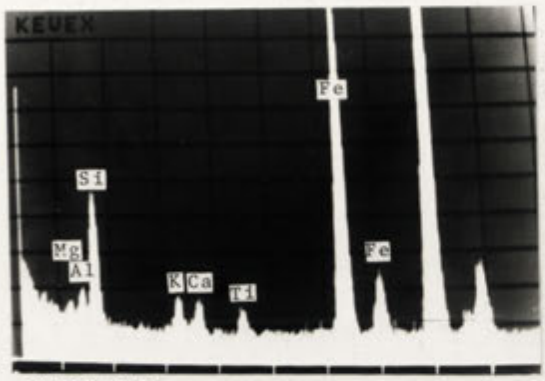

PLATE 6.11A: AMPHIBOLE SPECTRA

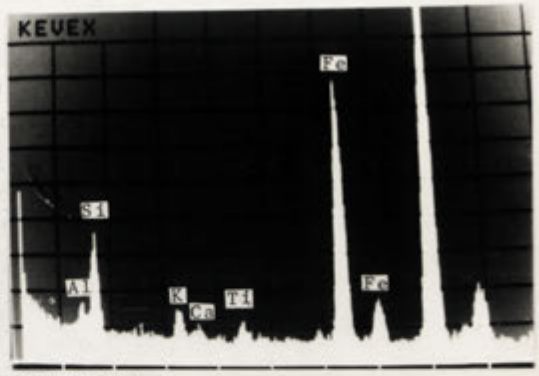

PLATE 6.11D: DARK SEMI-AMORPHOUS MATERIAL.

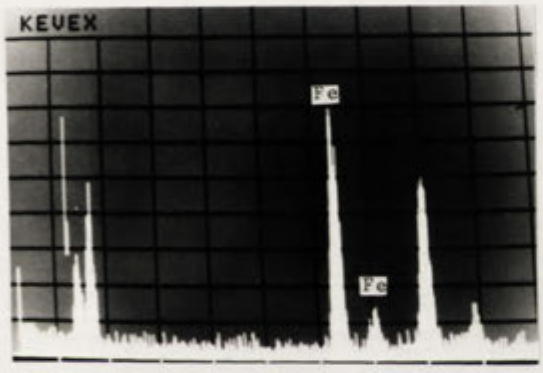

PLATE 6.11B: PARTLY CRYSTALLINE MATERIAL.

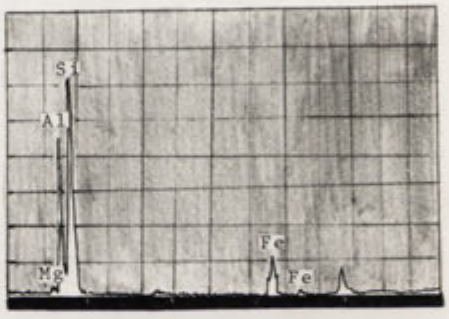

(TRACING)

PLATE 6.11E: PRIMARILY KAOLINITE.

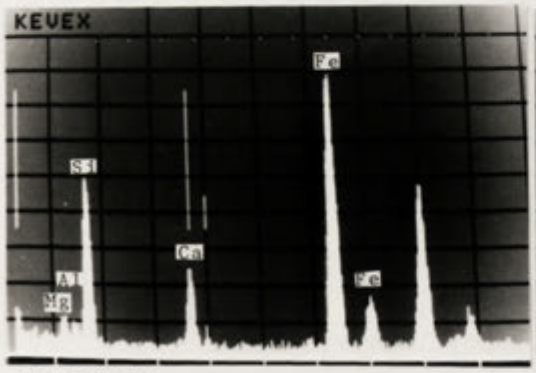

PLATE 6.11C: CURVING LATHS OF CLAY.

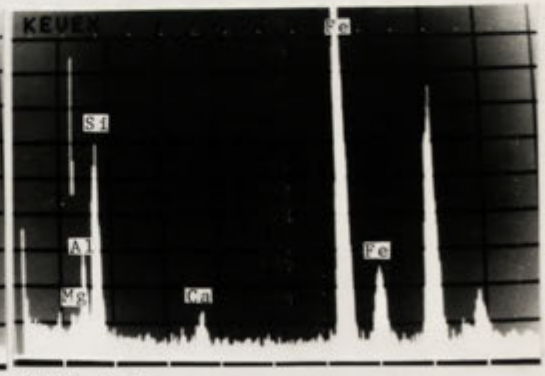

PLATE 6.11F: VERMICULITE AFTER CHLORITE.

crystallization of kaolinite was observed indicate the coexistence of this phase with a phase poorer in Al, and enriched in Fe and Mg. The presence of smectite (nontronite) in this material would be consistent with the chemical data; as kaolinite appears to be the late stage alteration product of amphibole, it would seem logical that mixtures of this phase and smectite occur. However, as a mixture of stilpnomelane and kaolin would also be consistent with the chemical data the possibility that smectite alters to kaolinite via a phase such as stilpnomelane could also be tentatively suggested.

The spectra reproduced in Plate 6.11f for the phase replacing chlorite suggests that it is vermiculite. The vermiculite, like its parent is comparatively rich in Al. The development of vermiculite as a weathering product of amphibole derived chlorite contrasts with the observation that biotite derived chlorite is apparently replaced by kaolinite.

Microprobe data for the weathering products in amphibole were also obtained. The major feature of these analyses is their enormous variability. This is interpreted to reflect the coexistence of many intimately mixed phases on a scale far smaller than the beam size of the probe. This can be clearly demonstrated in TEM images. The most interpretable analyses are presented below.

SMECTITE

K	Ca	Mn	Mg	Fe	Al	Al	Si
.02	.28	.19	2.49	2.83	.31	.63	7.37
-	.42	.20	2.93	3.09	-	.30	7.44

VERMICULITE

.06	2.72	4.09	.43	3.28	4.72
.04	2.15	3.30	.16	2.42	5.58
.03	1.82	3.52	-	3.13	4.87
.04	1.61	3.21	-	2.95	5.05

SECTION 4

SEM OBSERVATIONS

SEM observations of weathered amphibole illustrate the way in which dissolution proceeds, and the development of alteration products within the crystallographically bounded regions produced by dissolution.

Observations serve to reinforce the description of amphibole weathering obtained using the TEM.

Plate 6.12a clearly illustrates elongate etches developed parallel to cleavages. A thin coating of clay can be observed on many of the exposed surfaces. Plate 6.12b provides a much higher magnification image of this clay coating, and illustrates the tendency for alteration to concentrate in large channels or cracks developed within amphibole.

Saw-tooth fragments formed as a result of dissolution along cleavage directions are clearly illustrated in Plate 6.13a. Although most cleavage fragments are coated with fine grained alteration products, some much coarser clay material can be observed towards the centre of this plate. A higher magnification image of this material is provided in Plate 6.13b. The curving bands of clay developed fairly randomly within the etched amphibole structure strongly resemble smectite observed in the TEM.

SECTION 5

CONCLUSIONS

A study of weathered amphibole from the Bemboka profile has revealed that this phase begins to alter relatively early in comparison to other granitic minerals. The initial stage is dissolution, which occurs along crystallographically controlled lattice directions. In thin section this is indicated by widening of cleavages, in the SEM by the development of channels parallel to cleavage bound fragments, and in the TEM by the appearance of regularly spaced etches whose orientation is very strongly controlled by {110} lattice planes. These etches develop along pre-existing dislocations, and result in the appearance of cleavage bound fragments with a saw-tooth appearance.

Disaggregation of amphibole appears to occur, resulting in the development of areas of semi-amorphous material. These recrystallize to form increasingly regular, large laths of clay whose lattice dimensions resemble those of smectite. Qualitative chemical data indicate that this smectite is nontronite. Remaining poorly crystalline material is apparently enriched in Fe and Ti; these components presumably concentrate until Fe and Ti oxides can crystallize. Ca and K released

PLATE 6.12A: SEM PHOTOGRAPH OF THE DEVELOPMENT OF CRYSTALLOGRAPHICALLY CONTROLLED ETCHES.

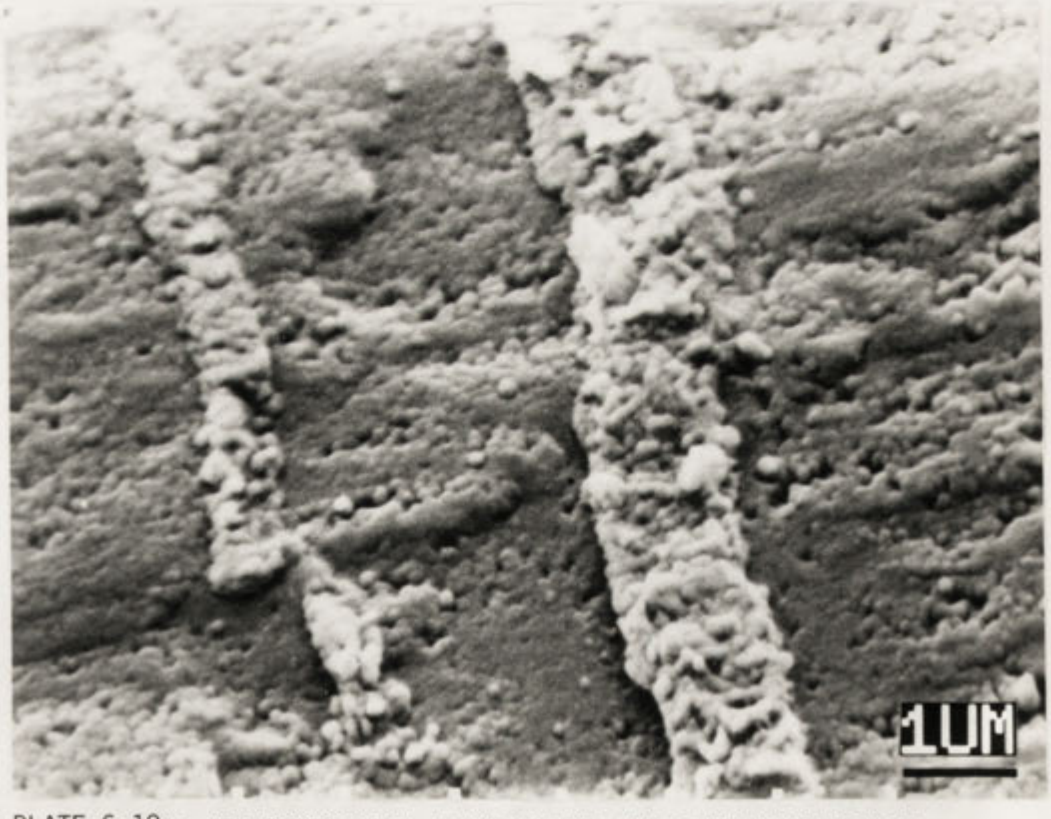

PLATE 6.12B: SEM PHOTOGRAPH ILLUSTRATING THE CONCENTRATION OF ALTERATION PRODUCTS ALONG CRACKS OR CHANNELS.

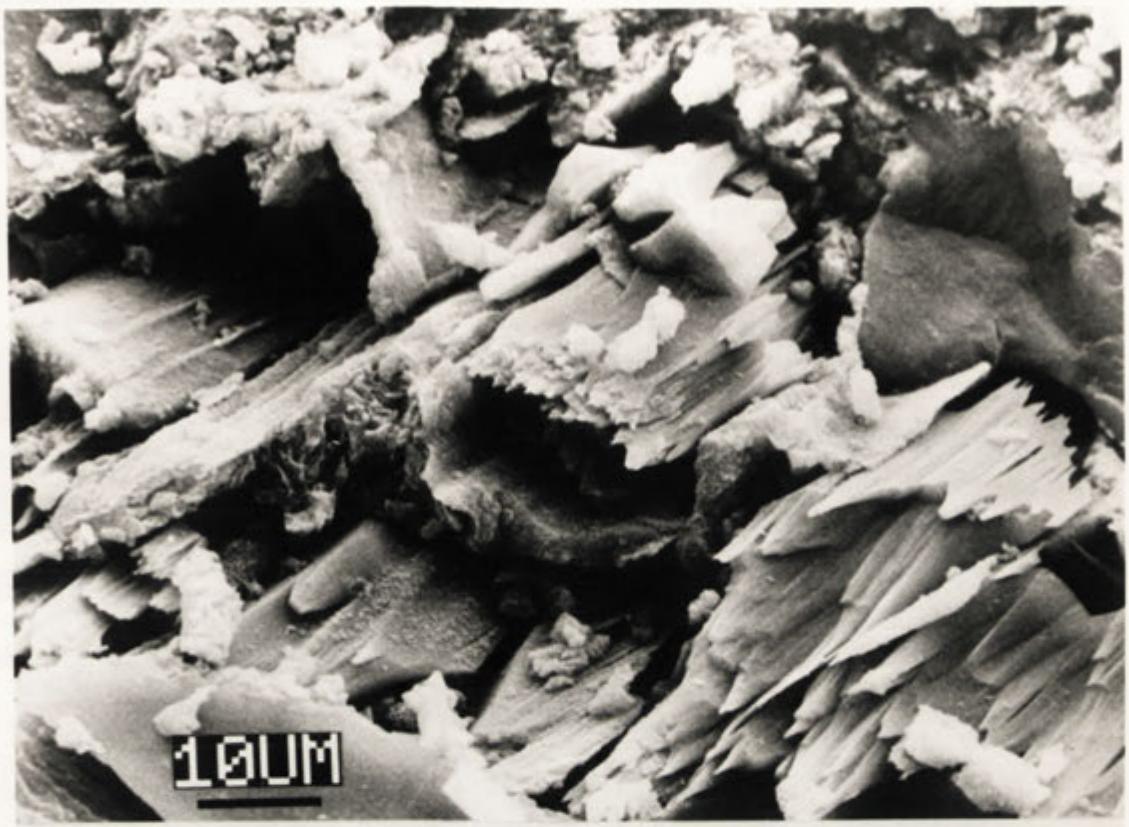

PLATE 6.13A: SAW - TOOTH AMPHIBOLE FRAGMENTS PRODUCED BY CRYSTALLOGRAPHICALLY CONTROLLED DISSOLUTION.

PLATE 6.13B: ALTERATION PRODUCTS DEVELOPED BY REPLACEMENT OF AMPHIBOLE (HIGH MAGNIFICATION PHOTOGRAPH OF ABOVE).

from amphibole are also associated with this material, and are adsorbed onto clays.

As in the case of K-feldspar and plagioclase feldspar weathering, breakdown of amphibole proceeds via a sequence of phases which become unstable as weathering proceeds, and are replaced. Like the feldspars, amphibole is converted via an amorphous stage to a smectite whose chemistry strongly reflects that of the parent phase, and later to kaolin. Kaolin appears to be the final product of weathering of all these phases. There is a possibility that a phase such as stilpnomelane develops as an intermediate between smectite and kaolinite in some areas. This is suggested by the development of well crystalline laths in mixtures of weathering products with diffraction patterns and images which are difficult to attribute to any other phase.

Vermiculite also present in the alteration assemblage develops as a result of chlorite weathering. The composition of this phase reflects the Al rich nature of the parent chlorite, resembling the development of Al poor, Fe rich smectite from the hornblende.

Chlorite is present within unweathered amphibole, and like talc, appears to have formed as a result of the hydrothermal alteration of amphibole.

Chapter 7

THE REPLACEMENT OF APATITE, AND THE BEHAVIOUR OF R.E.E. DURING WEATHERING

ABSTRACT

A Scanning Electron Microscope (SEM) examination of biotite from weathered Bemboka granodiorite revealed the presence of a number of phases which have formed in pits after apatite, and as rinds on relic apatite crystals. These phases have developed a range of distinctive morphologies, including 'donut' shaped objects (about 3μm in diameter), ropes and chains of donuts, platelets, and a variety of crystallites. These occur as rinds on the apatite parent.

Qualitative energy dispersive SEM, and quantitative wavelength dispersive Cameca probe analyses indicated that these alteration products were composed of LREE*, Al, P, with smaller quantities of Fe, Ba, Ca, and heavier REE. Analyses of material with a range of morphologies revealed that at least three quite distinct fractionation patterns could be identified. These were associated with highly variable proportions of the major components.

An SEM, TEM, AEM, XRD and light optics study revealed that both the donuts and the altered rims of apatite are composed of poorly crystalline material and larger, radiating crystals of florencite, $[(LREE)Al_3(PO_4)_2(OH)_6]$. Two varieties of florencite were identified, distinguished by their LREE fractionation patterns. The chondrite normalised REE pattern of the first is La rich, with a strong negative Ce anomaly, whereas the second has a gently sloping LREE pattern, with La>Ce>Nd⩾Sm. Where the surfaces of the donuts are disrupted, observations suggest the presence of an Al enriched coating, presumably clay.

Chemical data indicate the presence of a phase co-existing with florencite containing abundant REE and Al and which is apparently devoid

* Light Rare Earth Elements

of P. X-ray data and the prismatic form of these crystals suggests that this mineral may be a phase with characteristics similar to either ancylite or davidite.

Numerous crystallites exhibiting variable external form and style of development were observed in apatite pits. One variety, with a prismatic crystal form, was observed in the same pit as the more Ce rich florencite. This material contains about 50% REE and has a horizontal chondrite normalised LREE pattern with a strong negative Ce anomaly. Another of the more commonly encountered examples of crystallites was characterised by a hexagonal cross section. Electron diffraction patterns and qualitative chemical analyses indicated that this material was Nd rich rhabdophane $[(LREE)PO_4.H_2O]$.

SEM observations of unweathered through to strongly weathered samples demonstrate that apatite is rapidly etched, and chemically transformed by loss of Ca and addition of Al, Ba, Pb, Fe, and variable quantities of REE. Whole rock chemical data indicate that a substantial quantity of REE have been introduced from outside the sampled zone. Neutron activation analysis results suggest that this occurs early in weathering, after which these elements remain immobile. The net result is to enrich the profile in all REE without substantially changing the relative abundances of these components. With the exception of Ce which probably remains immobile as Ce^{4+} under oxidising conditions, replacement of apatite concentrates most REE to a similar extent. This is despite the fact that the phases responsible for accommodating these elements fractionate the REE dramatically. The lack of fractionation is interpreted to indicate that elements were introduced from elsewhere in the granite profile, and not from an external source.

The development of donut shaped REE-P phases has also been observed in the Island Bend profile. This is associated with a slight enrichment in the weathered zones of MREE[1] and HREE[2], while La is just conserved, and some Ce lost. This provides additional evidence that the REE display considerable mobility, particularly during the early stages of granite weathering.

[1] Middle Rare Earth Elements

[2] Heavy Rare Earth Elements

SECTION 7.1

PREVIOUS WORK

In granitic rocks the majority of the lanthanides are hosted in accessory phases, such as the silicate allanite, and phosphates such as monazite and xenotime. Although apatite generally contains significant quantities of these elements, this phase accounts only for a small proportion of the total REE content of the rock.

Nance and Taylor (1977) reported that REE were generally believed to be resistant to supracrustal fractionation. Similarly, Hanson (1980) stated that unless processes such as hydrothermal alteration and weathering were severe, they did not cause major changes in the patterns or abundances of REE. These views are contradictory to a large volume of literature, (often Russian), and are not supported by subsequently published reports. Work on a wide variety of rocks by has established that differential REE mobility, and resulting concentration and depletion commonly occurs as a result of weathering (Vlasov [1966]; Burkov and Podporina [granite weathering crusts, 1967]; Krasil'nikov [granites, 1969]; Blashov and Kudinov [carbonatites, 1966]; Kholodov [phosphorites, 1972]; Nesbitt [granodiorite, 1979]; Podporina et. al. [granites and migmatites, 1980]; Morris et. al., [nickeliferous laterite, 1980]; Schau and Henderson [saprolite and granite basement, 1983]; Koicki et. al. [bauxite, 1983]; Ludden and Thompson [seafloor basalt weathering, 1978]; Urritia Fucugauchi [seafloor basalt, 1979]; and Bonnot-Courtois [seafloor basalt, 1980]).

Nesbitt (1979) observed a progressive enrichment of REE in moderately weathered granodiorite; HREE were enriched by up to 300%, LREE by 100-200%. The model which he advanced to explain this involves mobilization of REE in response to changes in groundwater and soil pH. These elements are transported by acidic solutions down the profile, and deposited in areas where rock-water interactions have resulted in the development of alkaline conditions. Nesbitt attributed the observed fractionation of these elements at least partly to preferential adsorption of HREE by vermiculite, relict hornblende, and biotite. Kaolinite and illite were nominated to be phases which preferentially accommodated the LREE.

The work of Burkov and Podporina (1967) described observations similar in many respects to those of Nesbitt (1979). These authors assessed the role of clay minerals in adsorbing REE and discovered that these phases could account for up to 17% of the total REE content of the rock. They noted that Ce earths were preferentially adsorbed by clays.

Duddy (1980) documented an example of a granite weathering profile where REE were substantially enriched in certain zones. He proposed a model similar to that of Nesbitt (1979), and reported that up to 10.1% La+Ce+Nd+Y were fixed in vermiculte.

Ludden and Thompson (1978) studied the distribution of REE in submarine basalt weathering rinds. They described a substantial enrichment of REE which they attributed to uptake of these elements from seawater.

The weathering of primary REE bearing phases has not been the subject of many investigations. Under leaching conditions fluorapatite is reported to be relatively resistant to weathering, while hydroxyapatite is relatively unstable. Chlorapatite has a stability intermediate between the two (Loughnan, 1969). Rimsaite (1982) considered the alteration of a number of accessory phases including monazite, allanite, and apatite. She noted that allanite contained numerous REE, U, Th, P, carbonate and silicate bearing phases which alter under hydrous oxidising conditions with the allanite host. Leached elements may reprecipitate in secondary minerals and crusts. About apatite, Rimsaite comments:

> "Although apatite is relatively stable in hydrothermal and in weathering environments, shattered crystals partly replaced by an unidentified U-Nb bearing phase were found in relatively fresh pyrochlore pegmatite from the Bancroft area". p259

The belief that apatite should be relatively stable in the weathering environment is also expressed by Wolfendon (1965), who states:

> "..much of the apatite in the parent andesite must have been dissolved, despite the known resistance of apatite to weathering".

Gusev et. al. (1976) studied the weathering of apatite by analysing

fresh and weathered phosphate and experimentally leached apatite. The conclusions to this work were that monovalent anions such as fluorine were the first to be lost from the lattice, probably followed by Ca and then P.

A number of REE phases, commonly phosphates and carbonates are found in weathering crusts, soils and residual deposits. The link between the formation of these phases and the primary minerals in fresh rock has not been investigated thoroughly. The significance of some of these phases as hosts for phosphorus in soils has resulted in the intensive study, particularly of the plumbogummite series ($(Ca,Sr,Pb,Ba,REE)(Al_3)(PO_4)\ .H_2O$) by soil scientists, (eg. Norrish, 1968; Botinelly, 1976). Botinelly (1976) noted that members of the alunite-jarosite, beudantite, and plumbogummite groups were formed at low temperatures under slightly acid, oxidising conditions. Similarly, McKie (1962) reported that goyazite, florencite, and gorcexite in carbonatites appeared to have crystallized during the late stage of the replacement process or under supergene conditions, ($<500^{o}C$). He suggested that the phosphorus for these phases may be derived by dissolution of apatite.

It would seem that the weathering of accessory phases such as apatite and allanite is poorly understood. The variable susceptibility of apatite to dissolution is commonly noted. Literature concerned with the behaviour of REE reports that these elements are mobile and can be fractionated despite the fact that they have been considered generally to be resistant to fractionation in the weathering environment.

SECTION 7.2

APATITE WEATHERING

INTRODUCTION

Apatite in fresh Bemboka granite is unetched and unaltered, (Plate 7.1A). Modification of apatite by dissolution (Plate 7.1B) and exchange of chemical components occurs during the very early stages of weathering, and results in the development of a complex assemblage of secondary phases. These replacement phases display an enormous range in external morphology, occurring as rims and crusts, a spectacular range of "donut" like objects, and as a variety of crystallites. The following sections describe the form and distribution of these phases, their mineralogy and chemistry, and the net effects of the assemblage on the bulk chemistry of the weathering profile.

SECTION 7.2.1

MORPHOLOGY AND DISTRIBUTION

In the Bemboka granite apatite is generally present as euhedral crystals enclosed in biotite. Consequently replacement phases are developed in prismatic or hexagonal pits which occasionally contain relict apatite. These phases may form a featureless shell on the apatite, or occur as a sculptured rim. Donut shaped objects can be observed evolving in this rim with more extensive alteration. This sequence is illustrated in Plate 7.2A.

The second group of replacement phases occur as crystallites which display a variety of forms. A commonly encountered example is illustrated in Plate 7.2B. These crystallites frequently fill a considerable volume of the pit, but only rarely coexist with apatite. This suggests that crystals develop at a later stage in weathering.

It is rare to observe donuts and crystals in the same pit. Plate 7.3 illustrates one of the few examples where these phases have formed in close proximity. Massive material developing a more rounded, donut-like morphology is also present in this pit.

Some examples exhibiting the range in form of the donuts,

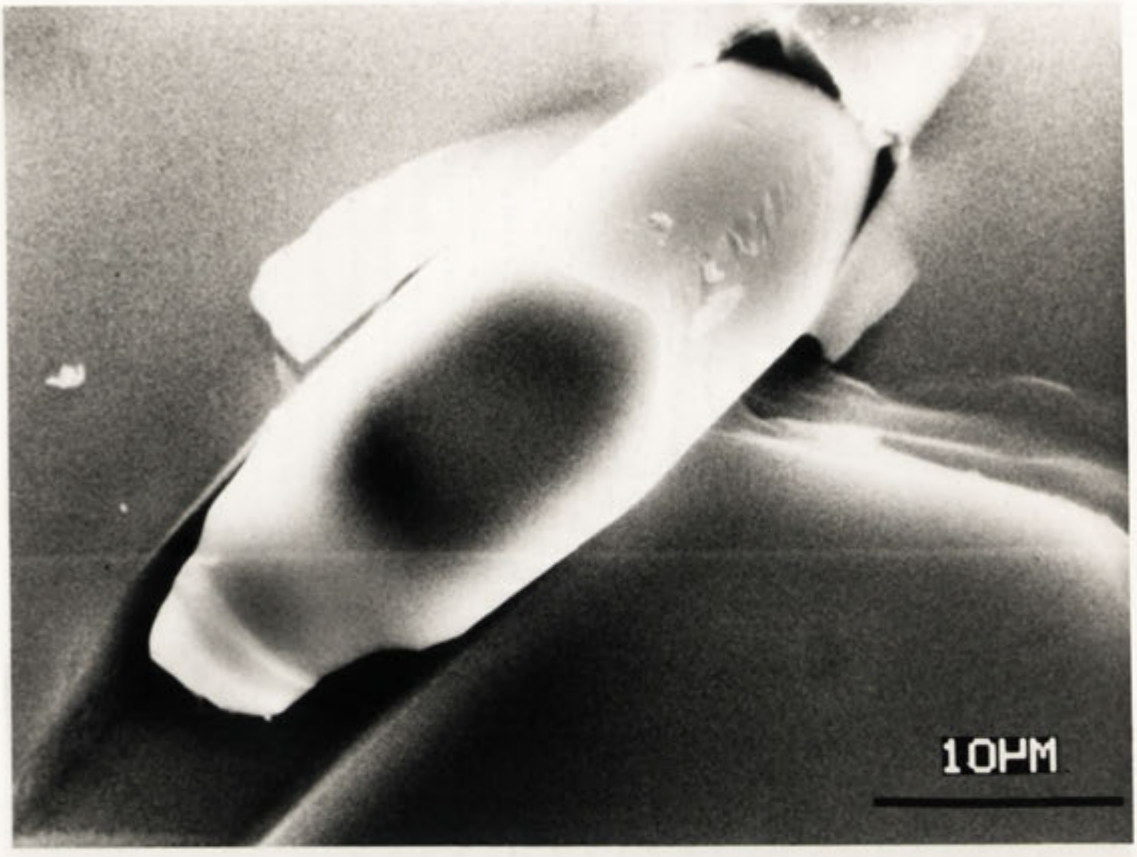

PLATE 7-1A: UNALTERED APATITE CONTAINED IN BIOTITE FROM FRESH ROCK.

PLATE 7-1B: ETCHING OCCURS DURING THE EARLY STAGES OF GRANITE WEATHERING.

Plate 7.2

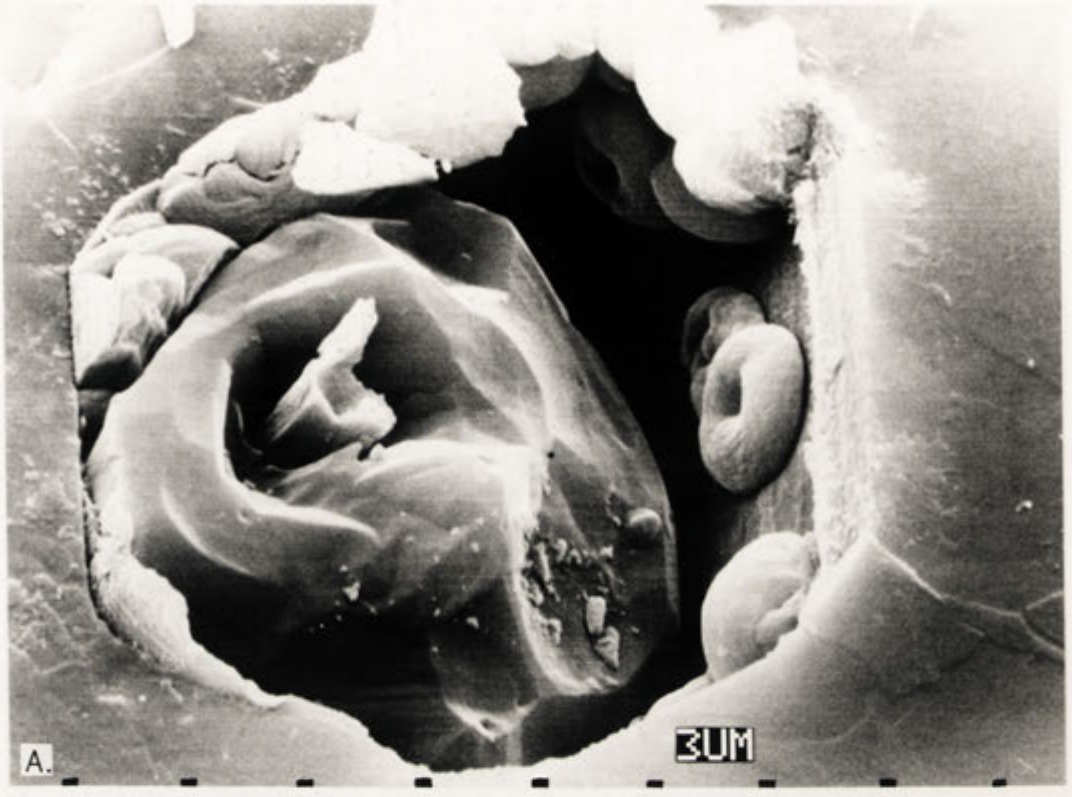

: A. Donuts.

: B. Crystals of rhabdophane.

REPLACEMENT OF APATITE CRYSTAL IN BIOTITE BY R.E.E.-PHOSPHATE PHASES.

Plate 7.3:

RARE EARTH ELEMENT-PHOSPHATE MINERALS DEVELOPED AFTER APATITE IN A BIOTITE CRYSTAL

crystallites, and rims are given in Plates 7.4, 7.5, and 7.6. Plate 7.4A reveals that the surface of donuts is not smooth, but covered in numerous concentric ridges. This may reflect the internal structure of these objects. In most cases where the shape of the donuts is well developed they have a central circular depression. In many cases they resemble a spiral coil, with a step developing in the donut ring (Plates 7.4A and 7.4B). Variation in size of these objects can be seen in Plate 7.4.B, and in Plate 7.4C where they form a rope-like mass.

The explanation for the central depression in the donuts is not clear. It is unlikely that it is an artifact caused by the vacuum in the coater or SEM as no other signs of collapse or distortion were observed, even when this material was subjected to a beam (during analysis) for quite considerable periods of time. Furthermore, as illustrated in Plate 7.4D, donuts occasionally contain holes rather than depressions, presumably implying that there is a structural basis for the development of the features observed. The role of internal organisation in controlling the external morphology of this material is also indicated in Plate 7.5A where the surface has been disrupted. This appears to indicate a structure dominated by radiating platelets, or crystallites.

Rims or rinds on remnant apatite generally develop as a thick shell, separated to some extent from the parent phase by regions where dissolution has occurred. In Plate 7.5B, for example, the central core was analysed using the CAMECA probe, and shown to be completely unmodified apatite. The rim on this crystal contained about 18% La_2O_3, and virtually no Ca, indicating that transformation to a completely new chemistry has occurred by this stage. Plate 7.5C also illustrates the apatite dissolution replacement sequence, with donut shapes developing in the altered rim. The further development of this sequence is shown in Plate 7.5D where apatite has been completely replaced by aggregates of donut like objects.

Some rinds do not exhibit a tendency to form rounded, donut like shapes. For example, Plate 7.6A illustrates a knobbly rind of material developed over apatite which has undergone only minor dissolution. The crystallographic control on the way in which apatite dissolution occurs can be clearly observed where concentric hexagonal ridges in the apatite surface reflect the structure of this phase. Although Plate 7.6B also

PLATE 74A

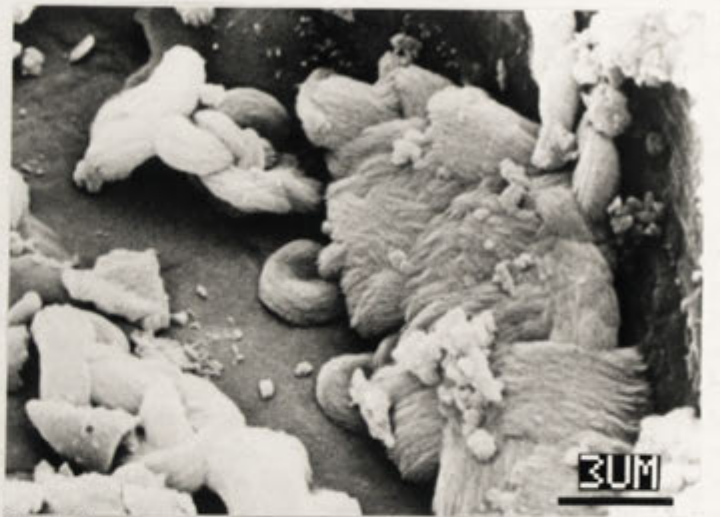

PLATE 74C

PLATE 74B

PLATE 74D

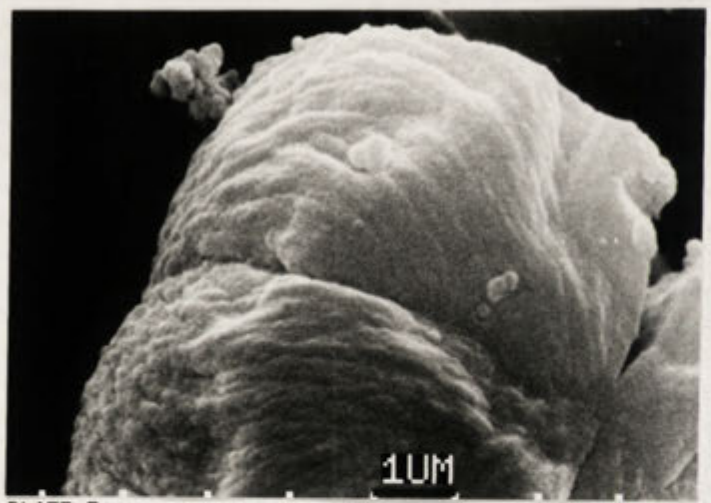

PLATE 75A

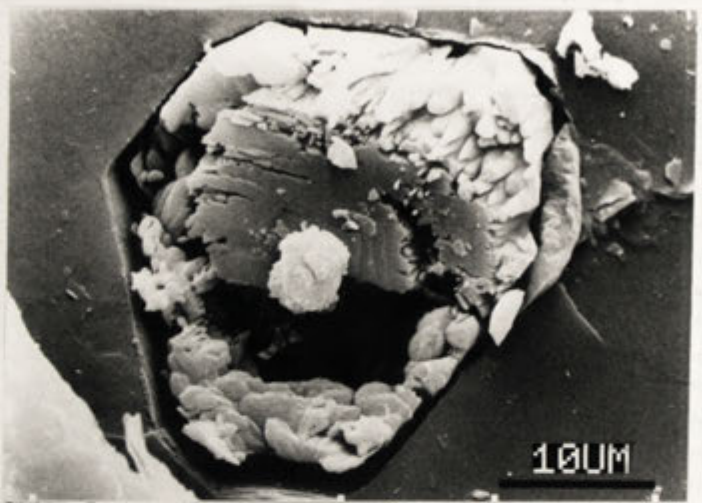

PLATE 75C

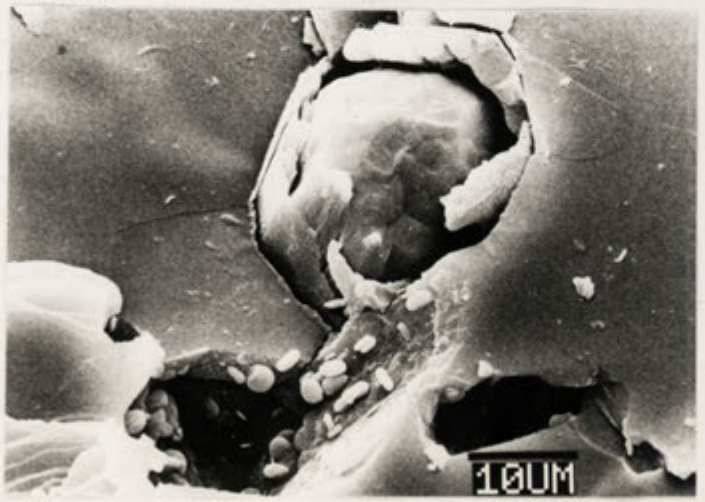

PLATE 75B

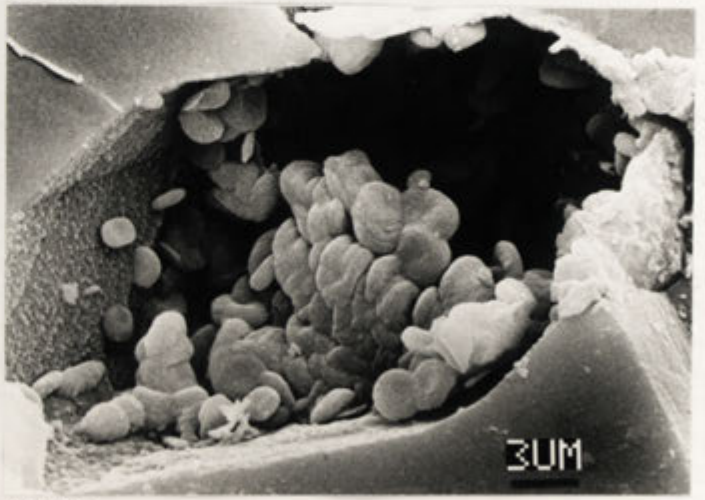

PLATE 75D

PLATE 7.6A

PLATE 7.6D

PLATE 7.6B

PLATE 7.6E

PLATE 7.6C

PLATE 7.6F

illustrates the development of a sheet like area of secondary material, this example differs in that where this phase is less continuous an array of underlying crystallites can be observed. These have apparently formed from the altered crust. Plates 7.6C, 7.6D, 7.6E, 7.6F illustrate pits containing crystals which appear to have grown from a similar material. These vary in size and shape within these pits, as well as differing in form between them.

Donuts, crystallites, and rims on apatite are present in very slightly weathered samples (Bemboka 2), and have been identified in successively more altered samples in the sequence, through to very strongly weathered material (Bemboka 6) where the parent apatite generally can not be recognised.

SECTION 7.2.2

DONUT AND RIM MINERALOGY

Introduction

Qualitative chemical information was obtained by examination of spectra produced by the SEM. These indicated that the donuts and rims are composed of a mixture of MREE and LREE, Al and P. Peaks indicating the presence of small quantities of Fe, Ca, Ba, Pb, HREE and possibly Ti were also detected. An example of the spectra obtained for this material using the SEM is given in Figure 7.1. Some variation was observed in the size of peaks, particularly for the REE from replacement phases. CAMECA probe analyses revealed that this reflected the presence of two varieties of this material characterised by distinct LREE fractionation patterns. These data are discussed in Section 7.2D.

Small quantities of material which had been located in the SEM were extracted and examined in an optical microscope, the TEM and STEM. An X-ray film was also obtained for one sample. These data revealed that the bulk of the rim and donut material was florencite, a REE-Al-phosphate. The coexistence of a second phase with florencite is strongly suggested by chemical and d space data.

FIGURE 7.1 SEM SCAN OF ALTERATION PRODUCTS.

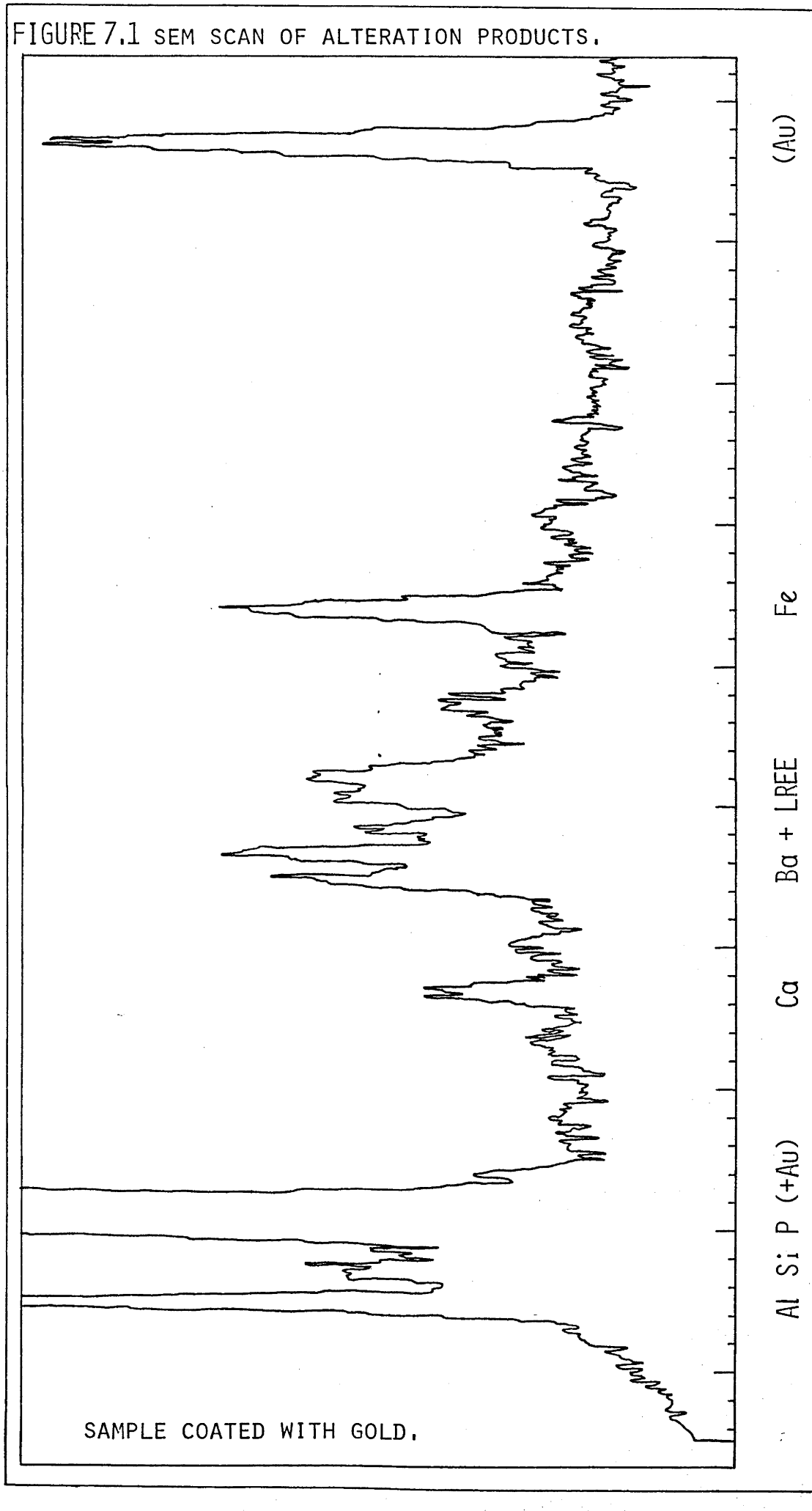

Optical microscopy

Two pits located on biotite flakes and containing donuts were identified initially in the SEM, and are shown in Plate 7.7. In transmitted light, donuts are transparent, pale greenish yellow in colour, with a refractive index estimated between 1.52 and 1.6, (A sample extracted for X-ray film was also tested, and appeared to have an R.I. in this range). Donuts do not appear to be pleochroic, and have a low birefringence, (first order grey). Under crossed polars they display an extremely strange behaviour, simulating a biaxial positive interference figure with an apparent 2V of about 30^{o}. The explanation for this phenomenon is not clear. The apparent interference figure may simply be caused by the small lense shape of the objects or could indicate that donuts are composed of crystallites arranged in such a way that they go to extinction in a symmetric sequence which simulates an interference figure.

Transmission electron microscopy

Phases were extracted from the pit shown in Plate 7.8, and examined in a TEM. In many cases donut and rim material was identified, but the sample was too thick to allow the minerals to be examined, or identified by their diffraction patterns. Where appropriate material occurred it was apparent that donuts consisted of radiating aggregates of a phase with a very fine net or cell like structure. This material produced poor diffraction patterns, containing a few broad rings. These powder rings exhibit a strong preferred orientation, indicating the presence of many very small, apparently crystalline units arranged in a regular manner. In Plates 7.9, 7.10A, 7.10B, 7.10C these subaligned crystallites can be observed to form lath-shaped domains. Single crystal spots are also present in many diffraction patterns. Many of these spots lie on the powder rings, or display a regular relationship with the maxima and minima in them, (Plate 7.10D). This is interpreted to indicate the coexistence of larger crystals with a poorly crystalline variety of the same phase (which produces the powder rings).TEM data are listed in Table 7.1. Results were obtained on the RSES 200kV microscope operated by John Fitzgerald using standardized conditions which allowed an accuracy of +/- 1%.

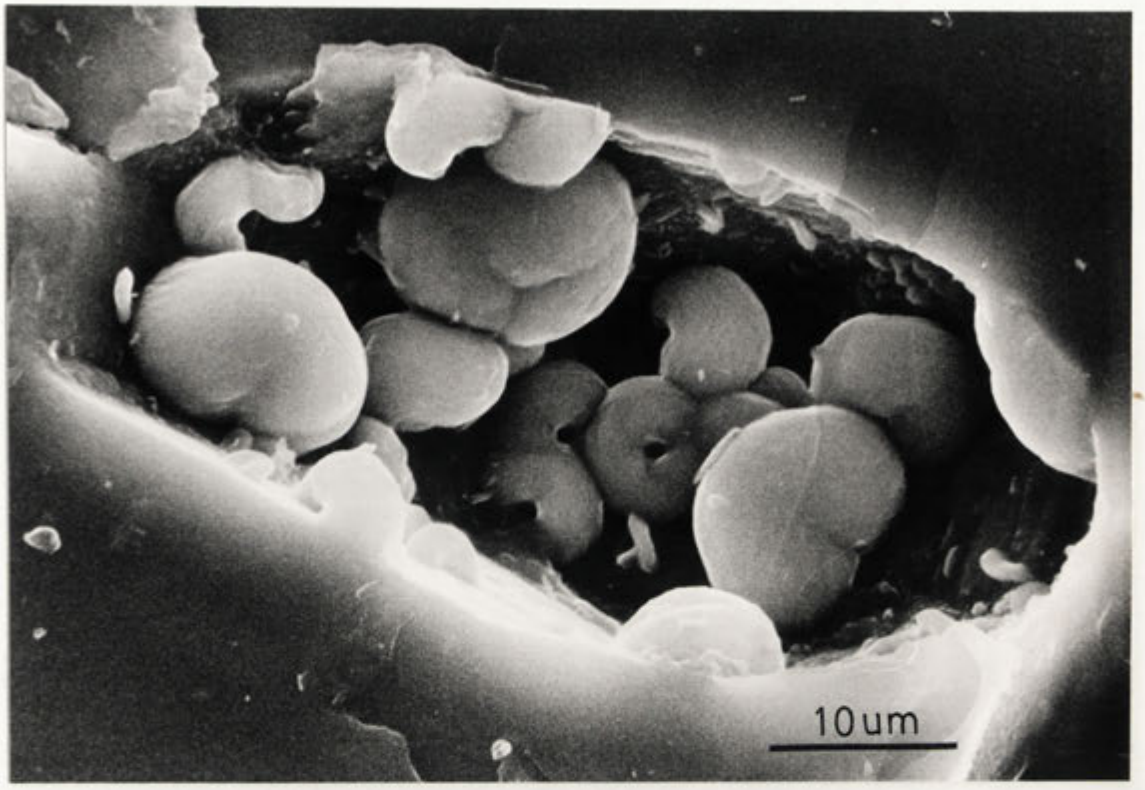

PLATE 7.7A: SEM photomicrograph of donuts in pit before extraction.

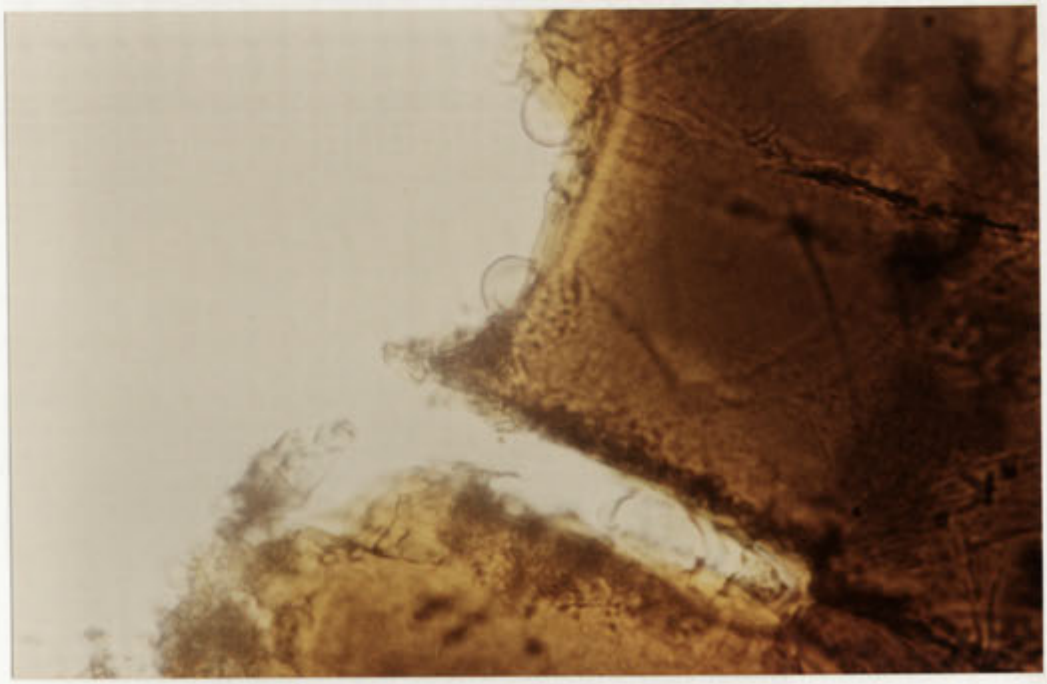

PLATE 7.7B: Donuts on biotite flake after extraction from pit shown above. Plane polarised light.

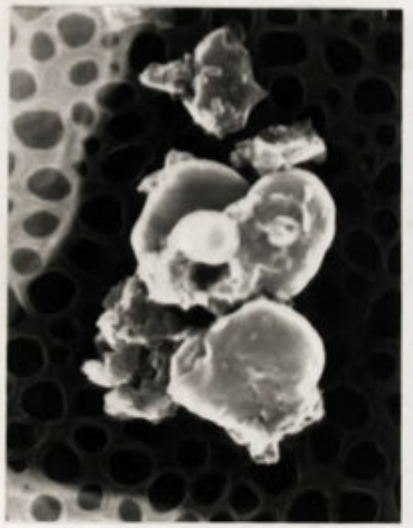

4 µM

PLATE 78B: APATITE REPLACEMENT PHASES USED FOR THE TEM STUDY ON A HOLEY CARBON GRID. (PHOTO: RSES ELECTRON MICROSCOPE BY J. FITZGERALD).

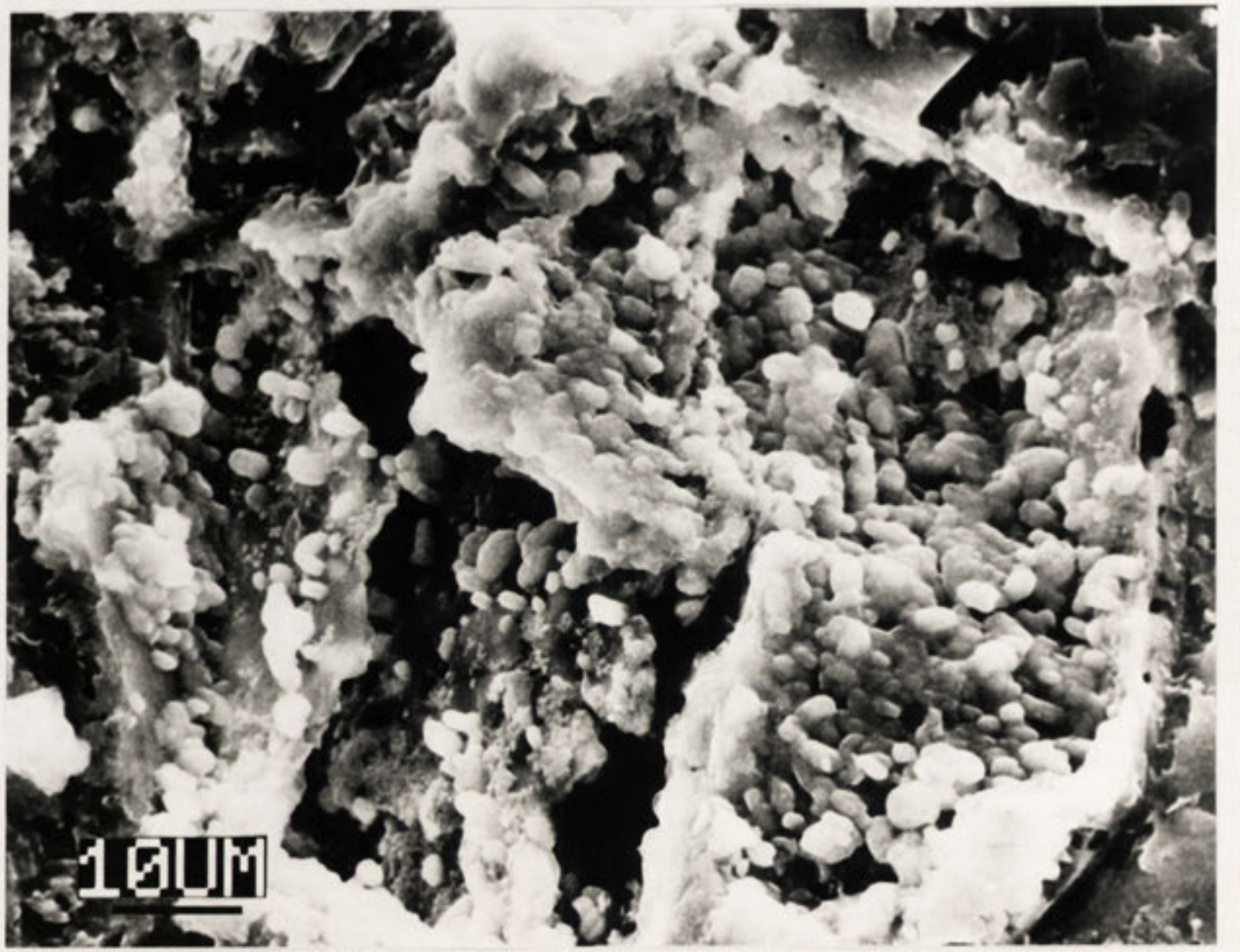

PLATE 78A: APATITE REPLACEMENT PHASES IN A PIT IN BIOTITE BEFORE EXTRACTION FOR EXAMINATION IN THE TEM.

Plate 7.9 :

REE-Al-Phosphate: Florencite

PLATE 7·10A: RADIATING FIBRES IN A DONUT FRAGMENT.

PLATE 7·10B: DIFFRACTION PATTERN FOR PLATE 10A.

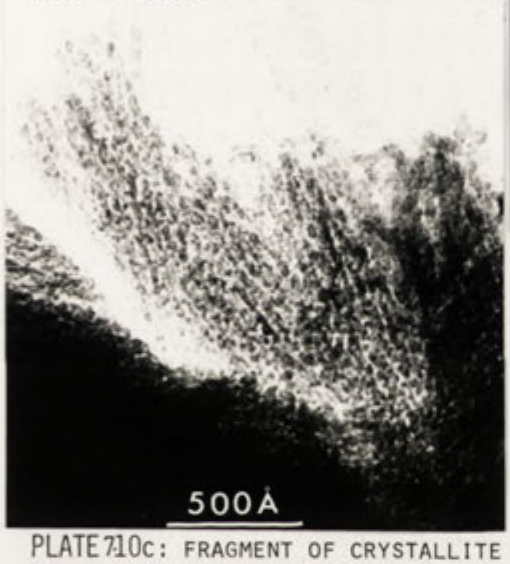

PLATE 7·10C: FRAGMENT OF CRYSTALLITE SHOWING BUILDING BLOCK TEXTURE.

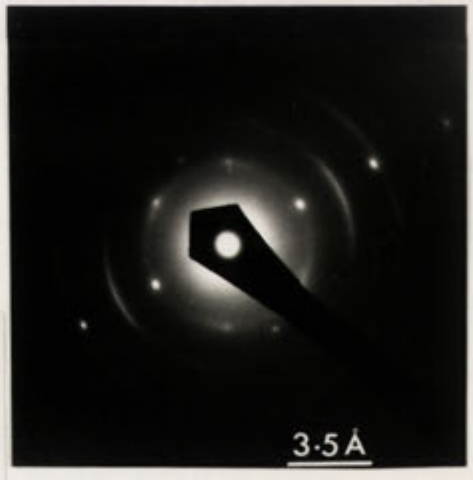

PLATE 7·10D: DIFFRACTION PATTERN CONTAINING SPOTS ON THE POWDER RINGS.

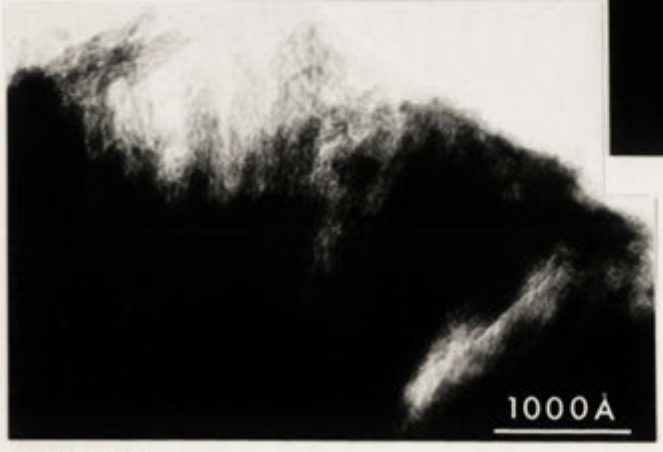

PLATE 7·10E: RADIATING CRYSTALLITES OF MORE CRYSTALLINE MATERIAL.

Table 7.1

TEM data for rings and associated spots:

spots and ring	3.49 Å\spots
spots	2.97 Å
ring	2.35 Å
ring	1.90 Å
spots	1.74 Å
ring	1.69 Å
ring	1.50 Å
ring	1.38 Å
ring	1.27 Å
spots	1.16 Å

Dark field images of some of these crystals were obtained using these single crystal spots. Photomicrographs were of poor quality, but did show what appeared to be prismatic crystals often over 1000 Å in length, (see bright field image of these crystallites in Plate 7.11D). Some radiating laths of more crystalline material are shown in Plate 7.10E, again suggesting that donuts are composed essentially of a mixture of coarsely, and very finely (or poorly) crystalline radiating fibres.

Plate 7.11 illustrates some additional examples of donut material, and the diffraction patterns obtained from it. The DP in Plate 7.11C contains an additional set of reflections which do not appear to belong to the phase described above. The presence of reflections at about 4.2 Å, and at 3.7 Å is noted in a number of diffraction patterns, suggesting the presence of a second phase. These reflections often appear to develop perpendicular or parallel to the maxima in the powder rings or single crystal spots, indicating that if a second phase is present it may have developed in an orientation which is crystallographically controlled by the first material.

X-ray diffraction

A small quantity of alteration products were extracted from an apatite pit, mounted on a glass fibre, and X-rayed using a 114mm Gandolfi camera. A long exposure (20 hours) was necessary as very little sample was available. The reflections present are listed in Table 7.2. These have been indexed as apatite, florencite, ($CeAl_3(PO_4)_2(OH_6)$) and a phase 'A?'which may be similar to ancylite (a Sr,Ca-LREE-carbonate) in structure. These phases are broadly consistent with the chemical composition of the material determined from qualitative energy dispersive SEM data before extraction.

PLATE 711A: SINGLE CRYSTAL SPOTS EXHIBIT SOME REGULAR DISTRIBUTION RELATIVE TO MAXIMA IN POWDER RINGS.

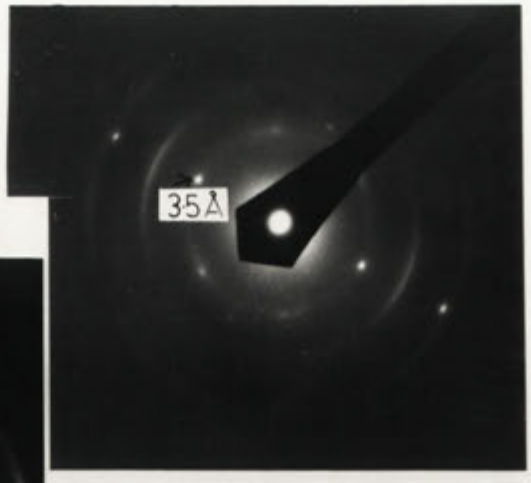

PLATE 711B: MAXIMA AND MINIMA IN POWDER RINGS INDICATING STRONG PREFERRED ORIENTATION.

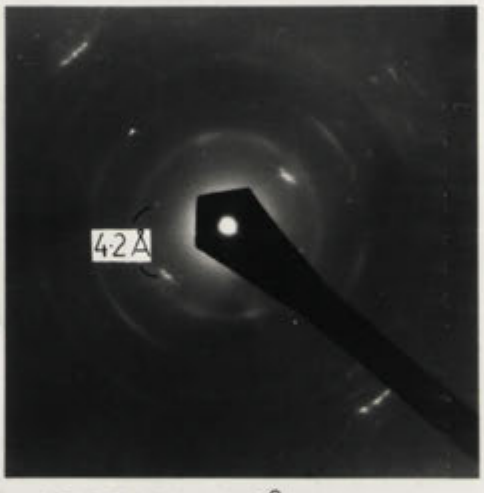

PLATE 711C: 4.2Å SPOTS ARE APPARENTLY ASSOCIATED WITH A SECOND PHASE.

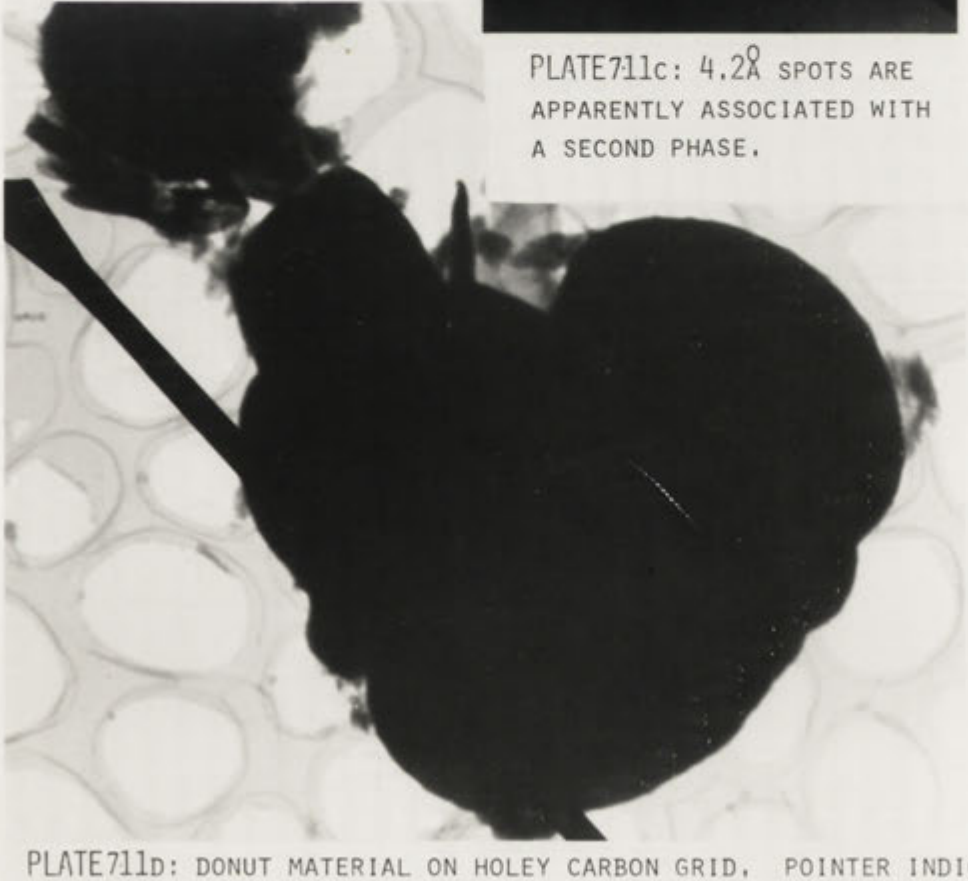

PLATE 711D: DONUT MATERIAL ON HOLEY CARBON GRID. POINTER INDICATES THE PRESENCE OF COARSER CRYSTALLITES.

Table 7.2: X-ray d space data

5.65 Å	broad	Florencite
4.18 Å	strong	? A
3.72 Å	moderate	? A
3.50 Å	mod-weak	Florencite
3.40 Å	mod-weak	Apatite,?A
3.18 Å	weak	Apatite
3.07 Å	weak	Apatite
2.93 Å	moderate	Apat;Flor;?A
2.81 Å	mod-strong	Apat; Flor
2.77 Å	moderate	Apat;?A
2.71 Å	moderate	Flor; Apat.
2.63 Å	mod-weak	Apat;??A
2.60 Å	v weak(?)	?
2.39 Å	weak	Flor;?A
2.25 Å	weak	Flor; Apat.
2.14 Å	v weak	Apat;Flor;?A
2.03 Å	v weak	Apat;Flor;?A
1.94 Å	weak	Apat;?A
1.88 Å	moderate	Flor;Apat;?A
1.84 Å	moderate	Apat;?A
1.80 Å	weak	Apat.
1.77 Å	v weak	Apat.
1.75 Å	v weak	Flor;Apat;?A
1.72 Å	v weak	Apat;?A
1.68 Å	v weak	Flor;Apat.

The reflections at 4.2 Å and 3.7 Å are amongst the strongest in the above list. These reflections (also recognised as spots in TEM diffraction patterns) are associated with relatively few minerals and could not be firmly assigned to any phase. Ancylite has been suggested as a possibility, although a mineral similar to davidite, a REE-Fe-Ti oxide, may be an alternative.

It is probably significant that many of the reflections may be attributed to both florencite and apatite. This may indicate that florencite crystallizes quite readily onto the apatite structure. Similarly, the phase associated with the 4.2 Å and 3.7 Å reflections probably shares many of the reflections which have been assigned to apatite and florencite.

SECTION 7.2.3

CRYSTALLITE MINERALOGY

Rhabdophane

A large variation in the size and shape of crystallites developed after apatite was observed. Rhabdophane has been identified as one of the more common forms by indexing the two diffraction pattern zones obtained for crystals (Plate 7.2A, 7.12A,B), extracted from a pit shown in Plates 7.12C and Plate 7.2B. The formula of rhabdophane is $CePO_4.H_2O$; the phase is hexagonal, and was described by Mooney (1950) as a modification of monazite (which is monoclinic). Rhabdophane readily converts monazite at moderately high temperatures. The hexagonal nature of this phase is apparent in the external morphology of crystals such as those in Plate 7.12C.

The identity of these crystallites was confirmed by examining the analytical spectra obtained from an STEM, (Plate 7.12D). This spectra indicated that the LREE assemblage was dominated by Nd and La, and contained virtually no detectable Ce. Similar Nd dominated rhabdophane compositions have been reported by Bowles and Morgan (1984). These authors noted that rhabdophane from magmatic rocks tends to be more Ce rich, while rhabdophane from sediments and limonitic ores can contain significant quantities of Nd.

Prismatic crystallites

A second variety of crystallite was also examined. This phase, illustrated in Plate 7.13, is sitting upon a REE-Al phosphate rim developed after apatite. The distinctly prismatic crystals were chemically analysed using the CAMECA probe. Their distinct REE fractionation pattern is given in Figure 7.2. Prismatic crystallites do not appear to contain significant P, and are rich in Al and REE, (particularly Nd and Sm). Probe totals for this material were low, (50-72%), suggesting that this phase may be a carbonate, oxide, or fluoride. The possibility that this phase may be the same as that producing the single crystal spots in diffraction patterns is considered in the following section.

PLATE 7·12

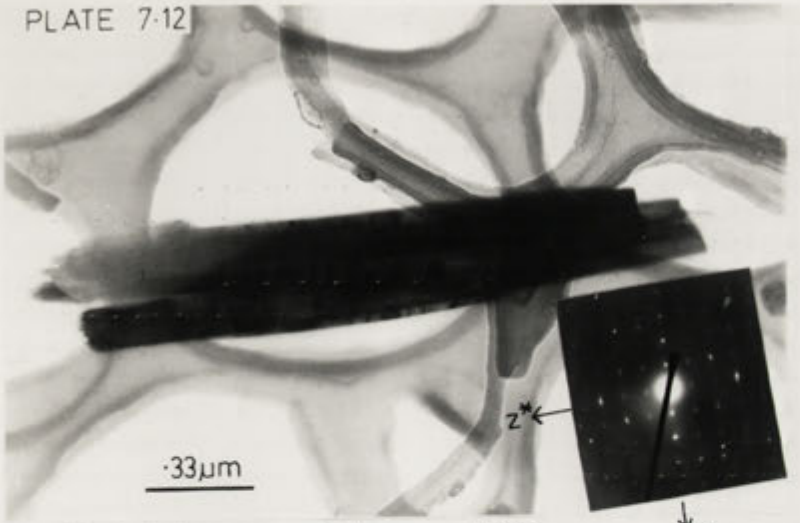

Rhabdophane crystals on a H.C.G.

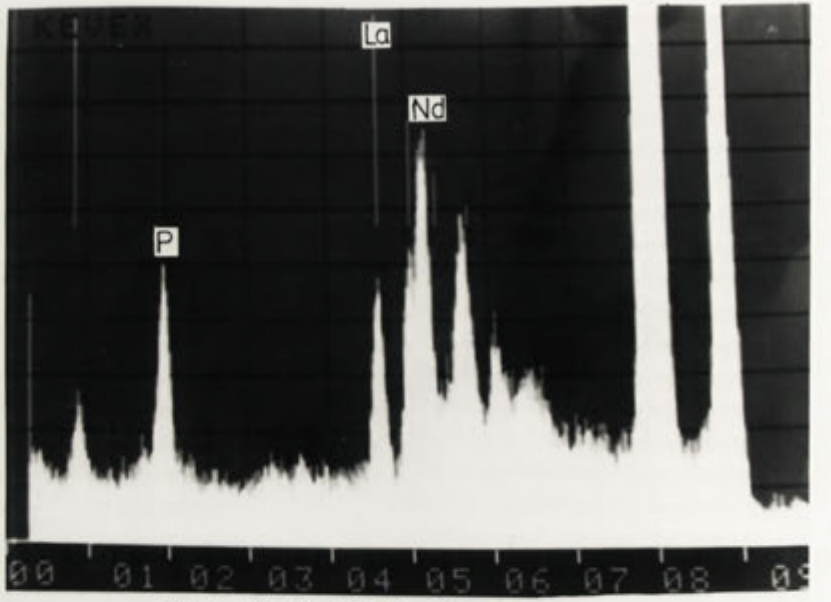

Plate 7·12 D: STEM Spectra

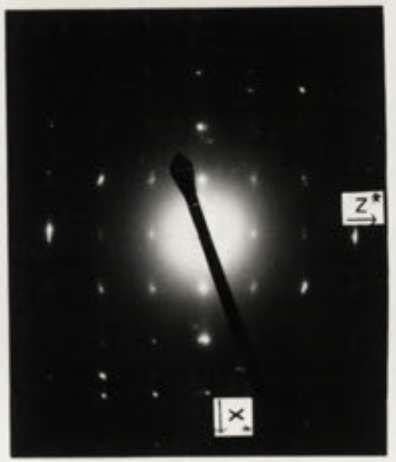

0°

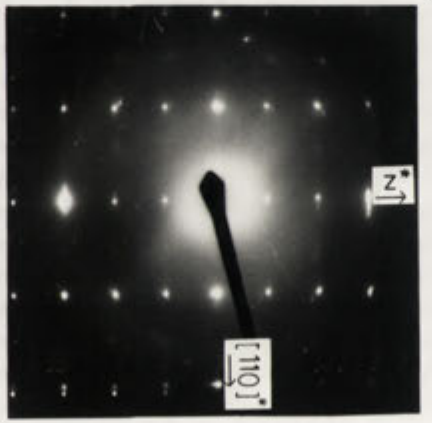

+30°

Plate 7·12 B
Diffraction patterns

Plate 7·12 C:
Hexagonal crystals.

1µm

Plate 7.13:

Prismatic crystallites: Nd-rich crystals on a relatively Ce-rich substrate.

FIGURE 7.2

CHONDRITE NORMALISED LREE ABUNDANCES

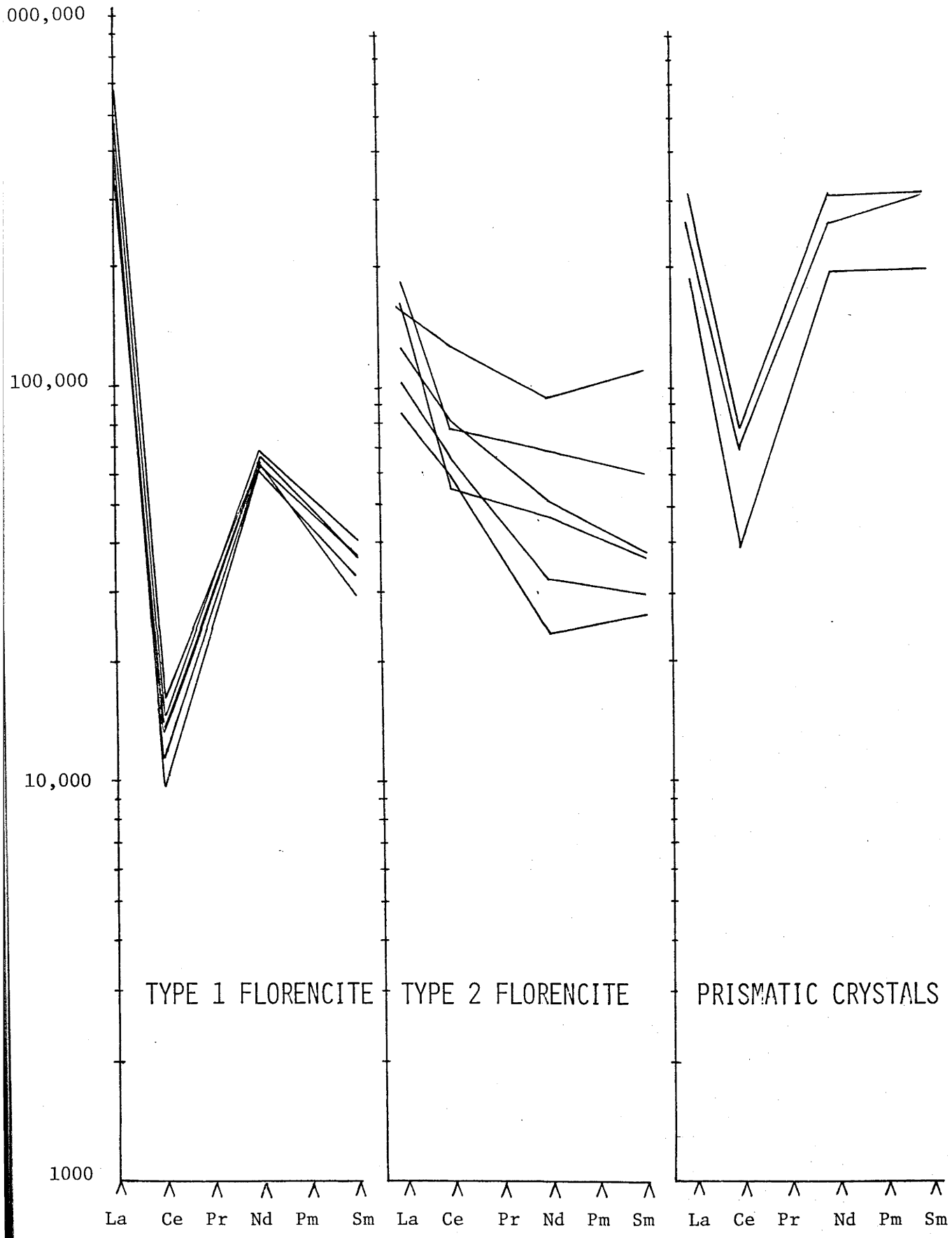

SECTION 7.2.4

MINERAL CHEMISTRY

CAMECA microprobe data for the donuts and rims were obtained from material located first in the SEM. The probe was calibrated for as many REE and trace elements as possible by N. Ware (RSES). Quantities of other components (eg. Pb, HREE) were estimated as closely as possible. Totals varied from about 50% for some prismatic crystallites, to 100.0% for unaltered apatite. Most totals for alteration products ranged between 80% and 98%; a mean value of about 89% is close to that expected for phases such as florencite, which generally contains about 10-12% H_2O^+. Lower totals are not necessarily interpreted to indicate the presence of an undetected component as analyses were not obtained from smooth surfaces, and much of the material examined was located relatively low in apatite pits. Similarly, the effects of concave curved surfaces may explain higher than expected totals. The effect of absorption of the REE spectra by other elements is not known. It is probable that this will effect components such as P and Al in a similar fashion.

One of the most obvious characteristics of the semi-quantitative chemical data obtained was the presence within it of three quite clearly distinguished LREE distribution patterns. Two of these REE distribution patterns were from donuts and rims on apatite composed essentially of florencite. Although these two forms of florencite were also chemically separable on the basis of their total REE and Ba contents, they were not distinguishable morphologically. The third REE distribution pattern was obtained from the prismatic crystallites developed on a substrate composed of the more Ce rich REE-Al phosphate material. LREE data for Type 1 florencite, Type 2 florencite, and for the prismatic phase were plotted as chondrite normalised abundances in Figure 7.2.

The second feature of the chemical data is the enormous variation in the proportions of the components. This provides a further indication that this material does not represent a single phase. Table 7.3 lists this chemical data, and illustrates the way in which analyses from rims and donuts can be subdivided into two chemically distinct groups.

TABLE 7.3: Weight percent oxide data.

TYPE 1 sample	La	Ce	Nd	Sm	Ba	Ca	Fe	P	Al	tot
14	15.8	1.1	4.0	0.7	1.8	1.0	1.7	10.8	26.2	63
15	15.6	1.2	5.0	0.8	2.2	1.1	1.7	11.6	39.7	79
16	16.3	1.6	4.9	0.9	2.2	1.0	2.4	22.4	34.1	86
18	13.9	1.1	4.7	0.8	1.1	0.9	2.5	22.6	36.7	84
19	11.8	0.7	3.7	0.5	0.0	0.7	3.3	15.2	26.4	62
2	18.0	0.8	5.5	0.9	1.3	8.5	2.5	22.1	33.4	93
3	11.4	1.1	3.2	0.6	1.0	0.9	3.8	17.9	33.4	73
5	13.9	2.6	4.1	0.6	2.1	0.6	2.7	26.8	45.0	98
23	16.0	1.7	4.7	0.9	3.0	3.5	2.0	8.1	22.8	63
4	16.8	0.8	4.9	0.8	2.0	2.9	4.6	18.1	30.1	81

TYPE 2 sample	La	Ce	Nd	Sm	Ba	Ca	Fe	P	Al	tot
12	5.9	6.5	4.6	1.2	4.0	1.1	1.9	11.8	36.7	74
13	4.0	8.3	4.9	1.6	1.6	0.7	3.1	8.0	25.0	57
6	3.7	5.7	1.0	0.7	5.4	1.3	1.5	28.9	44.3	93
7	3.2	5.7	1.9	0.6	7.2	2.2	1.3	27.5	35.0	85
8	3.9	6.6	2.6	0.7	5.5	1.7	1.9	20.1	44.7	88
21	3.5	5.7	2.9	0.6	0.3	1.1	3.6	16.1	28.0	62
25	5.2	4.6	4.2	1.1	Ti	0.9	6.6	15.4	40.2	78
26	6.1	5.8	4.0	0.9	3.5	3.2	12.5	11.3	45.4	93
apatite	0.1	0.3	0.2	0.1	0.0	56.2	0.6	42.5	0.0	100

Chemical data given in the above table have been converted to molecular proportions assuming a formula for florencite calculated to 22 oxygens. The amount of florencite which could be produced from these components was then determined. In effectively all cases the limiting factor was the phosphorus content. For example, if a formula contained 1.0 P, then it was assumed that this represented 0.5 unit cells of florencite. This is expressed in Tables 7.4 and 7.5 as 50% florencite. After the required REE and Al were subtracted to construct .5 unit cells of florencite, the remaining components were examined. The result was that in every case there was a variable surplus of Al, and in many cases REE.

As illustrated in Tables 7.4 and 7.5 the surplus of Al reflects to some extent the REE surplus as the Al% remaining tends to be very roughly comparable to the remaining REE+Ca+Ba%. This may reflect the presence of a phosphorus free phase possibly containing REE and Al in molecular proportions of (very approximately) 1:3. In cases where this is not observed, there is only an Al surplus. Although the explanation for a surplus only of Al is not clear, it is tentatively suggested that

it may reflect the presence of an Al rich coating, possibly of clay or oxide on the surface of the donuts. This is consistent with the observed slightly lower Al content where the surface coating of a large donut had been disturbed (see Plate 7.5A). Alternatively, the Al and REE surpluses may be a consequence of the presence of abundant material composed of extremely small crystallites whose chemistry may not be strictly stoichiometric.

Tables 7.4 and 7.5 summarise the results of these calculations. They first list the amount of florencite which is assumed to be present, then the ratio of La:Ce:Nd:Sm; then the calculated weight percent surplus of REE+Ca+Ba after the florencite has been extracted, then the percent Al remaining, and finally the sample number.

TABLE 7.4: % Florencite, REE ratios, REE surplus, and Al surplus for Type 1.

%Flor.	La	Ce	Nd	Sm	REE+Ca+Ba xs.	Al+Fe xs.	No.
50	69	5	22	4	18%	33%	15
60	73	5	19	3	21%	23%	14
74	72	4	21	4	14%	15%	4
76	71	4	22	3	3%	17% *	19
74	70	7	20	4	1%	21%	3
78	71	3	22	4	15%	11%	2
82	68	6	23	4	0%	27%	18
83	69	7	21	4	5%	12%	16
82	66	12	19	3	0%	17%	5

*Large Fe content.

TABLE 7.5: % Florencite, REE ratios, REE+Ca+Ba surplus, Al+Fe surplus, and sample number for Type 2.

%Flor.	La	Ce	Nd	Sm	REE+Ca+Ba xs.	Al+Fe xs.	No.
40	36	35	24	6	18%	36% *	26
50	33	36	25	7	20%	33%	12
50	21	44	26	8	26%	29%	13
60	34	31	28	7	0%	31% *	25
69	28	50	19	5	0%	26%	8
78	27	45	23	5	0%	19%	21
90	33	51	9	6	0%	13%	6
96	28	50	17	5	6%	6%	7

* Containing significant Ti and or Fe.

The above semi-quantitative data supports the XRD and TEM data which suggested the coexistence of a second phase with the florencite.

The prismatic crystals may be the material responsible for the extra reflections in the XRD and TEM data. The chemical composition of this material is very poorly known, although there is some indication that it is a REE-Al phase, possibly a carbonate or oxide. As the prismatic phase had a REE distribution pattern readily distinguishable from those of the florencite, a modification in the LREE abundance patterns should be detected if this phase coexists with the florencite (Figure 7.2). Data shown in the above tables do not suggest a clear change in the REE ratios where excess REE and Al are present. It would appear that the modification observed is not sufficient to support the suggestion that the prismatic phase is a component of the donuts and rims.

SECTION 7.2.5

MINERALOGY CONCLUSIONS

CAMECA probe analyses discussed above do quite clearly indicate that apatite may be replaced by two forms of florencite which are distinguished by their LREE distribution patterns. Type 1 florencite is extremely La enriched with a strong negative Ce anomaly, whereas type 2 has a gently sloping chondrite normalised LREE pattern, and frequently contains a large quantity of Ba. Both these phases may develop as donuts or as rims on apatite. Analytical data indicate that the prismatic phase is composed of LREE and Al and is characterised by a third, quite clearly distinct LREE distribution pattern. This phase contains large quantities of Nd and Sm and has a significantly low Ce content. It is not possible to explain any of these fractionation patterns as combinations of other patterns. These phases reflect quite distinct fractionations of the REE in the weathering environment.

The presence of a phase coexisting with the florencite was indicated by the chemistry and reflections in d space data. Although this material is believed to be also composed of LREE and Al, LREE distribution patterns for the combined material do not support the view that this second component is the same as the prismatic phase. This is not surprising as information suggests that phases which form at different stages in weathering are clearly distinguished by their REE abundance patterns, as well as by differences in their chemistries. This is further illustrated by the chemistry of rhabdophane crystals, which contain no detectable Al or Ba, and are very enriched in Nd.

Clearly the range in both morphology and chemistry of phases replacing apatite is immense. Many crystallites occurred which did not resemble either the squat hexagonal prisms of rhabdophane, or the prismatic phase. For example, tapered crystallites were commonly observed in apatite pits, and it is probable that these also represent a chemically distinct (REE bearing) phase. A complete characterization of all minerals observed was not possible within the time constraints of this study.

SECTION 7.3

THE BEHAVIOUR OF REE IN THE WEATHERING PROFILE

NEUTRON ACTIVATION RESULTS

Introduction

Bulk XRF chemical data indicate that the REE content of samples from the profile increases dramatically as a result of weathering. Neutron activation analysis was employed to determine the extent to which REE had been mobilized, the nature of the overall effect of the numerous replacement phases upon the abundance of the individual REE, and the extent to which these phases controlled the distribution of the HREE as well as the M and LREE.

Samples analysed

14 samples were submitted for analysis by B.W. Chappell (ANU); results are presented in Table 7.6. Most samples analysed were from the Bemboka profile. Whole rock chemical data were obtained for a sequence of samples which had undergone variable degrees of weathering. The three clay samples which were also submitted were extracted from the more strongly weathered members of this sequence. Clay extraction procedures are described in Appendix 3.

As apatite is commonly present within biotite, the effect of apatite replacement on REE in the profile can be examined by comparison of the REE content of moderately weathered biotite with that of fresh biotite. The REE content of fresh biotite is due primarily to the presence within it of inclusions. A sample of biotite extracted from unweathered granite was also submitted for analysis to determine the combined REE of content inclusions and the biotite host.

TABLE 7.6:

NEUTRON ACTIVATION RESULTS

Element	JFB 1	JFB 6	JFB 19	JFB 13	JFB 14	JFB 15	JFB 16	JFB 17	JFB 18	JFB 24	JFB 23	JFB 22	JFB 25	JFB 26	Element
Na_2O	2.94	0.55	0.89	2.89	2.34	1.10	0.94	0.52	0.33	1.89	1.04	1.20	0.27	2.24	Na_2O
FeO	2.75	3.10	2.26	2.9	2.73	2.98	2.98	3.00	3.53	4.81	5.24	7.97	24.59	20.00	Feo
Sc	9.71	11.81	12.30	11.02	10.73	12.34	12.01	11.74	11.60	21.67	21.97	27.11	69.43	64.65	Sc
Cr	5.86	5.87	4.40	8.82	4.90	3.18	4.51	5.24	2.40	7.85	5.72	6.08	43.91	41.87	Cr
Rb	104.21	133.96	81.55	161.55	151.81	173.65	178.63	171.92	176.26	136.21	98.44	106.48	456.10	445.01	Rb
Sb	0.01	0.06	0.53	0.14	0.15	0.19	0.05	0.08	0.23	0.10	0.35	0.80	0.03	0.52	Sb
Cs	4.70	5.05	4.80	5.89	5.39	5.71	7.02	6.90	6.51	12.37	10.57	9.79	29.33	29.75	Cs
Ba	791.95	1009.57	713.89	699.87	675.97	935.80	837.00	812.50	808.10	1277.27	1082.33	1169.77	3393.40	2833.64	Ba
La	24.54	42.86	39.75	41.28	336.2	573.9	341.	376.8	411.6	615.6	620.6	634.2	18.20	1768.7	La
Ce	45.51	57.54	87.02	86.52	86.61	77.97	76.61	128.89	124.05	509.39	518.96	487.06	46.26	64.78	Ce
Nd	17.52	38.47	30.23	37.04	276.42	496.32	279.13	308.53	345.61	441.94	403.45	430.42	28.76	1554.98	Nd
Sm	3.20	7.79	6.78	7.20	60.95	100.50	56.90	61.80	68.00	88.01	81.67	86.28	9.00	323.72	Sm
Eu	0.79	2.10	1.98	1.16	10.15	16.34	9.28	10.11	10.96	14.48	13.62	14.09	0.34	48.90	Eu
Gd	2.97	7.22	6.91	6.73	63.69	99.36	58.54	63.97	68.42	91.64	85.19	85.65	9.71	283.41	Gd
Tb	0.46	1.12	1.18	1.04	8.56	11.57	7.09	8.03	8.79	13.81	12.51	12.85	1.48	29.83	Tb
Ho	0.64	1.62	2.03	1.21	11.01	13.33	8.73	10.14	11.35	18.52	17.23	17.89	2.76	36.37	Ho
Yb	2.02	5.12	5.75	3.82	22.56	28.55	20.64	23.44	25.36	43.28	38.16	39.33	7.43	79.24	Yb
Lu	0.32	0.82	0.88	0.56	3.36	4.18	3.12	3.55	3.85	6.40	5.63	5.82	1.15	11.70	Lu
Hf	2.07	2.29	2.15	5.47	5.10	5.61	5.61	6.00	6.95	2.82	2.16	2.98	10.69	17.63	Hf
Ta	1.55	0.86	0.69	1.57	1.02	0.71	0.41	0.53	0.75	1.02	0.90	1.14	3.89	1.68	Ta
Th	9.29	10.67	12.07	22.61	18.91	19.69	20.82	21.08	25.59	86.32	67.35	76.30	9.91	28.84	Th
U	2.66	3.05	6.49	4.47	3.84	4.28	2.96	2.84	3.67	9.01	7.03	7.53	6.37	7.79	U

Three samples were also submitted from the Island Bend profile to determine whether mobilization of the REE had also occurred as a result of weathering. Fresh and strongly weathered granite were analysed, as well as the clay fraction from the most weathered material.

RESULTS AND DISCUSSION

SECTION 7.3A

BEMBOKA PROFILE

Neutron activation results for the Bemboka profile clearly support those obtained by XRF (Chapter 8), indicating that a substantial enrichment of REE has occurred as a result of the weathering of the granite. Results in Table 7.6 have been recalculated assuming an isovolumetric weathering model[1] . Absolute element abundances, expressed as gm/cm^3, are used in Figure 7.3. Data have been normalised by dividing these volumetric abundances for each sample by abundances in the fresh rock, so that results reflect the actual enrichment which has occurred. Resulting concentrations are plotted against density, which provides an index for the extent of alteration. Consequently a horizontal line at the 1x mark in Figure 7.3 would indicate that had no gain or loss of REE occurred as a result of weathering. As shown in this figure, REE contents increase rapidly from normal levels in the fresh rock, confirming that the replacement of apatite is a weathering, and not a hydrothermal phenomenon. REE have been introduced from outside the sampled zone very early in alteration, abundances appear to peak, and then remain constant through to the final stages studied. This is attributed to fixation of these elements in phases which remain resistant to further weathering, at least under the conditions encountered in this part of the profile. The reason why enrichment appears to peak before stabilizing is not understood. This may be attributed to a number of factors, including sampling, variations in the physical conditions within the profile when initial weathering of these more strongly enriched samples occurred, etc. There does not appear to be any other evidence to suggest that this peak reflects an important

---

[1] based on the observation that during weathering mass is lost while texture and volume remain constant: see Chapter 8

FIGURE 7.3

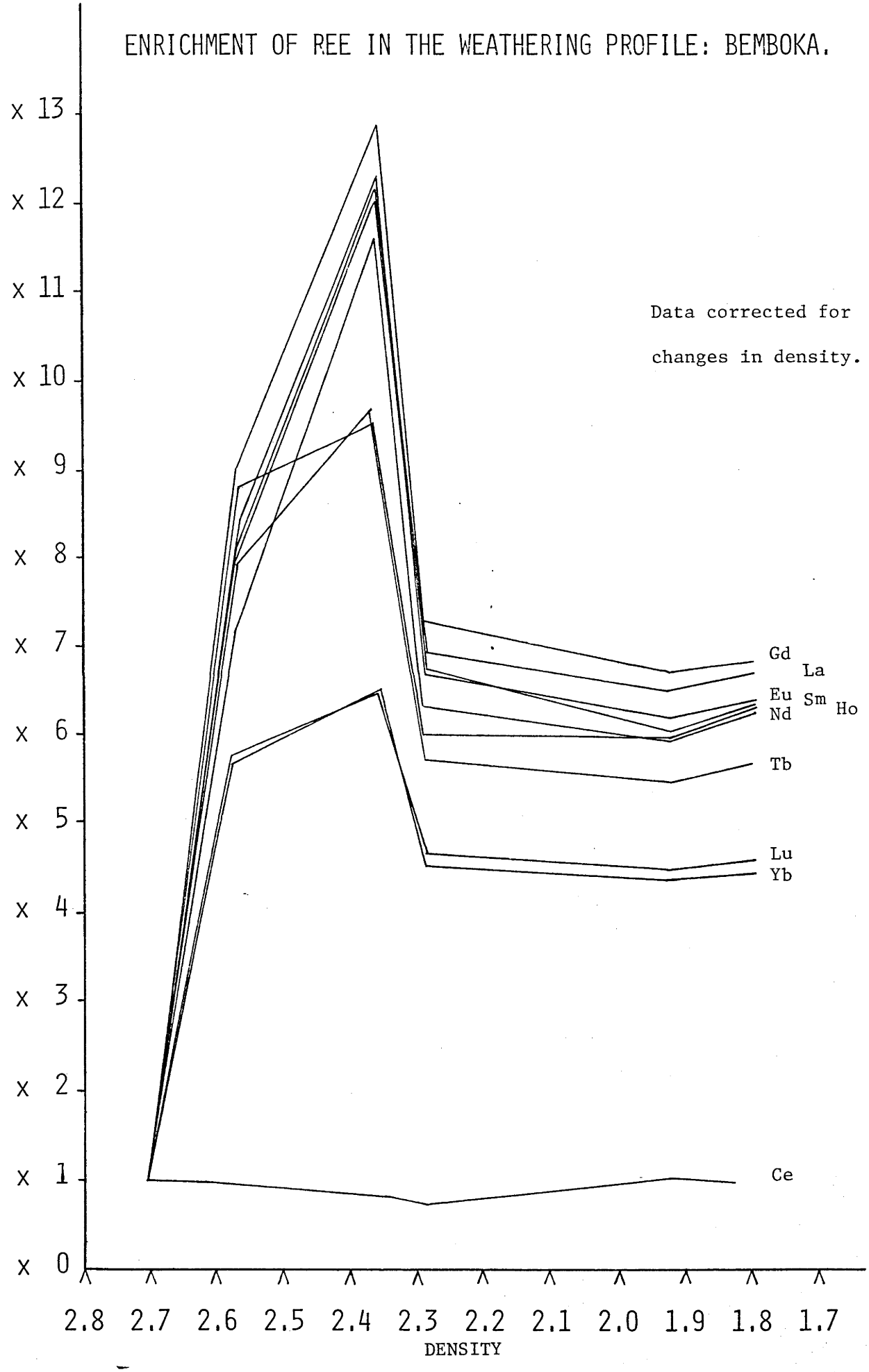
ENRICHMENT OF REE IN THE WEATHERING PROFILE: BEMBOKA.
x 13
x 12
x 11
x 10
x 9
x 8
x 7
x 6
x 5
x 4
x 3
x 2
x 1
x 0
Data corrected for
changes in density.
Gd
La
Eu
Sm
Ho
Nd
Tb
Lu
Yb
Ce
2.8 2.7 2.6 2.5 2.4 2.3 2.2 2.1 2.0 1.9 1.8 1.7
DENSITY

stage in the enrichment process. All elements have been enriched in weathered material except Ce, which appears to have remained immobile throughout the process. This element has effectively been fractionated from the remainder of the REE, probably because under oxidising conditions it exists as Ce^{4+}, and hence has remained relatively immobile.

In order to determine whether enrichment of the profile has been associated with a fractionation of the REE (other than Ce), data normalised to fresh rock have been plotted for all the REE determined. This method of processing data is analogous to chondrite normalisation of REE contents in that results reflect the relative enrichment of individual REE. Data have been plotted in Figure 7.4. It is apparent from this plot that replacement of apatite by a range of REE bearing phases has resulted in the enrichment of the REE, without significantly fractionating them. This is surprising when it is recognised that the phases which host these elements have fractionated the REE dramatically.

Figure 7.4 also throws some light upon the origin of the REE which have been added to the profile. Because the net effect of mobilization has been enrichment without modifying the relative abundance of these elements, it would seem probable that they have been derived from elsewhere in the granite, and not from an external source. For example, if these components had been released by weathering of a nearby basalt the relative abundances of REE would no longer resemble those in the unweathered granite.

The overall effect of apatite replacement also is examined in Figure 7.4. This is illustrated by plotting data for weathered biotite after the REE content of unweathered biotite has been subtracted. The resulting concentrations have then been normalized to Bemboka 1, so as to allow comparison of the enrichment of this phase with the enrichment of the whole rock. For this to represent the contribution of apatite replacement to the overall enrichment, this plot would have to be scaled down by a factor which reflected the biotite content of the rock, and the amount of apatite in the rock not present in biotite. The shape of this plot does quite strongly resemble that of the whole rock enrichment plots, possessing a strong negative Ce anomaly, and a relatively flat La-Nd-Sm-Eu-Gd pattern. Some difference in the shape of REE patterns can be observed in that the enrichment of the M and HREE in the biotite

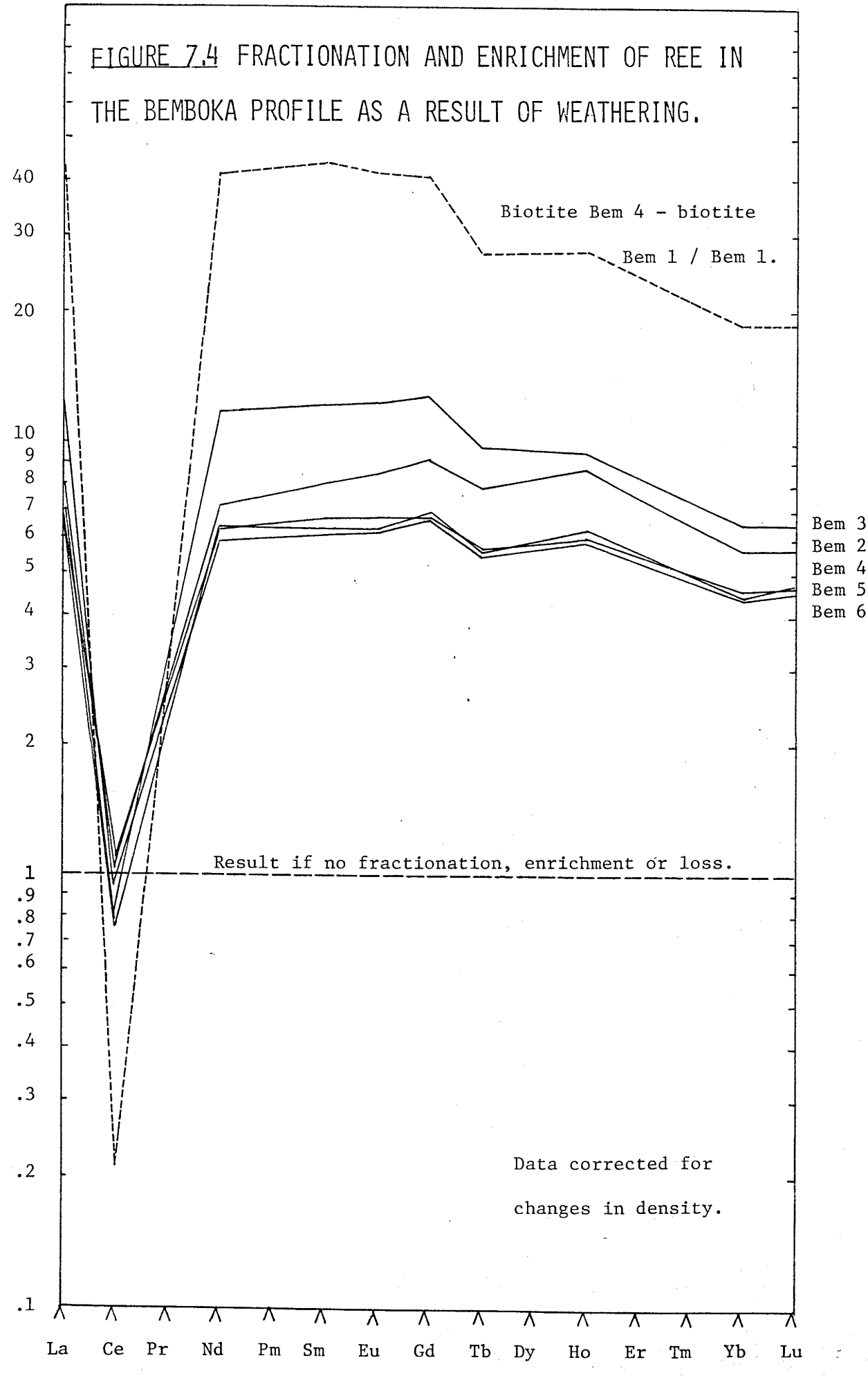
FIGURE 7.4 FRACTIONATION AND ENRICHMENT OF REE IN THE BEMBOKA PROFILE AS A RESULT OF WEATHERING.
40
30
20
10
9
8
7
6
5
4
3
2
1
.9
.8
.7
.6
.5
.4
.3
.2
.1
Biotite Bem 4 - biotite
Bem 1 / Bem 1.
Bem 3
Bem 2
Bem 4
Bem 5
Bem 6
Result if no fractionation, enrichment or loss.
Data corrected for
changes in density.
La
Ce
Pr
Nd
Pm
Sm
Eu
Gd
Tb
Dy
Ho
Er
Tm
Yb
Lu

plot are comparatively low, in contrast with the whole rock plots where enrichment of all elements has occurred to a similar extent. This suggests that M and heavy REE may be concentrated in phases not formed by replacement of apatite. The extent to which this has occurred is examined below.

The contribution of apatite replacement to whole rock REE enrichment.

The maximum contribution which the process of apatite replacement may make to the observed REE enrichment of the whole rock during weathering is examined by calculating the limiting factor by which the biotite plot in Figure 7.4 can be scaled down. This is determined to be .152, a factor larger than this would imply a greater enrichment of Sm than that is observed in the whole rock. Assuming that the biotite plot reflects the net effect of the apatite replacement process, the maximum REE enrichment which can be attributed to these phases can be determined. Data are listed in Table 7.7.

Table 7.7

Element	observed enrichment	-	.152x net effect	=	difference
La	6.94x	-	6.49x	=	.45x
Ce	.75x	-	.03x	=	.72x
Nd	6.33x	-	6.30x	=	.03x
Sm	6.64x	-	6.64x	=	.00x
Eu	6.72x	-	6.40x	=	.32x
Gd	7.31x	-	6.22x	=	1.09x
Tb	5.73x	-	4.17x	=	1.56x
Ho	6.06x	-	4.25x	=	1.81x
Yb	4.54x	-	2.88x	=	1.66x
Lu	4.68x	-	2.88x	=	1.80x

This calculation indicates that not only is a REE enrichment present which does not appear to be associated with apatite replacement phases, but this additional enrichment approaches twice the HREE content of the unweathered rock. This implies that heavier REE have been introduced to the profile from outside the sampled zone, and have been fixed in phases not associated with those observed within biotite replacing apatite. The identity of this phase, or of the phases responsible for concentrating these elements is not known. In an attempt to determine something about the distribution of this material, the REE contents of the clay and non clay fractions have been examined.

REE enrichment of the clay and non-clay fractions

The distribution of the REE between the clay and non-clay fractions has been examined by multiplying the measured REE content of the clay fraction by the percent clay in the rock from which the clay was extracted, and then comparing this contribution to the total enrichment observed. These data, listed in Table 7.8, are plotted in Figure 7.5 for the Bemboka 4 sample (for which the weathered biotite REE content is known).

Table 7.8

Element	REE clay/ REE whole rock	relative clay * enrichment
La	16.79%	1.16x
Ce	61.83%	.46x
Nd	14.72%	.93x
Sm	14.38%	.95x
Eu	14.55%	.97x
Gd	14.55%	1.06x
Tb	18.05%	1.04x
Ho	19.70%	1.19x
Yb	19.53%	.88x
Lu	19.23%	.89x

Rock contains 9.03% clay. *1.16x indicates the clay fraction contains 1.16x as much La as was present in the fresh rock.

Because the size of the crystallites, donuts, etc., may be as smaller than 1μm, it is probable that these phases account for much of the REE content of the clay as well as the non-clay fractions. However, Figures 7.5A,B clearly indicate that the REE distribution pattern of the clay fraction does differ from that of the non clay fraction in two ways. Firstly, a much larger proportion of the Ce present in weathered samples is located in the clay fraction. In the fresh rock this element is largely hosted in allanite, hence the weathering product of allanite may be located in the clay fraction and provide a host for this element, and possibly some of the La. Secondly, the clay fraction contains a larger proportion of the heavier REE than the non-clay fraction.

The distribution between the clay and non-clay fractions of REE which can not be attributed to apatite replacement can be examined. This data is listed in Table 7.9, and is plotted in Figure 7.6.

FIGURE 7.5a THE DISTRIBUTION OF THE REE BETWEEN THE CLAY AND NON-CLAY FRACTIONS IN BEMBOKA 4.

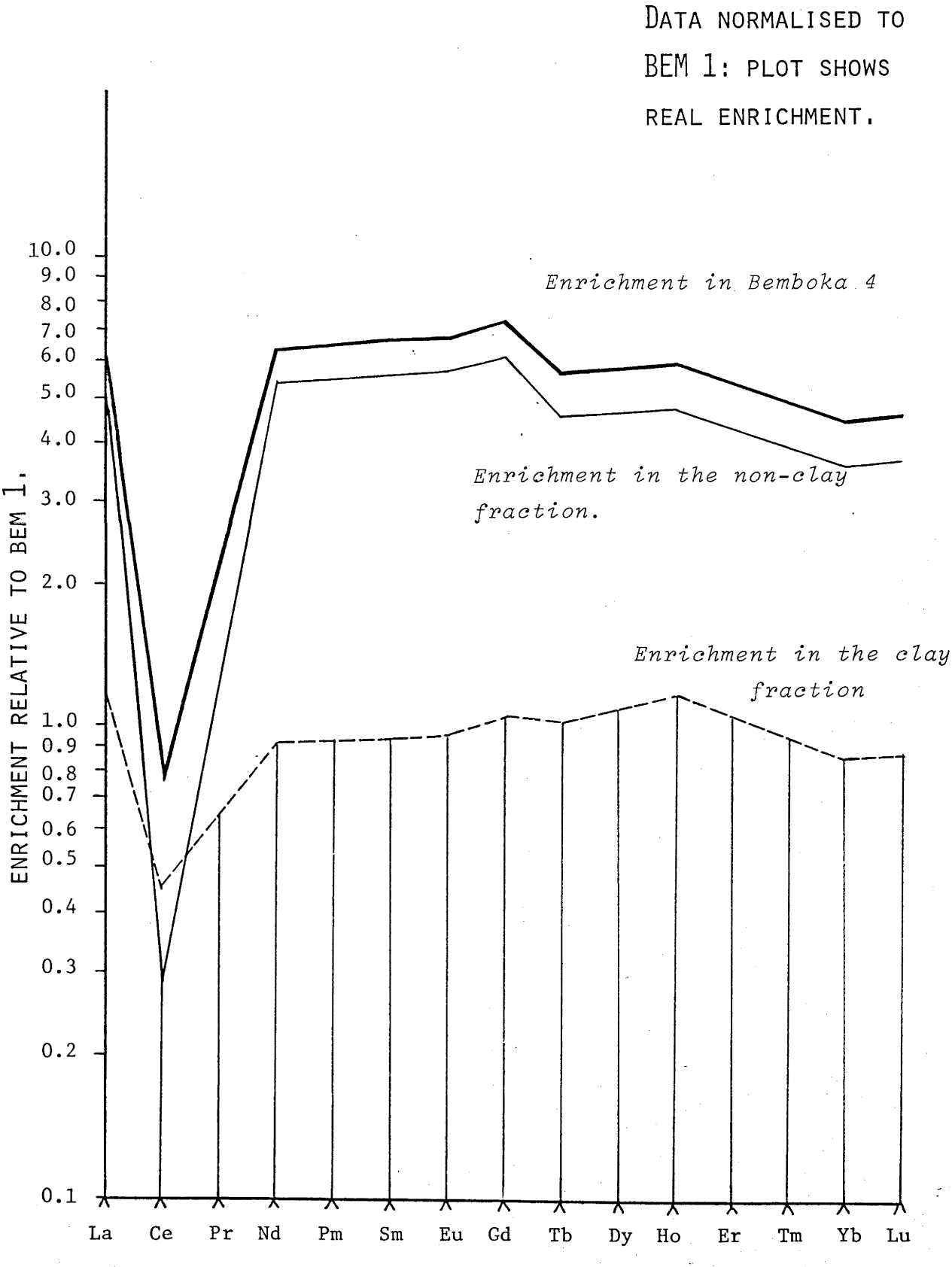

FIGURE 7.5b THE ROLE OF THE CLAY FRACTION IN CONTROLLING THE REE IN BEMBOKA 4.

ELEMENT	JFB 16	JFB 24 x % CLAY	REE CLAY/ REE WHOLE ROCK
La	341.0	57.3	16.8 %
Ce	76.6	47.4	61.8 %
Nd	279.1	41.1	14.7 %
Sm	56.9	8.2	14.4 %
Eu	9.3	1.4	14.6 %
Gd	58.5	8.5	14.6 %
Tb	7.1	1.3	18.1 %
Ho	8.7	1.7	19.7 %
Yb	20.6	4.0	19.5 %
Lu	3.1	0.6	19.2 %

Clay fraction controlling the HREE more strongly than the L & MREE, (except Ce which is strongly associated with the clay fraction).

FIGURE 7.6 DISTRIBUTION OF THE REE NOT ACCOUNTED FOR BY APATITE REPLACEMENT BETWEEN THE CLAY AND NON-CLAY.

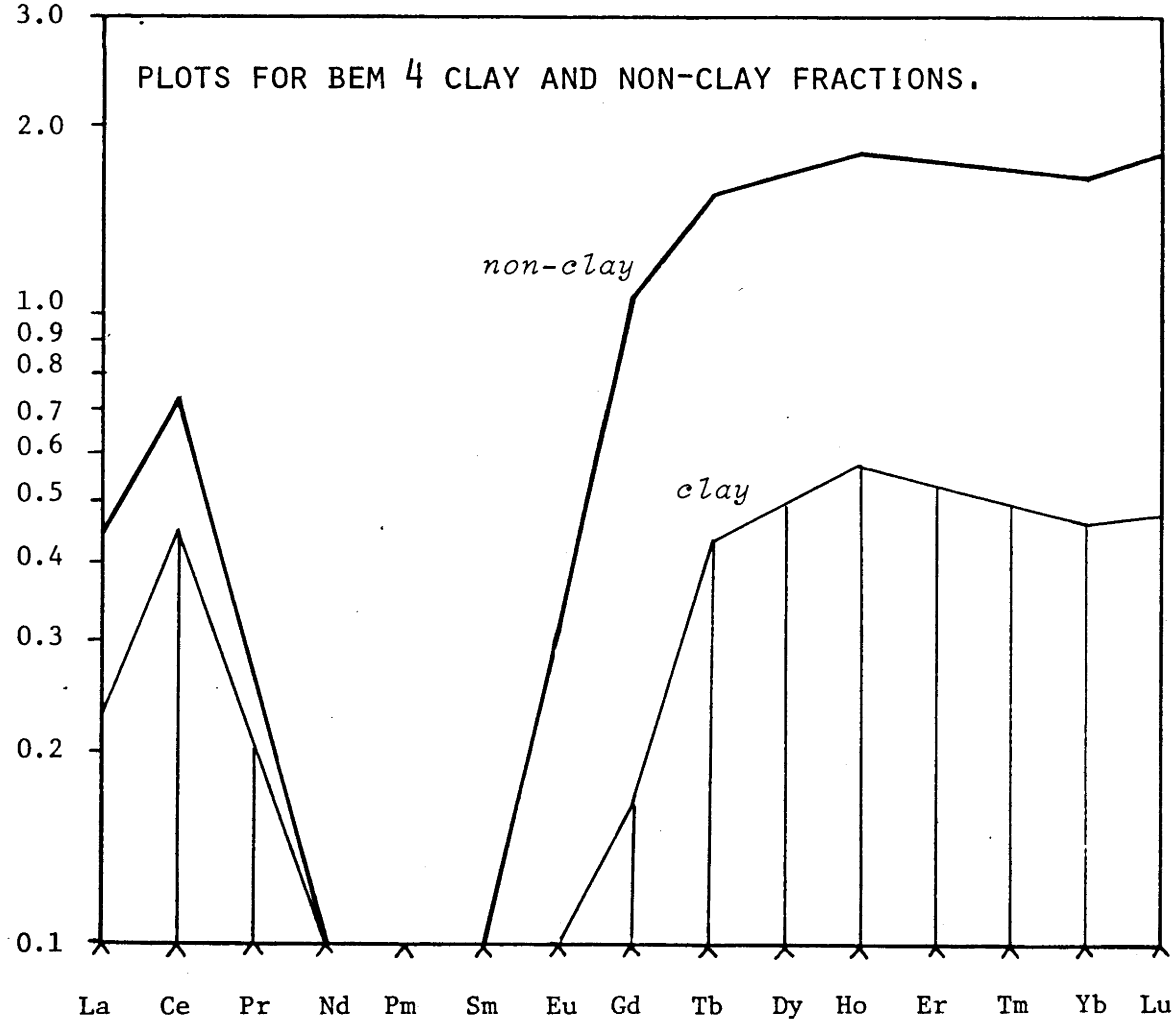

These data indicate that the REE present in Bemboka 4 which can not be associated with apatite replacement phases are concentrated to some extent more strongly in the clay than the non-clay fraction. As the data suggest formation of a HREE selective alteration product which is preferentially concentrated in the clay fraction only about twice as strongly as apatite alteration products it is considered unlikely that these elements are simply adsorbed by clay minerals. Ce, (and excess La) which are much more strongly associated with the clay than the non-clay fraction possibly may be hosted by clay and oxide minerals.

Table 7.9

Element	clay surplus		non-clay surplus		total surplus	clay/total surplus
La	.23x	+	.22x	=	.45x	51%
Ce	.46x	+	.26x	=	.72x	64%
Nd	.02x	+	.01x	=	.03x	
Sm	.00x	+	.00x	=	.00x	
Eu	.05x	+	.27x	=	.32x	16%
Gd	.17x	+	.92x	=	1.09x	16%
Tb	.44x	+	1.12x	=	1.56x	28%
Ho	.58x	+	1.23x	=	1.81x	32%
Yb	.47x	+	1.19x	=	1.66x	28%
Lu	.48x	+	1.32x	=	1.80x	27%

Bemboka 4 contains 9.03% clay.
(surpluses are relative to REE contents in fresh rock).

Neutron Activation results for other elements.

Neutron activation results for other elements are listed in Table 7.6. Whole rock enrichments and depletions occurring as a result of weathering are given in Table 7.10, (results are corrected for changes in density).

Table 7.10

Elt.	B2	B3	B4	B5	B6
Sc	x.93	x.98	x.92	x.75	x.71
Cr	x.54	x.31	x.43	x.42	x.18
Rb	x.91	x.93	x.93	x.75	x.74
Sb	x1.03	x1.18	x.30	x.41	x1.11
Cs	x.93	x.84	x1.00	x.83	x.75
Ba	x1.33	x1.17	x1.01	x.83	x.78
Hf	x.90	x.90	x.87	x.78	x.92
Ta	x.43	x.39	x.22	x.24	x.32
Th	x.81	x.76	x.77	x.66	x.76
U	x.83	x.84	x.55	x.46	x.55

These data indicate that none of the above elements are enriched to any extent comparable with the enrichment observed for the REE. Although Ba is concentrated in the apatite replacement phases, it is apparently derived from the host biotite. This is most clearly demonstrated by the data in Table 7.6 which indicate that the Ba content of weathered biotite is actually lower than the Ba content of unweathered biotite. Th (and to a lesser extent, Hf, U, and possibly Sb) are concentrated in the weathered biotite (presumably in apatite replacement phases) although they are lost slightly overall as a result of weathering.

SECTION 7.3B

ISLAND BEND PROFILE

Neutron activation results were obtained for the Island Bend profile in order to determine whether a similar process of mobilization and fixation of the REE could be observed. Results for fresh, weathered, and the clay fraction from the weathered material are listed in Table 7.6. These data have been plotted in Figure 7.7 after the appropriate corrections have been made to remove the effects of change in density. Although it is apparent that a small quantity of REE have been introduced to the profile from outside the sampled zone, the extent to which this has occurred is far less pronounced than in the Bemboka profile. Again Ce behaves differently to the other REE, in this profile. This element has apparently been lost during weathering, resulting in the presence of a negative Ce anomaly in the enrichment plot in Figure 7.7.

The overall enrichment in the most weathered samples is associated with a slight fractionation of the REE, the M and HREE being slightly added to the profile, while La is just conserved. Using the data for the clay fraction from the strongly weathered material it is possible to determine whether these effects can be linked with processes occurring specifically in the clay, or the non-clay fraction. Results are also plotted in Figure 7.7. As in the case of the Bemboka weathering profile, Ce is more strongly associated with the clay fraction, as are the heavier REE. The non-clay fraction is associated with slight concentration of all the REE except La and Ce; as in the Bemboka profile, the major process is enrichment, not fractionation.

FIGURE 7.7

ISLAND BEND ENRICHMENT WITH WEATHERING.

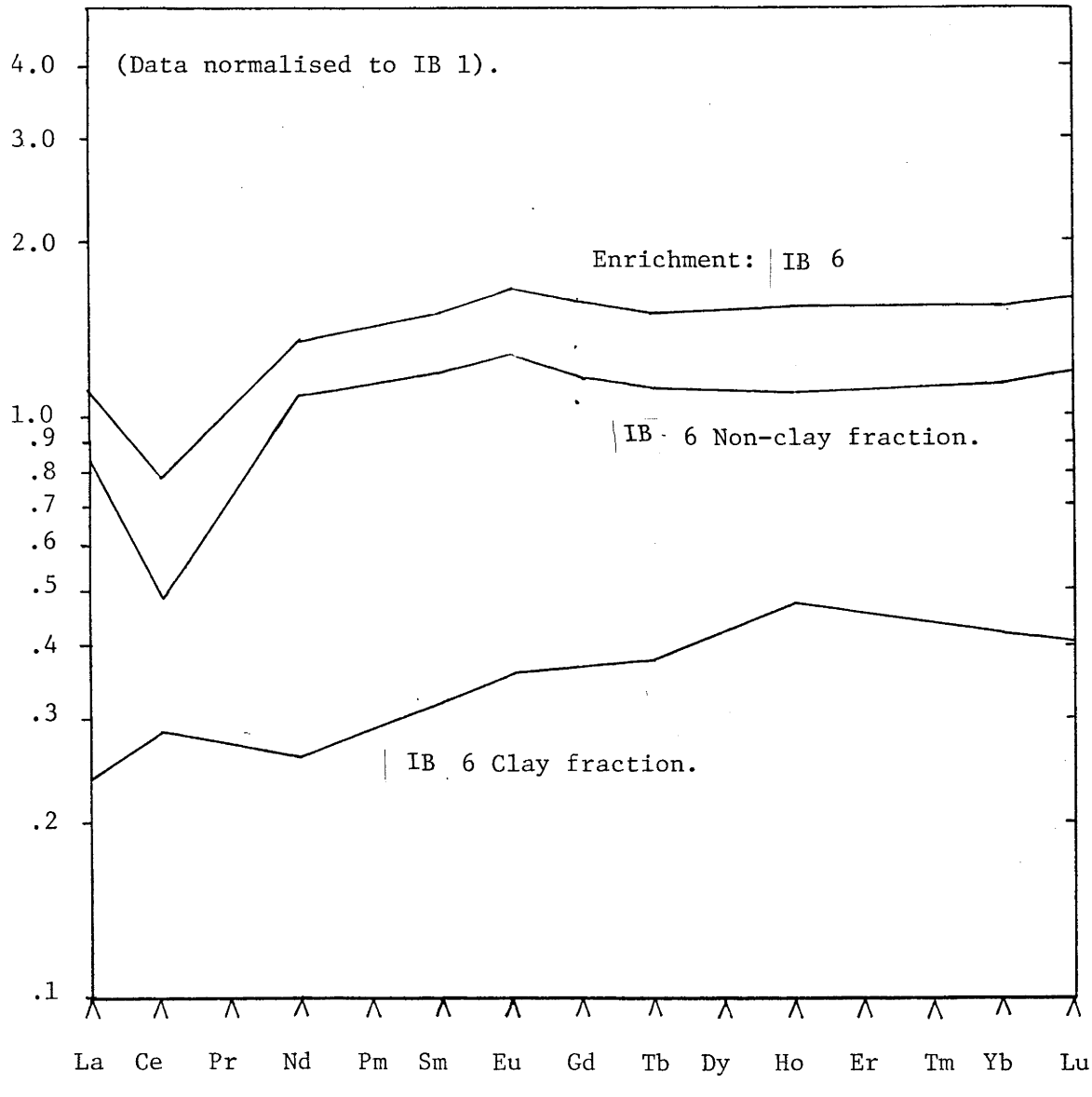

Results suggest that in the Island Bend profile REE behave in a similar fashion to that observed in the Bemboka profile, the major difference being the far less extreme nature of the process. Ce again is fractionated from the remainder of the REE during weathering. Apart from Ce, REE appear to be fixed in the zone at the weathering front, heavier REE showing some tendency to concentrate separately from the lighter REE, possibly in phases which occur more commonly in the clay fraction.

SECTION 7.4

THE ISLAND BEND PROFILE: APATITE WEATHERING

The major process during the early stages of apatite weathering in this profile appears to be dissolution. This results in the appearance of very pronounced, crystallographically controlled, etches and the development of only very minor quantities of secondary products. In the later stages of alteration very little unaltered apatite remains, and only small amounts of a secondary phase develop, generally coating the walls of the pits previously occupied by apatite. An examination of this material revealed that as in the case of the Bemboka profile, donut or disk shaped objects could be recognised. Qualitative SEM probe analysis of this material indicated that it contained primarily LREE and P. The example given in Plate 7.14 reflects the relatively minor volume occupied by this material. Although no further identification or characterisation of this material was attempted (for this reason), these observations are interpreted to support the conclusion that the same process of mobilization and fixation of REE by apatite replacement is occurring in this profile. The extent of replacement, however, is far less pronounced than observed in the Bemboka profile.

SECTION 7.5

CONCLUSIONS

1. REE are released from their host phases early in weathering. At this stage these elements are mobile, and may migrate through the profile.

2. REE are fixed at the weathering front by P released by weathering of apatite. This results in the development of a large range of secondary phases, generally phosphates or aluminium phosphates.

PLATE 7-14 : Weathering also results in replacement of apatite by 'donuts' in granite from Island Bend.

These phases frequently contain a range of minor elements which have been concentrated by this process, including Ba and Pb. The behaviour of Ce differs from that of the other REE. This element displays a low mobility, possibly because under oxidising conditions it exists in the 4^+ state, and hence is either conserved in the profile or is slightly lost. The behaviour of Ce observed in the bulk chemical data is reflected in the observation that in 3 of the 4 REE minerals examined the Ce content is notably low.

3. The major process associated with the migration and fixation of REE is enrichment. This is associated with very little fractionation of this group of elements (except from Ce). In the Bemboka profile, only a minor concentration of the MREE over the HREE occurs, whereas in the Island Bend profile a minor concentration of the M and HREE over the lighter REE is observed.

4. The preservation of near original REE distribution patterns is interpreted to indicate that the elements added to the sampled region of the profile were derived from elsewhere in the profile, and not from an external or foreign source.

5. Enrichment occurs during the earliest stages of weathering. REE appear to be fixed in phases which are then resistant to further alteration, at least under the conditions encountered in this section of the profile.

6. Phases which host these elements are characterised by a remarkable range in the contents of individual LREE. Three clear examples of quite readily distinguishable LREE fractionation patterns have been presented. Although the reason for the development of these different patterns is not clear, it is suggested that the formation of phosphate and aluminium phosphate phases which are resistant to further alteration may preserve any changes in the composition of the REE assemblage which is added to the profile over time. These changes must have occurred rapidly as no intermediate REE patterns were identified.

7. The process of mobilization and fixation of the REE appears to have been complex. In addition to a variety of LREE phases replacing apatite, chemical data indicates that heavier REE also have been added to the sampled zone and fixed independently of the lighter REE. This

implies that the HREE are hosted by at least one other phase. Although this phase has not been identified there is some evidence to suggest that it may be concentrated to some extent preferentially in the clay-size fraction.

8. The observation that in the Island Bend profile apatite is leached, and replaced by REE-phosphate phases which represent hosts for REE fixed after mobilization and migration as a result of weathering indicates that the process documented in the Bemboka profile does not represent an isolated phenomenon. This study indicates that REE are clearly mobile early in weathering, and that components may be added to a zone of a profile from elsewhere in the weathering system.

9. The reason why REE are mobilized from some regions of the weathering profile and concentrated in others is not clear. This may indicate that in some regions, weathering of individual minerals proceeds under differing conditions which exert different controls on the behaviour of elements in the profile.

Chapter 8

GEOCHEMISTRY OF THE WEATHERING PROFILE

INTRODUCTION

Bulk chemical analyses have been obtained for samples of fresh and successively more weathered material from three profiles. Clays extracted from some of the strongly altered samples have also been analysed for major and trace elements. (Table 8.1). This chapter discusses the behaviour of many of these elements during weathering approached firstly by considering the rates at which elements are released from their host phases either to form clays or into solution. The relative rates at which these minerals weather can then be estimated from these data.

The chemistry of the weathering profile is the net result of the interaction of the rate at which phases alter, and the extent to which secondary phases retain the components which are released. Consequently the tendency for the clay fraction to retain individual elements is examined for the three profiles studied. The results for these profiles can be compared in order to determine whether generalizations can be made about the relative mobilities of components during weathering. The behaviour of the rare earth elements will not be discussed in this chapter as it this topic has been covered in Chapter 7.

The texture of granite is preserved during weathering as mass has been lost without a change in the volume. The process is described as occurring isovolumetrically, so that the density of a sample is a measure of the extent to which it has been altered.

If an element is conserved in the profile during weathering its weight percent abundance increases as other components are removed. Many workers have approached the study of the chemical changes which have occurred by assuming one component, usually Al or Ti remains immobile, and scaled other components accordingly. This method has not

TABLE 8.1a

Chemical analyses for the Island Bend, Jindabyne and Bemboka profiles. Samples prefixed R collected by RAE.

	ISLAND BEND PROFILE													
	R22	R23	R24	J1	J2	R25	J3	J4	J5	R26	R27	R28	J6	Clay J19
SiO_2	69.60	69.63	69.39	69.89	69.28	69.34	68.73	69.19	68.38	67.53	68.72	68.28	66.80	43.48
TiO_2	.28	.29	.30	.27	.28	.28	.29	.29	.30	.31	.30	.31	.32	.45
Al_2O_3	15.13	15.05	15.20	15.72	15.52	15.18	15.40	15.34	15.63	17.19	16.43	16.72	16.86	36.25
Fe_2O_3	1.21	1.36	1.50	1.23	1.41	1.42	1.71	1.85	2.22	2.90	2.83	2.78	2.94	2.22
FeO	1.52	1.51	1.50	1.45	1.43	1.41	1.20	1.08	.78	.39	.40	.41	.40	-
MnO	.08	.08	.08	.08	.08	.08	.08	.08	.08	.10	.08	.10	.09	.18
MgO	1.20	1.26	1.31	1.18	1.20	1.23	1.24	1.19	1.20	1.23	1.22	1.22	1.23	.91
CaO	3.03	3.34	3.28	3.00	3.05	2.96	2.97	2.82	2.62	.54	.48	.40	.33	.05
Na_2O	3.17	3.23	3.18	3.19	3.18	2.99	3.40	3.00	3.09	.76	.71	.65	1.07	?
K_2O	3.10	2.82	2.78	2.91	2.76	2.86	2.90	2.78	2.59	2.92	3.14	3.14	3.22	.82
P_2O_5	.12	.13	.13	.12	.09	.12	.11	.09	.10	.03	.02	.02	.02	?
S	.01	.01	-	.02	.01	-	.01	.01	.01	-	-	-	.01	.01
H_2O^+	.87	.79	.92	1.05	1.04	1.19	1.22	1.40	1.90	4.69	4.46	4.70	4.86	
H_2O^-	.28	.19	.24	.32	.29	.35	.36	.36	.67	.88	.69	.77	1.21	
CO_2	.08	.04	.01	.05	.06	.08	.17	.15	.10	.06	.05	.08	.16	
O=S				.01			.01	.01					.01	
TOTAL	99.66	99.72	99.80	100.48	99.66	99.49	99.78	99.63	99.66	99.51	99.53	99.56	99.51	
Ba	375	710	735	795	760	765	755	770	770	925	905	880	1010	650
Rb	117	108	112	106	101	108	101	101	89	119	130	130	131	78
Sr	442	472	458	441	440	428	439	430	401	126	124	113	100	16
Zr	86	91	91	67	64	93	66	61	75	94	84	87	82	69
Y	22	21	21	19	19	20	20	21	19	48	22	20	41	44
La	20	22	24	21	20	20	21	22	20	40	21	17	40	34
Ce	42	48	48	43	43	44	44	37	36	66	43	40	45	83
V	53	58	58	58	55	57	55	57	55	58	54	53	65	37
Cr	6	6	6	6	6	6	6	6	5	8	6	6	6	4
Pb	23	21	20	22	20	21	21	24	21	24	23	25	25	48
Ni	1	1	1	<1	<1	<1	<1	1	2	<1	<1	<1	3	3
Cu	3	5	3	7	3	2	2	3	3	1	1	2	<1	14
Zn	42	44	46	39	37	44	39	37	38	54	51	52	48	60
Nb	9	9	9	8	8	8	9	7	8	10	9	9	9	9

TABLE 8.1b

	JINDABYNE PROFILE							
	J7	J8	J9	J10	J11	J12	Clay J21	Clay J20
SiO_2	70.09	69.81	69.73	68.48	67.85	68.90	41.89	42.90
TiO_2	.56	.54	.55	.54	.52	.54	1.35	1.23
Al_2O_3	14.05	13.91	14.04	14.13	14.43	14.48	24.81	27.58
Fe_2O_3	.34	1.39	.97	3.37	3.71	3.66	10.53	10.77
FeO	3.41	2.38	2.77	.62	.27	.40	-	-
MnO	.06	.05	.05	.04	.03	.05	.08	.13
MgO	1.63	1.58	1.65	1.47	1.51	1.49	3.27	2.81
CaO	2.21	1.74	1.63	1.13	.63	1.22	.44	.33
Na_2O	2.29	2.21	2.30	1.98	1.76	1.85	?	?
K_2O	3.80	3.88	4.13	3.90	4.28	3.58	2.79	3.11
P_2O_5	.10	.09	.10	.09	.04	.07	?	?
S	.04	.01	.01	.01	.01	.01	.02	.07
H_2O^+	1.21	1.42	1.36	2.09	2.83	2.39		
H_2O^-	.14	.36	.24	.91	1.11	.59		
CO_2	.33	.13	.08	.15	.28	.58		
O=S	.02	.01	.01					
TOTAL	100.23	99.50	99.59	98.91	99.25	99.81		
Ba	480	490	490	490	475	455	350	385
Rb	184	187	195	168	173	180	220	236
Sr	117	108	106	94	75	93	69	56
Zr	174	180	179	177	154	169	73	70
Y	32	31	32	30	24	28	29	23
La	29	27	25	32	29	30	52	51
Ce	67	63	57	66	51	62	116	106
V	68	71	70	89	89	85	171	166
Cr	35	35	37	44	43	42	90	77
Pb	27	26	26	28	25	27	41	43
Ni	12	12	12	12	12	13	32	31
Cu	13	12	8	17	14	10	47	46
Zn	58	58	60	66	58	54	161	155
Nb	12	12	12	12	10	11	26	20

TABLE 8.1c

BEMBOKA PROFILE

	J13	R1	R2	R3	J14	R4	R5	R6	R7	J15	J16	R8	J17	J18	R9	Clay J24	Clay J23	Clay J22
SiO_2	71.19	71.47	71.99	72.23	71.52	71.19	71.54	71.22	70.98	69.91	69.94	68.95	70.33	70.48	67.46	42.90	42.76	42.10
TiO_2	.38	.41	.36	.35	.39	.41	.41	.41	.40	.43	.43	.44	.42	.48	.43	.96	.79	.91
Al_2O_3	13.72	13.64	13.54	13.52	13.51	13.83	13.79	13.77	14.16	13.95	14.43	15.21	14.55	14.66	17.01	32.08	33.60	32.82
Fe_2O_3	.74	.74	.73	.86	1.03	1.27	1.50	1.43	1.64	1.79	1.91	2.03	2.16	3.31	2.96	5.25	5.91	8.87
FeO	21.05	2.14	1.87	1.64	1.82	1.73	1.53	1.57	1.29	1.34	1.25	1.28	1.00	.37	.21	-	-	-
MnO	.05	.05	.05	.05	.05	.06	.06	.06	.06	.06	.06	.07	.07	.07	.09	.15	.21	.25
MgO	.90	.91	.82	.75	.87	.84	.82	.83	.78	.80	.81	.84	.75	.50	.46	1.03	.98	1.14
CaO	2.92	3.00	2.72	2.50	2.62	1.92	1.82	1.96	1.69	1.03	.96	.44	.37	.05	.04	.45	.12	.62
Na_2O	2.87	2.89	2.88	2.73	2.79	2.31	3.16	2.41	2.20	1.22	1.24	.50	.61	.61	.11	?	?	?
K_2O	3.47	3.27	3.33	3.34	3.27	3.33	2.65	3.27	3.31	3.46	3.47	3.48	3.25	3.63	3.26	1.21	1.04	1.19
P_2O_5	.05	.08	.07	.06	.06	.07	.07	.06	.05	.02	.01	.02	.01	.01	.03	?	?	?
S	.04	.01	.01	.01	.01	.01	-	.03	-	-	-	-	-	-	.01	.02	.01	.01
H_2O^+	.84	.89	.99	1.06	1.17	1.73	1.75	1.74	2.17	3.09	3.28	4.11	4.17	4.31	5.26			
H_2O^-	.13	.14	.22	.26	.27	.66	.58	.64	.93	1.50	1.21	1.98	1.56	1.26	2.11			
CO_2	.73	.06	.14	.12	.19	.08	.23	.13	.15	.18	.13	.20	.10	.12	.19			
O=S	.02	.01		.01		.01		.02							.01			
TOTAL	100.06	99.71	99.54	99.48	99.56	99.41	99.90	99.52	99.80	99.78	99.13	99.53	99.33	99.87	99.63			
Ba	645	555	610	605	635	700	520	660	700	990	925	895	940	905	610	1170	960	995
Rb	154	148	151	158	160	170	141	165	191	184	193	197	179	182	177	134	116	105
Sr	159	160	153	148	149	121	129	121	104	72	68	40	36	26	22	38	17	18
Zr	184	186	180	176	184	200	191	196	185	203	215	217	205	247	207	85	89	110
Y	35	33	199	205	268	135	198	100	131	340	261	300	292	321	337	429	411	434
La	34	27	52	251	340	177	274	141	180	785	442	445	510	487	439	585	610	675
e	74	62	71	78	91	110	98	110	151	106	99	106	166	147	176	496	545	499
V	47	50	43	37	46	47	47	48	44	61	59	53	58	72	56	65	75	?
Cr	7	7	6	5	6	8	7	8	8	9	8	7	9	7	6	10	9	?
Pb	15	15	15	16	14	16	14	16	16	18	20	18	16	19	19	48	46	55
Ni	2	2	<1	<1	<1	<1	<1	1	<1	<1	<1	<1	<1	<1	<1	<1	<1	6
Cu	4	4	1	<1	2	1	2	1	<1	<1	2	<1	<1	<1	<1	25	12	11
Zn	37	41	36	36	38	46	45	44	45	65	63	74	67	74	58	188	153	180
Nb	9	9	10	9	12	10	10	10	9	14	13	12	13	15	12	20	19	23

been used in this study as there is considerable evidence to indicate that this assumption may be invalid (eg. Gardner et. al., 1978; Milnes 1984; this study). Weight based data have been converted to volumetric concentrations (gm/cm^3), using density measurements for samples. (Table 8.2).[2] The approach follows that described by Gardner et. al. (1978, 1981); gm/cm^3 abundances are plotted against density, allowing a comparison of the rate and extent of loss of individual components. Major and trace element data for the three profiles are presented in Figures 8.1 - 8.14.

MAJOR ELEMENT CHEMISTRY: RESULTS

One of the most outstanding features of Figures 8.1-8.4,(Bemboka Profile) 8.7, (Jindabyne Profile) and 8.11 (Island Bend Profile) is the number of oxides whose abundances, at least in the initial stages, decrease in a linear fashion. The slope of each plot is the net result of two process: the extent of release of components from parent phases, and retention in clay products. In the profiles studied it would appear that the most significant contribution to these trends is the rate at which elements are released. Clays occupy a comparatively small volume of the total, particularly early in weathering, and contain relatively small quantities of oxides other than Al, Fe, and Si (see Table 8.1).

Previous chapters have illustrated that weathering proceeds by development of a series of secondary phases which are intermediate in composition between the parent and the final alteration product. Although these phases, often smectites, accommodate significant quantities of elements such as Mg, Fe, Ca, K, (Na), in their structures, they occupy a relatively small volume, and are rapidly converted to stable alteration products, generally kaolin. Consequently, although the process occurring may be A->B->C->D->E, the bulk chemical data reflects the net result of A->E, and not A->B, B->C, etc. The small volume occupied by secondary products is apparent in studies of the weathering of individual phases, and is further illustrated by the XRD results which failed to clearly indicate the presence of smectite in alteration assemblages.

---

[2]Density measurements were obtained by determining the weights of wax coated samples in air and in water. Results were corrected for the parafin wax. Several measurements were made for each result, and care was taken to prevent the development of bubbles.

TABLE 8.2a

Chemical analyses in gm/cm^3 x 100 and ppm/cm^3 x 100 for the Island Bend, Jindabyne and Bemboka profiles. Samples prefixed R collected by RAE.

	ISLAND BEND PROFILE													
	R22	R23	R24	J1	J2	R25	J3	J4	J5	R26	R27	R28	J6	Clay J19
SiO_2	183.05	185.21	178.32	181.71	181.52	178.9	172.52	166.07	162.74	135.73	113.39	116.08	106.88	69.57
TiO_2	.74	.78	.78	.71	.74	.73	.73	.68	.70	.63	.50	.52	.50	.72
Al_2O_3	39.79	40.04	39.07	40.88	40.65	39.16	38.64	36.82	37.20	34.55	27.11	28.43	26.97	58.00
Fe_2O_3	3.17	3.62	3.84	3.21	3.70	3.67	4.30	4.44	5.29	5.82	4.66	4.73	4.71	3.55
FeO	4.00	4.02	3.83	3.77	3.75	3.64	3.01	2.59	1.86	.78	.66	.70	.64	-
MnO	.21	.22	.21	.20	.20	.21	.20	.19	.18	.19	.14	.16	.14	.29
MgO	3.15	3.35	3.36	3.08	3.14	3.17	3.12	2.86	2.86	2.48	2.01	2.07	1.97	1.46
CaO	7.96	8.87	8.43	7.79	7.98	7.63	7.46	6.78	6.23	1.08	.79	.67	.52	.08
Na_2O	8.33	8.60	8.16	8.30	8.32	7.72	8.53	7.20	7.34	1.53	1.17	1.11	1.71	?
K_2O	8.15	7.49	7.15	7.56	7.23	7.38	7.27	6.68	6.17	5.87	5.18	5.33	5.16	2.91
P_2O_5	.32	.33	.33	.32	.23	.32	.26	.21	.24	.05	.03	.03	.03	?
S	.02	.02	-	.04	.01	.01	.03	.02	.02	.01	-	-	.02	.02
H_2O^+	2.29	2.10	2.36	2.73	2.72	3.07	3.06	3.36	4.52	9.43	7.36	7.99	7.78	
H_2O^-	.74	.51	.62	.83	.76	.90	.90	.86	1.59	1.77	1.14	1.31	1.94	
CO_2	.21	.11	.03	.13	.16	.21	.43	.36	.24	.12	.08	.14	.26	
Density gm/cm^3	2.63	2.66	2.57	2.60	2.62	2.58	2.51	2.40	2.38	2.01	1.65	1.70	1.60	(1.60) 14.9% clay
Ba	1933.1	1888.6	1889.0	2067.0	1991.2	1973.7	1895.1	1848.0	1832.6	1859.3	1493.3	1496.0	1616.0	1040.0
Rb	307.7	287.3	287.8	275.6	264.6	278.6	253.5	242.4	211.8	239.2	214.5	221.0	209.6	124.8
Sr	1162.5	1255.5	1177.1	1146.6	1152.8	1104.2	1101.9	1032.0	954.4	253.3	204.6	192.1	160.0	25.6
Zr	226.2	242.1	233.9	174.2	167.7	239.9	165.7	146.4	178.5	188.9	138.6	147.9	131.2	110.4
Y	57.9	55.9	56.5	49.4	49.8	51.6	50.2	50.4	45.2	96.5	36.3	34.0	65.6	70.4
La	52.6	58.5	61.7	54.6	52.4	51.6	52.7	52.8	47.6	80.4	34.7	28.9	64.0	54.4
Ce	110.5	127.7	123.4	111.8	112.7	113.5	110.4	88.8	85.7	132.7	71.0	68.0	72.0	132.8
V	139.4	154.3	149.1	150.8	144.1	147.1	138.1	136.8	130.9	116.6	89.1	90.1	104.0	59.2
Cr	15.8	16.0	15.4	15.6	15.7	15.5	15.1	14.4	11.9	16.1	9.9	10.2	9.6	6.4
Pb	60.5	55.9	51.4	57.2	57.6	54.2	52.7	52.8	50.0	48.2	38.0	42.5	40.0	76.8
Ni	2.6	2.6	-	-	-	-	-	2.4	4.8	-	-	-	4.8	4.8
Cu	7.9	13.3	5.1	18.2	7.9	5.2	5.0	7.2	7.1	2.01	1.65	3.4	-	22.4
Zn	107.8	117.0	118.2	101.4	96.9	113.5	97.9	88.8	90.4	108.5	84.2	88.4	76.8	96.0
Nb	23.7	23.9	23.1	20.8	19.7	20.6	21.3	16.8	19.0	20.1	14.9	15.3	14.4	13.6

TABLE 8.2b

JINDABYNE PROFILE								
	J7	J8	J9	J10	J11	J12	Clay J21	Clay J20
SiO_2	191.35	178.02	182.00	160.92	147.92	158.48	91.32	98.67
TiO_2	1.53	1.38	1.43	1.26	1.12	1.25	2.94	2.83
Al_2O_3	38.34	35.46	36.63	33.21	31.45	33.30	54.09	63.43
Fe_2O_3	.93	3.54	2.54	7.93	8.10	8.42	22.96	24.77
FeO	9.31	6.07	7.23	1.46	.59	.92	-	-
MnO	.15	.12	.12	.10	.07	.11	.17	.30
MgO	4.44	4.04	4.30	3.45	3.29	3.42	7.13	6.46
CaO	6.03	4.44	4.25	2.66	1.38	2.81	.96	.76
Na_2O	6.25	5.64	6.00	4.66	3.83	4.26	?	?
K_2O	10.38	9.89	10.79	9.17	9.32	8.23	6.08	7.15
P_2O_5	.27	.23	.25	.21	.08	.15	?	?
S	.12	.03	.04	.01	.02	.01	.35	.15
H_2O^+	3.30	3.62	3.55	4.91	6.17	5.50		
H_2O^-	.38	.92	.63	2.14	2.42	1.36		
CO_2	.90	.33	.21	.35	.61	1.33		
Density gm/cm^3	2.73	2.55	2.61	2.35	2.18	2.30	(2.18) 18.8% clay	(2.30) 11.5% clay
Ba	1310.0	1250.0	1279.0	1152.0	1036.0	1047.0	763.0	885.5
Rb	502.3	476.9	508.9	394.8	377.1	414.0	479.6	542.8
Sr	319.4	275.4	276.7	220.9	163.5	213.9	150.4	128.8
Zr	475.0	459.0	467.0	416.0	336.0	389.0	159.1	161.0
Y	87.4	79.1	83.5	70.5	52.3	64.4	63.2	52.9
La	79.2	68.9	65.3	75.2	63.2	69.0	113.4	117.3
Ce	182.9	160.7	148.8	155.1	111.2	142.6	252.9	243.8
V	185.6	181.1	182.7	209.2	194.0	195.5	372.8	381.8
Cr	95.6	89.3	96.6	103.4	93.7	96.6	196.2	177.1
Pb	73.7	66.3	67.7	65.8	54.5	62.1	89.4	98.9
Ni	32.8	30.6	31.3	28.2	26.2	29.9	69.8	71.3
Cu	35.5	30.6	20.9	40.0	30.5	23.0	102.5	105.8
Zn	158.3	147.9	156.6	155.1	126.4	124.2	351.0	356.5
Nb	31.4	29.3	30.0	30.5	21.8	24.2	55.6	46.0

TABLE 8.2c

BEMBOKA PROFILE

	J13	R1	R2	R3	J14	R4	R5	R6	R7	J15	J16	R8	J17	J18	R9	Clay J24	Clay J23	Clay J22
SiO_2	192.93	190.82	191.50	189.97	186.67	182.24	173.84	171.65	166.80	164.99	159.45	143.41	135.74	128.97		97.81	82.52	77.04
TiO_2	1.04	1.09	.96	.92	1.02	1.05	1.01	.98	.94	1.01	.97	.92	.81	.87		2.20	1.52	1.66
Al_2O_3	37.17	36.41	36.01	35.56	35.26	35.39	33.50	33.19	33.28	33.93	32.91	31.63	28.07	26.83		73.14	64.85	60.06
Fe_2O_3	2.01	1.98	1.95	2.26	2.68	3.24	3.65	3.45	3.86	4.23	4.36	4.22	4.16	6.06		11.97	11.41	16.23
FeO	5.56	5.71	4.97	4.31	4.75	4.43	3.72	3.78	3.03	3.16	2.85	2.66	1.93	.68		-	-	-
MnO	.14	.14	.14	.13	.14	.14	.14	.13	.13	.13	.13	.14	.14	.12		.34	.41	.45
MgO	2.43	2.42	2.17	1.96	2.27	2.16	2.00	2.01	1.82	1.90	1.84	1.74	1.44	.92		2.37	1.89	2.09
CaO	7.92	8.00	7.23	6.57	6.83	4.90	4.41	4.73	3.96	2.43	2.19	.91	.71	.10		1.03	.23	.11
Na_2O	7.78	7.72	7.66	7.17	7.27	5.91	7.68	5.81	5.18	2.87	2.82	1.03	1.18	1.12		?	?	?
K_2O	9.40	8.72	8.86	8.79	8.54	8.52	6.44	7.88	7.79	8.17	7.91	7.24	6.27	6.65		2.77	2.00	2.18
P_2O_5	.14	.20	.18	0.17	.15	.17	.16	.15	.11	.05	.03	.04	.02	.02		?	?	?
S	.09	.02	.02	.04	.01	.03	.01	.07	.01	.01	-	.01	.01	.01		.03	.02	.02
H_2O^+	2.28	2.38	2.63	2.79	3.05	4.43	4.25	4.19	5.10	7.29	7.48	8.55	8.05	7.89				
H_2O^-	.35	.37	.59	.68	.70	1.69	1.41	1.54	2.19	3.54	2.76	4.12	3.01	2.31				
CO_2	1.98	.16	.37	.32	.50	.20	.56	.31	.35	.42	.30	.42	.19	.22				
Density gm/cm^3	2.71	2.67	2.66	2.63	2.61	2.56	2.43	2.41	2.35	2.36	2.28	2.08	1.93	1.83	?	(2.28) 9.31% clay	(1.93) 14.43% clay	(1.83) 17.23% clay
Ba	1748.0	1481.9	1622.6	1591.2	1657.4	1792.0	1263.6	1591.0	1645.0	2336.4	2109.0	1862.0	1814.2	1656.2		2667.6	1852.8	1820.9
Rb	417.3	395.2	401.7	415.5	417.6	435.2	324.6	397.7	448.9	434.2	440.0	409.8	345.5	333.1		305.5	223.9	192.2
Sr	430.9	427.2	407.0	389.2	388.9	309.8	313.5	291.6	244.4	169.9	155.0	83.2	69.5	47.6		86.6	32.8	32.9
Zr	498.6	496.6	478.8	462.9	480.2	512.0	464.1	472.4	434.8	479.1	490.2	451.4	395.7	452.0		193.8	171.8	201.3
Y	94.9	88.1	529.3	539.2	699.5	345.6	481.1	241.0	307.9	802.4	595.1	624.0	563.6	587.4		978.1	793.2	794.2
La	92.1	72.1	138.3	660.1	887.4	453.1	665.8	399.8	423.0	1852.6	1007.8	925.6	964.3	891.2		1333.8	1177.3	1235.3
Ce	200.5	165.5	188.7	205.1	237.5	281.6	238.1	265.1	355.0	250.2	225.7	220.5	320.4	269.0		1130.9	1051.9	913.2
V	127.4	133.5	114.4	97.3	120.1	120.3	114.2	115.7	103.4	144.0	134.5	110.2	111.9	131.8		148.2	144.8	?
Cr	19.0	18.7	16.0	13.2	15.7	20.5	17.0	19.3	18.8	21.2	18.2	14.6	17.4	12.8		22.8	17.4	?
Pb	40.7	40.1	39.9	42.1	36.5	41.0	34.0	38.6	37.6	42.5	45.6	37.4	30.9	34.8		109.4	88.8	100.7
Ni	5.4	5.3	-	-	-	-	-	2.41	-	-	-	-	-	-		-	-	11.0
Cu	10.8	10.7	2.7	-	5.2	-	4.86	2.41	-	-	4.56	-	-	-		57.0	23.2	20.1
Zn	100.3	106.8	95.8	94.7	99.2	115.2	109.4	106.0	105.8	153.4	143.6	153.9	129.3	135.4		428.6	295.3	329.4
Nb	23.0	24.0	26.6	23.7	30.3	25.6	24.3	24.1	21.2	33.0	28.5	25.0	24.1	27.5		44.5	30.9	42.1

When mineral crushes of strongly weathered granite are examined it is apparent that they contain a mixture of material from unaltered crystals through to phases which have been completely replaced. This further indicates that the composition of the bulk assemblage is controlled primarily by the balance between the proportions of unweathered minerals and the nature and abundance of the clay products, rather than the extent to which alteration has proceeded.

The rate of release of components is a direct result of the rate at which the host minerals weather. As indicated by the straight line trends in the figures, these rates appear to be fairly constant, at least in the early stages, and before host phases are consumed. Many workers have reported linear kinetics of dissolution for a range of minerals, implying that phases dissolve by release of components at a constant rate. These linear trends are interpreted to be a reflection of this behaviour.

To obtain an indication of the rates at which components are released during weathering the quantity of each element remaining in the clay fraction must be subtracted from the amount of each component remaining in the weathered rock. This contribution can be calculated by multiplying the amount of the oxide in the clay by the measured abundance of the clay in the whole rock. Where possible, release rate trends have been plotted with whole rock trends for the Bemboka profile in Figures 8.1-8.6. Resulting release rates are listed in Table 8.3.

To determine the relative rates at which host phases weather from release rates requires an understanding of the contribution which individual minerals make to control the distribution of elements. Consequently the calculation involves the use of modes and microprobe data for individual phases. As a number of assumptions and simplifications must be made, this study aims only to provide very general, comparative results for the relative weathering rates of the major minerals.

An example of the calculation of results given below is presented in Appendix 4, probe data are included in Appendix 2, and the bulk chemical and clay data are presented in Tables 8.1 and 8.2. The method used is described below:

KEY FOR FIGURES

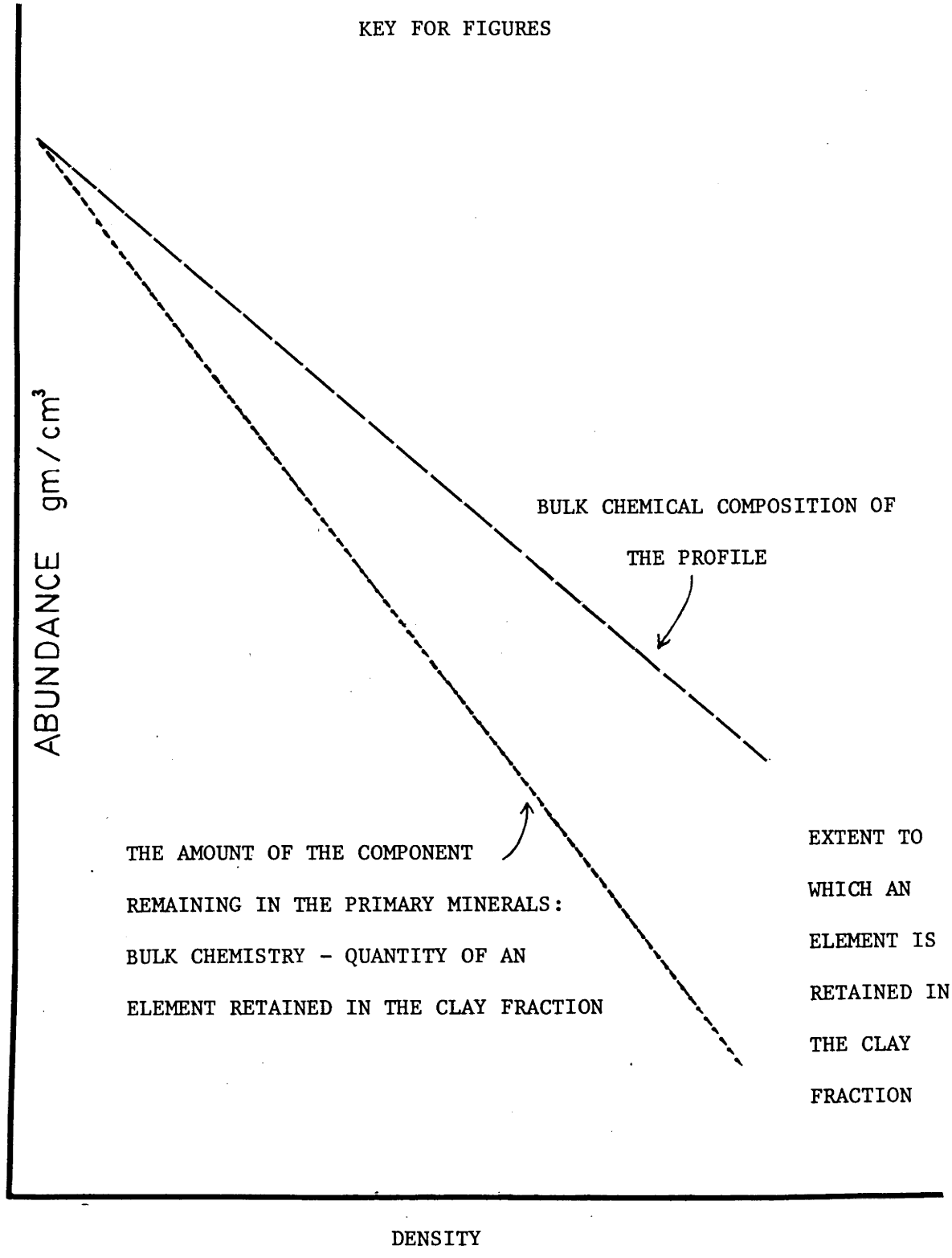

FIGURE 8. 1 gm / cm^3 ABUNDANCES OF OXIDES PLOTTED AGAINST DENSITY.

BEMBOKA PROFILE

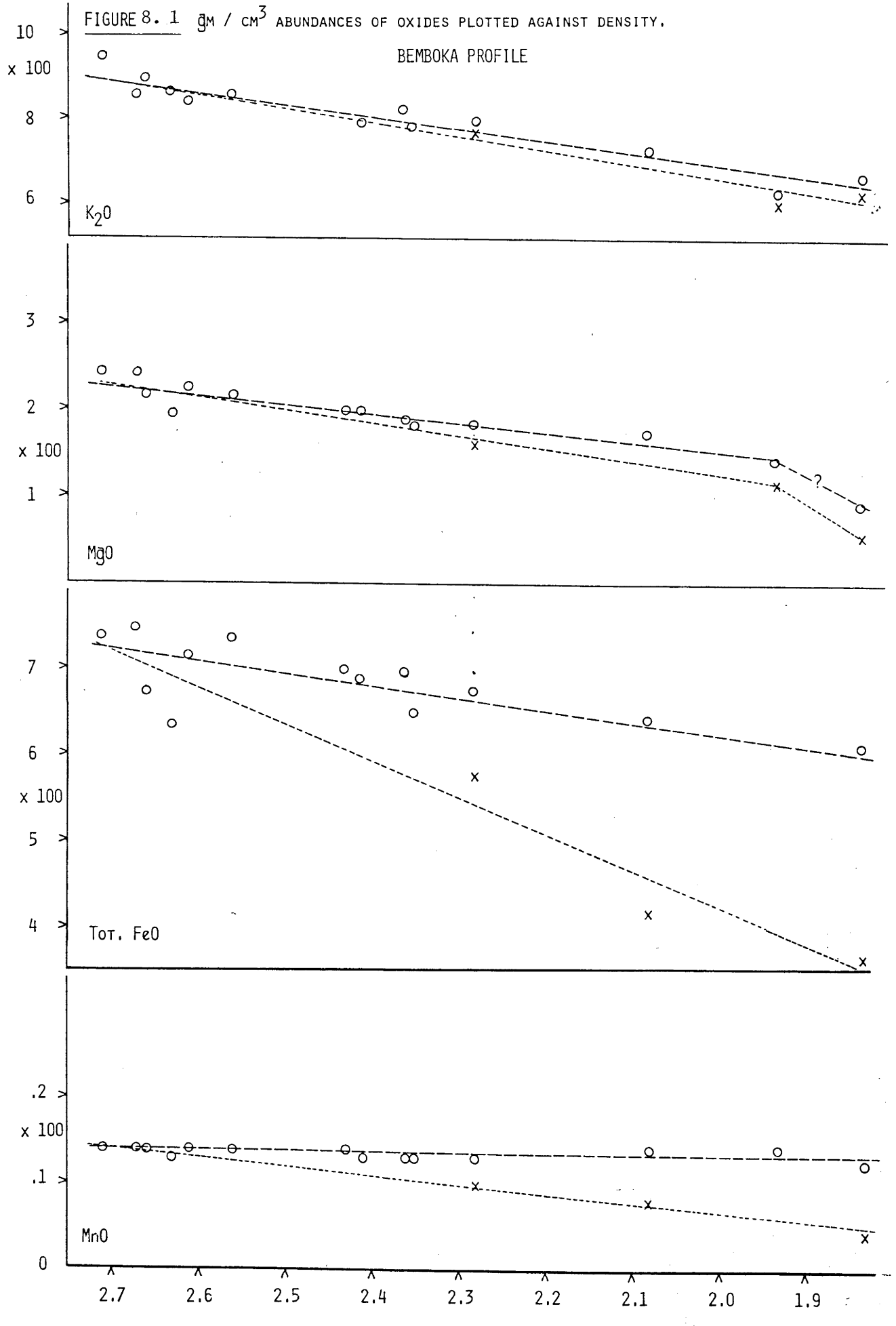

FIGURE 8.2 : gm / cm^3 ABUNDANCES OF OXIDES PLOTTED AGAINST DENSITY

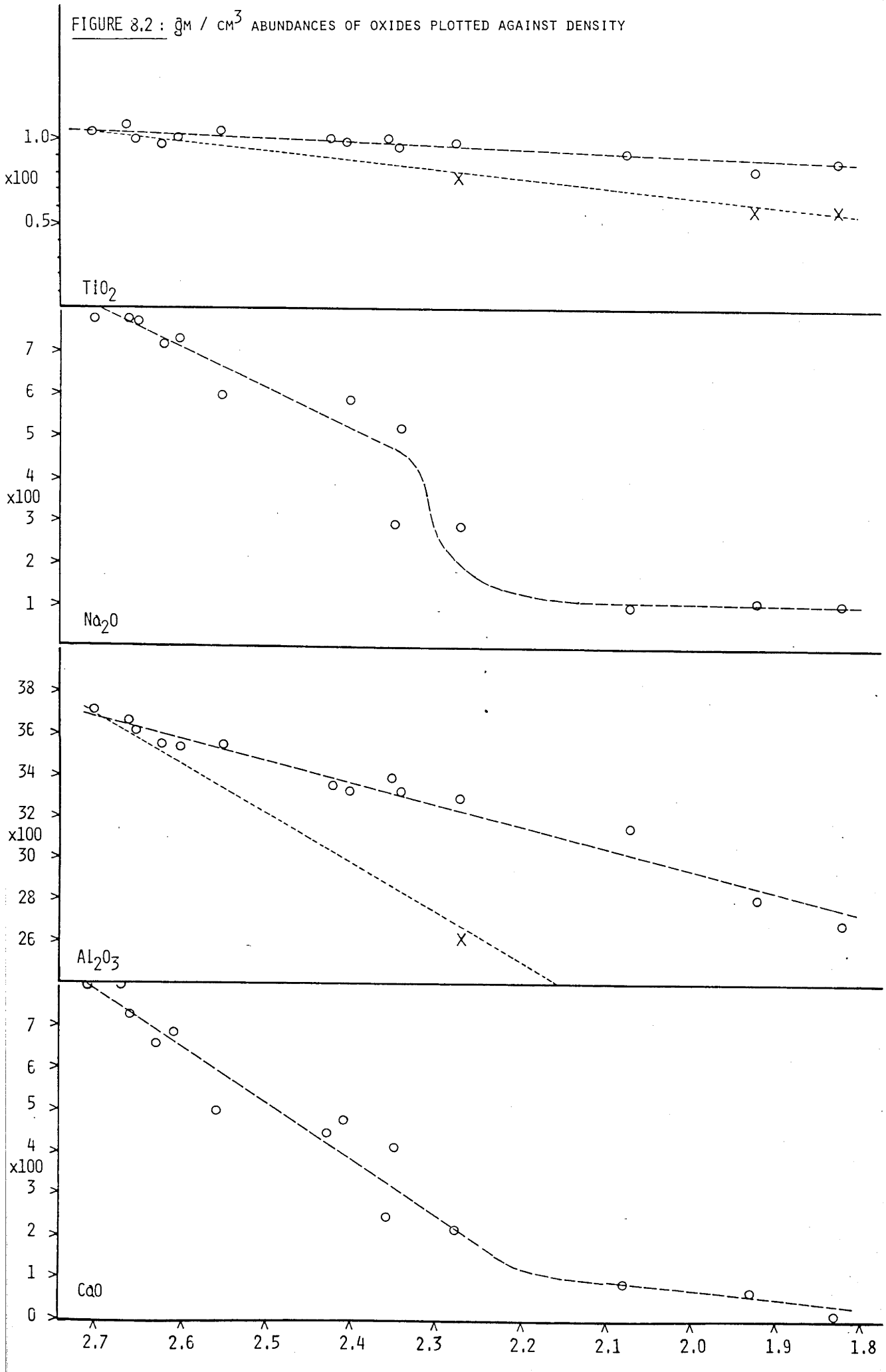

FIGURE 8.3 gm/ cm^3 AND PPM/ cm^3 ABUNDANCES OF ELEMENTS PLOTTED AGAINST DENSITY.

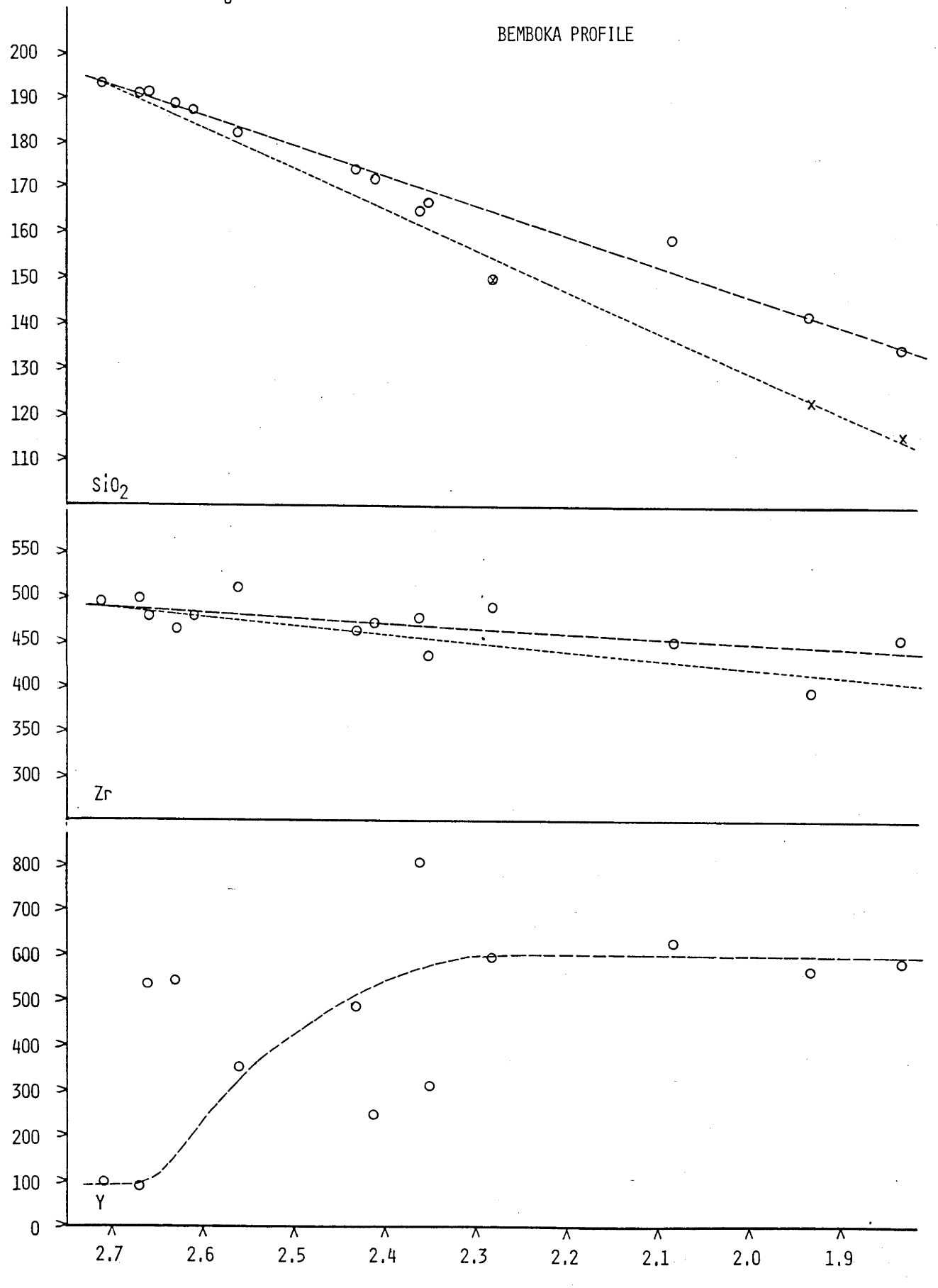

FIGURE 8.4 : gm / cm ^{3} OXIDE ABUNDANCES AND RATIOS PLOTTED AGAINST DENSTIY.

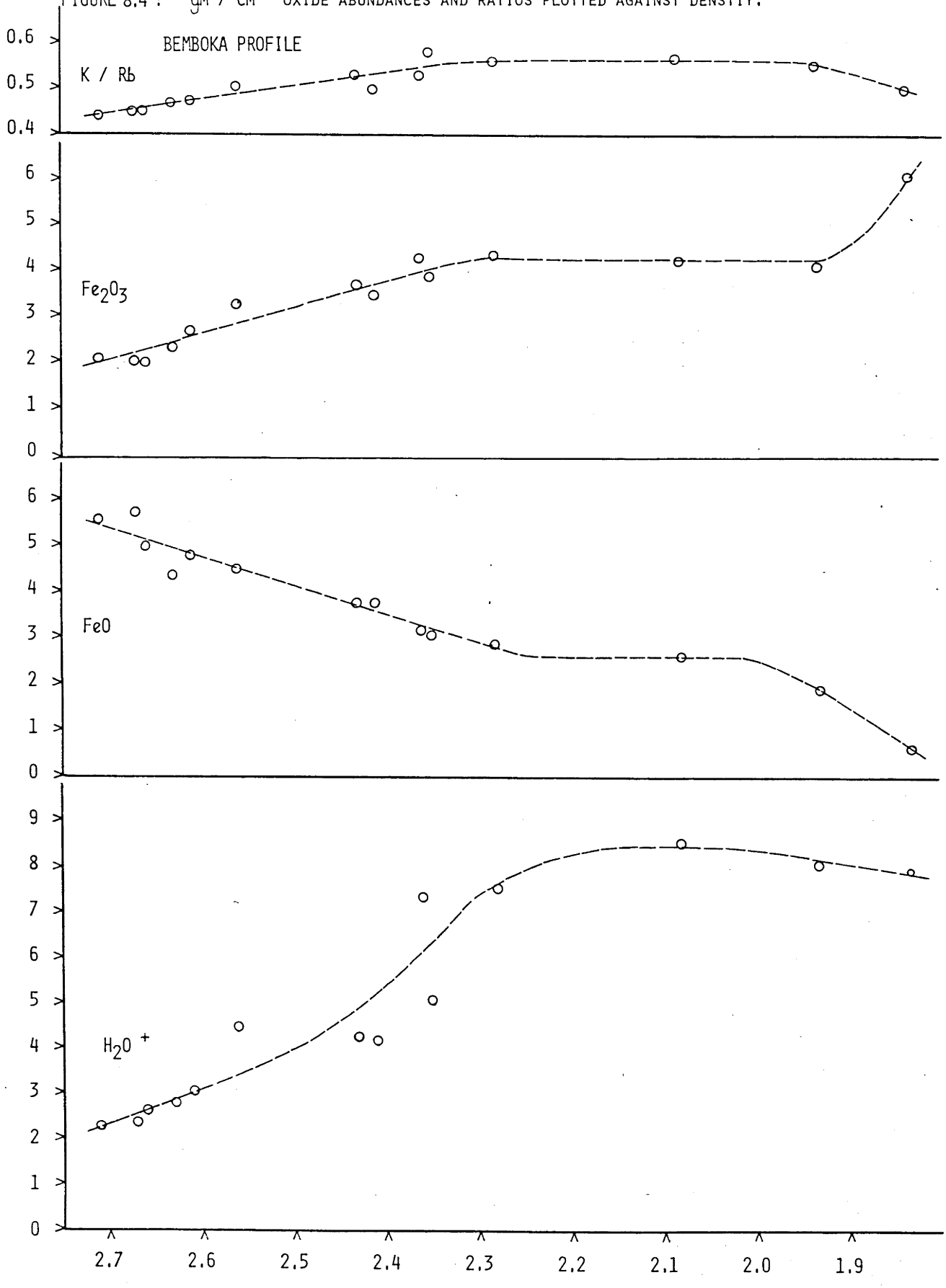

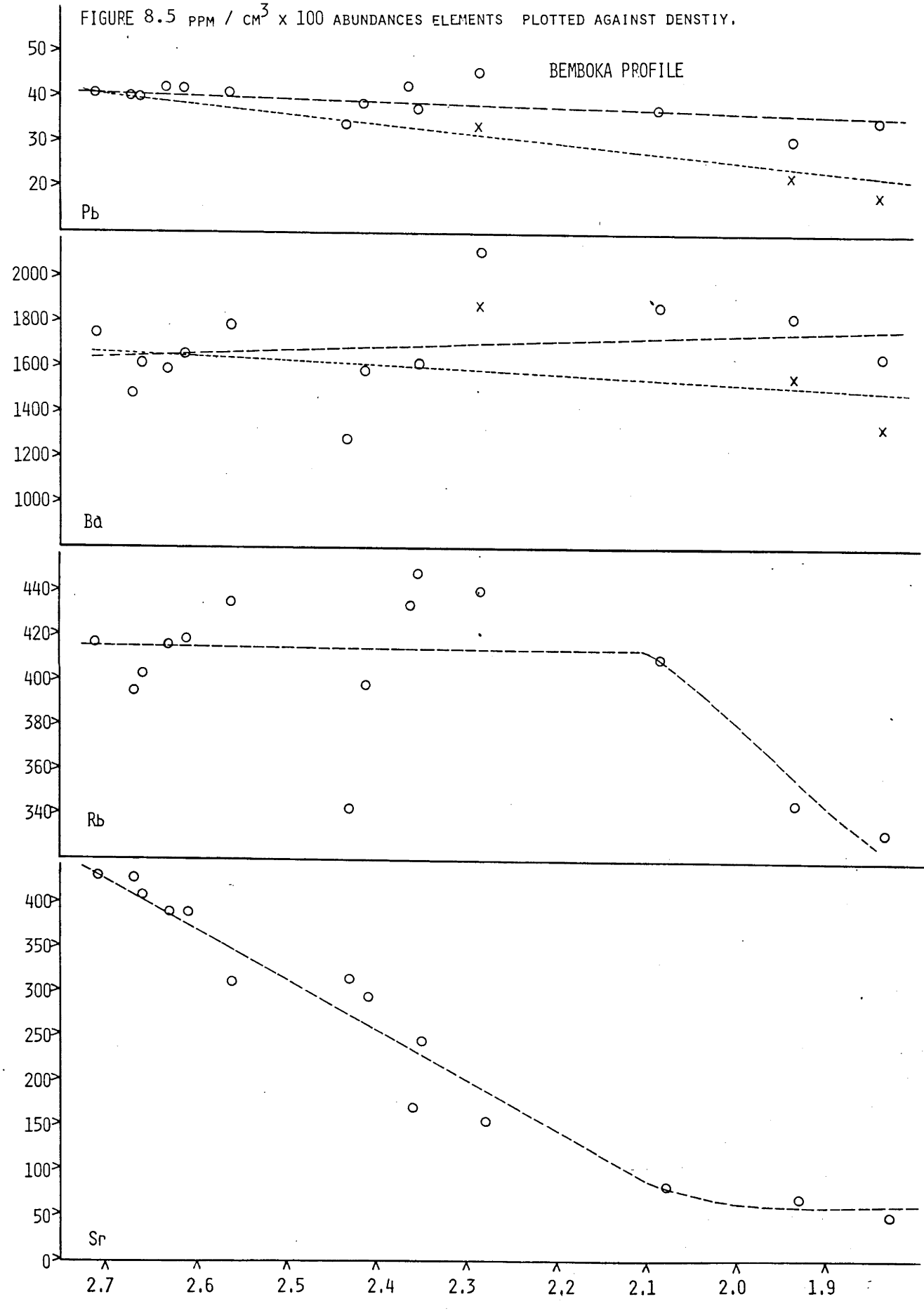
FIGURE 8.5 PPM / CM3 X 100 ABUNDANCES ELEMENTS PLOTTED AGAINST DENSTIY.
BEMBOKA PROFILE
Pb
Ba
Rb
Sr
50
40
30
20
2000
1800
1600
1400
1200
1000
440
420
400
380
360
340
400
350
300
250
200
150
100
50
0
2.7
2.6
2.5
2.4
2.3
2.2
2.1
2.0
1.9

FIGURE 8.6 PPM / CM^3 ABUNDANCES OF ELEMENTS PLOTTED AGAINST DENSITY.

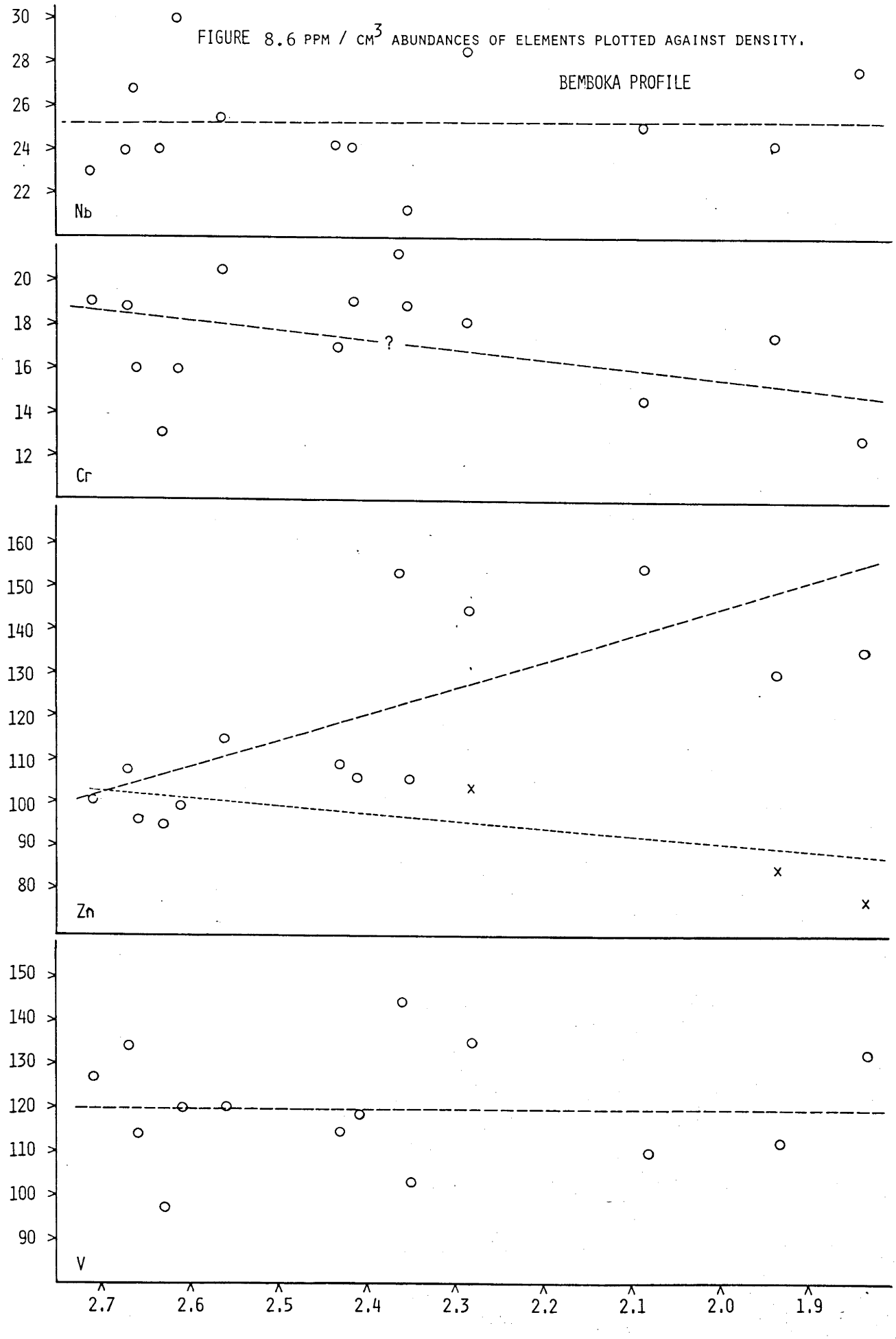

FIGURE 8.7 gm /cm ^{3} x 100 oxide abundances plotted against density.

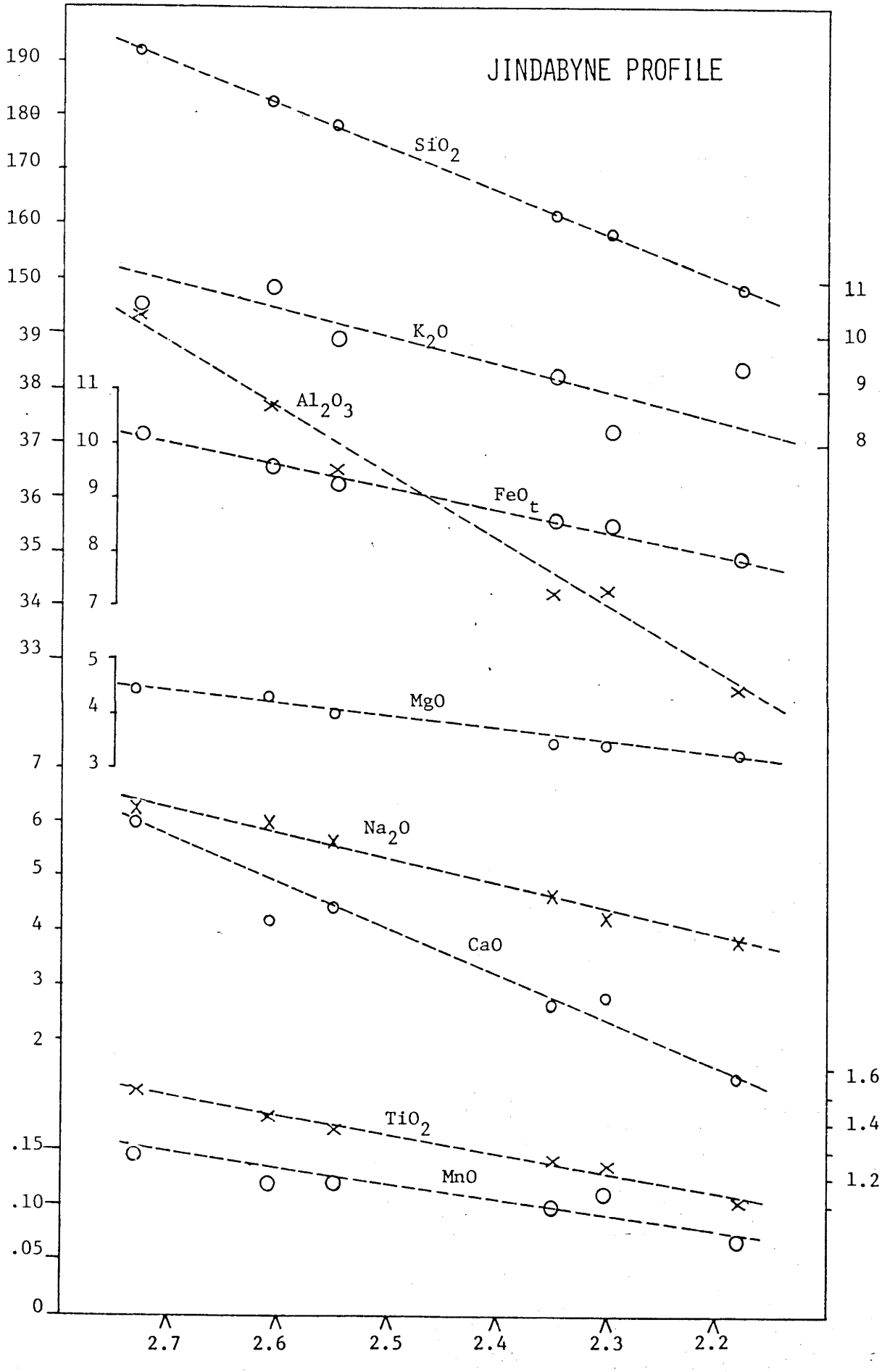

FIGURE 8.8 gm /cm ^{3} x 100 oxide abundances plotted against density.

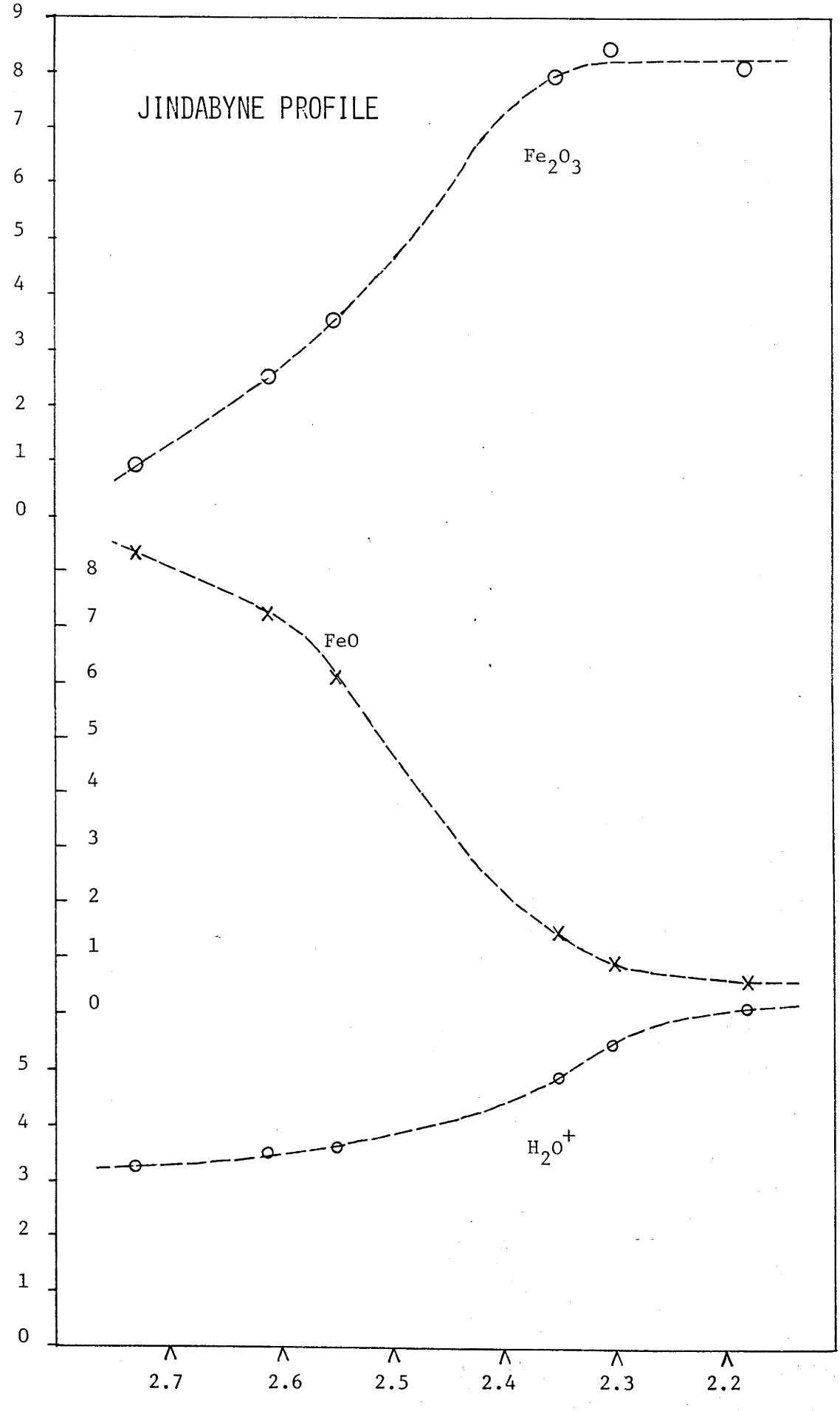

FIGURE 8.9 ppm /cm ^{3} x 100 abundances plotted against density.

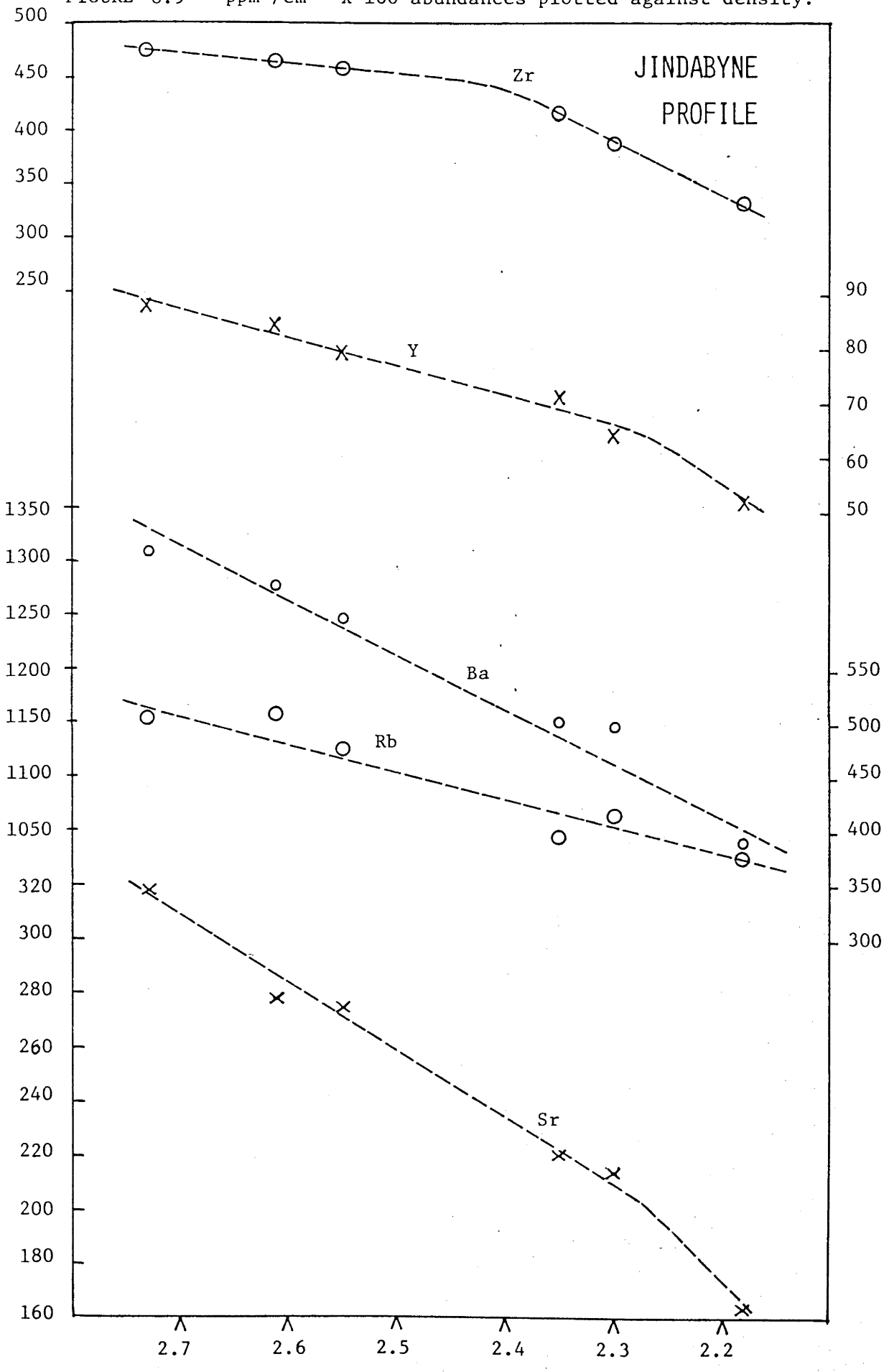

FIGURE 8.10 ppm /cm ^{3} x 100 abundances plotted against density.

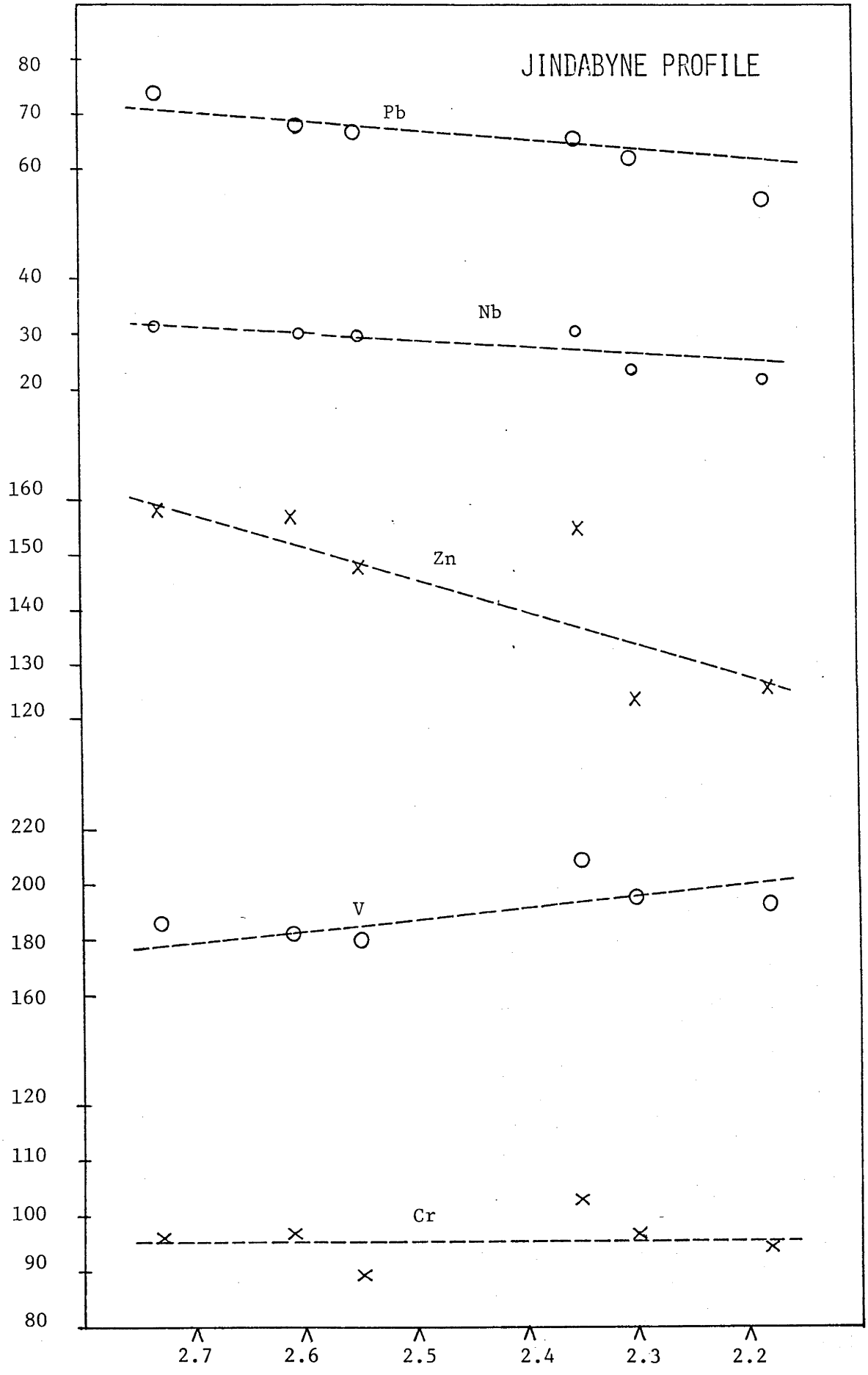

FIGURE 8.11 gm / cm^3 x 100 oxide abundances plotted against density.

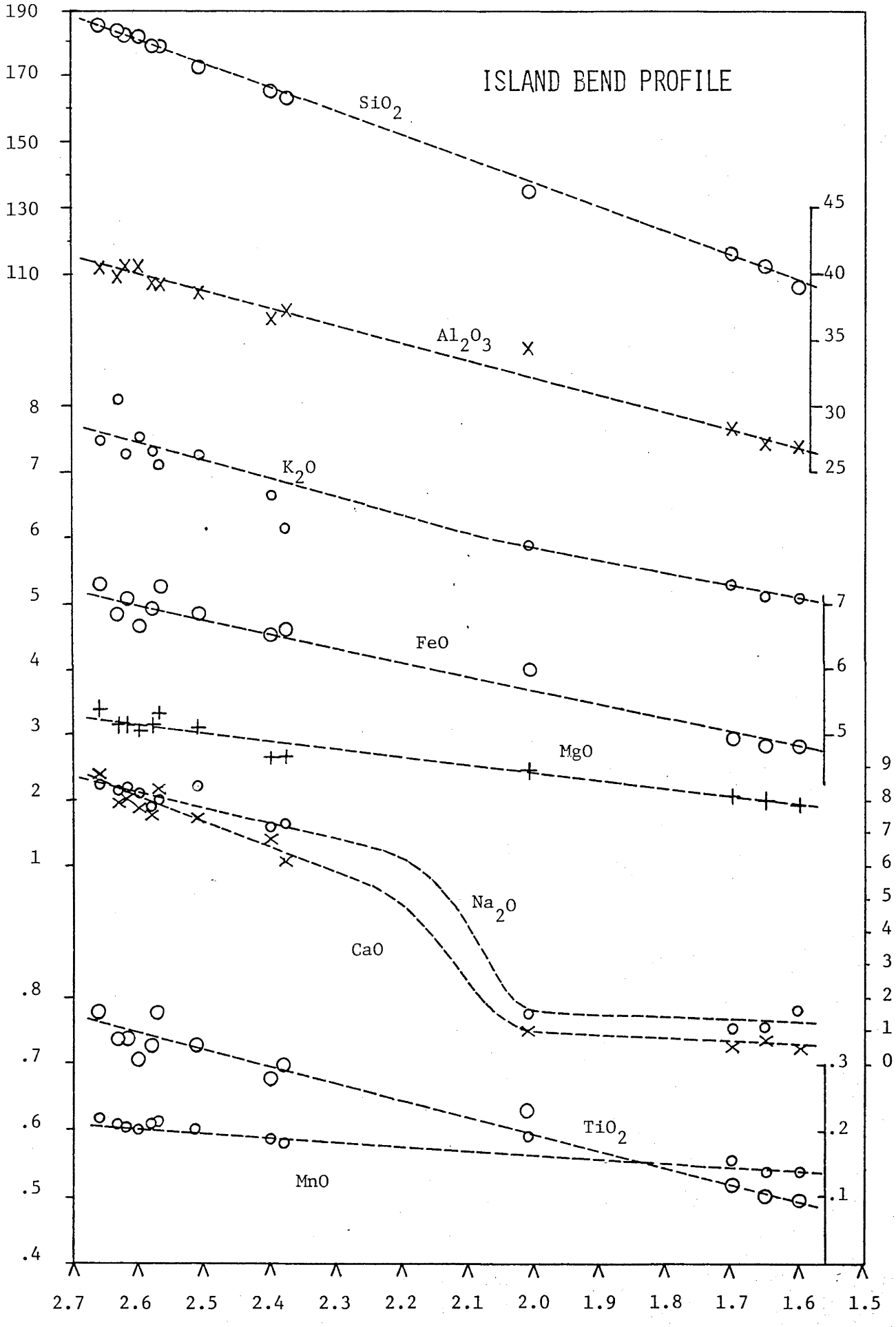

FIGURE 8.12 ppm / cm ^{3} x 100 abundances plotted against density.

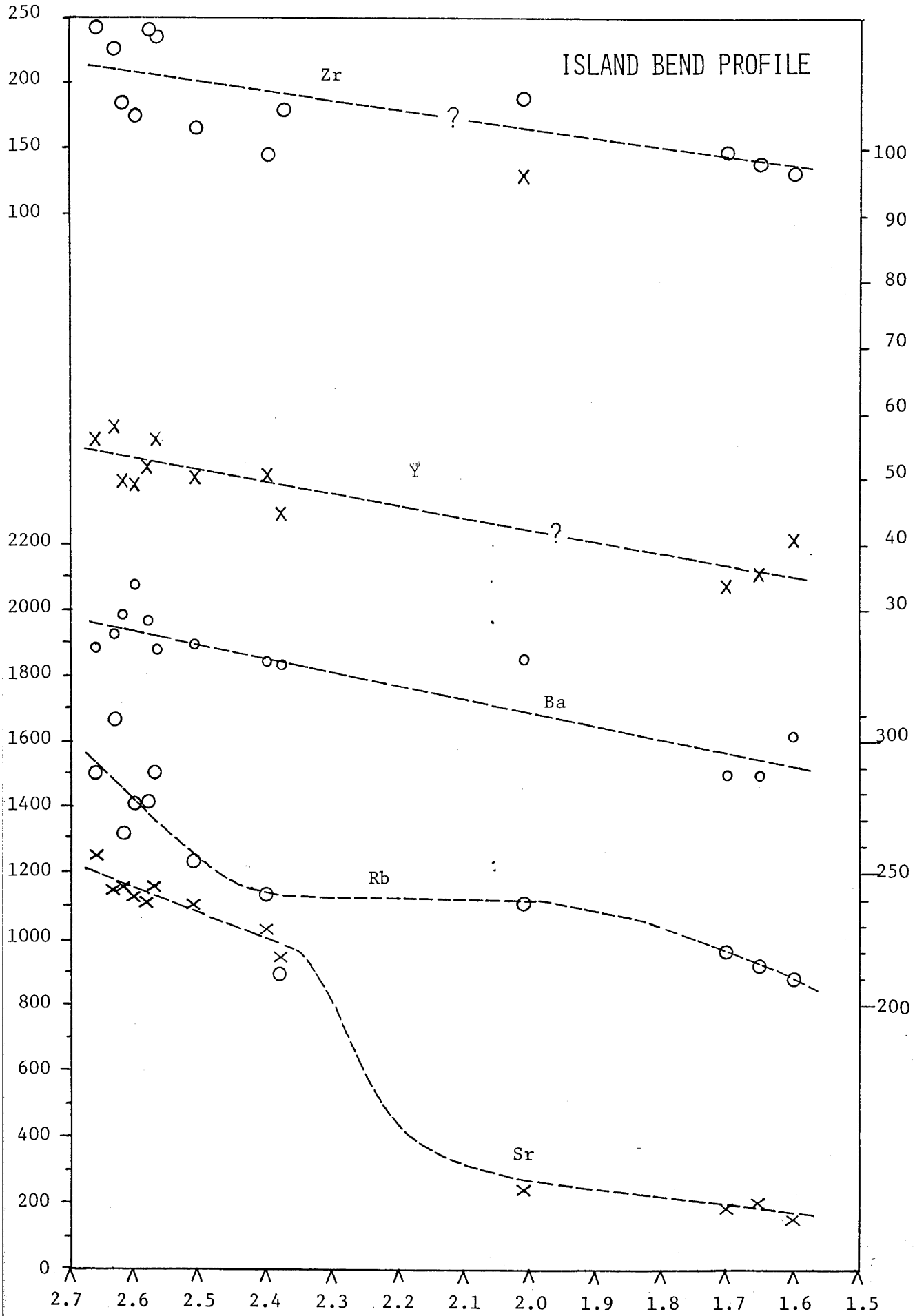

FIGURE 8.13 ppm / cm ^{3} x 100 abundances plotted against density.

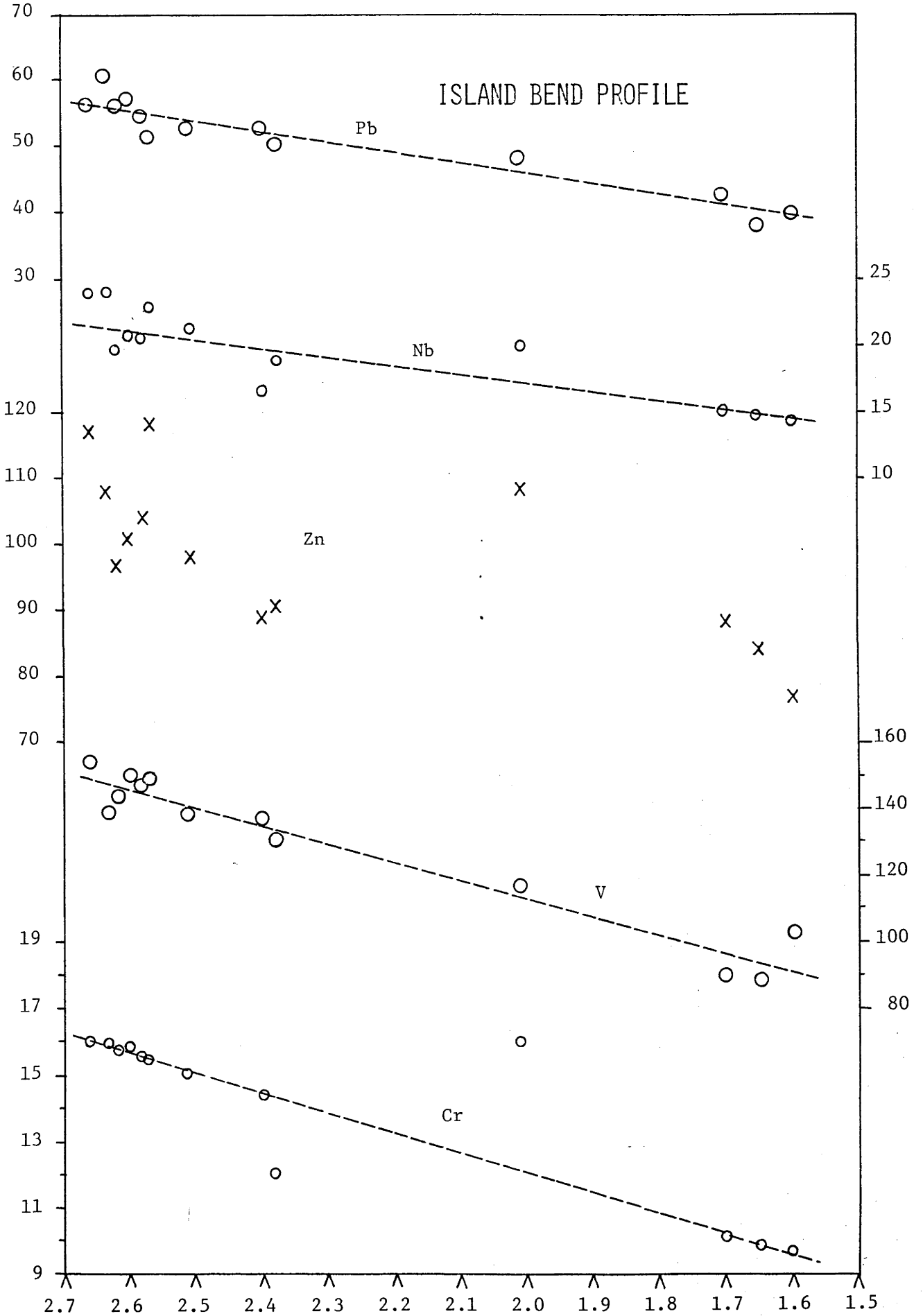

FIGURE 8.14 gm /cm ^{3} x 100 oxide abundances plotted against density.

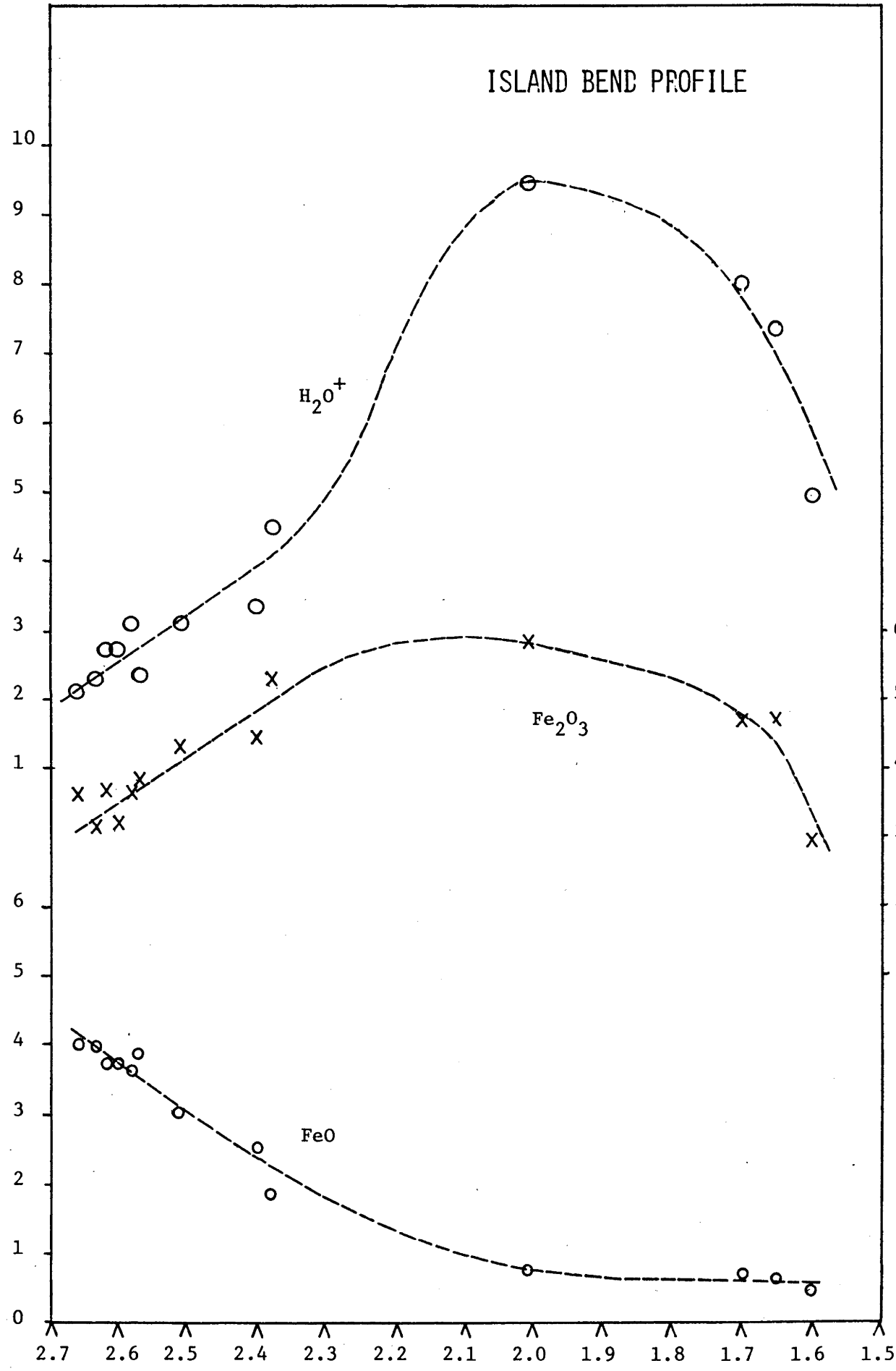

1. As effectively all the Mg, Ti, and most of the Fe are contained in biotite, the extent to which these components have been released should be the similar, and reflect the extent of destruction of biotite.

2. The amount of K which will be removed with the quantity of biotite determined in step 1. is calculated, and subtracted from the amount of K which has been released from the rock overall. As the remaining amount of K must have come from the breakdown of K-feldspar, the fraction of K-feldspar which has released its components to form clays or into solution can be obtained by dividing this quantity into the amount of K contained in K-feldspar before weathering commenced.

3. The rate at which plagioclase feldspars weather is more difficult to determine, primarily because the composition of the plagioclase is so varied, and as the different compositions weather at different rates. To overcome this problem probe data were examined, and a mixture of two selected compositions of plagioclase determined which would account for the abundance of Na and Ca in the whole rock. The two compositions of plagioclase used represent the calcic cores, at An_{45}-An_{50}, and the more sodic rims and laths at An_{10}- An_{20}. Plagioclase intermediate between these compositions is assumed to be accounted for by mixtures of these two end members. The relative quantities of the more calcic and more sodic plagioclase which must have been broken down were modeled using the amounts of Ca and Na released from the whole rock. A comparison of these quantities with the amounts of biotite and K-feldspar removed at this stage allows the determination of the relative rates at which the major phases in the rock have weathered.

The results of these calculations are given in Table 8.3. For the Bemboka profile the effect of the presence and alteration of amphibole and epidote have also been examined as these phases do accommodate an amount of Ca. Although the incorporation of these phases in the calculation does modify the result, the change in the general relative extents to which phases are inferred to breakdown is not of significance.

Table 8.3

PROPORTIONS OF COMPONENTS RELEASED FROM PRIMARY MINERALS INTO SOLUTION OR TO FORM CLAYS.

	BEMBOKA	JINDABYNE	ISLAND BEND
SiO_2	22%	22%	24%
TiO_2	22%	40%	23%
Al_2O_3	30%	30%	29%
Tot. FeO	25%	39%	19%
MnO	32%	45%	24%
MgO	22%	39%	22%
CaO	72%	53%	45%
Na_2O	50%	32%	33%
K_2O	15%	26%	20%

Quantities expressed per release of 25% of the original components in the rock.

MODES

QUARTZ	35%		34%		34%
PLAGIOCLASE:	An_{11} 19%		An_{13} 14%		An_{20} 21%
	An_{48} 13%		An_{50} 18%		An_{50} 23%
K-FELDSPAR	16%		12%		12%
BIOTITE	10%		18%		9%
AMPHIBOLE	3%		-		tr
MUSCOVITE	-		3%		-
EPIDOTE	4%		?		?
ACCESSORIES	tr		1%		1%

AMOUNT OF EACH PHASE REMOVED TO GENERATE THE LOSSES LISTED ABOVE

BIOTITE	22%	39%	23%
K-FELDSPAR	13%	14%	18%
Ca-PLAG.	70%	61%	52%
Na-PLAG.	35%	15%	21%
AMPHIBOLE	100%*		
EPIDOTE	100%		

*All amphibole assumed to have weathered as this phase is observed to be rapidly removed.

The above table illustrates that phases in the two profiles developed from I type granite, the Bemboka and Island Bend profiles, weather at broadly similar rates. The S type Jindabyne profile displays some similarity in the relative rates of removal of K-feldspar, and the two types of plagioclase, but considerably more of the biotite has been replaced or dissolved. This difference in the behaviour of biotite may be a reflection of the greater abundance of biotite in the fresh granite, or may indicate that the biotite in the Jindabyne profile is

more susceptible to weathering. As S-type granites tend to contain more reduced Fe in biotite than I types, the greater rate of destruction of this mineral may reflect a tendency for the presence of oxidizable Fe to accelerate the weathering of this phase.

Differences in the style of weathering of the three profiles are indicated by the nature of the weathered material produced. At a density of 2.18 material from the Jindabyne profile contains 18% clay, at 1.93 the Bemboka profile contains 14% clay, and at 1.60 the Island Bend profile contains 15% clay. This illustrates that the density of a sample does not reflect the extent to which it has been weathered.

The rates of release of elements in the above table, and the rates of destruction of minerals calculated from these data apply to the initial stages of weathering. The indications are that during this stage the breakdown of calcic feldspar (cores) contributes very significantly to the overall quantity of material released. As indicated in Figures 8.2, 8.11, this stage of weathering is terminated when the calcic feldspar is consumed. Chemical data indicate that of the abundant minerals K-feldspar* is the most resistant at this stage, and that sodic plagioclase and biotite are generally intermediate in their susceptibility to weathering. This is consistent with SEM, TEM, and optical microscope observations of mineral alteration.

Release rates for Al and Si were also obtained. To check the internal consistency, these rates are compared in Table 8.4 with the calculated quantities of Al and Si released by destruction of minerals in the quantities listed in Table 8.3. e.g. Calculated release rate =

% mineral$_{\text{fresh rock}}$ x % element mineral x % mineral dissolved / fresh rock

Data in the above table indicate that the amount of aluminium which has actually been lost from the profile is lower than the amount which would appear to be associated with the removal of phases in the calculated proportions. Although the reason for this is not clear, several sources of error can be identified. Firstly, complete separation of the clay from the non-clay fraction may not have been achieved as sonification may not extract all the alteration products, particularly those associated with the centres of relatively unaltered

* after quartz

crystals. The STEM study of the composition of alteration products in such areas indicated that this material is enriched in aluminium, and relatively depleted in Ca, K, and Na relative to the parent phases.

Table 8.4a
Al removed

	BEMBOKA	JINDABYNE	ISLAND BEND
BIOTITE	.3	1.3	.3
K-FELDSPAR	.4	.3	.4
Ca-FELDSPAR	2.5	3.1	3.5
Na-FELDSPAR	1.4	.5	1.1
(OTHER)	.6	-	-
	5.2	5.2	5.3
	5.2wgt%/14wgt% =39% compared with 30% (calculated)	5.2wgt%/14wgt% =37% compared with 30% (calc.)	5.3wgt%/15wgt% =35% compared with 29% (calc.)

Table 8.4b
Si removed

	BEMBOKA	JINDABYNE	ISLAND BEND
BIOTITE	.8	2.5	.8
K-FELDSPAR	1.3	1.1	1.4
Ca-FELDSPAR	5.0	5.9	6.9
Na-FELDSPAR	4.3	1.3	2.9
OTHER	2.5	-	-
	13.9	10.8	12.0
	13.9wgt%/72wgt% =19% compared with 22% (calculated)	10.8wgt%/70wgt% =15% compared with 22% (calc)	12wgt%/70wgt% =17% compared with 24% (calc.)

If the surplus of Al is associated with unextracted clay, the amount of Si actually removed should also be less than that calculated. As shown in Table 8.4b, data indicate the reverse. This observation suggests that some quartz dissolution has occurred. The presence of some Al in unextracted clay can not be ruled out using these data.

The second alternative is that a Ca rich, Al poor phase has been altered. This will strongly affect the estimate of the total Al removed (see Table 8.4a). The third suggestion is that the difference between the estimated and observed rates of Al loss is the net result of the assumptions and associated errors in the calculation.

RESULTS: TRACE ELEMENTS

Many of the trace elements, when plotted as ppm per cm^3 against density, also display straight line trends (Figures 8.4-8.6, 8.9, 8.10, 8.12, 8.13). For these elements a similar calculation of rate of loss can be performed using trace element data for the clay fractions. As in the case of the major elements, the measured rate of loss is a reflection of the rates at which the phases which host these elements weather. These rates of release can not easily be used to calculate the rate of weathering of host phases, as the distribution of each trace element between the host phases is generally not known. Data for the initial rates of release for trace elements are listed in Table 8.5.

TABLE 8.5

Fraction of original trace element released after 25% of the components in the whole rock have been released.

Element	BEMBOKA	JINDABYNE	ISLAND BEND
Ba	.09	.24	.15
Rb	trend unclear	.32	trend unclear
Sr	.72	.29	.26
Zr	.07	.07	trend unclear
Y	follows REE	.27	trend unclear
V	.??	.16	.21
Cr	.??	.24	.22
Pb	.25	.28	.26
Zn	.10*	.42	trend unclear
Nb	? *	.41	.20

*= some gain in the profile as a result of weathering.

As Zr in the granite is hosted in zircon, the release rates listed in the above table reflect the comparatively low tendency of this phase to weather. Data suggest that zircon does release some Zr, displaying a resistance to alteration in the early stages which is apparently only about twice that of K-feldspar. Zirconium is present in the clay fractions of the granites. It would seem unlikely that this is due to the presence of very small crystals of zircon, (<2μm) as the observed size of zircon in the fresh rock is frequently >50μm.

Sr, Ba, and Rb are contained in the feldspars, Rb and Ba are also present in biotite. The behaviour of Sr generally resembles that of Ca, being lost relatively rapidly compared with other components. There is some indication that Sr-feldspar is more resistant to alteration than Ca-feldspar. Rates of Rb and Ba release appear generally similar to those of K. Pb which also presumably replaces K in feldspars and possibly in biotite, appears to be released at a slightly faster rate than K. Zn appears to be contained within biotite, so that its release rates generally reflect the rate of destruction of this phase. V and Cr are commonly hosted by opaque oxide phases, their release rates resemble those of Fe and Mn. This may suggest that the rate of weathering of opaques is broadly similar to that of biotite.

In general it would appear that trace elements are released at rates which are generally similar to the rates of release of the major elements whose sites they occupy. Because the distribution of the trace elements between phases is complex, and as minor phases may control their distribution (and consequently their behaviour during weathering), the significance of measured rates of release for individual trace elements is difficult to determine. Consequently it is not possible to comment on the tendency for phases to preferentially release or retain these components.

THE CHEMISTRY OF THE CLAY FRACTION

The clay minerals have the ability to retain certain of the elements released during weathering. As kaolin and oxides are among the major alteration products of most granitic minerals, elements such as Fe, Mn, and Al should be clearly enriched in the clay sized fraction of the weathered granite. Other less abundant constituents are also enriched in this fraction, presumably by adsorption onto oxides and clay phases, or as constituents of less abundant clay phases. In this section the role that the clay fraction plays in determining the abundances of elements in weathered rock is examined. This has been approached by determining the proportion of the quantity of each component released during weathering which is retained in the clay fraction. An example of the procedure used to determine the results listed in Table 8.6 is given in Appendix 5.

TABLE 8.6

THE PROPORTION OF MAJOR AND TRACE ELEMENTS RELEASED WHICH ARE RETAINED IN CLAYS

ELEMENT	JINDABYNE	BEMBOKA	ISLAND BEND
V	1.00	.57-1.00	.16
Cr	.98	.66	.13
Ni	.70	-	-
Cu	.64	-	-
Zn	.62	added	.26
Tot. FeO	.60	.65	.15
Al_2O_3	.60	.53	.41
La	.57	added	added
TiO_2	.56	.62	.28
Pb	.48	.65	.41
Nb	.48	added	.17
MgO	.48	.24	.15
MnO	.41	.85	.36
Ce	.41	added	.27
Rb	.41	.31	.18
Ba	.32	added	.35
K_2O	(.52-).28	.09	.12
SiO_2	.27	.20	.13
Y	.24	added	added
Sr	.19	.02	<.01
Zr	.18	.19-.80	.13
CaO	.03	.01	<.01

Data are calculated from the averaged results obtained for each of the clay fractions analysed, and not from the general trends used for calculation of extent of release of components.

Data in Table 8.6 clearly indicate the variable degree to which components have been incorporated into the clay fraction. Some very general comments can be made regarding the tendency for elements such as Ca and Sr to be removed in solution, and Al, Ti, Mn, Fe to be retained by the clay fraction. However, even in the three examples above, a considerable range in the extent to which these elements are retained is apparent. Furthermore, is quite clear that although in some cases elements such as V, Cr, and other transition elements are strongly retained by alteration products, this does not occur in all cases.

For an element to be termed immobile it must either be retained in secondary minerals, or be contained in a mineral which does not alter. Clearly no element in the above list is completely retained in the clay fraction of all three profiles, although in individual cases this does appear to occur. There also does not appear to be a mineral in the

granite which does not weather. Although zircon is the most likely candidate, this mineral does appear to undergo some dissolution. The estimation of how mobile a component is becomes more complicated when it can be clearly demonstrated that components derived elsewhere in the profile may be added to the sampled zone. The most obvious examples are the components associated with apatite replacement, the REE, Ba, and Y. In other cases, the abundance (gm/cm^3) of elements in weathered material is only slightly higher than the abundance in fresh granite, possibly as the result of errors in measurements. However, the cases where additions can clearly be demonstrated draw attention to the problem that if components appear to be completely retained in the profile they are considered to have been immobile, yet if the abundance has increased, perhaps to 120%, the component must be described as very mobile. This aspect, combined with the variable degree to which almost all components are observed to be retained in the clay fraction, makes it impossible to nominate an element which can be assumed to have been conserved for use in the interpretation of bulk chemical data.

The range in the ability of the clay fraction to accommodate elements released during weathering is almost certainly due to differences in the nature of the clays which are developed in each profile. The nature of the clay fraction is in turn observed largely to reflect the mineralogy of the granite before weathering commenced. For example, in the Jindabyne profile the unweathered granite contained approximately twice the biotite content of the Island Bend and Bemboka granites. Consequently weathering has resulted in the development of considerably more vermiculite in the Jindabyne profile, and it is this phase which appears to be responsible for the extensive retention of the transition elements. Comparatively small quantities of these components are retained in the Island Bend profile, probably as the result of the dominance of the kaolin minerals in the alteration assemblage. This difference in the nature of weathering products is illustrated in XRD scans presented in Figure 8.15 for the clay fractions of the Island Bend and Jindabyne profiles.

THE NET RESULT: COMPONENTS RELEASED FROM THE PROFILE

The initial rates at which components are released from the profiles can be determined from the trends of straight lines for the bulk chemical data plotted in Figures 8.1-8.1.4 Results have been scaled

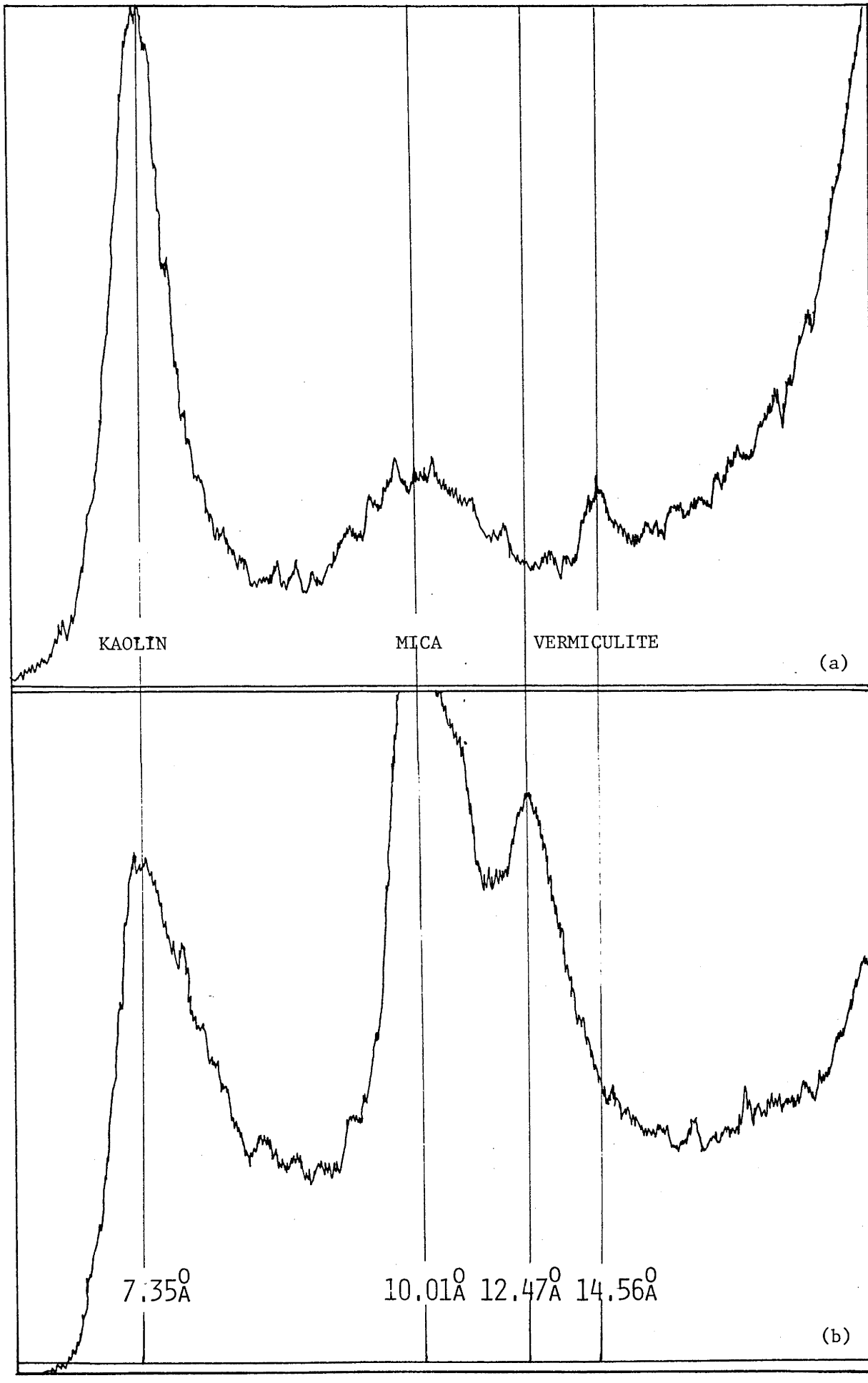

FIGURE 8.15 XRD scans for clay from the (a) Island Bend and (b) Jindabyne profiles. (Tc 4, 4 x 10^2, Co 40/ 20 radiation).

to represent the loss from the profile after 25% of the original components have been released, either to form clays or into solution, and are listed in Table 8.7. These data can then be compared directly with data representing proportions of components released from minerals at this stage (Table 8.3).

TABLE 8.7

PROPORTIONS OF COMPONENTS LOST FROM THE PROFILES AFTER 25% OF THE COMPONENTS IN THE FRESH ROCK HAVE BEEN RELEASED

ELEMENT	BEMBOKA	JINDABYNE	ISLAND BEND
SiO_2	.17	.16	.21
TiO_2	.08	.17	.16
Al_2O_3	.13	.12	.17
Tot. FeO	.08	.14	.15
MnO	<.01	.25	.14
MgO	.19	.20	.19
CaO	.72	.53	.45
Na_2O	.50	.32	.33
K_2O	.12	.18	.19
Ba	*	.15	.09
Rb	?	.20	?
Sr	.72	.29	.26
Zr	.04	.06	?
Y	*	.20	?
V	.00	*	.17
Cr	?	.00	.20
Pb	.10	.13	.16
Zn	*	.14	?
Nb	*	.18	.16

* = material added to the profile overall.
? = data does not exhibit a clear trend.

The results in the above table suggest that the rates at which components are released from the weathering profiles into the environment are relatively similar for many elements, although the proportions of individual components released from their host phases vary to some extent, and the degree to which these components are retained in the clay fraction varies in some cases quite dramatically.

LATER STAGE ALTERATION OF THE PROFILES

The above discussion has concentrated upon the initial stages of weathering when the breakdown of minerals appears to occur at relatively constant rates, and no primary phases have been consumed. Although in

the Jindabyne profile this stage is not exceeded, weathering of the Island Bend and Bemboka profiles has proceeded past the point where effectively all the plagioclase feldspar has been consumed.

In the Bemboka profile, chemical data indicate that destruction of the more calcic plagioclase is associated with a slight increase in the rate at which the more sodic plagioclase alters, followed by the maintenance of the abundance of Na, Ca, and Sr at a constant, low level. The trends for most other elements in the profile remain linear, suggesting that the removal of plagioclase has not resulted in a dramatic modification of the relative rates of weathering of other phases. There is a reduction in the rate of the oxidation of iron at this stage, and a change from addition to loss of bound water, possibly reflecting the replacement of more hydrous clays by kaolinite. This also corresponds to a change from the preferential loss of K relative to Rb to a stage where the relative abundance of these elements remains constant (see Figure 8.4)

Weathering of the Island Bend profile appears to occur initially by breakdown of the major minerals at approximately constant rates. This is followed by a second stage when the relative rate at which plagioclase feldspar is destroyed increases dramatically, resulting in its almost total removal. The effect of this can be observed in the K trend, which indicates that the rates at which biotite and K-feldspar weather have been reduced. The acceleration of the rate of destruction of plagioclase corresponds with a decrease in the extent of oxidation of Fe; the total removal of this mineral is associated with a change from gain to loss of bound water. The final stage of weathering of this profile resembles that of the Bemboka profile in that it is associated with the general resumption of the constant rates of loss of components.

CONCLUSIONS

The way in which the bulk chemistry of the profile changes as weathering proceeds reflects the operation of a number of processes.

1. The composition of weathered material reflects the assemblage of primary phases which remains at any stage. In the profiles examined in this study, this factor appears to exert the greatest control. Because the chemical loss occurs, at least in the initial stages, at constant

rates, it would appear that the relative rates at which minerals in the profile weather remains fairly constant. There is some evidence to suggest that the rate at which plagioclase feldspar is broken may accelerate, possibly with increased access of solution to the structure, before this phase is completely removed.

2. The initial mineralogy of the granite controls the relative abundance and chemistry of secondary phases. In the later stages of weathering the bulk chemistry of the profile reflects to a greater extent the composition of these phases. The nature of this assemblage will control the chemistry of the profile in two ways. Firstly, the minerals which develop incorporate certain elements into their structures, and secondly result in the retention of other components by adsorption. Data indicate that the composition of the clay fraction may vary dramatically between profiles. Vermiculite appears to be associated with a far greater retention of the trace elements, particularly the transition elements in the profile than kaolinite.

3. The composition of the solution which is present during alteration may control the chemistry of the profile. The ability of the solution to remove components released during weathering presumably exerts a strong influence upon the nature of the clays formed, and their abundance. A more difficult effect of solution chemistry to evaluate is the extent to which this phase is capable of introducing into a section of the profile components derived from elsewhere in the weathering granite. Because in a few cases this can be clearly demonstrated to have occurred, the possibility that introduction of other components whose final abundance does not exceed that of the unweathered rock can not be ruled out. This behavior appears to be associated mainly with the trace elements, hence the use of these components in calculations which assume their immobility would appear to be extremely inadvisable. Clearly the data discussed indicate that the assumption that components such as Al, Ti and Zr will be completely retained in the profile can not be made. A conclusion to this study must be that it can not be assumed that any element will remain immobile during weathering. Consequently no component can be used to provide an indication of the extent to which a profile has been weathered.

The bulk chemistry of the profile does not reflect the details of the way in which the weathering of primary minerals occurs, but rather

is the net result of the assemblage of secondary phases which develops, and the composition of the remaining unweathered material.

Chapter 9

CONCLUSIONS

The aim of this thesis has been to achieve an understanding of the mechanism of granite weathering through examination of the detailed processes by which individual minerals in the granite are converted to secondary phases. Conclusions to these studies have been presented in the final sections of Chapters 4-7, and are summarized in Figure 9.1. The net chemical effect of these reactions and the relative rates at which they occur control the bulk composition of the profile.

The weathering of most granitic minerals involves the conversion of the original phase to a sequence of alteration products as weathering proceeds. A number of aspects of these mineral reactions have been examined, including the mechanisms by which structural and chemical modifications occur, and the factors which influence the chemistry and morphology of the phases formed.

An investigation of the mineralogy, structure, and distribution of weathering products has revealed that a reaction may involve crystallization of a secondary phase from solution, such as when halloysite tubes grow into dissolution cavities; direct epitactic growth, such as when kaolinite develops on preexisting sheet silicates; epitactic recrystallization of poorly crystalline or semi-amorphous material, which may be the case when goethite develops in an orientation controlled by the crystallography of enclosing sheets; recrystallization of poorly crystalline, or semi-amorphous material, such as when smectite forms from K-feldspar; or proceed by direct structural modification, such as when biotite is replaced by vermiculite. The major control on the pathway observed is the structure of the parent mineral and of the phase replacing it. Hence, it appears that when the parent phase has a framework structure, such the feldspars, or a chain structure, such as amphibole, the clay mineral can not form directly from it because the parent structure does not contain units which can be readily inherited.

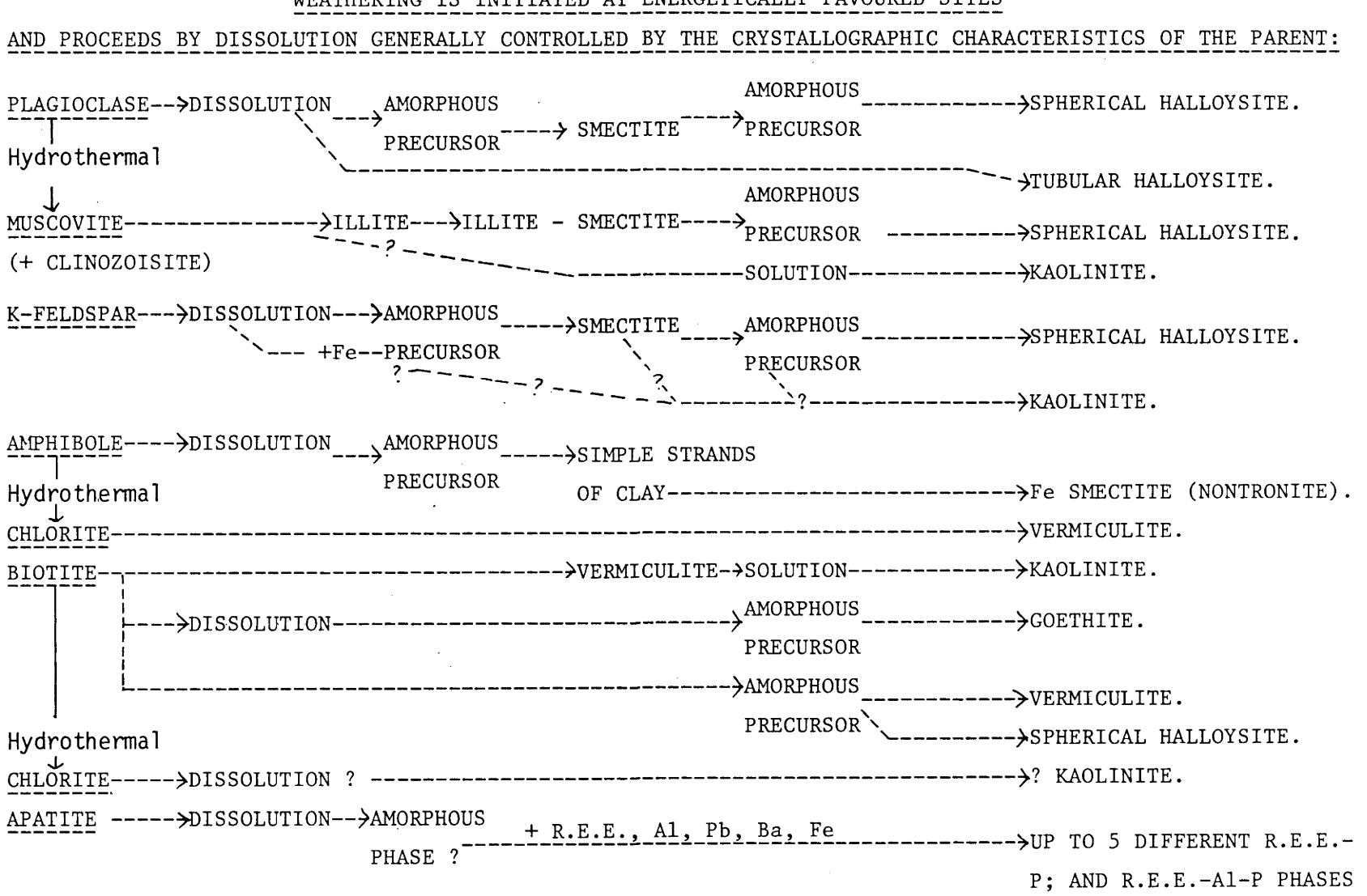
WEATHERING IS INITIATED AT ENERGETICALLY FAVOURED SITES
AND PROCEEDS BY DISSOLUTION GENERALLY CONTROLLED BY THE CRYSTALLOGRAPHIC CHARACTERISTICS OF THE PARENT:
PLAGIOCLASE
Hydrothermal
DISSOLUTION
AMORPHOUS PRECURSOR
SMECTITE
AMORPHOUS PRECURSOR
SPHERICAL HALLOYSITE.
TUBULAR HALLOYSITE.
MUSCOVITE
(+ CLINOZOISITE)
ILLITE
ILLITE - SMECTITE
AMORPHOUS PRECURSOR
SPHERICAL HALLOYSITE.
SOLUTION
KAOLINITE.
K-FELDSPAR
DISSOLUTION
AMORPHOUS PRECURSOR
+Fe
SMECTITE
AMORPHOUS PRECURSOR
SPHERICAL HALLOYSITE.
KAOLINITE.
AMPHIBOLE
Hydrothermal
DISSOLUTION
AMORPHOUS PRECURSOR
SIMPLE STRANDS OF CLAY
Fe SMECTITE (NONTRONITE).
CHLORITE
VERMICULITE.
BIOTITE
VERMICULITE
SOLUTION
KAOLINITE.
DISSOLUTION
AMORPHOUS PRECURSOR
GOETHITE.
AMORPHOUS PRECURSOR
VERMICULITE.
SPHERICAL HALLOYSITE.
Hydrothermal
CHLORITE
DISSOLUTION ?
? KAOLINITE.
APATITE
DISSOLUTION
AMORPHOUS PHASE ?
+ R.E.E., Al, Pb, Ba, Fe
UP TO 5 DIFFERENT R.E.E.-P; AND R.E.E.-Al-P PHASES

FIGURE 9.1

The secondary products tend to develop from an intermediate, semi-amorphous material derived by breakdown of the parent mineral. In contrast, 2:1 sheet silicates structurally resemble 2:1 clay products sufficiently that redistribution, introduction, and removal of components can proceed without complete disaggregation of the original structure. No clear evidence has been observed for the formation of 1:1 sheet silicates such as kaolinite from 2:1 sheet structures. In most cases, the reoganization necessary for this to occur would appear to be too great, and secondary phases crystallize from solution.

This study has demonstrated that weathering of many minerals does involve a semi-amorphous, or poorly crystalline stage. This material generally does not appear to be capable of controlling the breakdown of parent minerals by limiting diffusion. In the case of plagioclase, this component is so rapidly replaced that it is never developed in abundance. In K-feldspar weathering semi-amorphous material is patchily developed so much of the corroded feldspar surface remains exposed to solution. Amphibole alteration products do not appear to form a tightly adhering coating, and are so readily removed that they can not be identified on fragments in grain mount TEM samples.

The mechanism by which crystallization occurs appears to be the single most important factor in determining the morphology of the alteration products. Hence smectite formed by recrystallization of semi-amorphous material developed as small, curved, generally randomly oriented laths. In contrast, the smectite which replaced illite formed large clay laths which pseudomorphed the parent mica. Minerals crystallized epitactically also assume the parent orientation, and may form quite large clay laths, such as in the case of kaolinite. By contrast, spherical halloysite developed from an apparently semi-amorphous, or allophane-like intermediary derived by breakdown of smectite. It is suggested that this form of halloysite may be the result of spherical growth from nucleii in this cell-textured material. Tubular halloysite characteristically developed in dissolution cavities appeared to have crystallized from solution, possibly by spiral growth.

The type of secondary mineral formed is dependent primarily upon two factors: the mineralogy of the parent phase, and the micro-environment in which the reaction occurs. Of these factors, micro-environment appears to be more significant. Hence, smectite is

formed from K-feldspar, K-mica, plagioclase, and amphibole in the initial stages of mineral weathering. At this stage access of solution to the alteration front is very limited, the volume of solution is small, and the composition of the fluid is almost certainly modified by interaction with the surrounding phase. Modification of the micro-environment as weathering proceeds results in replacement of smectite by phases which are stable under the new conditions. Similarly, biotite is replaced by vermiculite in areas where the reaction proceeds slowly, while in areas where access of the fluid is greater, particularly in the later stages of weathering, large areas of biotite are dissolved, and replaced by kaolinite and goethite.

Although the micro-environment appears to be very significant in determining the type of secondary mineral which forms, this factor generally does not play the major role in determining the chemistry of the alteration product. Rather, this is strongly dependent on the chemistry of the mineral from which it is derived. For example, the smectite which replaces Fe-rich, Al-poor amphibole is nontronite, whereas smectites replacing feldspars are relatively Al-rich. Furthermore, the smectites which replace plagioclase, K-feldspar, and K-mica can be clearly distinguished from each other by their chemistry (Figure 9.2).

FIGURE 9.2

Compositions of smectite produced by weathering of Feldspars, Muscovite, and Amphibole.

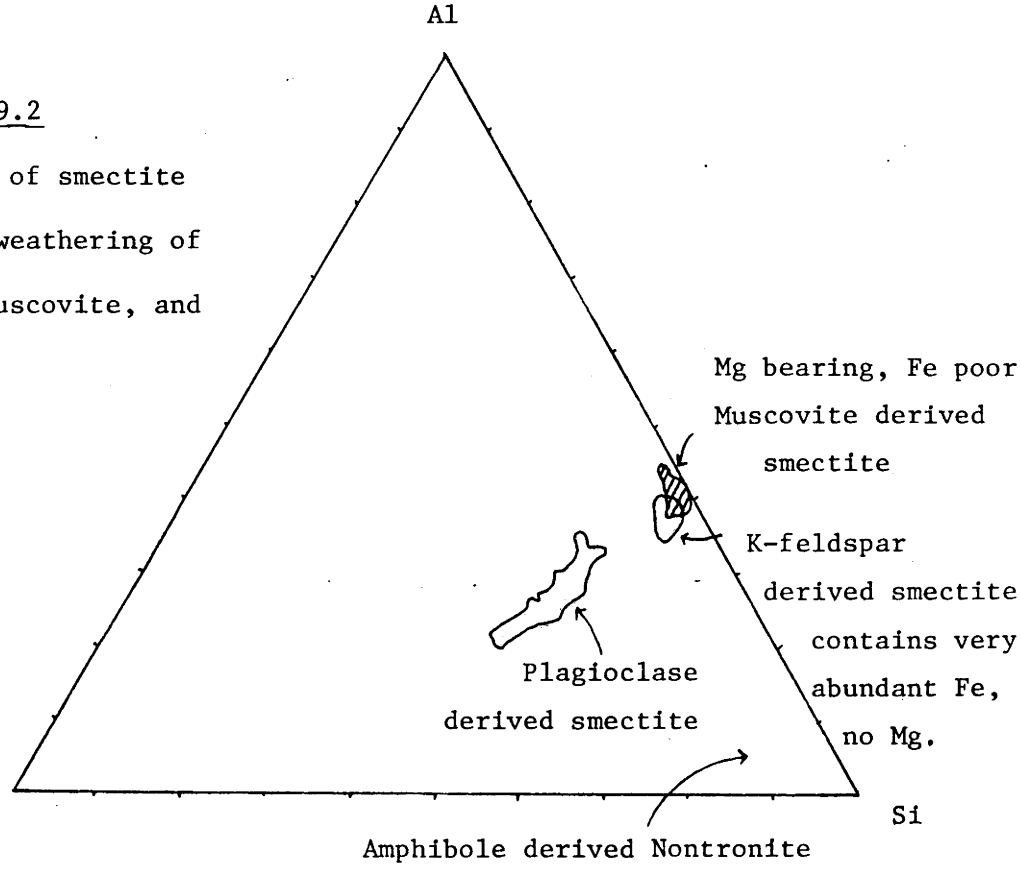

This chemical distinction is preserved when the smectites exist in very close proximity, although the mechanisms by which they crystallize differ. Consequently, in the mineral assemblages studied, weathering is characterised by very small scale equilibrium. This is emphasised by the presence in a single crystal of a range of sequentially developed phases outward from the alteration front.

The final products of the weathering of major minerals in the profiles appear to be kaolinite and oxides. These phases are predicted to be in equilibrium with surface water (see Figure 4.10c, from Loughnan, 1969). This suggests that as the micro-environment changes with improved access of solution, the assemblage approaches equilibrium with surficial conditions.

The pathways of many cations during weathering is more complex than release from the parent phase, retention of elements such as Mg, Fe, Si, Ca, K, (Na) in secondary phases, followed by release of many of these elements from the profile when transitional phases are destroyed. For example, abundant Fe is introduced and incorporated into initially formed, poorly crystalline K-feldspar derived material. The quantity of Fe in the semi-amorphous phase exceeds that which is incorporated into the smectite which crystallizes from it. Some Fe is also introduced into plagioclase derived alteration products, whereas Mg is introduced into muscovite-illite derived alteration products. These observations suggest that weathering reactions of different minerals do not proceed independently of each other. It is not clear whether, for example, the Fe at the K-feldspar reaction front has simply been scavenged by the amorphous component, or whether its presence implies that it may be more directly involved either in the destruction of the feldspar, or recrystallization to form clay. It is clear, however, that individual mineral weathering reactions should not be visualized as independent systems. This factor is generally not recognised in experimental studies.

The weathering of apatite illustrates the involvement of introduced components in secondary phases. Many elements, particularly the REE, are added to the profile studied from elsewhere in the weathering granite. The REE were mobilized and fixed early in weathering by P released from apatite to form a complex and varied range of secondary minerals. These observations again demonstrate that the weathering of a single crystal

can not be considered a discrete process, and illustrate that weathering profiles may represent systems to which components other than meteoric water are added.

The bulk composition of weathered material is a result of original granite mineralogy, the relative rates at which primary minerals weather, and the extent to which released components are retained in secondary phases. In the profiles studied, the major control on composition is the relative weathering rates of phases, particularly in the early stages. The role of transitional phases in determining the bulk profile chemistry is small. These phases are generally developed at the interface between the parent mineral and its stable alteration product, hence are never present in abundance. The bulk chemistry primarily reflects the composition of unweathered phases, and of the final alteration products, it does not clearly reflect the process by which weathering occurs. The ability of the clay sized fraction to host released components, particularly the trace elements was also examined. Results for the three profiles indicate that the extent to which components are retained by clay varies considerably, apparently due to differences in the clay mineral assemblages. Abundant vermiculite in the alteration assemblage is associated with strong retention of minor components, particularly the transition elements, whereas kaolin dominated assemblages contain very low abundances of these components. For an element in a weathering profile to be termed immobile it must be either contained in a mineral which does not weather, or be retained completely by the alteration products. In the profiles studied, results suggest that no mineral can be assumed to be resistant to weathering, and no element is always retained by the clay fraction.

As, at least in the early stages, components are released from the profiles at constant rates, the relative mineral weathering rates can be calculated by subtracting from the bulk composition the effect of retention of elements by the clay fraction. Results for the three profiles indicate that of the major minerals, K-feldspar tends to be most resistant to weathering, while calcic plagioclase is the phase which is most rapidly destroyed. Considerable variability was observed in the calculated weathering rates of the major minerals, possibly reflecting that the extent to which phases weather is dependent upon a number of factors, one of which may be original granite mineralogy.

BIBLIOGRAPHY

Aagaard, P., & Helgeson, H.C., 1982. Thermodynamic and kinetic constraints on reaction rates among minerals and aqueous solutions. I. Theoretical considerations. Am. Journ. Sci., Vol. 282, 237-285.

Anand, R.R., Gilkes, R.J., Armitage, T., & Hillyer, J., (manuscript). The influence of microenvironment on feldspar weathering in lateritic saprolite.

Anderson, A.T., Clayton, R.N., & Mayeda, T.K., 1971. Oxygen isotope thermometry of mafic igneous rocks. J. Geol., Vol. 79, 715-729.

Beams, S.D., 1980. Magmatic evolution of the southeast Lachlan Fold Belt, Australia. Unpubl. Ph.D. Thesis, A.N.U., Canberra.

Berner, R.A., & Holdren, G.R. (Jr), 1977. Mechanism of feldspar weathering. I. Some observational evidence. Geology, Vol. 5, 369-372.

Berner, R.A., & Holdren, G.R., (Jr), 1979. Mechanism of feldspar weathering. II. Observations of feldspars from soils. Geochim. Cosmochim. Acta, Vol. 43, 1173-1186.

Berner, R.A., & Schott, J., 1982. Mechanisms of pyroxene and amphibole weathering. II. Observations of soil grains. Am. Journ. Sci. Vol. 282, 1214-1231.

Blashov, Yu. A., & Kudinov, Yu. A., 1966. Separation of Ce from REE during weathering of calcite parisite from carbonatites. Tr. Mineral. Muz., Akad. Nauk SSSR. Vol, 17, 176-179. (Russian) CA:67(24)110441-k.

Bonnot-Courtois, C., 1980. Behaviour of Rare Earth Elements during submarine weathering and its implications. Chem. Geol., Vol. 31. No. 1-2, 119-131.

Bottinelly, T., 1976. A review of the minerals of the Alunite - Jarosite, Beulandite, and Plumbogummite Groups. J. Res. USGS. Vol. 4, No.2, 213-216.

Bottinga, Y., & Javoy, M. 1973. Oxygen isotope equilibrium between muscovite and water. J. Geophy. Res., Vol. 74, 6012-6022.

Bottinga, Y., & Javoy, M. 1975. Oxygen isotope partitioning among minerals in igneous and metamorphic Rocks. Rev. Geophys. Space Phys., Vol. 13, 401-418.

Brindley, G.W., & Brown, G. (Eds), 1980. Crystal structures of clay minerals and their X-ray identification. Min. Soc. Monograph, No. 5, Min. Soc., London.

Bowles, J.F.W., & Morgan, D.J., 1984. The composition of Rhabdophane. Min. Mag. Vol. 48, 146-148.

Brown, B.E., & Jackson, M.L., 1958. Clay mineral distribution in soils of Northern Wisconsin. Clays and Clay Minerals. Vol. 5, 213-226.

Burkov, V.V., & Podporina, E.K., 1967. Rare Earths in the weathering crusts of granitoids. Dokl. Akad. Nauk SSSR., Vol. 177, No. 3, 691-694. (Russian).

Burnham, C.W., 1975. Water and magmas: A mixing model. Geochim. Cosmochim. Acta. Vol. 39, 1077-1084.

Carroll, D., 1970. Rock Weathering. Plenum Press, N.Y. - London.

Chappell, B.W., & White, A.J.R., 1974. Two contrasting granite types. Pacific Geology, Vol. 8, 173-174.

Churchman, G.T. 1980. Clay minerals formed from micas and chlorite in some New Zealand soils. Clay Minerals, Vol. 15, 59-76.

Churchman, G.J., Whitton, J.S., Claridge, G.G.C., & Theng, B.K.G., 1984. Intercalation method using formamide for differentiating halloysite from kaolinite. Clays and Clay Minerals. Vol. 32, 241-248.

Coleman, N.T., Le Roux, F.H., & Cady, I.G., 1963. Biotite - hydrobiotite- vermiculite in soils. Nature, Vol. 198, 409-410.

Correns, C.W., 1940. Die Chemische Verwitterung der silicate. Naturw, Vol. 28, 369-376.

Correns, C.W., 1963. Experiments on the decomposition of silicates,

and discussion of chemical weathering. Clays and Clay Minerals, Vol. 12, 443-460.

Correns, C.W., & VonEnglehardt, W., 1938. Chemie der Erde, Vol. 12, 1-22. in: Nixon, R.A. 1979.

Delvigne, J., 1965. Pédogenèse en zone tropicale la formation des minéraux secondaires en milieu ferrallitique. O.R.S.T.O.M., Dunod ed. Paris. p 177; in Proust, 1982.

DeVore, G.W.M., 1959. The surface chemistry of feldspars as an influence on their decomposition products. in: Proc. Nat. Conf. Clays and Clay Minerals, 6th Berkley, California. London Permagon Press, 26-41.

Droste, J.B., Battacharya, H., & Sunderman, J.A., 1962. Clay mineral alteration in some Indian soils. Clays and Clay Minerals, Vol. 9, 329-343.

Duddy, I.R., 1980. Redistribution and fractionation of Rare Earth and other elements in a weathering profile. Chem. Geol. 30, 363-381.

Eggleton, R.A., & Banfield, J.F., The alteration of granitic biotite to chlorite. American Mineralogist. Accepted for publication.

Eggleton, R.A., & Boland, J.N., 1982. Weathering of Enstatite to Talc through a sequence of transitional phases. Clays and Clay Minerals, Vol. 30, No. 1, 11-20.

Eggleton, R.A., & Busek, P.R., 1980. High resolution electron microscopy of feldspar weathering. Clays and Clay Minerals, Vol. 28, 173-178.

Eggleton, R.A., & Chappell, B.W., 1978. The crystal structure of Stilpnomelane. Part III: Chemical and physical properties. Min. Mag., Vol. 42, 361-368.

Erberl, D., & Hower, J., 1976. Kinetics of illite formation. G.S.A. Bull. 87, 1326-1330.

Erberl, D., Whitney, G., & Khoury, H., 1978. Hydrothermal reactivity of smectite. Am. Min. Vol. 63, 401-409.

Eswaran, H., & Bin, W.C., 1978. A study of a deep weathering profile on granite in Peninsular Malaysia. III. Alteration of feldspars. Soil Sci. Soc. Am. J., Vol. 42, 154-158.

Exley, C.S., 1976. Observations on the formation of kaolinite in the St Austell granite, Cornwall. Clay Minerals, Vol. 11, 51-63.

Farmer, V.C., Russell, J.D., & McHardy, W.J., 1971. Evidence for the loss of protons and octahedral iron from oxidised biotite and vermiculite. Min. Mag., Vol. 38, No. 294, 121-137.

Faure, G., 1977. Principles of Isotope Geology. John Wiley & Sons, New York.

Ferry, J.M., 1979. Reaction mechanisms, physical conditions, and mass transfer during hydrothermal alteration of mica and feldspar in granitic rocks from south central Maine, USA. Cont. Mineral. Petrol., Vol. 68, 125-139.

Feth, J.H., Roberson, C.E., & Polzer, W.L., 1964. Sources of mineral constituents in water from granitic rocks, Sierra Nevada, California, and Nevada. U.S.G.S. Water Suply Paper, 1531-1, 170.

Field, J. (Manuscript). Weathering and soil formation, New England, NSW. A case study.

Fieldes, M., & Swindale, L.D., 1954. Chemical weathering of silicates in soil formation. J. Sci. Tech. New Zealand, Vol. 56, 140-154.

Frederickson, A.F., 1951. Mechanism of weathering. G.S.A. Bull., Vol. 62, 221-232.

Gardner, L.R., 1983. Models for incongruent feldspar dissolution. Sci. Geol., Mem., 71, Strasbourg, 1983, 55-62.

Gardner, L.R., Kheoruenromne, I., & Chen, H.S., 1978. Isovolumetric

investigations of a buried branite saprolite near Columbia, S.C. Geochim. Cosmochim. Acta., Vol. 42, 417-424.

Gardner, L.R., Kheoruenromne, I., & Chen, H.S., 1981. Geochemistry and mineralogy of an unusual diabase saprolite near Columbia, South Carolina. Clays and Clay Minerals Vol. 29, III, 184-190.

Garrels, R.M., 1984. Montmorillonite/Illite stability diagrams. Clays and Clay Minerals, Vol. 32, No. 3, 161-166.

Gilkes, R.J., & Little, I.P., 1972. Weathering of Chlorite and some associations of trace elements in Permian phyllites in SE Queensland. Geoderma, Vol. 7, 233-247.

Gilkes, R.J., & Suddhiprakarn, A., 1979. Biotite in deeply weathered granite. I.Morphologic, mineralogical and chemical properties. Clays and Clay Minerals, Vol. 27, 349-360. AND: II. The oriented growth of secondary minerals. Clays Clay Minerals, Vol. 27, 361-367.

Greer, R.T., 1970. Submicron unmixing of phases in the feldspar group of minerals as related to growth and optical properties. Proc. 3rd Ann. SEM Symposium. Chicago, 377-384.

Guilbert, J.M., & Sloane, R.L., 1968. Electron optical study of hydrothermal fringe alteration of plagioclase in quartz monzonite, Butte District, Montana. Clays and Clay Minerals, Vol. 16, 215-221.

Gschneidner, K.A. (Jr)., and Eyring, LeRoy, (Eds)., 1979. Handbook on the Physics and Chemistry of Rare Earths. Vol. 3. Non Metalic Compounds. North Holland Publishing Company.

Gusev, G.M., Zanin, Yu. N., Krivolutskaya, L.M., Lemina, N.M., & Yusupov, T.S., 1976. Transformation of Apatite during weathering and leaching. Doklady Akad. Nauk SSSR, Vol. 229, 146-147.

Hanson, G.N., 1980. Rare Earth Elements in petrogenetic studies of igneous systems. An. Rev. Earth & Plan. Sci. 371-406.

Helgeson, H.C., 1971. Kinetics of mass transfer among silicates and aqueous solutions. Geochim. Cosmochim. Acta, Vol. 35, 421-469.

Hemni, T., & Wada, K., 1976. Morphology and composition of allophane. Am. Min. 61, 379.

Hine, R., Williams, I.S., & Chappell, B.W., 1978. Contrasts between I- and S-type granitoids of the Kosciusko Batholith. J. Geol. Soc. Aust., Vol. 25, 219-234.

Hiroji, & Hironma, 1978. D/H ratios of Biotite and Chlorite correlated with their $^{18}O/^{16}O$ ratios. in: Short Papers of the 4th Int. Conf. Geochronology, Cosmochronology, and Isotope Geology. Geol. Survey File Report, 180-182.

Hoefs, J., & Binns, R.A., 1978. Oxygen isotope compositions in Archean rocks from Western Australia, with special reference to Komatiites. in: Short Papers of the 4th Int. Conf. on Geochronology, Cosmochronology, and Isotope Geology. Geol. Survey Open File Report, 180-182.

Holdren, G.R. (Jr), and Berner, R.A., 1979. Mechanism of feldspar weathering. I. Experimental Studies. Geochim. Cosmochim. Acta, Vol. 43, 1161-1171.

Hough, D.J., 1982. Surficial features and landscape features of the Eden - East Gippsland region. Report to Harris - Daishowa (Australia) Pty Ltd. A.N.U., Canberra.

Huang, W.H., & Keller, W.D., 1970. Dissolution of rock forming minerals in organic acids. Am. Min., Vol. 55, 2076-2094.

Hughes, J.C., & Brown, G., 1977. Two unusual minerals from a Nigerian soil: I. Fibrous kaolin; II. Bastnaesite. Clays and Clay Minerals, Vol. 12, 319-329.

Ildefonse, P., Copin, E., Velde, B., 1979. A Soil Vermiculite formed from a Meta-Gabbro, Loire-Atlantique, France. Clay Minerals, Vol. 14, 201-210.

Ildefonse, Ph., Proust, D., Meunier, A., & Velde, B., 1978. Rôle des phènomènes de déstabilisation - recristallisation successifs dans l'alteration des roches crystallines au sein des microsystèms chimiques. Sci. Sol - Bull. AFES. 2-3, 239-257.

Ildefonse, Ph., Proust, D., Meunier, A., & Velde, B., 1978. Rôle de la structure dans l'altération des roches cristallines au sein des microsystèms Mise en évidence de la succession des phénomènes de destabilisation - recristallisation . Sci. Soc.-Bull. AFES, 2-3, 239-257.

James, W.C., Mack, G.H., & Suttner, L.J., 1981. Relative alteration of microline and sodic plagioclase in semi - arid and humid climates. J. Sed. Pet., Vol. 51, No.1, 151-164.

Jayaraman, N., 1940. Alteration of Tremolite to Talc in the dolomitic marbles of Yellandu Warangal District (Hyderbad, Dn). Proc. Indian Acad. Sci., Sect. A 12, 65-71; in Proust, 1982.

Keller, W.D., 1970. Environmental aspects of clay minerals. J. Sed. Petrol., Vol. 40, 788-813.

Keller, W.D., 1977. Scan electron micrographs of kaolin collected from diverse environments of origin. Pt IV; Georgia kaolin; kaolinizing source rocks. Clays and Clay Minerals, Vol. 25, 311-346.

Keller, W.D., 1978. Kaolinization of feldspar as displayed in Scanning Electron Micrographs. Geology, Vol. 6, 184-188.

Keller, W.D., Balgord, W.D., Reesman, A.L., 1963. Dissolved products of artificially pulverised silicate minerals and rocks. J. Sed. Pet., Vol 33, 191-204.

Kholodov, V.N., 1972. Rare Earths in weathering of Kara-Tau phosphorites. Geokhimiya, No. 9, 1063-70. CA:78(22)138833-r.

Kirkman, J.H., 1981. Possible structure of halloysite disks and cylinders observed in some New Zealand rhyolitic tephras. Clay Minerals, Vol. 12, 199-215.

Koicki, S., Koicki, A., & Maksimovic, Z., 1983. Neutron activation analysis of lanthanides in Yugoslav bauxites. Glas. Srp. Akad. Nauka Umet., Od. Prir.- Mat. Nauka. (1980). Vol 46, 37-48. (Serbo-Croation) CA: 96(12) 88761-q.

Krasil'nikov, A.V., 1969. Behaviour of Rare Elements in weathering profiles developed on granitic rocks. Geol. Razedka. 141-142. (Russian) CA:75(14)90186-r.

Kulla, J.B., & Anderson, T.F., 1978. Experimental oxygen isotope fractionation between kaolinite and water. Short Papers of the 4th International Conference Geochronology, Cosmochronology, Isotope Geology. Geol. Survey Open File Report. 78-701, 234-235.

Lagache, M., Wyart, J., Sabatier, G., 1961. Dissolution des feldspaths alcalins dans l'eau pure ou chargee de CO_2 a 200°C. Acad. Sci. Paris., Comptes Rendus, Vol. 253, 2019-2022.

Lawrence, J.R., & Taylor, H.P., 1971. Deuterium and Oxygen 18 correlation: clay minerals and hydroxides in Quaternary soils compared to meteoric Wwater. Geochim. Cosmochim. Acta, Vol. 35, 993-1003.

Leneuf, N., 1959. L'alteration des granites calcoalcalins et dans granodiorites en Côte d'Ivore forestière et les sols qui en sont dérivés. These Science; in Proust, 1982.

Lin, F-C., & Clemency, C.V., 1981. The kinetics of dissolution of muscovites at 25°C and 1 atm. CO_2 partial pressure. Geochim. Cosmochim. Acta, Vol. 45, 571-576.

Lodding, W., 1972. Conditions for the direct formation of gibbsite from K-feldspar. Discussion. Am. Min., Vol. 57, 292-294.

Loughnan, F.C., 1969. Chemical weathering of silicate minerals. American Elsevier Publishing Company Inc.

Luce, R.W., Bartlett, R.W., & Parkes, G.A., 1972. Dissolution kinetics of magnesium silicates. Geochim. Cosmochim. Acta., Vol. 36, 35-50.

Ludden, J.N., & Thompson, G., 1978. Behaviour of Rare Elements during submarine weathering of tholeiitic basalt. Nature, Vol. 274, 147-149.

Lundstrom, I., 1970. Etch pattern and twinning in two plagioclases. Arkiv. Mineralogi och Geologi, Vol. 5, 63-91.

MacDonald, J.A., & Grubb, P.L.C., 1971. Genetic implications of shales in the Brockman iron formation from Mount Tom Price and Wittenoom gorge, Western Australia. Geol. Soc. Aust. J. Vol. 18. Part 1, 81-86.

MacEwan, D.M.C., 1953. Cardenite, a trioctahedral montmorillonoid derived from biotite. Clay Min. Bull. Vol. 2, No. 11, 120-126.

Marshall, C.E., 1962. III. Reactions of feldspars and micas with aqueous solutions. Econ. Geol., 57, 1219-1227.

Marshall, C.E., & McDowell, L.L., 1965. The surface activity of micas. Soil Sci., Vol. 99, 115-131.

McConnell, A.D., 1979. A landscape history of the Wantabadgery Area, New South Wales. Unpubl. MSc Thesis, A.N.U., Canberra.

McKie, D., 1962. Goyazite and Florencite from two African carbonatites. Min. Mag., 33, 281-297.

Meunier, A., & Velde, B., 1976. Mineral reactions at grain contacts in the early stages of granite weathering. Clay Minerals, Vol. 11, 235-240.

Meunier, A., & Velde, B., 1978. Biotite weathering in granites of western France. in: Developments in Sedimentology, 27. International Clay Conference, 1978. Eds. Mortland and Farmer; Elsevier.

Meunier, A. & Velde, B., 1982. Phengitization, sericitization, and potassium beidellite in a hydrothermally altered granite. Clay Minerals, Vol. 17, 285-299.

Milnes, A.R., 1984. Direct evidence for titania mobility in silcretes. Aust. Clay Minerals Soc. 9th Biennial Conference, Canberra, A.C.T. (Poster).

Minato, H., 1981. On the problem of genesis in kaolinite and halloysite by hydrothermal water. J. Min. Soc. Japan, Vol. 13. (Min. Abst. 32, 81-0150).

Mooney, Rose C.L., 1950. X-ray Diffraction study of cerous

phosphate and related crystals. I. Hexagonal modification. Acta Cryst. 3, 337-341.

Morris, D.F.C., Ghariba, A., & Saber, H., 1980. Distribution of Lanthanum, Europium, Germanium, Tin, Phosphorus, and Sulphur in nickeliferous lateritic profiles. Min. Mag. Vol. 43, 816-820.

Murray, H.H., & Leininger, R.K., 1956. Effect of weathering on clay minerals. Clays and Clay Minerals, Vol. 4, 340-347.

Nagasawa, K., & Miyazaki, S.,1976. Mineralogical properties of halloysite as related to its genesis (Abst). in Int. Clay Conf., Abstracts, 223 -224, Univ. Nac. Anton. Mexico., Inst. Geol., Mexico.

Nance, W.B., & Taylor, S.R., 1977. Rare earth element patterns and crustal evolution., II. Archean sedimentary rocks from Kalgoorlie, Aust. Geochim. Cosmochim. Acta., Vol. 41, 225-231.

Nesbitt, H.W., 1979. Mobility and fractionation of Rare Earth Elements during weathering of a granodiorite. Nature, Vol. 279, 206-210.

Nicolas, J., & Sagn, J.P., 1966. Alteration en talc d'une diabase au Sud de Quintin (Côtes - du - Nord). Bull. Gr. Fr. Arg., XVIII, 14, 47-50.

Nixon, R.A., 1979. Differences in incongruent weathering of plagioclase and microline - cation leaching versus precipates. Geology, Vol. 7, 221-224.

Norrish, K., 1968. Some phosphate minerals in soils. in: Trans. 9th Conf. Int. Soil Sci. Soc., Adelaide. 2, Elsevier, N.Y. 713-723.

Norrish, K., 1972. Factors in the weathering of mica to vermiculite. Proc. 1972 Int. Clay Conf., Chairman's Introduction, 419-432.

O'Neil, J.R., & Silberman, M.L., 1974. Stable isotope relations in epithermal Au-Ag deposits. Econ. Geol. Vol. 69, 902-909.

O'Neil, J.R., & Taylor, H.P., 1969. Oxygen isotope equilibrium between muscovite and water. J. Geophys. Res., Vol 74, 6012-6022.

Ojanuga,A.G., 1973. Weathering of biotite in soils of a humid tropical climate. Soil Sci. Soc. Am. Proc., Vol. 37, 644-646.

Parneix, J.C., & Meunier, A., 1982. Les paragenèses de replacement des biotites utilisées comme marqueurs des conditions de température et de composition des fluides dan les altérations hydrothermale et supergène du granite de Mayet- de - Montage (Allier, France). Bull. Mineral. 105, 662-672.

Parry, W.T., & Downey, L.M., 1982. Geochemistry of hydrothermal chlorite replacing igneous biotite. Clays and Clay Minerals. Vol. 30, No. 2, 81-90.

Petrovic, R., 1976. Rate control in feldspar dissolution. I. Study of residual feldspar grains by X-ray photoelectron spectroscopy. Geochim. Cosmochim. Acta, Vol. 40, 537-548. AND II. The protective effect of precipitates. Geochim. Cosmochim. Acta, Vol. 40, 1509-1521.

Petrovic, R., Berner, R.A., & Goldhaber, M.B., 1976. Rate control in dissolution of alkali feldspars. I. Study of residual grains by X-ray photoelectron spectroscopy. Geochim. Cosmochim. Acta, Vol. 40, 537-548.

Podporina, E.K., & Burkov, V.V., 1977. Rare Elements during weathering of biotite pyroxenites. Litol. Polezn. Iskop. No. 4., 39-53. (Russian) CA:88(16) 40029-q.

Podporina, E.K., Lyapunov, C.M., & Sonkin, L.S., 1980. A Study of the fractionation of Rare Earths during the weathering process with the aid of Neutron Activation analysis. in: Mineralogical - Geochemical Studies with the aid of Neuclear Physical Methods. (Russian). 41-46.

Praham, W.E., 1982. Formation of halloysite from feldspar: low temperature artificial weathering versus natural weathering. Clays and Clay Minerals, Vol. 17, 13-22.

Proust, D., 1982. Supergene alteration of metamorphic chlorite in an amphibolite from Massif Central, France. Clay Minerals, Vol. 17, 159-173.

Proust, D., 1982. Supergene alteration of hornblende in an

amphibolite from Massif Central, France. In: Developments in Sedimentology, 35. International Clay Conference, 1981. Eds. H. Van Olphen & F. Veniale, Elsevier.

Proust, D., & Velde, B., 1978. Beidellite crystallization from plagioclase and amphibole precursors. Local and long range equilibrium during weathering. Clay Minerals, Vol. 13, 199-209.

Rausell-Colom, J., Sweatman, T.R., Wells, C.B., & Norrish, K., 1965. Studies in the artificial weathering of mica. Proc. 11th Easter School Agr. Sci., 40-72. University of Nottingham. Experimental Petrology. Butterworth, London.

Reesman, A.L. & Keller, W.D., 1965. Calculation of apparent standard free energies of formation of six rock forming silicate minerals from solubility data.

Rimsaite, J., 1975. Natural alteration of mica and reaction between released ions in mineral deposits. Clays and Clay Minerals, Vol. 23, 247-255.

Rimsaite, J., 1976. Natural amorphous materials, their origin and identification procedures. in Developments in Sedimentology, 27. Int. Clay Conf., 1978. Eds. M. M. Mortland, V.C. Farmer, 567-576.

Rimsaite, J., (1982). The leaching of radionucleides and other ions during alteration and replacement of accessory minerals in radioactive rocks. Pap. Geol. Survey, Canada, 82-1B, 253-266.

Robertson, H.E., & Lahann, R.W., 1981. Smectite to illite conversion rates. Effects of solution chemistry. Clays and Clay Minerals, Vol. 29, No.2, 129-135.

Ronov, A.B., Blashov, Yu. A., & Migdisov, A.A., 1967. Geochemistry of Rare Earths in the sedimentary cycle. Geokhimiya, 1., 3-19. (Russian) CA:66(14)57924 -w.

Ross, G.J., 1975. Experimental alteration of Chlorites into Vermiculites by chemical oxidation. Nature, Vol. 255, 133-134.

Sales, R.H., & Meyer, C., 1948. Wall rock alteration at Butte, Montana: Am. Inst. Min. Eng. Mining Tech. Publ. 2400, 25. (quoted in Parry and Downey, 1982).

Schott, J., Berner, R.A., & Sjoberg, L., 1981. Mechanism of pyroxene and amphibole weathering. I. Experimental Studies of Iron-free Minerals. Geochim. Cosmochim. Acta, Vol. 45, 2123-2135.

Schultz, L.G., Shepard, A.O., Blackman, P.D., & Starky, H.C., 1971. Mixed layer Kaolinite - Montmorillonite from the Yucatan Peninsular, Mexico. Clays and Clay Minerals, Vol. 19, 137-150.

Shau, M., & Henderson, J.B., 1983. Archean chemical weathering at three localities in the Canadian Shield. Precambrian Res., Vol. 20, 2-4, 189-224.

Shieh, Y.N., & Schwarcz, H.P., 1974. Oxygen isotope studies of granite and migmatite, Grenville Province of Ontario, Canada. Geochim. Cosmochim. Acta, Vol. 38, 21-45.

Siefert, K.E., 1967. Electron microscopy of etched plagioclase feldspars. Am. Ceramics Soc. Journal, Vol. 50, 60.

Staatz, M.H., Shaw, V.E., & Wahlberg, J.S., 1972. Occurrence and distribution of Rare Earths in the Lemhi Pass thorium veins, Idaho and Montana. Econ. Geol., Vol. 67, 72-82.

Stephen, I., 1952. A Study of Rock Weathering with reference to the Soils of the Malvern Hills. II. Weathering of Appinite & Ivy Scar Rock. J. Soil Sci. Vol. 3, 219-237.

Stoch, L., & Sikora, W., 1976. Transformation of micas in the process of kaolinization of granites and gneisses. Clays and Clay Minerals, Vol. 24, 156-162.

Stringham, B.F., & Taylor, A., 1950. Nontronite at Bingham, Utah. American Mineralogist. Vol. 35, 1060-1066.

Sudo, T., & Shimoda, S., 1978. Clays and Clay Minerals of Japan. Kodansha Ltd, Tokyo.

Tardy, Y., Bocquier, G., Parquet, H., & Millot, G., 1973. Formation of clay from granite and its distribution in relation to climate and topography. Geoderma, Vol. 10, 271-284.

Taylor, H.P. (Jr)., 1974. The application of oxygen and hydrogen isotope studies to problems of hydrothermal alteration and ore deposition. Econ. Geol., Vol. 69, 843-883.

Taylor, R.M., 1984. Rapid formation of crystalline double hydroxyl salts and other compounds by controlled hydrolysis. Manuscript, submitted to Clays and Clay Minerals.

Tazaki, K., 1978. Micromorphology of halloysite produced by weathering of plagioclase in volcanic ash. in: Developments in sedimentology, Vol. 27. International Clay Conference. M.M. Mortland, & Farmer, V.C., (Eds) Elsevier.

Tazaki, K., 1978. Analytical electron microscope studies of halloysite formation processes. Morphology and composition of halloysite. in: Developments in Sedimentology, Vol. 27, Int. Clay Conf.. M.M. Mortland and V.C. Farmer, (Eds). Elsevier.

T'Serstevens, A., Rouxhet, P.G., & Herbillon, A.J., 1978. Alteration of mica surfaces by water and solutions. Clays and Clay Minerals, Vol. 13, 401.

Tsuzuki, Y., & Kawabe, I., 1983. Polymorphic transformations of kaolin minerals in aqueous solutions. Geochim. Cosmochim. Acta, Vol. 47, 59-66.

Urrutia Fucugauchi, J., 1979. Effects of low temperature seafloor weathering on the Rare Earth Elements of tholeiitic basalts. Geofis. Int. Vol. 18, No. 4, 385-394.

Velbel, M.A., 1983. A dissolution - reprecipitation mechanism for the pseudomorphous replacement of plagioclase feldspar by clay minerals during weathering. Svi. Geol. Mem., 71, Strasbourg, 1983, 139-147.

Vlasov, K.A. (Ed.), 1966. Geochemistry and Mineralogy of Rare Elements and genetic types of their deposits. Vol. III, Mineralogy of

the Rare Elements. Translation Z. Lerman. Israel Program for Scientific Translations. Jerusalem.

Walker, G.F., 1949. The decomposition of biotite in the soil. Min. Mag., Vol. 28, 693-703.

Walker, P.H., & Coventry, R.J., 1976. Soil profile development in some alluvial deposits of eastern New South Wales. Aust. J. Soil Res., Vol 14, 305-317.

Walker, P.H., & Hutka, J., 1979. Size characteristics of soils and sediments with special reference to clay fractions. Aust. J. Soil Res., 17, 383-404.

White, A.J.R., Williams, I.S., & Chappell, B.W., 1977. Geology of the Berridale 1:100,000 Sheet 8625. Geol. Survey of N.S.W. Dept. Mines.

Wilke, B.S., Schwertmann, U., & Murad, E., 1978. An occurrence of polymorphic halloysite in granite sapprolite of the Bayerischer Wald, Germany. Clay Minerals, Vol. 13, 67-77.

Wilson, M.J., 1966. The weathering of biotite in some Aberdeenshire soils. Min. Mag., Vol. 35, 1080-1093.

Wilson, M.J., 1970. A study of weathering in a soil derived from a biotite -hornblende rock. I, Weathering of biotite. Clay Minerals, Vol. 8, 291-303.

Wilson, M.J., Bain, D.C., & McHardy, W.J., 1971. Clay mineral formation in deeply weathered boulder conglomerate in northeast Scotland. Clays and Clay Minerals, Vol. 19, 345-352.

Wolfendon, E.B., 1965. Geochemical behaviour of trace elements during bauxite formation in Sarawak, Malaysia. Geochim. Cosmochim. Acta., Vol. 29, 1051-1062.

Wollast, R., 1967. Kinetics of the alteration of K-feldspar in buffered solutions. Geochim. Cosmochim. Acta, Vol. 31, 635-648.

APPENDIX A

PAPER SUBMITTED TO

GEOCHIMICA ET COSMOCHIMICA ACTA

AS A LETTER.

1985

SOURCE ROCK WEATHERING: A MECHANISM FOR RESIDUAL MONAZITE IN S-TYPE GRANITES

Wayne N Sawka

Jillian F Banfield

and

Bruce W Chappell

Geology Department

The Australian National University

Canberra, ACT

ABSTRACT

The S-type granite suites comprising more than a quarter of the extensively developed granites in the Lachlan Fold Belt, Australia, contain ubiquitous residual monazite related to the chemical weathering of the sedimentary source rocks. We report a process whereby chemical weathering fixes mobile rare-earth elements (REE) in hydrous phosphate phases of such as florencite and rhabdophane. This material contains up to 50wt% LREE and occurs as very small particles (~3μm). Dehydration of these hydrous REE phases during anatexis directly yields monazite. The low solubility of phosphorous in S-type granite melts inhibits dissolution of both monazite and apatite. Refractory monazite is thus entrained and transported in S-type granites similarly to inherited zircon. Since both Th and the light REE are major components in monazite, materials containing this minute phase may be of widespread geochemical significance in both granites and metamorphic rocks.

INTRODUCTION

The S-type granite suites of the Lachlan Fold Belt, Australia, are considered to have been derived from a largely sedimentary source material (Chappell and White, 1974). Compositionally equivalent S-type suites of ash flow tuffs also occur within this region (Wyborn et al., 1981). Many geochemical characteristics of these S-type suites are attributed to weathering of the sedimentary source materials (White and Chappell, 1983). The production of clays during the weathering cycles causes fractionation of both major and trace elements. On weathering K and Rb are retained by clays, whereas Na, Ca and Sr are lost in solution. Clays incorporate Cr and Ni during weathering so these elements are also retained in the sedimentary source. This overall weathering process increases Al relative to Na+ K+Ca, thus causing source materials to be peraluminous.

The recent experimental demonstration of the low accessory mineral solubilities in granite melts (Harrison and Watson, 1984; Watson and Harrison, 1983) is particularly relevant to S-type granites. Zircon has been known to be a residual phase in S-type granites from inherited U-Pb ages (Williams, 1977; Williams et al., 1984). Yet due to the rapid diffusion rates in the phosphate accessory minerals (Harrison and Watson, 1984 and pers. comm. Bob Rapp, 1985), inherited ages are not preserved in those minerals. Both apatite and monazite are likely to be refractory phases in S-type granites and residual source materials. The high concentrations of Th and LREE in monazite makes this mineral extremely important

geochemically as a residual phase. Monazite could be incorporated into S-type source regions initially as heavy mineral sands. Even though the process might be reasonable, widespread and regionally significant occurrences are doubtful. We find that the widespread occurrence of monazite in S-type granites is related to the weathering cycle of the source rocks.

Weathering as a cause of widespread monazite in peraluminous granites and refractory source regions and also metasedimentary rocks is of potential global significance to heat flow (Sawka and Chappell, 1985; Chappell and Sawka, 1984) and other trace element processes, involving REE.

REE DURING WEATHERING

Scanning electron microscope (SEM) observations of unweathered through to strongly weathered granite samples demonstrate that apatite is rapidly etched, and chemically transformed by loss of Ca and addition of Al, Ba, Pb, Fe and REE (Banfield, 1985; Banfield and Eggleton, 1984). This process is responsible for REE fixation after mobilisation and migration as a result of weathering. This process occurs early in weathering, after which these elements remain immobile. The net result is to enrich the weathering profile in all REE without substantially changing the relative abundances of these components. With the exception of Ce which remains immobile as Ce^{4+} under oxidising conditions, the replacement of apatite concentrates most REE to a similar extent. The lack of overall fractionation is

interpreted to indicate that elements were introduced from elsewhere in the weathering profile, and are not from an external or foreign source.

The weathered samples contain a number of phases which have formed in pits after apatite, and as rinds on relict apatite crystals. These phases have developed a range of distinctive morphologies, including 'donut'-shaped objects (about 3μm in diameter), ropes and chains of donuts, platelets, and a variety of crystallites (Plates 1A and 2B). Quantitative wavelength dispersive microprobe analyses indicate that at least three quite distinct REE fractionation patterns could be identified within this material (Banfield, 1985).

The donuts and alteration rims are composed of poorly crystalline material, and larger radiating crystals of florencite, $[(LREE)Al_3(PO_4)_2(OH)_6]$. Two varieties of florencite have been identified, distinguished by their LREE fractionation patterns. One of the chondrite-normalised REE patterns is La-rich, with a strong negative Ce anomaly, whereas the other has a gently sloping LREE enriched pattern (Figure 1A). A commonly encountered form of hexagonal crystallites were identified using electron diffraction patterns and energy dispersive analyses as Nd-rich rhabdophane, $[(LREE)PO_4 \cdot H_2O]$, a hydrous form of monazite (Vlasov, 1966). A second form of crystals with a prismatic form contain about 50wt% REE and have a horizontal chondrite-normalised LREE pattern with a strong negative Ce anomaly (Figure 1B).

Clearly the range in both morphology and chemistry of phases replacing apatite is immense. Complete details of this weathering process are presented elsewhere (Banfield, 1985; Banfield and Eggleton, 1984). The fixation of REE in phosphate phases is apparently not an isolated phenomenon. Such phases are common in soils and sandstones throughout the world (Vlasov, 1966; Pettijohn et al., 1973; Burkov and Podlorina, 1967).

The hydrous REE phosphate phases adhere strongly to host phases, normally biotite. Thus, upon dispersal by sedimentary processes these phosphate phases should be deposited with the host sand grains. The other source for phosphates in sedimentary rocks is thought to be mainly organic, bone and shell fragments etc. (Pettijohn et al., 1973).

S-TYPE GRANITES

Phosphorous saturation is low in felsic and intermediate melts and suggests a high potential for residual phosphate phases after anatexis (Harrison and Watson, 1984). Apatite is now thought to be a common refractory phase in both I- and S-type granites (op cit.). The S-type granites on average contain sufficient concentrations of P_2O_5 (Figure 2), to exceed the saturation limit of the melt. Therefore, unmelted phosphate phases may be transported from the source region in many S-type granites.

We propose that REE phosphate weathering products are incorporated into S-type granites to become residual monazite. Compositional variations that distinguish between S-type granite suites reflect differences in the sedimentary source materials. The Bullenbalong and Dalgety suites are well characterised and contrasting examples of such source related variations (Chappell, 1984). The fractionation displayed by these S-type granites is thought to occur largely through the unmixing of refractory source material and melt (op. cit.). Therefore, the most mafic S-type granites contain the most refractory material, including monazite. It is the mafic S-type granites which typically contain the greatest La concentrations as shown for the two suites in Figure 3. Clearly such La enrichment in mafic S-type granites is evidence for the existence of monazite early in the magma fractionation.

In I-type granites, monazite is restricted in its occurrence to the most felsic varieties (Williams et al., 1983) whereas it is ubiquitous in S-type granites (Williams, 1977). The absence of monazite from mafic I-type granites high in P_2O_5 may be due to either reaction to apatite in the melt, or source rock effects. Since I-type granite source rocks do not go through a weathering cycle it is consistent that these rocks do not contain early or residual monazite, even though the apatite may be refractory. Monazite that occurs in felsic I-type granites is apparently related to a low Ca melt activity (Green and Pearson, 1984) and therefore is not an early crystallising phase.

DISCUSSION

The rate-limiting-step in apatite dissolution is phosphate diffusion away from the dissolving crystal (Harrison and Watson, 1984). For monazite, dissolution is governed by the slow diffusion of both phosphorous and the REE (pers. comm., Bob Rapp, 1985). Therefore both these phosphate phases will be insoluble once the melt is saturated with P_2O_5.

Rhabdophane dehydrates to monazite at about 400°C (Vlasov, 1966). Due to slow diffusion rates of P_2O_5 and REE in the melt, florencite may react to monazite in a similar manner by the exclusion of both Al and water.

It would seem that these REE-rich phosphate phases must be present before anatexis occurs to produce monazite in this manner. The low melt activities of REE compared to Ca during anatexis would probably inhibit direct monazite crystallisation, with most melt P_2O_5 going into apatite formation. The lack of inherited ages in phosphate phases does not necessarily indicate direct magmatic crystallisation but rather re-equilibration with the melt. Diffusion rates for REE^{3+} in apatite are relatively fast compared to the time scale for anatexis (Harrison and Watson, 1984). Similar or more rapid diffusion rates probably also apply to radiogenic Pb^{2+} in monazite and apatite due to the change in charge balance and/or ionic radius from that of the parent isotope.

In the Koetong S-type granite suite, Price (1983) found that schistose, granular biotite-rich and quartzite inclusions all contained higher REE concentrations than in the host granite. Monazite was cited as a possible explanation for the high REE abudances within these inclusions. Certainly it is consistent with our weathering model that these sedimentary, and probably restite, inclusions contain minute monazite crystals from the chemical weathering cycle.

In the felsic S-type Sweetwater Wash pluton, California, monazite was identified as a ubiquitous phase that controls the whole rock light REE variations (Miller et al., 1980; Mittlefehldt, 1983). Monazite was argued to be a liquidus phase throughout crystallisation of the pluton (op. cit.), but not a residual phase. However, the occurrence of monazite in the Sweetwater Wash pluton is precisely what would be expected for residual monazite from weathering. The most abundant site for monazite in the pluton is in biotite, which is also the main site for REE-rich phosphates produced by weathering. Monazite is also included in all other phases, suggesting that it may have been, as predicted, insoluble in the peraluminous melt. All monazite grains are extremely minute in the pluton, as are the hydrous forms produced during weathering. The changing REE composition of monazite with whole rock fractionation was implied to indicate early and continuous crystallisation from the melt (op. cit.). However, the minute size of these crystals combined with the rapid REE diffusion rates (pers. comm., Bob Rapp, 1985) could certainly cause REE variations by re-equilibration in the melt. As noted by Mittlefehldt and Miller (1983), the extremely low melt concentrations (activities)

of REE should tend to inhibit early monazite crystallisation. Both residual and magmatic monazite could be present in the Sweetwater Wash pluton, however, magmatic monazite should only occur as a late crystallising phase, when the melt REE activity begins to approach the calcium activity. It is predictable from kinetic considerations that unless the melt calcium activity is low, apatite would probably crystallise from the melt rather than monazite.

The LREE fractionation trends in the peraluminous South Mountain batholith, Nova Scotia (Muecke and Clarke, 1981) are typical of those expected with residual monazite. There appears little doubt that monazite is an extremely common and frequently overlooked phase (Mittlefehldt and Miller, 1983) in peraluminous granites.

The chemical weathering of source rocks appears to provide a consistent model for the ubiquitous occurrence of monazite in S-type granites. It is beyond the scope of this letter to cite all the potential implications of monazite as a widespread residual phase. However, partial melting will tend to concentrate phosphorous in residual materials (Watson and Capobianco, 1981). Thus, refactory monazite may be an important site for deep crustal radioactive heat production (Sawka and Chappell, 1985), heavy isotopes and decay products of Th and Nd, and REE in any rocks which have undergone a chemical weathering cycle.

Certainly much additional research is needed to fully test and understand the implications of the process. The submicroscope size of

the REE phosphate weathering phases will make common identification difficult. Yet, if some of the original REE-Th concentrations are preserved it may be possible to demonstrate such REE-rich weathering products in both granites and high-grade metamorphic rocks. Clearly, the stability and partitioning characteristics of monazite will be of critical importance in assessing the role of this residual phase in crustal evolution.

ACKNOWLEDGEMENTS

We thank T. M. Harrison for useful discussions and making us aware of B. Rapp's current experimental work at SUNY Albany. Research for this paper was supported by an Australian National University PhD and MSc scholarship to WNS and JFB respectively. We also thank N. Ware of the Research School of Earth Sciences for assistance with REE microprobe analyses. Thoughtful reviews of this manuscript were kindly provided by I. S. Williams, C. Johnson, M. T. McCulloch, R. L. Rudnick and D. Wyborn.

REFERENCES

BANFIELD, J. F., 1985: Mineralogy and chemistry of granite weathering. MSc Thesis, Australian National University, Canberra.

BANFIELD, J. F. and EGGLETON, R. A., 1984: The fixation of mobile REE during weathering by replacement of apatite. In: Geosciences in the Development of Natural Resources. Geol. Soc. Aust., Abst. 12, p. 51-52.

BURKOV, V. V., and PODLORINA, E. K., 1967: Rare earths in the weathering crusts of granitoids. Dokl. Akad. Nauk SSSR, 177, No. 3, 691-694 (In Russian).

CHAPPELL, B. W., 1984: Source rocks of I- and S-type granites in the Lachlan Fold Belt, southeastern Australia. Phil. Trans. R. Soc. Lond., Vol. A310, p. 693-707.

CHAPPELL, B. W., and WHITE, A. J. R., 1974: Two contrasting granite types. Pac. Geol., 8, p. 173-174.

CHAPPELL, B. W., and SAWKA, W. N., 1984: Vertical distribution of radioactivity in different types of granite crust: implications to heat flow in the Sierra Nevada batholith, USA and the Lachlan Fold Belt, Australia. Geol. Soc. Amer. Abst. with Prog., Vol. 16, No. 6, p.468.

GREEN, T. H., and PEARSON, N. J., 1984: Stability of REE-acceptor minerals at high pressures and temperatures. In: Geoscience in the Development of Natural Resources. Geol. Soc. Aust., Abst. No. 12, 197-199.

HARRISON, T. M., and WATSON, E. B., 1984: The behaviour of apatite during crustal anatexis: equilibrium and kinetic considerations. Geochim. et Cosmochim. Acta, Vol. 48, p. 1467-1477.

MITTLEFEHLDT, D. W., and MILLER, C. F., 1983: Geochemistry of the Sweetwater Wash Pluton, California: implications for 'anomalous' trace element behaviour during differentiation of felsic magmas. Geochim. et Cosmochim. Acta, Vol. 47, p. 109-124.

MUECKE, G. K., and CLARKE, D. B., 1981: Geochemical evolution of the South Mountain batholith, Nova Scotia: rare-earth-element evidence. Can. Mineral., Vol. 19, p. 133-146.

PETTIJOHN, F. J., POTTER, P. E., and SIEVER, R., 1973: Sand and Sandstone. Springer-Verlag, New York, 618p.

PRICE, R. C., 1983: Geochemistry of a peraluminous granitoid suite from north-eastern Victoria, South-eastern Australia. Geochim. et Cosmochim. Acta, Vol. 47, p. 31-42.

SAWKA, W. N., and CHAPPELL, B. W., 2985: The distribution of radioactive heat production in I- and S-type granites and residual source regions: implications to high heat flow areas in the Lachlan Fold Belt, Australia. Aust. J. Earth Sci. (submitted).

VLASOV, K. A., 1966: Geochemistry and mineralogy of rare elements and genetic types of their deposits. In: Mineralogy of Rare Elements, Volume 2. Israel Program for Scientific Translations Ltd., Jerusalem, p. 293-297.

WATSON, E. B., and HARRISON, T. M., 1984: Accessory mineral phases and the geochemical evolution of crustal magmatic systems: a summary of and prospectus of experimental approaches. Phys. Earth. Planet. Inst., Vol. 35, No. 1-3, p. 19-30.

WATSON, E. B., and HARRISON, T. M., 1983: Zircon saturation revisited: temperature and compositional effects in a variety of crusal magma types. Earth Planet. Sci. Lett., 64, p. 295-304.

WHITE, A. J. R., and CHAPPELL, B. W., 1983: Granitoid types and their distribution in the Lachlan Fold Belt, southeastern Australia. Geol. Soc. Amer., Mem. 159, p. 21-34.

WHITE, A. J. R., and CHAPPELL, B. W., 1977: Ultrametamorphism and granitoid genesis. Tectonophysics, 43, p. 7-22.

WILLIAMS, I. S., COMPSTON, W., and CHAPPELL, B. W., 1983: Zircon and monazite U-Pb systems and the histories of I-type magmas, Berridale Batholith, Australia. Jour. Petrol., Vol. 24, Pt. 1, p. 76-97.

WILLIAMS, I., 1977: The Berridale Batholith: a lead and strontium isotope study of its asge and origin. PhD Thesis, Australian National University, Canberra.

WYBORN, D., CHAPPELL, B. W., and JOHNSON, R. M., 1981: Three S-type volcanic suites from the Lachlan Fold Belt, Southeast Australia. Jour. Geophys. Res., Vol. 86, No. 11, p. 10335-10348.

FIGURE CAPTIONS

Figure 1A Chondrite normalised REE plots of the compositional type ranges of florencite.

Figure 1B Chondrite normalised REE plot of the compositional range of prismatic crystallites.

Figure 2 Harker variation diagram for 316 S-type granite samples from the Lachlan Fold Belt, Australia (published and unpublished data of B. W. Chappell). Dashed line is a least squares fit to all data. It should be noted that the P_2O_5 saturation limit is dependent on melt temperature and silica content (Harrison and Watson, 1984). In a granite magma crystal mush, actual melt compositions will probably be more silica-rich than the whole rock compositions which solidify (Chappell, 1984).

Figure 3 Harker variation diagram for La in the Dalgety (solid) and Bullenbalong (open) S-type granite suites. The decreasing La concentration with fractionation is attributed to restite unmixing of monazite. Total iron provides a better differentiation index for S-type granites (Chappell, 1984). However, silica is used here for simplicity (Data source as in Figure 2).

PLATE CAPTIONS

Plate 1 A hexagonal pit in biotite containing a central core of unaltered apatite which is rimmed by a florencite weathering product. Donut-shaped aggregates of this material adhere to the RHS of the pit wall.

Plate 2 Crystals of rhabdophane which formed by replacement of a euhedral apatite crystal in biotite.

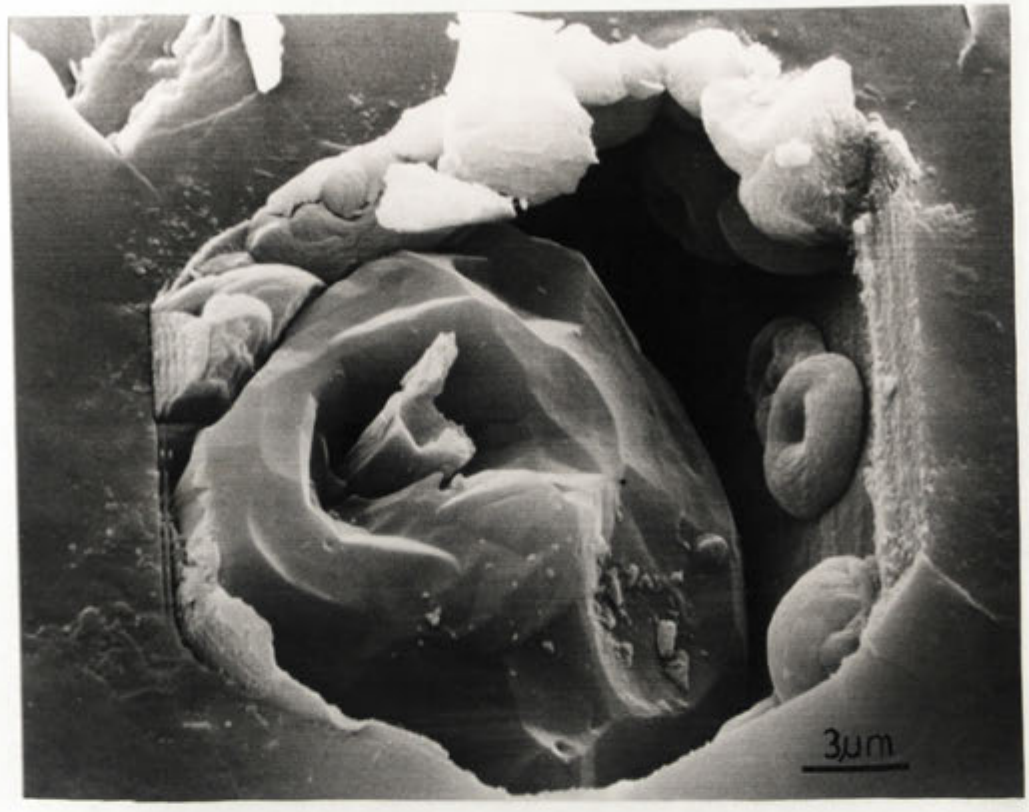

PLATE 1.

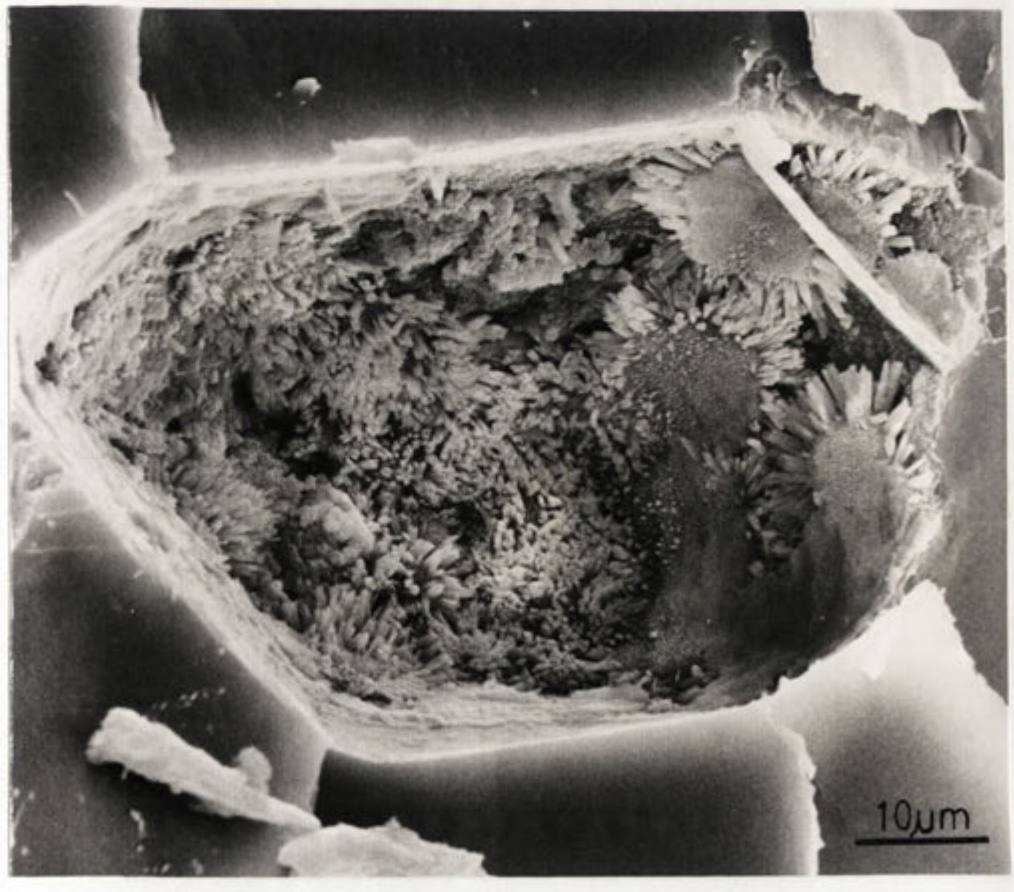

PLATE 2.

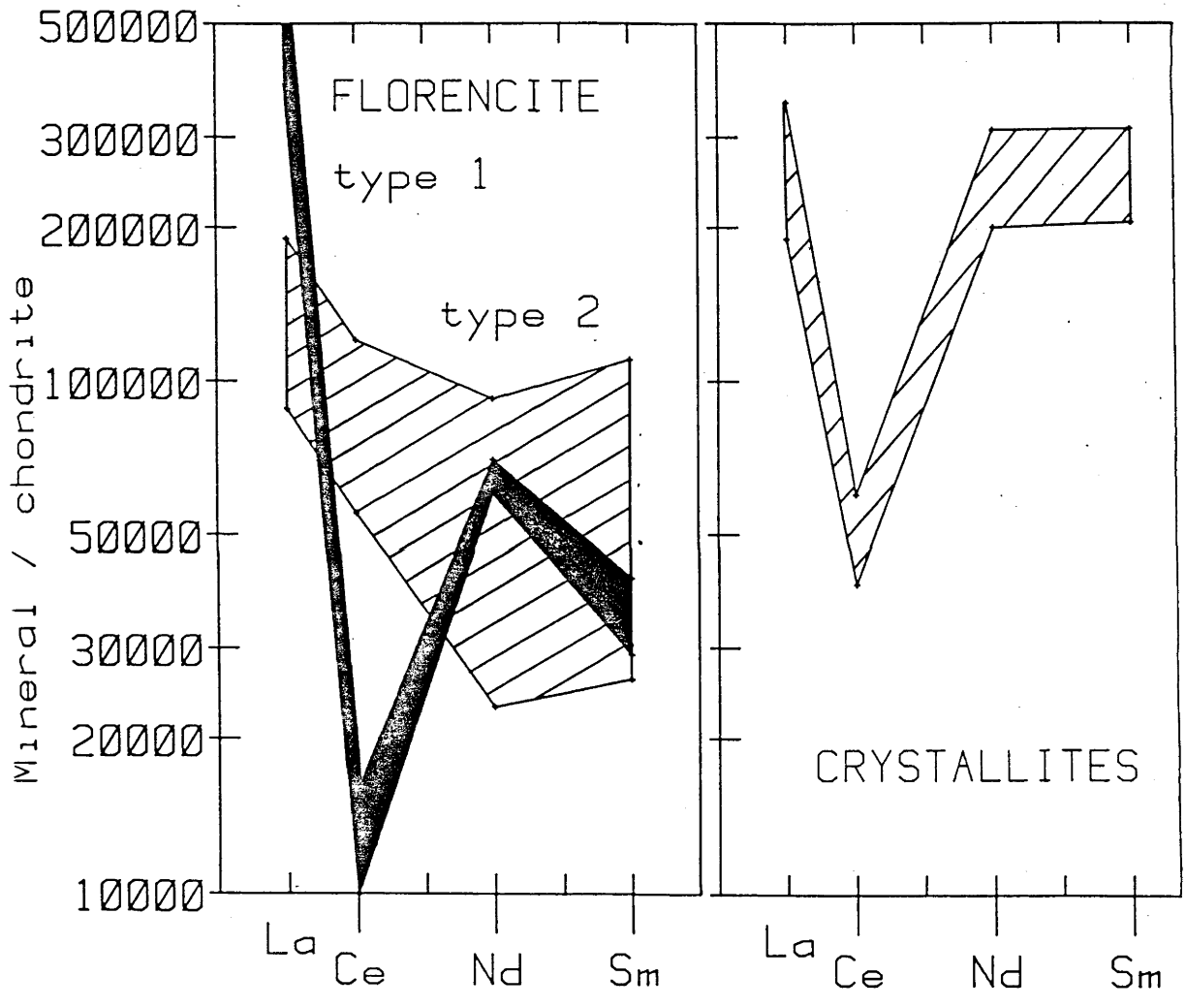
500000
300000
200000
100000
50000
30000
20000
10000
Mineral / chondrite
FLORENCITE
type 1
type 2
CRYSTALLITES
La
Ce
Nd
Sm
La
Ce
Nd
Sm

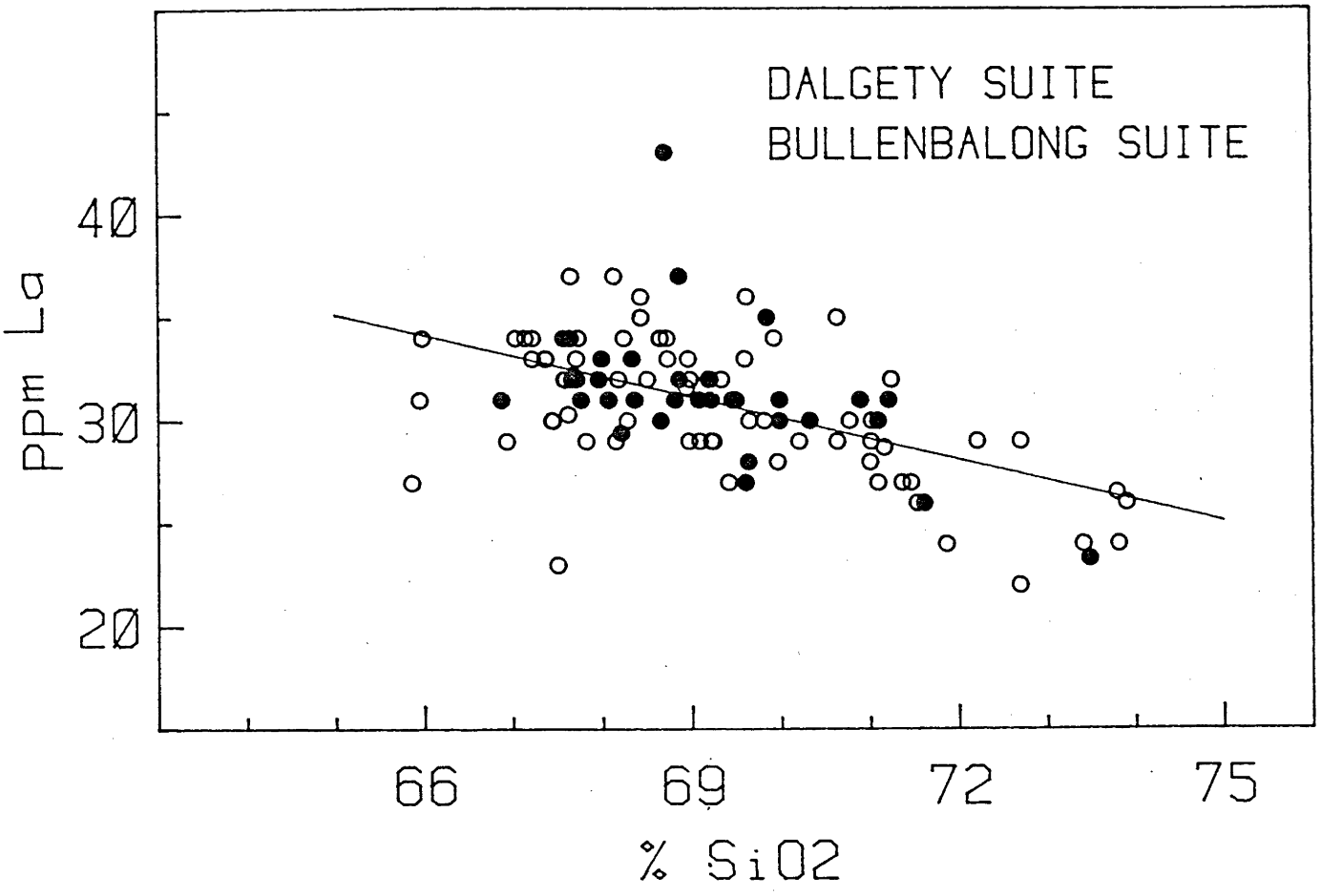
DALGETY SUITE
BULLENBALONG SUITE
40
30
20
PPm La
66
69
72
75
% SiO2

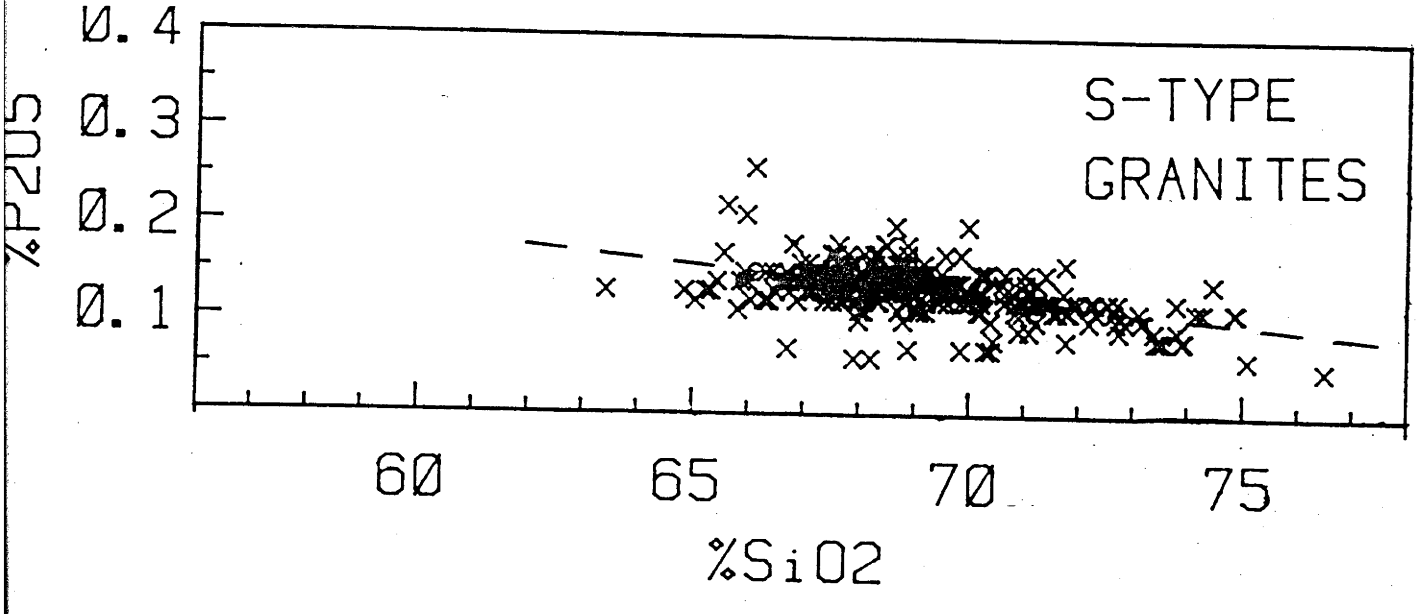
0.4
0.3
0.2
0.1
%P2O5
S-TYPE
GRANITES
60
65
70
75
%SiO2

Appendix B

OPTICAL MICROSCOPE DESCRIPTIONS OF THIN SECTIONS:

THE BEMBOKA PROFILE

The Bemboka Profile: Samples Bemboka 1 to 6 corresponding with analyses JFB 13 to JFB 18.

BEMBOKA 1

Fabric intact, minor veining of the fresh rock by quartz and mica (sericite?). No iron oxide staining.

GREENSCHIST FACIES ALTERATION OF GRANITE:

Biotite is replaced by vivid green chlorite developed parallel to host biotite sheets. This is associated with large lumps of pistachio green epidote, and fine grained, oriented clusters, possibly of sphene. There is some iron oxide (magnetite), and prehnite associated with these phases.

Plagioclase shows variable degrees of alteration to K-mica; this phase is often more strongly developed in the cores of this phase. Some large, (up to 300μm) epidote crystals (clinozoisite) crystals are also developed in these cores. Alteration appears to be more prominent along fracture planes in plagioclase; no strong correlation between twin planes and alteration is noted.

K-feldspar is distinctly less altered than plagioclase feldspar. Hydrothermal activity has resulted only in the development of a pale, dusty brown appearance in some areas of these crystals. If this dusty brown appearance can be attributed to the presence of a secondary phase, this material is too fine to be characterised in the optical microscope. Electron microscope observations of this phase suggest that this dusty appearance may be attributed to the presence of etch pits, (see Chapter 4). K-feldspar does contain some exsolution lamellae. These do not

appear themselves to be altered, but their margins with the enclosing K-feldspar are the sites for the development of small, oriented phyllosilicate laths.

Amphibole does not exhibit large areas of secondary, or hydrothermal alteration products. In some areas the green-brown amphibole has been replaced by paler, blue green amphibole (actinolite). Amphibole has also been replaced by small chlorite laths.

Allanite displays an outer, possibly metamict rim. The origin of this rim is not known; it may have developed during late stage crystallization of the granite or in response to a later hydrothermal event. Other phases present in the granite include zircon, apatite, magnetite, quartz. These phases do not appear to have been altered by any hydrothermal, or metamorphic events.

PROBE DATA
MAJOR MINERALS

	GREEN AMPHIBOLE		PALE AMPHIBOLE		BIOTITE		K-FELDSPAR	
SiO_2	44.1	6.94	51.1	7.93	37.0	5.68	64.9	12.00
TiO_2	.8	.10	-	-	3.8	.43	-	-
Al_2O_3	7.1	1.32	.7	.13	13.7	2.47	18.3	3.99
FeO	20.9	2.76	18.1	2.35	24.1	3.09	-	-
MnO	.9	.12	.4	.05	.2	.03	-	-
MgO	8.9	2.09	11.5	2.66	8.9	2.02	-	-
CaO	10.1	1.71	11.4	1.90	.2	.03	.2	.04
K_2O	.7	.14	-	-	9.2	1.81	14.9	3.51
Na_2O	1.3	.41	-	-	-	-	1.2	.44
Cl	.2	.06	-	-	.4	.09	-	-
tot.	95.0		93.2		97.3		99.5	
	15.70		15.01		15.65		19.97	
	23		23		22		-32	

	PLAGIOCLASE RIM		PLAGIOCLASE CORE		EPIDOTE		CLINOZOISITE	
SiO_2	65.2	11.53	56.1	10.17	35.3	5.54	39.5	6.16
TiO_2	-	-	-	-	-	-	-	-
Al_2O_3	21.4	4.47	28.3	5.98	18.8	3.47	28.5	5.24
FeO	-	-	-	-	15.5	2.04	6.2	.81
MnO	-	-	-	-	.2	.02	-	-
MgO	-	-	-	-	-	-	-	-
CaO	2.4	.45	9.9	1.90	21.7	3.65	24.0	4.00
K_2O	.3	.06	.1	.03	-	-	-	-
Na_2O	10.3	3.52	5.7	1.98	-	-	-	-
tot.	99.5		100.0		91.5		98.2	
	20.02		19.95		14.72		16.21	
	-32		-32		22		25	

BEMBOKA 2

Although the fabric of this sample remains essentially intact, networks of cracks present in the sample are coated with small quantities of orange-brown material.

Biotite which does not contain a significant quantity of chlorite remains unaltered. Chloritized biotite, however, displays signs that alteration has commenced with the development of narrow zones of orange vermiculite. Chlorite remains unaltered.

Weathering of plagioclase feldspar is apparent in this sample. Outlines of and interiors of plagioclase crystals are clearly distinguished from the surrounding granite by the dusty grey brown colour of their alteration products, and strongly altered cores. Fine grained, low birefringence weathering products are randomly distributed in the host feldspar. Coarser, higher birefringence micas display some tendency to parallel cleavage and twin planes. These micas are probably hydrothermally derived alteration products.

K-feldspar exhibits few signs of weathering in this sample. The dusty brown surface may be slightly more prominent than in fresh rock.

Anhedral or subhedral amphibole clots of blue green - green brown amphibole display early signs of weathering with the widening of cleavages and development of minor orange-brown discoloration, possibly associated with the development of clays.

Apatite exhibits some indications that dissolution of this phase has commenced. Some crystals have developed what appears to be a central, slightly browner rib.

Prehnite, green epidote, and clear clinozoisite appear to be resistant to weathering at this stage.

BEMBOKA 3

The fabric of this sample shows only minor signs of disruption, some holes have developed, and cracks widened. More prominent fractures are coated with orange brown material (Fe oxide?).

Biotite appears to be weathering slowly, orange vermiculite developed parallel to biotite cleavages is still relatively scarce. The correlation between more advanced weathering of biotite and the presence of interlayers of chlorite is quite apparent. Chlorite does not appear to be significantly altered at this stage. Prominent vermiculite is developed in biotite in this sample where the host biotite is located in close proximity to amphibole crystals, (such as in clots of mafic phases).

Plagioclase in this sample is significantly altered, few crystals contain any areas of unweathered feldspar of any appreciable size. Sodic rims, however, appear to be less altered than the more calcic regions of zoned crystals. Quite prominent holes have developed in the plagioclase, presumably as a result of dissolution. This etching is associated with the presence of abundant fine creamy-brown clays, and semi-randomly oriented laths of white phyllosilicate. The grainsize of alteration products is significantly larger in the cores of plagioclase crystals than in their rims.

K-feldspar again appears to be only marginally more altered in this sample than in the fresh rock. There is some tendency for the dusty brownish discoloration of the K-feldspar to be more prominently developed at the rims of crystals, and along exsolution lamellae.

Paler green brown amphibole in this sample contains numerous cracks. Dissolution of material has been strongly concentrated along cleavage planes. These fissures in the amphibole are generally lined with a orange brown alteration product. The remaining amphibole exists as cleavage-bound islands surrounded by weathering products and gaps.

Apatite shows further sign of dissolution.

Zircon, epidote, clinozoisite, prehnite, magnetite and quartz appear to be relatively resistant ot weathering at this stage.

BEMBOKA 4

The fabric of this sample is notably less intact than previous samples with gaps developed along cracks. These cracks are quite common, and strongly stained by orange brown material. This staining is also common around the margins of some phases, particularly plagioclase crystals.

The unchloritised biotite laths now show a minor development of orange vermiculite in zones paralleling cleavages. By this stage most chlorite has acquired an orange-green colour, possibly indicating that this phase is being replaced by either vermiculite or kaolinite. As noted in the Bemboka 4 sample, alteration is again more pronounced where biotite is developed in close proximity to amphibole. Where crystals have been strongly weathered their outlines have become ragged and internal zones contain abundant elongate cracks.

Many crystals of plagioclase feldspar have been altered right to their rims. Most alteration consists of semi-randomly oriented, fine, grey clays, and coarser, pinkish brown micas.

Although the dusty brown alteration of K-feldspar is quite strongly developed in this sample in some areas, apparently unaltered K-feldspar also persists. More pronounced zones of alteration appear to correlate with crystal margins more strongly than with exsolution lamellae or cleavages. A possible correlation also appears to exist between areas within a crystal which extinguish under crossed polars simultaneously and regions which have experienced similar degrees of weathering. This may indicate that feldspar in some orientations, or regions of greater strain may be more susceptible to weathering.

Amphibole is extensively altered by this stage, the crystals contain numerous cracks and holes, many of which are coated by orange clays.

Prehnite, epidote, and clinozoisite persist in this sample. Epidote, however, appears to have become less strongly coloured, particularly in the cores of this phase.

BEMBOKA 5

The fabric of this sample has become quite disrupted; numerous cracks and holes are present. Staining (by Fe?), particularly of plagioclase feldspar has become prominent.

Although fresh biotite remains in this sample, most crystals have been replaced, apparently by biotite-vermiculite mixtures. Partings between sheets are common, and occasionally appear to be filled in by slightly obliquely developed clay (possibly kaolinite). Most chlorite has been replaced by an orange-brown phase.

Plagioclase appears to have been very strongly replaced by creamy coloured clays which, when developed near the crystal margins, are stained brown.

K-feldspar exhibits an increased abundance of dusty brown alteration, and in some cases appears to have developed small quantities of coarser weathering products.

Amphibole can not be recognised in this sample. The pre-existence of this phase is indicated by holes, and a net like array of relic cleavage traces marked by remaining clays.

Some allanite was recognised in this sample. This phase has been strongly weathered, the pale relic core surrounded by a dark red altered rim.

The abundance of green epidote appears to have diminished in this sample. Clear clinozoisite is abundant, and appears to be stable at this stage.

Opaques are coarse, and abundant in this sample. Zircon persists unaltered.

Note: Some recrystallization of phyllosilicates into arrays composed of small groups of radiating crystals appears to have occurred by this stage. These arrays commonly pseudomorph the host phase.

BEMBOKA 6

The fabric of this sample is strongly disrupted, with cracks and gaps forming strips which isolate many crystals from surrounding crystal faces. Iron staining of cracks does not appear more pronounced than in Bemboka 5, but grain boundaries are extensively stained.

Only small quantities of biotite, and minor quantities of chlorite remain at this stage in weathering. Vermiculitized grains are very ragged in appearance, and contain a significant volume of cracks and voids.

Plagioclase is extremely altered by this stage, contains numerous voids, and abundant pale coloured clays, many of which have recrystallized to form coarser radiating aggregates. Staining of relic crystal margins is very prominent.

By this stage K-feldspar displays a some distinct signs of weathering. Crystals appear to be more fragmented, with the margins of these areas more strongly weathered to brown red material. Small very dark red brown aggregates of a secondary phase have developed within the feldspar. This material appears to be goethite.

Relic amphibole crystals can not easily be identified.

Although epidote is still a recognisable component of this sample this phase appears to be unstable, and appears to be altering at its margins to a browner phase.

THE JINDABYNE PROFILE

The Jindabyne profile: Samples 1 to 6 corresponding with analyses JFB 7 to JFB 12

JINDABYNE 1

Fabric undisturbed by weathering. No iron oxide staining.

GREENSCHIST FACIES ALTERATION OF GRANITE:

Red brown biotite is almost unchloritized. Minor development of some prehnite.

Plagioclase exhibits a minor development of K-mica, particularly in the cores of crystals.

K-feldspar appears to be almost unaltered.

No cordierite has been recognised in this sample. The former presence of this phase is suggested by the development of aggregates of white, green, and yellow brown micas, and possibly quartz.

Muscovite appears to be primary, and does not exhibit signs of alteration.

No accessory phases in this granite exhibit signs of hydrothermal alteration. Phases present include: Apatite, monazite, zircon, minor tourmaline, opaques.

Most phases in this sample have been quite strongly strained. Hand specimens indicate that this has been associated with the development of a foliation.

JINDABYNE 2

The fabric of this sample is notably less intact than that of Jindabyne 1, and exhibits veins and cracks which are occasionally stained by iron oxides.

Generally biotite in this sample is only marginally more altered than in Jindabyne 1. Some crystals show signs of disruption, and contain what appear to be faded areas. Some very minor development of vermiculite has occurred in narrow strips.

Plagioclase is notably more altered, clays present in this phase are generally coarser, and tend to concentrate in the cores of cystals, and along twin and cleavage planes. Coarser clays tend to parallel twins and cleavages in many cases.

K-feldspar has developed minor cloudy alteration which is associated in some cases with slightly coarser alteration products.

Apatite in this sample appears to have undergone some dissolution, and in rarer cases is associated with what appears to be Fe oxide staining.

Aggregates of white, green, and yellowish micas are now also associated with a more vivid yellow phase.

Zircon and tourmaline and opaques appear to be unaltered.

JINDABYNE 3

As in the case of Jindabyne 2, the fabric has been disrupted by cracks and holes; these have been stained, probably by Fe-oxides, to a minor extent.

Biotite remains reasonably fresh. The development of vermiculite is indicated in some areas by the presence of strips of paler material parallel to cleavages.

Plagioclase is associated with the development of reasonably coarse white mica with a dusty distribution. Lath orientation is strongly controlled by crystallography, and exhibits a strong preference for cleavage traces, and a lesser association with twin planes.

K-feldspar is associated with marginally more abundant dusty alteration than in Jindabyne 2.

Mica apparently pseudomorphing cordierite appears browner, and is associated with more abundant yellowish material in some areas.

Muscovite does not appear to have been modified by weathering at this stage.

Apatite appears to have undergone moderate dissolution by this stage.

Zircon and tourmaline appear to be unaltered.

Fe oxides are associated in some cased with Fe stains.

JINDABYNE 4

The fabric of this sample has been significantly disrupted, Fe oxide coated cracks are common.

Biotite now appears to be quite extensively converted to vermiculite, the colour is significantly paler, and crystals contain many strips and gaps.

Plagioclase is associated with relatively abundant fine dusty alteration, and the development of coarse, oriented white micas. A greater degree of alteration in the cores is now apparent, sodic rims are only marginally altered.

Dusty alteration of K-feldspar is marginally more prominent than in Jindabyne 3. Much K-feldspar remains unaltered, with only rare development of coarse micas. This phase contains occasional cracks which are coated with what appears to be iron oxide.

White mica appears to be very coarse and abundant in this sample.

Although apatite has undergone some dissolution, this phase persists at this stage of weathering.

Tourmaline and zircon do not appear to have been affected by weathering. Fe oxide is associated with some red brown staining.

JINDABYNE 6

Jindabyne 6 is less weathered by all criteria used to measure the extent of alteration than Jindabyne 5. Samples were similar in appearance when collected, and some doubt existed at the time as to which should be considered the more extensively weathered.

JINDABYNE 5

The fabric of this sample is extensively disrupted, and cracks stained with a thick coat of what appears to be iron oxide. Many crystals are separated by enlarged gaps. Biotites seem to have been broken and compressed into large aggregates of small flakes.

Biotite has essentially been replaced by vermiculite and kaolinite. Aggregates contain large strips and gaps. Some granular dark oxide is associated with this material, and kaolin appears to have developed in cracks and holes.

Remaining plagioclase crystals are strongly altered. Dusty grey rims are noted on some crystals. In places this phase has been extensively broken up, probably as a result of the disruption of fragile corroded crystals during the thin section making process.

K-feldspar is covered in fine dusty pale alteration, and is easily distinguished from plagioclase by its far less altered nature.

Mica aggregates have become a uniform yellow orange colour, and are associated with large clear mica crystals.

Some relatively unaltered apatite does persist, but most is etched and altered.

Zircon crystals are still present. This phase is difficult to recognise as crystals are frequently covered in clays and oxides.

THE ISLAND BEND PROFILE

The Island Bend profile: samples 1 to 6 correspond with analyse JFB 1 to JFB 6

ISLAND BEND 1

This sample has been mildly weathered, and therefore has not been used to represent fresh rock. Analysed sample RAE is representative of the unweathered granite.

The fabric of this sample shows some disruption, and has been mildly stained by Fe oxides (?) along fractures.

GREENSCHIST FACIES ALTERATION

Biotite contains quite prominently developed green chlorite, associated with large crystals of green epidote, dusty oxide, and possibly sphene.

Some plagioclase feldspar cores are very altered, and contain quite coarse epidote, and quite well formed K-micas. In some areas preferential replacement of one set of twin planes can be observed, in others both sets of twin planes control the development of alteration products.

K-feldspar in this sample is virtually unaltered. This phase contains quite prominent exsolution lamellae and tends to develop as interstitial crystals.

WEATHERING

Some vermiculite has developed within the biotite, and appears to be associated with a small amount of what appears to be iron oxide. Some clear K-mica appears to be developing within the biotite, generally associated with the chlorite interlayers.

Plagioclase has developed some very fine dusty alteration, with pale micas concentrated in the central parts of crystals, particularly just inside the core - rim boundary.

The dusty alteration associated with the K-feldspar is possibly attributable to weathering effects.

Some apatite crystals appear to have been fractured, most appear unaltered. This phase occurs in feldspar as well as in biotite laths.

Although amphibole is present in this granite, its abundance is very low. In this sample this phase does not appear to have been significantly altered by hydrothermal processes or by weathering.

Opaques are commonly present in this sample as large subhedral crystals, often occurring in clusters.

ISLAND BEND 2

The fabric of this sample is slightly more fractured than in the previous sample. Holes are more abundant, and Fe staining on cracks and mineral contacts is noted.

Biotite contains more abundant vermiculite, chlorite appears slightly more orangish brown in places. Vermiculite is more prominently developed along chlorite biotite contacts, and is more abundant in chloritized crystals than in unchloritized crystals.

Plagioclase has quite coarse mica developed along its twin planes, narrow twin lamellae are commonly selectively replaced. Alteration is generally most prominent just inside the core - rim boundary. In some cases the whole core has been replaced by an orangish phase, probably kaolin.

K-feldspar is associated with very fine, pale alteration. Exsolution lamellae are frequently more strongly altered than the host K-feldspar.

Rare small crystals of amphibole do not show signs of any significant degree of weathering.

Although most apatite crystals persist intact, some do show signs of alteration, particularly dissolution.

Zircon and opaques do not appear to have been altered.

ISLAND BEND 3

Although the fabric of this sample is cracked, it still remains essentially intact. Some iron oxide staining can be observed on the margins of some crystals.

Biotite crystals have become more ragged in appearance, with the development of more abundant vermiculite. Chlorite and epidote still persist in the biotite, chlorite still being more abundant than vermiculite.

Plagioclase in this sample appears to be only marginally more abundant in this sample than in the previous sample. Alteration still appears to be controlled to some extent by crystallographic features of the feldspar. Some coarser micas appear to be developing in central regions of crystals, and secondary phases around crystal margins appear to have become more prominent.

K-feldspar contains very fine grained alteration, concentrating to some extent towards the margins of crystals, where exsolution is more strongly developed. Cleavage traces in this phase appear to have been highlighted by weathering.

Amphibole is rare, and only shows minor signs of alteration.

Apatite has undergone some dissolution, and possibly has been replaced by secondary phases.

Zircon appears to be unaltered.

ISLAND BEND 4

The fabric of this sample has undergone a significantly greater degree of modification than previously observed. Many quite large gaps and cracks have developed, most are extensively stained by Fe oxides. Mineral contacts are also stained.

Biotite crystals appear far more ragged. Chlorite is still present, and has apparently been only slightly affected by weathering. This phase has developed a browner green colour. In some crystals vermiculite is quite prominently developed, whereas others are almost unaltered. Abundant epidote persists in most areas.

Plagioclase is moderately weathered at this stage to fine greyish clays. The development of alteration products seems to be controlled far less by twin and cleavage planes. Alteration of the more sodic rims is now far more pronounced.

K-feldspar remains relatively unaltered, and has developed only minor dusty alteration products at this stage. These secondary phases appear to be only marginally more strongly developed towards the rims of crystals.

Amphibole can still be recognised, and is not strongly altered.

Apatite exhibits distinct signs of dissolution in some cases.

Zircon persists, apparently unaltered.

ISLAND BEND 5

Gaps are commonly developed in this material, crystals are commonly separated by spaces, and their margins are frequently iron stained.

Biotite is notably vermiculitized at this stage. Chlorite persists, and is often still quite green.

Plagioclase is moderately altered in this sample, cores are still more altered than rims. Minor crystallographic control on the orientation of secondary products can be recognised, but is not nearly as predominant as in fresh samples.

K-feldspar is still markedly less weathered than plagioclase feldspar. More altered regions of this phase generally correspond with areas where plagioclase exsolution can be recognised.

Much of the original apatite in the rock has been removed by this stage. In the optical microscope, this phase appears to have been replaced by holes.

Zircon persists, and is particularly apparent in phases after biotite.

ISLAND BEND 6

The fabric of this sample is very disrupted, fractures and voids are apparent both within and between crystals. Fe staining does not appear to be as extensive as in the other profiles.

Biotite and vermiculite appear to have been almost completely converted to vermiculite and kaolin. Reddish oxide (Fe?) develops in cracks in this material.

Plagioclase has been very strongly altered and fragmented partly as a result of slidemaking. Most plagioclase appears to have been replaced by kaolinite, the relic crystals containing up to about 50% holes.

K-feldspar is also fragmented, but is far less altered than plagioclase. This phase has not been extensively replaced by secondary phases as a result of the degree of weathering experienced in this profile.

Amphibole was not recognised in this sample.

Virtually no apatite can be recognised in this sample.

Zircon persists, and is abundant in this sample.

Appendix C

CLAY MINERAL SEPARATION AND PARTICLE SIZE ANALYSIS OF WEATHERED GRANITES.

Analyses of the percentage clay in selected weathered samples, the distribution of the particles sizes within the clay fraction, and the extraction of clay separates (for XRD, IR, major and trace element chemistry, neutron activation, measurement of cation exchange capacity, and electron microscopy) was carried out at the Soils Division of CSIRO in Canberra, under the supervision of Dr. Pat Walker, and Mr John Hutka. The method outlined below very closely resembles that used routinely by CSIRO; it is a modification of the Steele and Bradfield (1934) method which has been described in Walker and Hutka(1979).

.1 SAMPLES STUDIED:

Of the sets of six samples from the three weathering profiles (labeled from 1 to 6 to reflect increasing degrees of weathering), samples 3,4,5, and 6 from each profile were selected for analysis of the amount of clay, size distribution of the clay fraction, and clay extraction.

.2 METHOD:

Measurement and extraction of the <2μm fraction was done by sedimentation and pipette analysis utilizing settling velocities as determined by Stoke's Law. Extraction and measurement of the <0.24μm fraction was achieved by centrifuging, a technique also employed to concentrate the clay fraction for chemical analysis etc. The procedure is outlined below.

1. The bulk sample was disaggregated by hand and air dried at <35°C.

2. A sub-sample was passed through a 2mm sieve after aggregates were broken down using a mortar and pestle. In all cases some of the

individual crystals were larger than 2mm in diameter, and required considerable crushing before the bulk sample would pass through the sieve. Consequently it should be noted that the abundance data for particles coarser than 2μm does not relate to the particle size distribution of the original rock, but also reflects the grindability of the sample, (and probably therefore will reflect the extent of weathering). It was considered unlikely that this approach would result in the production of any material finer than 2um as a result of grinding. This was infact the case; IR analysis of the extracted clay fraction did not contain detectable quartz.

3. After randomizing, 60 grams (3x20g subsamples) of material was sonified, for 20 minutes, allowed to cool, and then again sonified for 20 minutes. This process liberates clay minerals by further disaggregating the sample. Examination of the coarse fraction (31.2μm-2mm) (under a binocular microscope, and also using a scanning electron microscope) after the pipette analysis was completed indicated that this technique was effective, and very little clay remained on the primary minerals.

4. Samples did not appear to contain any organic matter. Consequently treatment with hydrogen peroxide was not considered necessary. This step was also avoided on the grounds that addition of another chemical and its removal by boiling was undesirable where clays were extracted for further analysis.

5. Samples were placed in 250ml plastic bottles with 5mls of 1N NaOH and 10mls of Na tripolyphosphate to disperse the clays. Bottles were placed on an end over end tumbler overnight to prevent sedimentation, and to thoroughly mix the samples.

6. Bottles were emptied into 1250ml cylinders and filled to 1250mls with distilled water. A blank 1250ml solution containing dispersing agent was prepared at this stage.

7. The temperature of the solution was measured before and during sedimentation as settling rates are temperature dependent. The times required for a 31.2μm and a 2μm particle to fall 10cm were then determined.

8. Samples were then thoroughly stirred and sedimentation of samples allowed to begin at 1 minute intervals. At 25°C a 31.2um particle requires 1 minute and 45 seconds to settle 10cm. Consequently sedimentation was allowed to proceed in each case for this period of time before a subsample was removed from a depth of 10cm. The exact volume of the pipette sample had previously been accurately determined to be 28.47mls. Similarly, the time required for a 2μm particle to settle 10cm is 7 hours and 5 minutes. Samples extracted by pipette were placed in clean, oven dried beakers, and dried overnight at 105°C, and reweighed. (The sample was then discarded).

9. A subsample of the <2μm fraction was collected at the appropriate depth and time, and 3ml aliquots placed onto glass slides. This sample was then allowed to dry at air temperature. Slides were recoated until sufficient sample thickness was obtained to allow XRD identification of the phases present in the clay fraction.

10. After removal of the <2μm samples about 800mls of the suspension was decanted for centrifuging. This process involves pipetting 100mls of the suspension into containers and determining the appropriate parameters, (eg. rpm, time) required for a particle of .24μm to fall 2cm at a given temperature. After centrifuging, a known volume (5.25 mls) of sample was removed by pipette from this depth, oven dried, and weighed. The process was repeated with the appropriate modifications to determine the abundance of particles <.06μm in diameter. The method used to prepare XRD slides is the same as that outlined above.

11. The H_2O^- content is measured by weighing a separate quantity of sieved sample before and after it is oven dried at 105°C.

12. The percent by mass of the sample between 31.2μm and 2mm was measured by repeatedly decanting (by suction) the <31.2μm fraction after the appropriate settling time. The residue was then oven dried and weighed.

13. In selected cases the clay fraction contained in the fluid after the clay size analysis was centrifuged for sufficient time to ensure that no significant quantity of material remained in suspension, (about 50mins at 7000rpm). The bulk of the fluid could then be poured

off, and the sample dried in an oven. Sufficient material was processed this way to provide at least 3g of clay for chemical analysis.

3 CALCULATION OF RESULTS:

3.1 For the 31.2µm to 2mm fraction:

wgt sample after decanting (dry) x 100/ 60g = %

3.2 For the <2µm and <31.2 µm factions:

wgt sample-wgt dispersing agent per 28.47mls x 1250 x 100/ 60g x 28.47mls = %

3.3 For the <.24µm and <.06µm factions:

wgt sample-wgt disp. agent per 5.25mls x 1250 x100/ 60g x 5.25mls = %

Results are listed in the following Tables.

PARTICLE SIZE ANALYSIS : BEMBOKA GRANODIORITE - RESULTS

SAMPLE NUMBER	<0.06 µm	<0.24 µm	<2.00 µm	<31.2 µm	2mm-31.2 um	H_2O^-
BEM 1	..... NOT STUDIED					
BEM 2						
BEM 3	0.37 %	1.92 %	5.62 %	16.03 %	83.05 %	1.82 %
BEM 4	-0.06* %	3.12 %	9.31 %	23.89 %	74.27 %	2.18 %
BEM 5	-0.01* %	4.69 %	14.43 %	32.65 %	65.86 %	2.69 %
BEM 6	-0.13* %	5.05 %	17.23 %	41.10 %	58.69 %	1.65 %

per cent in each fraction

	0.06 µm	0.24 µm	2.00 µm	31.2 µm	total - dispersing agent
BEM 3	0.37 %	1.55 %	3.70 %	10.41 %	100.38 %
BEM 4	-0.06 %	3.12 %	6.19 %	14.58 %	100.26 %
BEM 5	-0.01 %	4.69 %	9.74 %	18.22 %	101.13 %
BEM 6	-0.13 %	5.05 %	12.18 %	23.87 %	101.37 %

PARTICLE SIZE ANALYSIS: THE JINDABYNE PROFILE - RESULTS

SAMPLE NUMBER	<0.06 µm	<0.24 µm	<2.00 µm	<31.2 µm	2mm-32.2 um	H_2O^-
JIN 1	..... NOT STUDIED					
JIN 2						
JIN 3	0.51 %	1.62 %	3.67 %	12.37 %	88.06 %	0.54 %
JIN 4	1.36 %	4.44 %	11.56 %	27.33 %	72.51 %	0.22 %
JIN 5	1.93 %	7.31 %	18.75 %	37.11 %	60.89 %	2.05 %
JIN 6	0.68 %	4.73 %	11.52 %	27.01 %	66.00 %	1.40 %

per cent in each fraction

	0.06 µm	0.24 µm	2.00 µm	31.2 µm	total - dispersing agent
JIN 3	0.51 %	1.11 %	2.14 %	8.61 %	100.90 %
JIN 4	1.36 %	3.08 %	7.12 %	15.77 %	99.99 %
JIN 5	1.93 %	5.38 %	11.44 %	18.36 %	99.97 %
JIN 6	0.72 %	4.29 %	7.20 %	16.42 %	100 (corrected)%

PARTICLE SIZE ANALYSIS: ISLAND BEND PROFILE - RESULTS

SAMPLE NUMBER	<0.06 μm	<0.24 μm	<2.00 μm	<31.2 μm	2mm-31.2 um	H_2O^-
IB 1	..... NOT STUDIED					
IB 2						
IB 3	0.37 %	0.94 %	2.01 %	7.94 %	92.21 %	0.24 %
IB 4	-0.05* %	0.19 %	1.73 %	8.53 %	90.97 %	0.55 %
IB 5	-0.11* %	0.39 %	3.45 %	12.46 %	86.04 %	1.21 %
IB 6	-0.23* %	4.83 %	14.87 %	35.33 %	64.68 %	1.40 %

per cent in each fraction

	0.06 μm	0.24 μm	2.00 μm	31.2 μm	total - dispersing agent
IB 3	0.37 %	0.57 %	1.07 %	5.93 %	100.32 %
IB 4	-0.05 %	0.19 %	1.54 %	6.80 %	99.97 %
IB 5	-0.11 %	0.39 %	3.06 %	9.01 %	99.63 %
IB 6	-0.23 %	4.83 %	10.04 %	20.46 %	101.34 %

* -ve result due to experimental errors.

Appendix D

CALCULATION OF RELATIVE MINERAL WEATHERING RATES

CALCULATION FOR THE BEMBOKA PROFILE

The data required for this calculation are: 1. Modal proportions of minerals in the unweathered granite; 2. Composition of these phases; and 3. A measure of the rates at which components are released. Data have been expressed as proportions of the original quantity which remain at a given time, in this case, after 25% of the original components in the rock have been released from their host phases. The fate of these components after release, (eg. retained in clays or removed in solution) is not important in this calculation.

BEMBOKA MODE		% RELEASED AFTER 25% TOTAL RELEASED	
QUARTZ	35%	SiO_2	22%
An_{11}	19%	TiO_2	22%
An_{48}	13%	Al_2O_3	30%
K-FELDSPAR	16%	Tot. FeO	25%
BIOTITE	10%	MnO	32%
AMPHIBOLE	3%	MgO	22%
EPIDOTE	4%	CaO	72%
		Na_2O	50%
		K_2O	15%

Probe data for individual phases are listed in Appendix 1.

Data for the release of MgO, and TiO_2 indicate that at this stage approximately 22% of the biotite has been destroyed. Biotite contains 9% K_2O, and makes up 10% of the whole rock. Consequently this phase originally accounts for 0.9 wgt% K_2O. The result of the destruction of 22% of the biotite will be the release of .22 x 0.9wgt% K_2O from the whole rock = .20 wgt%.

Now: At this stage the whole rock has released 15% K_2O, which is equivalent to the release of .15 x 3.47 wgt% K_2O = .52 wgt% K_2O, and of this, 0.20 wgt% has been lost from biotite. Consequently .32 wgt% K_2O has been released from the other K-bearing phase, K-feldspar.

Now: K-feldspar originally contributed 16% x 15wgt% K_2O to the whole rock, = 2.4 wgt%; of this .32 wgt% has been released, which represents the destruction of .32/2.4 of the original quantity of K-feldspar, or 13%.

Consequently, the destruction of 22% of the biotite originally present is associated with the destruction of 13% of the original K-feldspar.

Two varieties of plagioclase feldspar have been selected to represent the core and rim compositions. As probe data indicate groupings around a maximum of An_{48}, and a minimum of An_{11}, these compositions have been chosen. As it is clear that calcic plagioclase is more susceptible to weathering than the more sodic plagioclase, it is hoped that this simplification will allow an estimate of the extent to which these varieties differ in their behaviour. The assumption has been made that the behavior of plagioclase with compositions intermediate between these end members will be approximated by weathering rates which are also intermediate.

Now: The two feldspars account for the following proportions of Na_2O and CaO in the fresh material:

	CaO	Na_2O	Al_2O_3
An_{11}	2.4 wgt%	10.3 wgt%	21.4 wgt%
x 19%	= .46wgt%	1.96wgt%	4.07wgt%
An_{48}	9.9 wgt%	5.7 wgt%	28.3 wgt%
x 13%	= 1.29wgt%	.74wgt%	3.68wgt%

In addition to these phases,

Epidote	22.0 wgt%	-	19.0 wgt%
x 4%	.88wgt%	-	.76wgt%

Amphibole	11.4 wgt%	-	.7 wgt%
x 3%	.35wgt%	-	.02wgt%

Note: rock contains 16 % k-feldspar, which accounts for .16wgt% Na_2O.

As it has been noted earlier, amphibole is weathered at an early stage, hence it is assumed that this phase, (and epidote) are completely removed. (This is the extreme case, and appears necessary to reduce the difference between the calculated and observed Al release rates. These phases were only incorporated for this profile, as calculations for the Jindabyne and Island Bend profiles produced results much closer to those expected).

Now: To account for the removal of 50% Na_2O and 72% CaO, the following quantities of the above phases are removed:

	CaO	Na_2O
35% An_{11}	.16wgt%	.69wgt%
70% An_{48}	.90wgt%	.52wgt%
100% Epidote	.88wgt%	
100% Amph.	.35wgt%	
	2.29wgt%	1.21wgt%

This implies that, very approximately, removal of 13% K-feldspar is associated with the removal of 22% biotite, 35% sodic, and 70% calcic plagioclase.

These results can be compared with those from the Island Bend and Jindabyne profiles in Chapter 8. In both the Island Bend and Bemboka profiles the calcic plagioclase weathers about twice as fast as the sodic plagioclase, and in all three profiles the removal of K-feldspar occurs comparatively slowly, but at a fairly consistent rate relative to the average rate of destruction of the granite.

Appendix E

CALCULATION FOR CLAY CHEMISTRY

A DETERMINATION OF THE EXTENT TO WHICH THE CLAY FRACTION RETAINS COMPONENTS RELEASED DURING WEATHERING: THE CALCULATION FOR THE JINDABYNE PROFILE.

1. The fraction of the original content of an element which is contained in the clay fractions examined:

wgt% element in clay x density whole rock x % clay in whole rock = contribution of clay fraction = "x" so that: x / gm cm^3 element in unweathered rock (COLUMN 2). -> COLUMN 3

2. The fraction of the original content of an element which is contained in the non-clay fraction at this stage:

(gm cm^3 element in weathered rock - x) / gm cm^3 element in unweathered rock -> COLUMN 4.

3. The fraction of the original content of an element which has been removed in solution:

100% - COLUMN 3 - COLUMN 4 -> COLUMN 5.

4. The fraction of the quantity of an element which has been released which has been retained in the clay fraction:

COLUMN 3 / (COLUMN 3 + COLUMN 5) -> COLUMN 6.

RESULTS FOR THE JINDABYNE PROFILE

ELEMENT	FRESH ROCK=	CLAY	NON-CLAY	SOLUTION	FRACTION RETAINED
SiO_2	191.4	6%	77%	17%	.26
		9%	68%	23%	.28
TiO_2	1.53	22%	60%	18%	.55
		36%	37%	27%	.57
Al_2O_3	38.3	19%	68%	13%	.59
		27%	56%	17%	.61
tot. FeO	10.2	25%	55%	20%	.56
		38%	40%	22%	.63
MnO	.15	20%	53%	27%	.43
		20%	27%	53%	.38
MgO	4.44	17%	60%	23%	.43
		30%	44%	26%	.54
CaO	6.03	1%	45%	50%	.02
		3%	20%	77%	.04
K_2O	10.4	8%	71%	21%	.28
Ba	1310	8%	72%	20%	.29
		11%	68%	21%	.34
Rb	502	12%	70%	18%	.40
		18%	57%	25%	.42
Sr	319	5%	62%	23%	.18
		9%	42%	49%	.16
Zr	475	4%	78%	18%	.18
		6%	64%	30%	.17
Y	87	7%	67%	26%	.21
		14%	46%	40%	.26
La	79	17%	70%	13%	.57
		27%	53%	20%	.57
Ce	183	15%	63%	22%	.41
		26%	35%	39%	.40
V	186	24%	82%	-6%	1.06
		38%	67%	-5%	1.05
Cr	96	21%	89%	-1%	1.01
		39%	59%	2%	.95
Pb	74	15%	69%	16%	.48
		23%	51%	26%	.47
Ni	33	25%	66%	9%	.74

		40%	40%	20%	.67
Cu	36	34%	31%	35%	.49
		54%	32%	14%	.79
Zn	158	26%	53%	21%	.55
		42%	38%	20%	.68
Nb	31	17%	60%	23%	.43%
		33%	36%	31%	.52%

AMENDMENTS

Page 6 Determination of the abundances of a number of minor components was performed by instrumental neutron activation analysis using a modified technique similar to that of Jacobs et. al. (1977). Samples were irradiated in a thermal neutron flux of 4×10^{12} n $cm^{-2} sec^{-1}$ for 24 hours, and six counts performed over a period of six months.

Page 7 I and S type granites were defined by Chappell and White (1974) in Vol. 8, Pacific Geology; pp 173-174.

Page 12 Palaeoenvironments have been also studied by a number of other workers, including Bowler et. al. (1975): Late quaternary climates of Australia and New Guinea; a summary: in Proc. WMO/ IAMAP symposium on long term climatic changes (Davies D.A.) World Met. Org. Publ. No. 421, p39 - 46, 1975.

Page 12 All sites before roadworks were located below the centre of the crests of moderately steeply sloping ridges, and would appear to be predominantly shedding rather than receiving drainage water from surrounding weathered material. The topography and vegetation associated with the Jindabyne profile resembles that associated with the Bemboka and Island Bend profiles, and is illustrated in Plate 3.1 Bii., p 7a.

Page 41 4.2.4: 1st sentence refers primarily to K-feldspar from the Jindabyne and Island Bend profiles. K-feldspar from the Island Bend profile was not examined in detail as it contained abundant exsolution lamellae. The identity of the primary phase associated with alteration products discussed and illustrated in this section was confirmed using the STEM to ensure that alteration of plagioclase exsolution lamellae was not confused with K-feldspar alteration.